Annual Report of the

Prado Basin Habitat Sustainability Committee

Water Year 2017

Final Report

June 2018

Prepared for:

Inland Empire Utilities Agency
&
Chino Basin Watermaster

Prepared by:

Wildermuth Environmental, Inc.

Table of Contents

List of Tables

List of Figures

List of Figures (cont'd)

Acronyms, Abbreviations, and Initialisms

ACOE	US Army Corps of Engineers
AF	acre-feet
AFY	acre-feet per year
AMP	Adaptive Management Plan for the PBHSP
Annual Report	Annual Report of the Prado Basin Habitat Sustainability Committee
BLM	Bureau of Land Management
CAL FIRE	California Department of Forestry and Fire Protection
CBMWD	Chino Basin Municipal Water District
CBWM	Chino Basin Watermaster
CCWF	Chino Creek Well Field
CDA	Chino Basin Desalter Authority
CDFM	Cumulative Departure from the Mean
CEQA	California Environmental Quality Act
Chino Basin	Chino Groundwater Basin
CIMIS	California Irrigation Management Information System
DBH	Diameter at Breast Height
FD	Fusarium Dieback
ft-bgs	feet below ground surface
FRAP	Fire and Resource Assessment Program
GIS	Geographic Information System
GMP	Groundwater Monitoring Program
HCMP	Hydraulic Control Monitoring Program
IEUA	Inland Empire Utilities Agency
LEDAPS	Landsat Ecosystem Disturbance Adaptive Processing System
MWD	Metropolitan Water District of Southern California
NDVI	Normalized Difference Vegetation Index

Acronyms, Abbreviations, and Initialisms (cont'd)

NASA	National Aeronautics and Space Administration
NEXRAD	Next Generation Radar
NPS	National Park Service
OBMP	Optimum Basin Management Program
OC-59	The OCWD's imported water turnout tributary to Prado Basin
OCWD	Orange County Water District
Parties	Parties to the Chino Basin Judgment
PBHSC	Prado Basin Habitat Sustainability Committee
PBHSP	Prado Basin Habitat Sustainability Program
POTWs	Publicly Owned Treatment Works
Prado Basin	Prado Flood Control Basin
PSHB	Polyphagous Shot Hole Borer - *Euwallacea fornicates*
QA/QC	Quality Assurance and Quality Control
RHMP	Riparian Habitat Monitoring Program
SAWA	Santa Ana Watershed Association
SCL	Scan Line Detector
SEIR	Subsequent Environmental Impact Report
SWMP	Surface-Water Monitoring Program
TDS	Total Dissolved Solids
USBR	United States Bureau of Reclamation
UCSB	University of California Santa Barbara
USGS	United States Geological Survey
USDA	United State Department of Agriculture
USFWS	United States Fish and Wildlife Service
VOCs	Volatile Organic Compounds
Watermaster	Chino Basin Watermaster

Acronyms, Abbreviations, and Initialisms (cont'd)

WEI	Wildermuth Environmental Inc.
WRCRWA	Western Riverside County Regional Wastewater Authority
WY	Water Year

Section 1 – Background and Objectives

This *Annual Report of the Prado Basin Habitat Sustainability Committee for Water Year 2017* (Annual Report) was prepared on behalf of the Prado Basin Habitat Sustainability Committee (PBHSC), convened by the Inland Empire Utilities Agency (IEUA) and the Chino Basin Watermaster (Watermaster) pursuant to the mitigation monitoring and reporting requirements of the Peace II Subsequent Environmental Impact Report (SEIR) (Tom Dodson, 2010).

This introductory section provides background on the general hydrologic setting of the Prado Flood Control Basin (Prado Basin); the Chino Basin Judgment, Optimum Basin Management Program (OBMP) and its Programmatic EIR, and Peace Agreement; the Peace II Agreement and its Subsequent EIR, the formation of the PBHSC and the development of the adaptive management plan (AMP) for the Prado Basin Habitat Sustainability Program (PBHSP).

1.1 Prado Flood Control Basin

Figure 1-1 shows the Prado Basin, located in the southern portion of the Chino Groundwater Basin (Chino Basin). The Prado Basin is the flood control area behind Prado Dam, which was constructed in 1941 as the major flood-control facility within the Santa Ana River Watershed. The US Army Corps of Engineers regulates releases of water from Prado Dam for both purposes of flood control and groundwater recharge in Orange County. Releases of water temporarily held in storage in Prado Basin for groundwater recharge in Orange County is coordinated with the Orange County Water District (OCWD). Approximately 4,300 acres of riparian habitat has developed within the Prado Basin, creating the largest riparian habitat in Southern California.

The Santa Ana River (SAR) flows through the Prado Basin from east to west. The tributaries of the SAR that flow into the Prado Basin include San Antonio/Chino Creek, Cucamonga/Mill Creek, and Temescal Creek. The major components of flow within the SAR and its tributaries are: runoff from precipitation, discharge of tertiary-treated effluent from wastewater treatment plants, rising groundwater, discharge of untreated imported water from OC-59 turnout conveyed through the Prado Basin for groundwater recharge in Orange County, and dry-weather runoff[1].

The Prado Basin is a hydrologically complex region of the lower Chino Basin. Groundwater in the Chino Basin generally flows from the forebay regions in the north towards Prado Basin in the south. Depth to groundwater is relatively shallow in the Prado Basin area, and the SAR and its tributaries are unlined across the Prado Basin, which allows for groundwater/surface-water interaction. Groundwater outflows in the Prado Basin occur via evapotranspiration by riparian vegetation and rising-groundwater discharge to the SAR and its tributaries.

To the north of Prado Basin, the Chino Basin Desalter Authority (CDA) owns and operates a municipal well field. Figure 1-1 shows the location of the existing CDA wells. The well field

---

[1] Dry-weather runoff consists of excess irrigation runoff, purging of wells, dewatering discharges, etc.

pumps groundwater with high concentrations of total dissolved solids (TDS), nitrate, and volatile organic compounds (VOCs). The CDA treats the groundwater at two regional facilities using reverse osmosis, ion exchange and blending to produce a potable water supply for the region. VOCs are currently treated through blending, and new treatment processes are being added to increase their removal. CDA operations are fundamental to achieving many of the management goals outlined in the Chino Basin OBMP and both Peace Agreements, which are discussed below.

1.2 Chino Basin Judgment, OBMP, and Peace Agreement

A 1978 Judgment entered in the Superior Court of the State of California for the County of San Bernardino (Chino Basin Municipal Water District *v.* City of Chino et al.) established pumping and storage rights in the Chino Basin. The Judgment established the Watermaster to oversee the implementation of the Judgment and provided Watermaster with the discretionary authority to develop an OBMP to maximize the beneficial use of the Chino Basin. The OBMP was developed by Watermaster and the Parties to the Judgment (Parties) in the late 1990s (WEI, 1999). The OBMP maps a strategy to enhance the yield of the Chino Basin and reliable high-quality water supplies for the development expected to occur. The goals of the OBMP are: to enhance basin water supplies, to protect and enhance water quality, to enhance the management of the Basin, and to equitably finance the OBMP.

In 2000, the Parties executed the Peace Agreement (Watermaster, 2000) which documented their intent to implement the OBMP. The Peace Agreement included an OBMP Implementation Plan, which outlined the time frames for implementing tasks and projects in accordance with the Peace Agreement and the OBMP. The OBMP Implementation Plan is a comprehensive, long-range water-management plan for the Chino Basin and includes: the use of recycled water for direct reuse and artificial recharge, the capture of increased quantities of high-quality storm-water runoff, the recharge of imported water when TDS concentrations are low, the desalting of poor-quality groundwater in impaired areas of the basin, the support of regulatory efforts to improve water quality in the basin, storage management, and the implementation of management activities that will result in the reduced discharge of high-TDS/high-nitrate groundwater to the SAR, thus ensuring the protection of downstream beneficial uses in Orange County.

The Chino Basin Municipal Water District (CBMWD) was the plaintiff in the legal action that resulted in the Judgment. The CBMWD was formed in 1950 to supply supplemental, imported water purchased from the Metropolitan Water District of Southern California (MWD) to the Chino Basin. On July 1, 1998, the CBMWD changed its name to the IEUA and expanded its role to become the regional supplier of recycled water for most of the Chino Basin. For OBMP implementation, the IEUA has served as the lead agency for compliance with the California Environmental Quality Act (CEQA). A Program Environmental Impact Report for the OBMP (SCH#2000041047) was certified by the IEUA in July 2000 (Tom Dodson, 2000).

1.3 The Peace II Agreement and its Subsequent EIR

To further implement the goals and objectives of the OBMP, the Parties executed the Peace II Agreement in 2007, which modified the OBMP Implementation Plan (Watermaster, 2007). The two main activities of the Peace II Agreement are: (i) increasing the controlled overdraft of the Chino Basin, as defined in the Judgment,[2] by 400,000 acre-feet (AF) through 2030 (re-operation) and (ii) refining the planned expansion facilities of the Chino Basin Desalter program from about 30,000 to 40,000 acre-feet per year (AFY) of groundwater production. Re-operation is allocated specifically to offset the production of the Chino Basin Desalters. Both re-operation and desalter expansion contribute to the attainment of "hydraulic control" of groundwater outflow from the Chino Basin to the SAR. The attainment and maintenance of hydraulic control is a requirement of Watermaster and the IEUA, as defined in the Water Quality Control Plan for the Santa Ana River Basin (California Regional Water Quality Control Board, Santa Ana Region, 2008). Hydraulic control ensures that the water management activities in the Chino Basin will not impair the beneficial uses designated for SAR water quality downstream of Prado Dam.

The expansion of the Chino Basin Desalters, described in the Peace II Agreement, is accomplished, in part, by the construction and operation of the Chino Creek Well Field (CCWF) in the southwest portion of Chino Basin (see Figure 1-2). During Peace II Agreement planning, the estimated capacity of the CCWF was about 5,000 to 7,700 AFY (WEI, 2007). The CCWF wells were constructed in 2011-2012; the actual capacity is 1,500 to 1,800 AFY.

In 2010, the IEUA certified the Peace II SEIR (Tom Dodson, 2010) to evaluate the environmental impacts that could result from implementing the Peace II Agreement. One of the potential impacts evaluated was the possible lowering of groundwater levels (drawdown) in the Prado Basin area, which could impact riparian vegetation that is dependent upon shallow groundwater. Watermaster performed modeling studies to predict the extent and magnitude of the drawdown associated with the implementation of the Peace II Agreement, using the planned capacity of 7,700 AFY of the CCWF (WEI, 2007). Figure 1-2 (modified from Figure 4.4-10 from the Peace II SEIR) shows the model-predicted drawdown in the Prado Basin area for the period of 2005 to 2030. The drawdown throughout most of the Prado Basin area was predicted to be less than five feet by 2030.

Although the available modeling work indicated that implementing the Peace II Agreement would not cause significant adverse effects on the Prado Basin riparian habitat, a contingency measure to address the potential for drawdown of groundwater levels and its impact on riparian vegetation was included in the Peace II SEIR as Mitigation Measure 4.4-3 (Biological Resources/Land Use & Planning section of the Mitigation Monitoring and Reporting Program).

[2] The Judgment established 200,000 AF of controlled overdraft over the period of 1978 to 2017. Re-operation increases the controlled overdraft to 600,000 acre-ft through 2030.

Mitigation Measure 4.4-3 was developed to ensure that the riparian habitat will not incur unforeseeable significant adverse effects from the Peace II implementation and to contribute to the long-term sustainability of the riparian habitat. Mitigation Measure 4.4-3 calls for:

1. Watermaster, the IEUA, the OCWD, and other stakeholders that choose to participate, to jointly fund the development of an adaptive management program to monitor Prado Basin riparian habitat extent and quality, and other factors, and to investigate and identify essential factors to the long-term sustainability of the riparian habitat.

2. Watermaster and the IEUA to convene the PBHSC, comprised of representatives from all interested parties to implement the adaptive management program.

3. The PBHSC to prepare annual reports pursuant the adaptive management program. Annual reports are to include recommendations for ongoing monitoring and any adaptive management actions required to mitigate any measured or prospective loss of riparian habitat resulting from Peace II activities.

1.4 Adaptive Management Plan for the PBHSP

Pursuant to Mitigation Measure 4.4-3 in the SEIR, Watermaster and the IEUA convened four meetings of the PBHSC, starting in late-2012, to develop the adaptive management plan for the PBHSP and facilitate its implementation. Watermaster and the IEUA adopted the final *2016 Adaptive Management Plan for the Prado Basin Habitat Sustainability Program* (AMP) in August 2016 (WEI, 2016).

The AMP is designed to answer the following questions to satisfy the monitoring and mitigation requirements of the Peace II SEIR:

1. *What are the factors that potentially can affect the extent and quality of the riparian habitat?*

2. *What is a consistent, quantifiable definition of "riparian habitat quality," including metrics and measurement criteria?*

3. *What has been the historical extent and quality of the riparian habitat in the Prado Basin?*

4. *How has the extent and quality of the riparian habitat changed during implementation of Peace II?*

5. *How have groundwater levels and quality, surface-water discharge, weather, and climate changed over time? What were the causes of the changes? And, did those changes result in an adverse impact to riparian habitat in the Prado Basin?*

6. *Are there other factors besides groundwater levels, surface-water discharge, weather, and climate that affect riparian habitat in the Prado Basin? What are those factors? And, did they (or do they) result in an adverse impact to riparian habitat in the Prado Basin?*

7. *Are the factors that result in an adverse impact to riparian habitat in the Prado Basin related to Peace II implementation?*

8. *Are there areas of prospective loss of riparian habitat that may be attributable to the Peace II Agreement?*

9. *What are the potential mitigation actions that can be implemented if Peace II implementation results in an adverse impact to the riparian habitat?*

The AMP outlines a process for monitoring, modeling, and annual reporting to answer and address the questions listed above. Appendix A to the AMP is the initial monitoring program: *2016 Monitoring Program for the Prado Basin Habitat Sustainability Program*. Annual reports are intended to document: monitoring and modeling activities, the analysis and interpretation of the monitoring and modeling results, and recommendations for changes to the PBHSP, which may include monitoring, modeling, and/or mitigation, if deemed necessary. Any future mitigation measures that are deemed necessary will be developed jointly by Watermaster and the IEUA.

1.5 Annual Report Organization

This Annual Report for water year (WY) 2017 is the second annual report prepared by Watermaster and the IEUA for the PBHSC. It documents the collection, analysis, and interpretations of the data and information generated by the PSHSP through September 30, 2017 and is organized into the following sections:

Section 1 – Introduction. This section describes the background of the PBHSP and the Annual Report.

Section 2 – Monitoring, Data Collection, and Methods. This section describes the collection of historical information and recent monitoring data, and the groundwater-modeling activities performed during WY 2017 for the PBHSP.

Section 3 – Results and Interpretations. This section describes the results and interpretations that were derived from the information, data, and groundwater-modeling.

Section 4 – Conclusions and Recommendations. This section summarizes the main conclusions derived from the PBHSP through the prior water year, and describes the recommended activities for the subsequent fiscal year as a proposed scope-of-work, schedule, and budget.

Section 5 – References. This section lists the publications cited in the report.

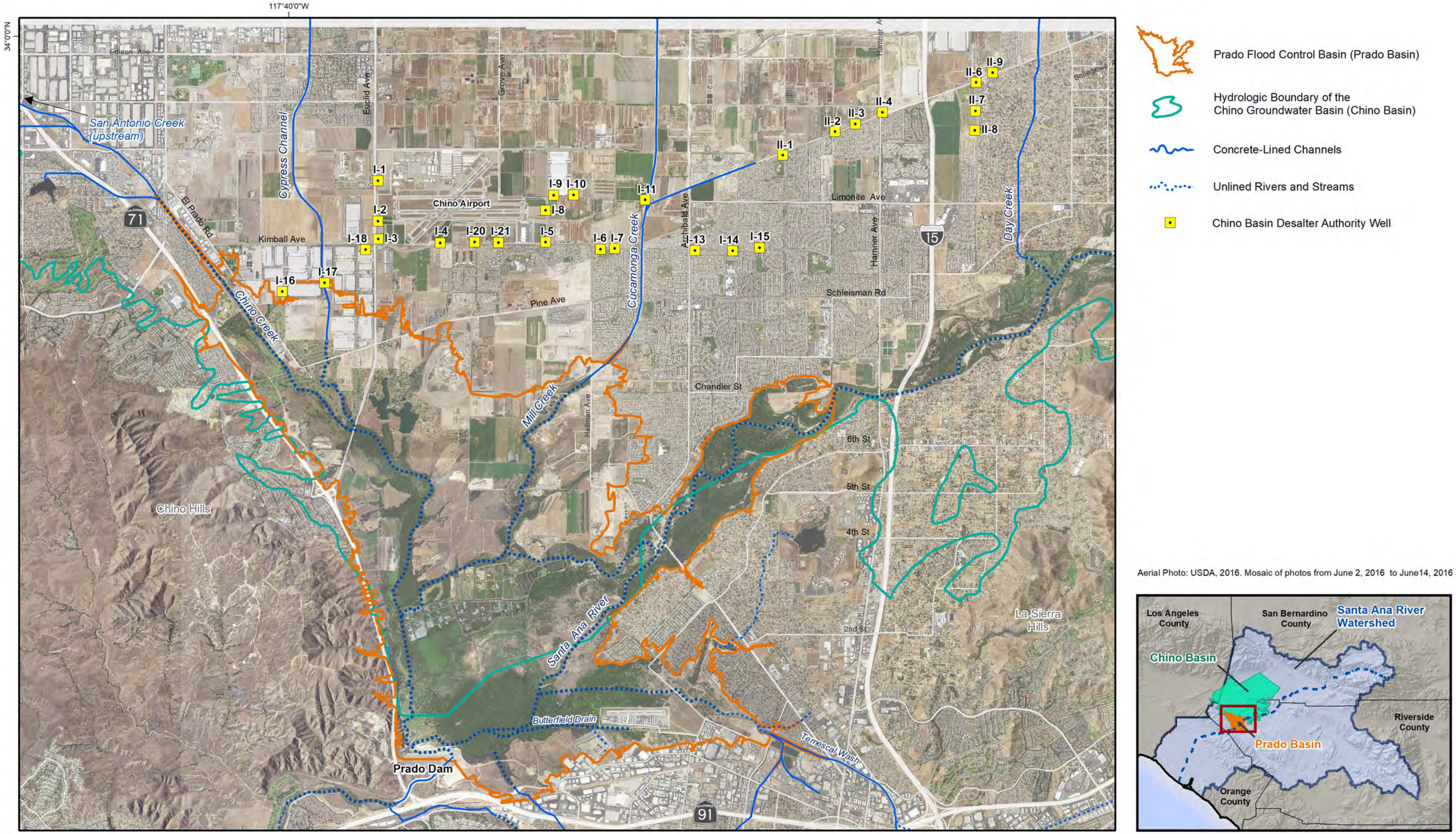

Prepared by:

WEI
Wildermuth Environmental, Inc.

Author: VMW
Date: 2/7/2018
File: 2017_Figure 1-1

2017 Annual Report

Prado Basin Habitat Sustainability Committee

Prado Basin Area

Figure 1-1

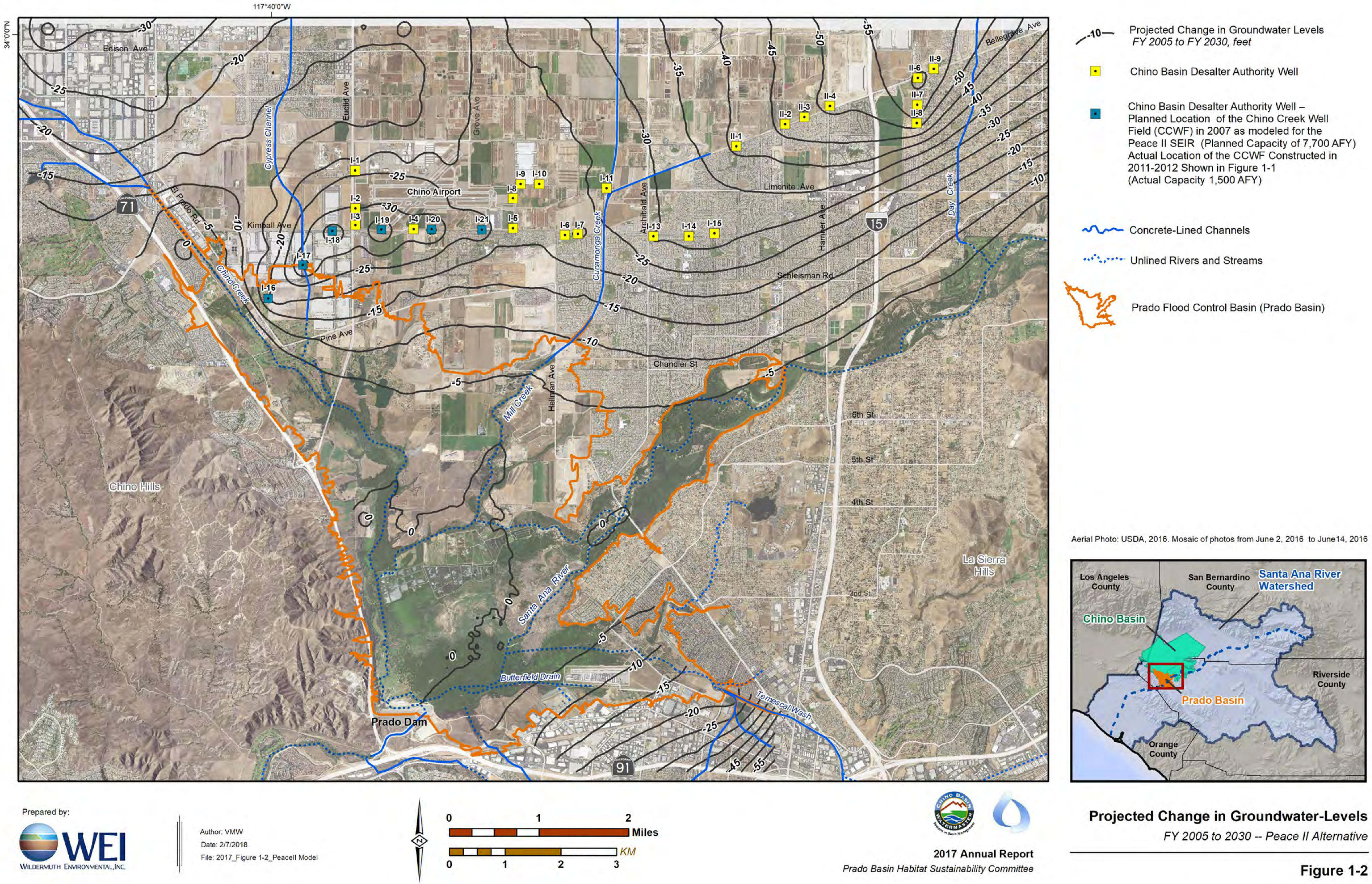

Prepared by:

WEI
WILDERMUTH ENVIRONMENTAL, INC.

Author: VMW
Date: 2/7/2018
File: 2017_Figure 1-2_PeaceII Model

2017 Annual Report
Prado Basin Habitat Sustainability Committee

Projected Change in Groundwater-Levels
FY 2005 to 2030 -- Peace II Alternative

Figure 1-2

Section 2 – Monitoring, Data Collection, and Methods

This section describes the collection of historical and recent monitoring data and the groundwater-modeling activities performed during WY 2017 for the PBHSP.

The PBHSP was designed, in part, to answer Question 1 from the AMP:

1. *What are the factors that potentially can affect the extent and quality of the riparian habitat?*

The main hydrologic factors that can potentially affect the extent and quality of the riparian habitat in Prado Basin include, but are not limited to, groundwater levels, surface-water discharge, weather events, and long-term climate. As such, the PBHSP includes an integrated monitoring and analysis programs for the riparian habitat, groundwater, surface water, and climate.

During the first year of AMP implementation in WY 2016, data collection efforts included the compilation of historical data through the present. The period of data available for each data type varies, but all span both pre- and post-Peace II implementation. Data collection efforts for WY 2017 focused primarily on recent monitoring data through the past water year. All data collected and compiled for this effort were uploaded to Watermaster's centralized relational database, HydroDaVE[SM], and used in the data analyses.

2.1 Riparian Habitat Monitoring

The objective of the Riparian Habitat Monitoring Program (RHMP) is to collect data to help answer questions 2, 3, and 4 from the AMP:

2. *What is a consistent quantifiable definition of "riparian habitat quality," including metrics and measurement criteria?*
3. *What has been the historical extent and quality of the riparian habitat in the Prado Basin?*
4. *How has the extent and quality of the riparian habitat changed during the implementation of Peace II?*

To answer these questions, the RHMP must produce a time series of data and information on the extent and quality of the riparian habitat in Prado Basin over a historical period that includes both pre- and post-Peace II implementation.

Figure 2-1 displays the features of the RHMP. Two types of monitoring and assessment are performed: regional and site-specific. Regional monitoring and assessment is appropriate because the main potential stress associated with Peace II activities is the regional drawdown of groundwater levels. The intent of the site-specific monitoring and assessment is to verify and complement the results of the regional monitoring.

2.1.1 Regional Monitoring of Riparian Habitat

Regional monitoring and assessment of the riparian habitat is performed by mapping the extent and quality of riparian habitat over time using: (i) multi-spectral remote-sensing data and (ii) air photos. Both are discussed below.

2.1.1.1 Multi-Spectral Remote Sensing Data

The Normalized Difference Vegetation Index (NDVI), derived from remote sensing measurements by Landsat Program satellites, is used to assess the extent and quality of the riparian vegetation in the Prado Basin over a long-term historical period.

This sub-section provides background information on the NDVI, explains why the NDVI was chosen as an analytical tool for the PBHSP and its advantages and limitations, and describes how NDVI estimates were compiled and used for this annual report.

Background. Multi-spectral remote-sensing measurements of the Earth's surface from satellites are a verifiable means of deriving complete spatial coverage of environmental information. Remote-sensing measurements have been collected in a consistent manner over time. They are updated regularly and can be analyzed retrospectively, which has made these measurements useful in various types of ecological and environmental monitoring, including vegetation monitoring (USDA, 1996; Schidt and Karnieli, 2000; Campbell, 2007; Lillesand et al., 2008; Xie et al., 2008; Jones and Vaughnan, 2010).

Remote sensing-based methods of vegetation monitoring commonly use vegetation indices that can be calculated from the wavelengths of light absorbed and reflected by vegetation (Jensen, 2007). The NDVI is a widely used numerical indicator of vegetation extent and quality that is calculated from remote-sensing measurements (Ke et al., 2015; Xue,J and Su, B.,2017). Moreover, the NDVI is an index of greenness correlated with photosynthesis and can be used to assess temporal and spatial changes in the distribution, productivity, and dynamics of vegetation (Pettorelli, 2013). The NDVI is calculated from the visible and near-infrared radiation reflected by vegetation using the following formula:

$$NDVI = \frac{(NIR - VIS)}{NIR + VIS}$$

Where: NIR = spectral reflectance of near infrared radiation
VIS = spectral reflectance of visible (red) radiation

Healthy vegetation during photosynthesis absorbs incoming visible light and reflects a large portion of the near-infrared radiation. Unhealthy or dormant vegetation absorbs less visible light and reflects less near-infrared radiation. The figure[3] below illustrates how the formula for NDVI works:

[3] http://earthobservatory.nasa.gov/Features/MeasuringVegetation/measuring_vegetation_2.php

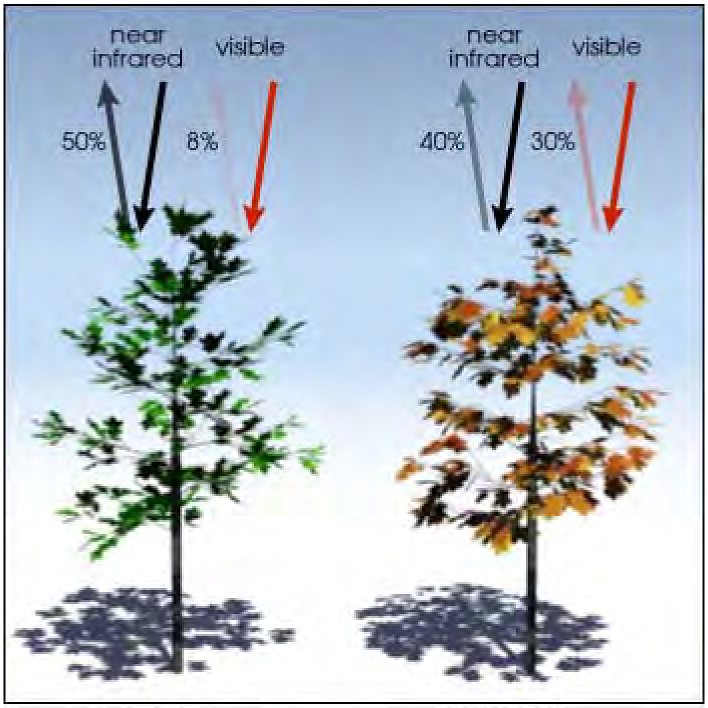

$$\frac{(0.50 - 0.08)}{(0.50 + 0.08)} = 0.72 \qquad \frac{(0.4 - 0.30)}{(0.4 + 0.30)} = 0.14$$

The near-infrared radiation and visible light spectral reflectance are both expressed as ratios of the reflected radiation over the incoming radiation (values between 0 and 1); therefore, NDVI estimates range between -1.0 and 1.0. Negative NDVI estimates correspond to standing water, and low positive values (0 to 0.1) correspond to non-vegetated areas such as barren rock and sand, snow, and water. NDVI estimates ranging from 0.1 to 1.0 correspond to vegetated areas, with very low-end estimates indicating sparse, unhealthy, or dormant vegetation, and increasing estimates towards 0.9 indicating higher amounts of dense, healthy green vegetation.

Advantages and Limitations. The NDVI was chosen as a method for characterizing and monitoring the riparian habitat for the PBHSP for the following reasons:

- Peace II activities could cause regional changes in groundwater levels, which potentially could result in regional impacts to the riparian habitat that is dependent on shallow groundwater. The regional scale of the NDVI makes it an appropriate "first indicator" of regional changes in the extent and quality of riparian vegetation. And, it has been widely used in the past to support similar environmental monitoring and management programs (Peters et al., 2002; Pinzon et al., 2004; Wang et al., 2004; Weiss et al., 2004; Intera, 2014; Verbesselt et al, 2010; Gandhi et al. 2015).

- There is a long time-series of historical NDVI (early 1980s to present) that spatially covers the entire Prado Basin. These datasets can be used to characterize the history of the spatial extent and quality of the riparian vegetation prior to and after the implementation of Peace II activities (2007).

- In the future, it is likely that multi-spectral remote sensing will include the collection of the commonly measured spectral bands that are used to calculate the NDVI (red and near-infrared) and that these data will be available for use as part of the PBHSP at low cost.

Like most monitoring tools, the NDVI has its limitations, which can reduce its reliability and usefulness. Important examples include:

- Cloud cover, water vapor, and atmospheric contaminants can lead to false decreases in NDVI estimates compared to clear days (Tanre et al., 1992; Achard and Estreguil, 1995; Chen et. al., 2004; Hird and McDermid, 2009).

- Satellite degradation, sensor errors, and data transmission errors can lead to false increases in NDVI estimates (James and Kalluri, 1994).

- Changes in soil moisture can lead to changes in NDVI estimates that are not necessarily related to changes in vegetation (Pettorelli, 2013).

- The NDVI is a composite view of plant species diversity, form, structure, density, and vigor. Therefore, changes in the NDVI may be caused by various changes in the riparian habitat (Markon et al., 1995; Markon and Peterson, 2002). In other words, the NDVI does not provide a complete picture of how and why vegetative changes are occurring; it simply indicates a change in vegetation.

- In densely vegetated areas, NDVI estimates have been shown to plateau during the growing season, which indicates that the NDVI can underestimate the green biomass in densely vegetated areas (Tucker et al., 1986).

These limitations demand that the NDVI be screened and filtered to identify or remove errors and noise in the data. To reduce or eliminate noise in the NDVI, processing algorithms can be applied to "smooth" the time-series data and reveal patterns of change over time. An example of a smoothing technique applied in this report is the averaging of all of the NDVI from the growing season months. The average values are then plotted on time-series charts to display long-term trends in growing season vegetation quality.

The limitations listed above also demand that the NDVI not be interpreted in isolation. Interpretations of the NDVI (vegetative changes) should be (i) verified with other georeferenced datasets, such as air photos and field vegetation surveys, and (ii) explained by comparison to datasets of causal factors of vegetative changes, such as water availability.

2.1.1.2 Landsat Program and NDVI

The USGS and the National Aeronautics and Space Administration (NASA) jointly manage the Landsat Program,[4] a series of Earth-observing satellite missions that began in 1972 with sensors

[4] https://landsat.gsfc.nasa.gov/about/

that observe the Earth's surface and transmit information to ground stations that receive and process multi-spectral remote-sensing data. Landsat satellites use technology that collects scenes of remote sensing measurements at the same time and location on the Earth's surface at a temporal frequency of about every two weeks. Landsat remote sensing measurements (Landsat imagery) is acquired in scenes that are approximately 106 by 115 miles. Landsat imagery is the only data source with more than thirty-years of continuous records of global land surface conditions at a spatial resolution of tens of meters (Tuck et al. 2004). Landsat imagery is among the most widely used satellite imagery in ecology and conservation studies (Pettorelli, 2013), and the data have been available for no cost since about 2010.

The United States Geological Survey (USGS), in compliance with the Global Climate Observing System,[5] produces spectral indices products from Landsat imagery to support land surface change studies, which includes the NDVI from 1982 to present (USGS, 2016). The USGS uses remote sensing imagery from the Landsat satellites—*Landsat 4, Landsat 5, Landsat 7, and Landsat 8* (*Landsat 4, 5, 7, and 8*)—to generate the NDVI estimates of the Earth's surface at a 30 x 30-meter pixel resolution. A specialized software called Landsat Ecosystem Disturbance Adaptive Processing System (LEDAPS) is used by the USGS to post-process the Landsat imagery to apply the necessary atmospheric corrections to generate a surface reflectance product (USGS 2015; 2017a). This surface reflectance product is then used to determine the NDVI among the other spectral indices post-processed by the USGS.

2.1.1.3 NDVI Methods for the PBHSP

The NDVI determined from Landsat imagery for the period 1982 to 2017 were collected from the USGS, using the Earth Resources Observation and Science (EROS) Center Science Processing Architecture (ESPA) On Demand Interface[6] (USGS 2017b). The interface requires a bulk request in the form of a text file list of specific Landsat scenes using the Landsat scene identifier ID.[7] To obtain complete spatial coverage of the Prado Basin area, the NDVI was requested for all Landsat scenes for Path 040, Rows 036 and 037.[8] The table below summarizes the Landsat satellites and the periods for which the NDVI was obtained to produce a near-continuous NDVI record from 1982 through 2017.

---

[5] http://www.wmo.int/pages/prog/gcos/

[6] https://espa.cr.usgs.gov/login?next=https%3A%2F%2Fespa.cr.usgs.gov%2F

[7] Landsat imagery is captured in scenes that are about 106 by 114 miles. Each Landsat scene has a unique scene ID based on the specific Landsat satellite, the Landsat path number, the Landsat row number, and the date the image was collected.

[8] Prado Basin is in an area of the Landsat path 040 that straddles Rows 036 and 037. Landsat scenes from Path 040 Row 036, and Path 040 Row 037 overlap each other throughout most of the Prado Basin region, but both are required to obtain complete spatial coverage of the Prado Basin.

Satellite	Instrument	Launched	Ended	Period of NDVI Data Obtained from USGS
Landsat 4	Thematic Mapper	Jul 16, 1982	Dec 14, 1993	1982 - 1983
Landsat 5	Thematic Mapper	Mar 1, 1984	Jun 5, 2013	1984 - 2011
Landsat 7	Enhanced Thematic Mapper	Apr 15, 1999	Still active	1999 - 2017
Landsat 8	Operational Land Imager	Feb 11, 2013	Still active	2013 - 2017

For this Annual Report, NDVI estimates were collected for WY 2017 and for some historical dates that were not acquired during prior efforts to collect historical NDVI. This included NDVI from *Landsat 4, 5, 7, and 8* with scenes that have cloud cover greater than 20 percent from 1982 to 2016, and all NDVI from *Landsat 7* from 1999 to 2011.

In total, NDVI from about 1,600 scenes from the *Landsat 4*, *5, 7,* and *8* satellites were obtained from the USGS for the period 1982 through 2017. The NDVI from all 1,600 Landsat scenes were cataloged, processed, and uploaded into HydroDaVE^{SM}, a database management software that manages gridded-data sets.[9] HydroDaVE^{SM} was used to compute a date-by-date stacked average for Landsat scenes from Path 040, Rows 036 and 037, where they overlap, for each NDVI pixel in a defined area.[10] The NDVI from the 1,600 Landsat scenes collected from the USGS for Path 040, Rows 036 and 037, were averaged date-by-date, resulting in about 970 individual dates with a NDVI estimates between 1982 through 2017.

The source and frequency of availability of NDVI for the 970 dates over the period of record varies:

- From 1982 to 1989, NDVI is from *Landsat 4 and 5* and is patchy, ranging from a frequency of eight days to one year.
- From 1990 to 1999, NDVI is from *Landsat 5* at a frequency of 16 days.
- From 1999 to 2012, NDVI is from *Landsat 5 and 7* at a frequency of eight days.
- From 2013 to 2017, NDVI is from *Landsat 7 and 8* at a frequency of eight days.

---

[9] http://www.hydrodave.com/company/

[10] Not all dates will have Landsat scenes for both Rows 036 and 037 if cloud cover was greater than 20 percent in one of them; Landsat scenes with a percent cloud cover greater than 20 percent were not obtained from the USGS for this study.

The spatial NDVI for the 970 dates were reviewed for disturbances that can be caused by cloud cover, unfavorable atmospheric conditions, or satellite equipment malfunction. In HydroDaVE[SM], maps were prepared of the spatial NDVI for the entire Prado Basin region for all 970 dates. The maps were reviewed and documented to identify specific dates that should not be used for analysis due to cloud cover or other disturbances. Erroneous NDVI estimates were discernable because the NDVI patterns of permanent landscape features were distorted and/or NDVI estimates were clearly not consistent with the estimates typically observed for a particular area both seasonally and over time. About 201 dates with NDVI from the *Landsat 4, 5, 7, and 8* satellites (21 percent) were identified as erroneous and excluded from the analysis. Most of the dates were rejected because of cloud coverage in the Prado Basin region, which was further ground by referencing the specific Landsat scene on the USGS EarthExplorer website.[11] After reviewing for these disturbances, NDVI estimates for 769 dates out of the original 970 dates from *Landsat 4, 5, 7, and 8* satellites remained for analysis of the historical period. This includes only one date for 1982, and no dates for 1983.

Of the 769 dates with NDVI estimates available for analysis, 307 of them were derived from *Landsat 7* satellite imagery from 1999 to 2017. The NDVI estimates for these 307 dates had to be further reviewed date-by-date for the occurrence of spatial data gaps, resulting from the failure of the Scan Line Corrector (SLC) on the *Landsat 7* satellite, which accounts for the satellite's forward motion. SLC failure results in data gaps along scan line paths of variable widths and occurrences. An estimated 22 percent of any given *Landsat 7* scene is lost because of SLC failure; however, the imagery acquired between these gaps is valid and useable for analysis.[12] All NDVI estimates derived from the *Landsat 7* satellite imagery from 1999 to 2017 for the 307 dates were evaluated spatially date-by-date to determine if the valid data covers the areas of interest used for the analysis of NDVI temporally in the time series discussed in Section 3 of this report. Date-by-date analysis is necessary because the spatial position and size of the data gaps varies for each date. Generally, areas of interest for NDVI analysis that are larger than about 400 square meters could not use any NDVI determined from the *Landsat 7* satellite imagery because it would include a data gap area; while areas of interest less than 400 square meters could use about 70 percent of the NDVI from the *Landsat 7* satellite imagery.

In addition to determining a stacked average for each NDVI pixel for Landsat scenes that overlap, HydroDaVE[SM] contains features to average and extract a date-by-date spatial average NDVI for a designated area and time period. The NDVI spatial average data can be plotted in time-series charts to analyze seasonal and temporal changes for a defined area.

When viewing time-series charts of NDVI for the period of record, it should be noted that differences between the technology of the *Landsat 4, 5, and 7* satellites, and the *Landsat 8* satellite is a methodological factor that can affect the observed NDVI trends. The *Landsat 4, 5, and 7* satellites use thematic mapper technology to scan the land surface, whereas *Landsat 8* uses operational land imager sensors. It has been well documented that the NDVI estimates obtained

---

[11] https://earthexplorer.usgs.gov/

[12] https://landsat.usgs.gov/slc-products-background

from the operational land imager sensors used on the *Landsat 8* satellite generates slightly higher index values for vegetated land cover (Xu and Guo 2014; She et al., 2015). The *Landsat 8* satellite was launched in orbit in 2013, and ever since, the NDVI is available from both *Landsat 7 and 8* satellites. In order to analyze time-series of NDVI derived across all Landsat satellites for the period of record, a bias-correction factor of +0.05 that was derived from a literature review (Li et al., 2014; Flood, 2014: and Ke et al., 2015) and was used to transform all *Landsat 8* NDVI estimates so that all historical NDVI estimates could be analyzed collectively (Roy et al., 2016). Time-series charts of NDVI for various areas in the Prado Basin are first introduced in Section 3.1 of this report.

2.1.1.4 Collection and Analysis of Air Photos

Georeferenced air photos are used to visually characterize the spatial extent of the riparian habitat in Prado Basin over the historical period. The air photos also serve as an independent check on interpretations from the analysis of NDVI, which involves visually comparing the extent and density of the riparian habitat as shown in the air photos to NDVI maps. Table 2-1 summarizes the air photos that have been compiled and analyzed for the Prado Basin region. In total, fifty-eight air photos were collected for the period 1938-2017. For some years, there are more than one air photo. The air photos vary in scale, coverage, and quality.

For the first annual report, all available historical air photos for the Prado Basin area were compiled, cataloged, and georeferenced for the historical period of 1938-2016. These air photos were collected from: USGS Earth Explorer, the United States Department of Agriculture (USDA) Aerial Photography Field Office, Eagle Aerial Solutions, the University of California Santa Barbara (UCSB) Aerial Imagery Research Service, the United State Bureau of Reclamation (USBR), and the archives of the IEUA, the OCWD, Watermaster, and WEI.

The acquisition of the 2017 air photo included a custom flight that was performed by Eagle Aerial Solutions on July 3, 2017 which produced a high-resolution (3-inch resolution) image of the visible spectrum for the entire Prado Basin. The cost to acquire the 2017 air photo was shared with the OCWD.

2.1.2 Site-Specific Monitoring of Riparian Habitat

The objective of the site-specific monitoring of riparian habitat is to collect data that can be used to ground-truth the interpretations derived from the regional monitoring and assessment of the riparian habitat. The NDVI from remote sensing measurements should be integrated with georeferenced field observations for validation (Pettorelli, 2013). Site-specific monitoring performed in the Prado Basin prior to the implementation of the AMP included vegetation surveys performed by the USBR in 2007 and 2013 (USBR, 2008b; 2015) and seasonal ground-based photo monitoring performed by the OCWD since 2010 (OCWD, 2015; Harvey, 2015). In 2016, the USBR performed vegetation surveys at 38 sites: 24 previously established USBR sites and 14 new sites primarily located near the PBHSP monitoring wells. Details of the 2016 USBR surveys are described in the *2015/16 Annual Report for the PBHSC* (WEI, 2017) and the USBR's 2016 vegetation survey report (USBR, 2017). Figure 2-1 shows the locations of the USBR vegetation surveys and the OCWD photo-monitoring stations.

In WY 2017, research was performed to refine the site-specific monitoring program to employ methods favorable for validation of the NDVI values. Results of this research are discussed in Appendix A.

2.2 Factors that Potentially Affect the Riparian Habitat

The main factors that can potentially affect riparian habitat in Prado Basin include, but are not limited to: groundwater levels, surface-water discharge, and climate. This section describes the methods employed to collect and analyze information on these factors to help answer the questions 5, 6, and 7 from the AMP:

5. *How have groundwater levels and quality, surface-water discharge, weather, and climate changed over time? What were the causes of the changes? And, did those changes result in an adverse impact to riparian habitat in the Prado Basin?*

6. *Are there other factors besides groundwater levels, surface-water discharge, weather, and climate that affect riparian habitat in the Prado Basin? What are those factors? And, did they (or do they) result in an adverse impact to riparian habitat in the Prado Basin?*

7. *Are the factors that result in an adverse impact to riparian habitat in the Prado Basin related to Peace II implementation?*

2.2.1 Groundwater Monitoring Program

A primary result of implementation of the Peace II Agreement is the lowering of groundwater levels (drawdown) in the southern portion of Chino Basin. Hence, drawdown is a factor that is potentially related to Peace II implementation and could adversely impact the riparian habitat.

The Groundwater Monitoring Program (GMP) includes the collection of three types of data: groundwater production, groundwater level, and groundwater quality. Watermaster has been implementing a groundwater monitoring program across the entire Chino Basin to support various basin management initiatives and activities, and all data within Watermaster's centralized relational database are available to the GMP.

Watermaster's groundwater monitoring network was expanded in 2015 specifically for the PBHSP with the construction of 16 new piezometers at nine sites located along the fringes of the riparian habitat, between the riparian habitat and the CDA well field. These wells, along with two existing monitoring wells, HCMP-5/1 and RP2-MW3, are specifically monitored for the PBHSP and are called the "PBHSP monitoring wells."

Figure 2-2 shows the extent of the study area for which the GMP data are compiled and used for the PBHSP. The area covers Prado Basin and the upgradient areas to the north that encompass the CDA well field. Figure 2-2 also shows the wells in the study area where groundwater data was available in WY 2017.

2.2.1.1 Groundwater Production

Groundwater production strongly influences groundwater levels and groundwater-flow patterns. Groundwater-production data are analyzed together with groundwater-level data to characterize the influence of groundwater production on the extent and quality of riparian habitat. Groundwater-production data are also used as an input to the Chino Basin groundwater-flow model to evaluate past and future conditions in the Chino Basin, which, for the PBHSP, supports the analysis of prospective losses of riparian habitat (see Section 2.3).

Watermaster collects quarterly groundwater-production data for all active production wells within the Chino Basin. The data are checked for quality assurance and quality control (QA/QC) and uploaded to Watermaster's centralized relational database. The active production wells within the study area include CDA wells and privately-owned wells used for agricultural, dairy, or domestic purposes.

During WY 2017, Watermaster collected groundwater-production data at about 119 wells in the GMP study area.

2.2.1.2 Groundwater Level

Monitoring groundwater levels in the Prado Basin is a key component of the PBHSP: the potential for declining groundwater levels related to Peace II implementation could be a factor that adversely impacts riparian habitat. Groundwater-level data are analyzed together with production data to characterize how groundwater levels have changed over time in the GMP study area and to explore the relationship(s) to any observed changes that occurred in the extent and quality of the riparian habitat. Groundwater-level and production data are also used as input to the Chino Basin groundwater flow model to evaluate past and future conditions in the Chino Basin, which, for the PBHSP, supports the analysis of prospective losses of riparian habitat (see Section 2.3).

Watermaster collects groundwater-level data at various frequencies at wells in the GMP study area to support a variety of groundwater management initiatives. The data are checked for QA/QC and uploaded to Watermaster's centralized relational database.

During WY 2017, Watermaster collected groundwater-level data at 209 wells in the study area (see Figure 2-2). At 96 of these wells, water levels were measured by the well owners at varying frequencies and provided to Watermaster. The remaining 113 wells are CDA wells, dedicated monitoring wells, or private wells that are monitored by Watermaster using manual methods once per month or with pressure transducers that record water levels once every 15 minutes. Groundwater-levels at the 18 PBHSP monitoring wells have been measured manually and with pressure transducers since May 2015.

2.2.1.3 Groundwater Quality

Water-quality data can be used to understand the relative sources of groundwater in the Prado Basin. For the PBHSP, groundwater-quality data are compared to surface-water-quality data to characterize groundwater and surface-water interactions in the Prado Basin and assess the importance of those interactions to the extent and quality of the riparian habitat.

Watermaster collects groundwater-quality data from wells in the GMP study area to support a variety of groundwater management initiatives. These data are checked for QA/QC and uploaded to Watermaster's centralized relational database.

During WY 2017, groundwater-quality data were collected from 160 wells in the study area (see Figure 2-2). Of these wells, 101 were sampled by the well owners at varying frequencies. The remaining 59 wells are dedicated monitoring wells or private wells sampled by Watermaster either quarterly, annually, or triennially (every three years). The PBHSP monitoring wells were sampled quarterly during water year 2016/17 (December 2016, March 2017, June 2017, September 2017) and analyzed for the parameters listed in Table 2-2. The WY 2017 quarterly groundwater-quality sampling occurred during.

2.2.2 Surface-Water Monitoring Program

Surface-water discharge in the Prado Basin is another factor that can influence the extent and quality of riparian habitat and can influence groundwater levels. Surface-water discharge data are evaluated for the PBHSP to characterize historical and current trends in the discharge of the SAR and its tributaries in the Prado Basin and to explore the relationship(s) to any observed changes that occurred in the extent and quality of the riparian habitat. Surface-water discharge data are also used as input to the Chino Basin groundwater-flow model to evaluate past and future conditions in the Chino Basin, which, for the PBHSP, supports the analysis of prospective losses of riparian habitat (see Section 2.3). And, as noted in Section 2.2.1.3, surface-water quality is compared to groundwater-quality data to characterize groundwater and surface-water interactions in the Prado Basin and the importance of those interactions to the extent and quality of the riparian habitat.

The surface-water monitoring program for the PBHSP involves collecting existing, publicly available, surface-water discharge and quality data from sites within or tributary to the Prado Basin. Figure 2-3 shows the location of the surface-water monitoring sites used in the PBHSP. These sites include publicly-owned treatment works (POTWs) discharge locations, USGS stream gaging stations, Watermaster and IEUA Maximum-Benefit Monitoring Program surface-water-quality monitoring sites, and the OCWD's discharge of untreated imported water from OC-59 turnout tributary to Prado Basin.

Surface-water discharge and quality data are collected annually for these sites. All surface-water discharge and quality data were collected and compiled, checked for QA/QC, and uploaded to Watermaster's relational database.

2.2.3 Climatic Monitoring Program

Climatic data are used to characterize how the climate has changed over time in the study area and to explore the relationship(s) to any observed changes that occurred in the extent and quality of the riparian habitat. Climatic data is also used for the Chino Basin groundwater-flow model to evaluate past and future conditions in the Chino Basin, which, for the PBHSP, supports the analysis of prospective losses of riparian habitat (see Section 2.3).

The climatic monitoring program for the PBHSP involves collecting existing, publicly-available precipitation, temperature, evaporation, and potential evapotranspiration data in the vicinity of the Prado Basin. Figure 2-3 shows the location of the stations where data are available and collected for the PBHSP. These sites include monitoring stations for the California Irrigation Management Information System (CIMIS) for potential evapotranspiration data, the Los Angeles County Department of Public Works pan evaporation station, and the spatially gridded climate datasets from Next-Generation Radar (NEXRAD) and the PRISM Climate Group for regional precipitation and temperature data. The Chino Basin boundary was used to extract the spatially-gridded data for precipitation, and the Prado Basin boundary was used to extract the spatially-gridded data for maximum and minimum temperature. Climatic data are collected annually and uploaded to Watermaster's relational database.

2.2.4 Other Factors That Can Affect Riparian Habitat

The AMP recognizes that there are potential factors other than groundwater, surface water, and climate that can affect the riparian habitat in the Prado Basin. These factors include, but are not limited to: fire, disease, pests, and invasive species. To the extent necessary, data and information on these factors are collected and analyzed to explore for relationships to changes in the extent and quality of the riparian habitat.

During WY 2016, two specific factors were identified as potential impacts to the Prado Basin riparian habitat: wildfires and an invasive pest known as the Polyphagous Shot-Hole Borer - *Euwallacea fornicates* (PSHB). Data was collected for these two factors in WY 2016 and updated in WY 2017. The following describes the information that was collected for these two factors and how they are used to explore for relationships to changes that have occurred in the extent and quality of the riparian habitat.

2.2.4.1 Wildfires

Wildfires occur periodically in the Prado Basin and can reduce the extent and quality of the riparian habitat. For the PBHSP, the occurrence and location of wildfires are used to corroborate trends observed in riparian vegetation extent and health based on the analysis of NDVI.

To map wildfires, fire-perimeter data were collected from the Fire and Resource Assessment Program (FRAP) of the California Department of Forestry and Fire Protection (CAL FIRE) for 1950-2016.[13] CAL FIRE, the USDA Forest Service Region 5 Remote Sensing Lab, the Bureau of Land Management (BLM), and the National Parks Service (NPS) jointly developed a GIS database of the fire perimeters for the State of California.[14] The methods to compile the data varied over time: data from 1950 to 2001 include CAL FIRE fires ≥300 acres and US Forest Service (USFS) fires ≥10 acres; data from 2002 to 2016 include BLM and the NPS fires ≥10 acres, and CAL FIRE expanded criteria to include timber fires ≥10 acres, brush fires ≥50

[13] Data for 2017 will not be available until April 2018, past the period of data collection and analysis for this annual report for water year 2016/2017.

[14] http://frap.fire.ca.gov/projects/fire_data/fire_perimeters_index

acres, and wildland fires that destroyed three or more structures or caused $300,000 or more in damage.

The FRAP database is the most complete digital record of fire perimeters in the State; however, it is still incomplete in many aspects: fires may be missing altogether because historical records were lost or damaged, fires were too small for the minimum cutoffs, documentation was inadequate, or fires have not yet been incorporated into the database. Currently, wildfire data is uploaded to the database annually during the month of April for the previous year.

2.2.4.2 Polyphagous Shot-Hole Borer (PSHB)

The PSHB is a recently identified pest within the Prado Basin and has the potential to negatively impact the riparian habitat vegetation (USBR, 2016; Palenscar, K., verbal communication, 2016; McPherson, D., verbal communication, 2016). For the PBHSP, the occurrence of PSHB in the Prado Basin is used to corroborate trends observed in riparian vegetation extent and health based on the analysis of the NDVI time series

The PSHB is a beetle that burrows into trees, introducing a fungus (*Fusarium euwallacea*) into the tree bark, which spreads the disease Fusarium Dieback (FD).[15,16] FD destroys the food and water conducting systems of the tree, eventually causing stress and tree mortality. The PSHB was first discovered in Southern California in 2003 and has been recorded to have caused branch die-back and tree mortality for various tree specimens throughout the Southern California region (USDA, 2013). OCWD biologists in the Prado Basin have been working with the University of California at Riverside, the United States Fish and Wildlife Service (USFWS), and the Santa Ana Watershed Association to actively monitor the occurrence and impact of PSHB within Prado Basin riparian habitat (Zembal, R., personal communication, 2017); to date, no reports have been prepared by the agencies.

Information on PSHB occurrence in the Prado Basin was obtained from the University of California, Department of Agriculture and Natural Resources' online PBHB/FD Distribution Map[17] for 2016 and 2017, from the USBR vegetation surveys of Prado Basin riparian habitat performed in 2016, and from the OCWD's PSHB trap deployment and monitoring from 2016 to 2017.

2.3 Prospective Loss of Riparian Habitat

Monitoring and mitigation requirement 4.4-3 in the Peace II SEIR calls for annual reporting for the PBHSP:

> *Annual reports will be prepared and will include recommendations for ongoing monitoring and any adaptive management actions required to mitigate any measured loss or* ***prospective loss*** *of riparian habitat that may be attributable to the Peace II Agreement (emphasis added).*

---

[15] http://ucanr.edu/sites/pshb/

[16] http://cisr.ucr.edu/polyphagous_shot_hole_borer.html

[17] http://ucanr.edu/sites/pshb/Map/

The meaning of "prospective loss" in this context is "future potential loss" of riparian habitat. Predictive modeling of groundwater levels can be used to answer question 8 from the AMP:

8. *Are there areas of prospective loss of riparian habitat that may be attributable to the Peace II Agreement?*

Watermaster's most recent groundwater-modeling results can be used to evaluate forecasted groundwater-level changes within the Prado Basin under current and projected future conditions in the Basin, including, but not limited to, plans for pumping, storm-water recharge, and supplemental-water recharge. To perform this evaluation, the predictive model results are mapped and analyzed to identify areas (if any) where groundwater levels are projected to decline to depths that may negatively impact riparian habitat in the Prado Basin.

For this annual report, Watermaster's most recent groundwater model projections for Scenario 1A using the 2017 Chino Basin groundwater-flow model (WEI, to be published in 2018), were used to characterize past and future groundwater-level conditions in the Prado Basin study area.

Table 2-1
Summary of Collected Historical Air Photos for the Prado Basin Region

Year	Source	Date	Percent Coverage of the Prado Basin	Resolution (meters)	Quality	Georeferenced	Comments
1938	UCSB	5/27/1938 to 10/17/1938	100%	1.2	Good	no	Scanned black and white photo.
1946	USGS	12/29/1946	75%	0.7	Good	yes	Scanned black and white photo. The image borders need to be cropped.
1948	USGS	7/10/1948 to 7/20 1948	100%	0.5	Good	yes	Scanned black and white photo. Some image borders need to be cropped.
1952	USGS	6/30/1952	100%	0.8	Good	yes	Scanned black and white photo. The image borders need to be cropped.
1953	UCSB	9/22/1953 to 2/16/1954	100%	1	Very Good	no	Scanned black and white photo.
1959	UCSB	9/5/1959 to 11/6/1959	100%		Okay	no	Scanned black and white photo.
1959	USDA	10/15/1959 to 11/6/1959	100%	0.3	Very Good	no	Scanned black and white photo.
1960	UCSB	6/27/1960 to 7/13/1960	100%	0.6	Good	yes	Scanned black and white photo.
1960	Watermaster	2/9/1960	100%		Okay	yes	Scanned black and white photo.
1962	UCSB	1/30/1962	100%		Poor	no	Scanned black and white photo.
1965	UCSB	3/3/1965	100%		Good	yes	Scanned black and white photo.
1966	USGS	4/16/1966	100%	0.7	Okay	yes	Scanned black and white photo. Some image borders need to be cropped.
1967	UCSB	5/15/1967	100%		Good	no	Scanned black and white photo.
1968	UCSB	9/23/1968	100%		Good	no	Scanned black and white photo.
1973	UCSB	1/20/1973 to 1/23/1973	100%	1.1	Okay	yes	Scanned black and white photo.
1974	WEI	8/27/1974	100%	3.2	Good	yes	Scanned Colored photo.
1974	USGS	11/6/1974 to 9/18/1975	100%	7	Okay	yes	Scanned black and white photo.
1977	UCSB	2/1/1977	100%	1.1	Good	yes	Scanned black and white photo.
1977	WEI	11/2/1977	80%	3.1	Okay	yes	Scanned Colored photo.
1980	USGS	11/21/1980 to 12/24/1980	100%	2.1	Okay	yes	Scanned black and white photo.
1980	WEI	11/12/1980 to 12/24/1980	100%		Okay	no	Scanned black and white photo.
1980	UCSB		100%		Okay	no	Scanned black and white photo.
1984	WEI	2/12/1984	50%	1.2	Okay	no	Scanned Colored photo.
1985	USGS	9/13/1985	100%	5	Okay	yes	Scanned infared photo.
1985	USDA	7/28/1985	100%	0.7	Good	yes	Scanned infared photo.
1990	USGS		100%	3.5	Okay	yes	Scanned infared photo.
1990	UCSB	5/21/1990 to 5/22/1990	100%		Good	no	Scanned black and white photo.
1994	WEI	6/1/1994	100%	1	Okay	yes	Scanned black and white photo. A black line runs through the photo center.
1994	USGS	6/1/1994	100%	2.8	Okay	yes	Scanned black and white photo.
1994	USDA	6/1/1994	100%	0.5	Good	no	Scanned black and white photo. Some image borders need to be cropped.

Table 2-1
Summary of Collected Historical Air Photos for the Prado Basin Region

Year	Source	Date	Percent Coverage of the Prado Basin	Resolution (meters)	Quality	Georeferenced	Comments
1999	UCSB	1/14/1999	100%	1.8	Good	yes	Digital Colored photo.
2001	Eagle Aerial		100%	1	Good	yes	Digital Colored photo.
2002	Watermaster		100%	0.6	Very Good	yes	Digital Colored photo.
2003	Watermaster		100%	0.6	Very Good	yes	Digital Colored photo.
2003	USBR	12/2/2003	80%	0.2	Excellent	yes	Digital Colored photo.
2004	IEUA		100%	0.6	Very Good	yes	Digital Colored photo.
2005	Watermaster		100%	0.3	Very Good	yes	Digital Colored photo.
2005	IEUA		100%	0.3	Excellent	yes	Digital Colored photo.
2006	Watermaster		100%	0.3	Very Good	yes	Digital Colored photo.
2006	IEUA		100%	0.3	Excellent	yes	Digital Colored photo.
2007	Watermaster		100%	0.3	Very Good	yes	Digital Colored photo.
2007	IEUA		100%	0.3	Excellent	yes	Digital Colored photo.
2008	Watermaster		100%	0.3	Very Good	yes	Digital Colored photo.
2008	IEUA		100%	0.3	Good	yes	Digital Colored photo.
2009	Watermaster		100%	0.3	Very Good	yes	Digital Colored photo.
2009	OCWD	4/21/2009 to 5/8/2009	100%	0.1	Excellent	yes	Digital Colored photo.
2009	OCWD	1/26/2009 to 3/25/2009	100%	0.3	Excellent	yes	Digital Colored photo.
2010	Watermaster		100%	0.3	Very Good	yes	Digital Colored photo.
2010	IEUA		100%	0.3	Good	yes	Digital Colored photo.
2012	Watermaster		100%	1	Very Good	yes	Digital Colored photo.
2012	IEUA	1/28/2012 to 3/14/2012	100%		Very Good	no	Digital Colored photo.
2012	OCWD		100%	0.3	Very Good	yes	Digital Colored photo.
2012	OCWD		100%	0.1	Very Good	yes	Digital Colored photo.
2014	USDA	April and May 2014	100%	1	Good	yes	Digital Colored photo.
2014	OCWD	6/5/2014 to 6/6/2014	100%	0.1	Excellent	yes	Digital Colored photo.
2015	IEUA	5/11/2015	100%	0.1	Excellent	yes	Digital Colored photo.
2016	USDA	5/3/2016 to 6/14/2016	100%	0.6	Good	yes	Digital Colored photo.
2017	Eagle Aerial Custom Flight	7/3/2017	100%	0.08	Excellent	yes	Digital Colored photo.

Table 2-2
Parameter List for the Groundwater-Quality Monitoring Program

Analyte	Method
Alkalinity in CaCO3 units	SM2320B
Ammonia Nitrogen	EPA 350.1
Bicarbonate as HCO3 *Calculated*	SM2320B
Boron Total ICAP	EPA 200.7
Calcium Total ICAP	EPA 200.7
Carbonate as CO3 *Calculated*	SM2320B
Chloride	EPA 300.0
Flouride	SM 4500-C
Hydroxide as OH *Calculated*	SM2320B
Kjeldahl Nitrogen	EPA 351.2
Magnesium Total ICAP	EPA 200.7
Nitrate as Nitrogen by IC	EPA 300.0
Nitrate as NO3 *Calculated*	EPA 300.0
Nitrite as Nitrogen by IC	EPA 300.0
Organic Nitrogen *Calculated*	EPA 351.2
PH (H3=past HT not compliant)	SM4500-HB
Potassium Total ICAP	EPA 200.7
Sodium Total ICAP	EPA 200.7
Specific Conductance, 25 C	SM2510B
Sulfate	EPA 300.0
Silica	EPA 200.7
Total Dissolved Solids (TDS)	E160.1/SM2540C
Total Hardness as CaCO3 by ICP *Calculated*	SM 2340B
Total Organic Carbon	SM5310C/E415.3
Turbidity	EPA 180.1

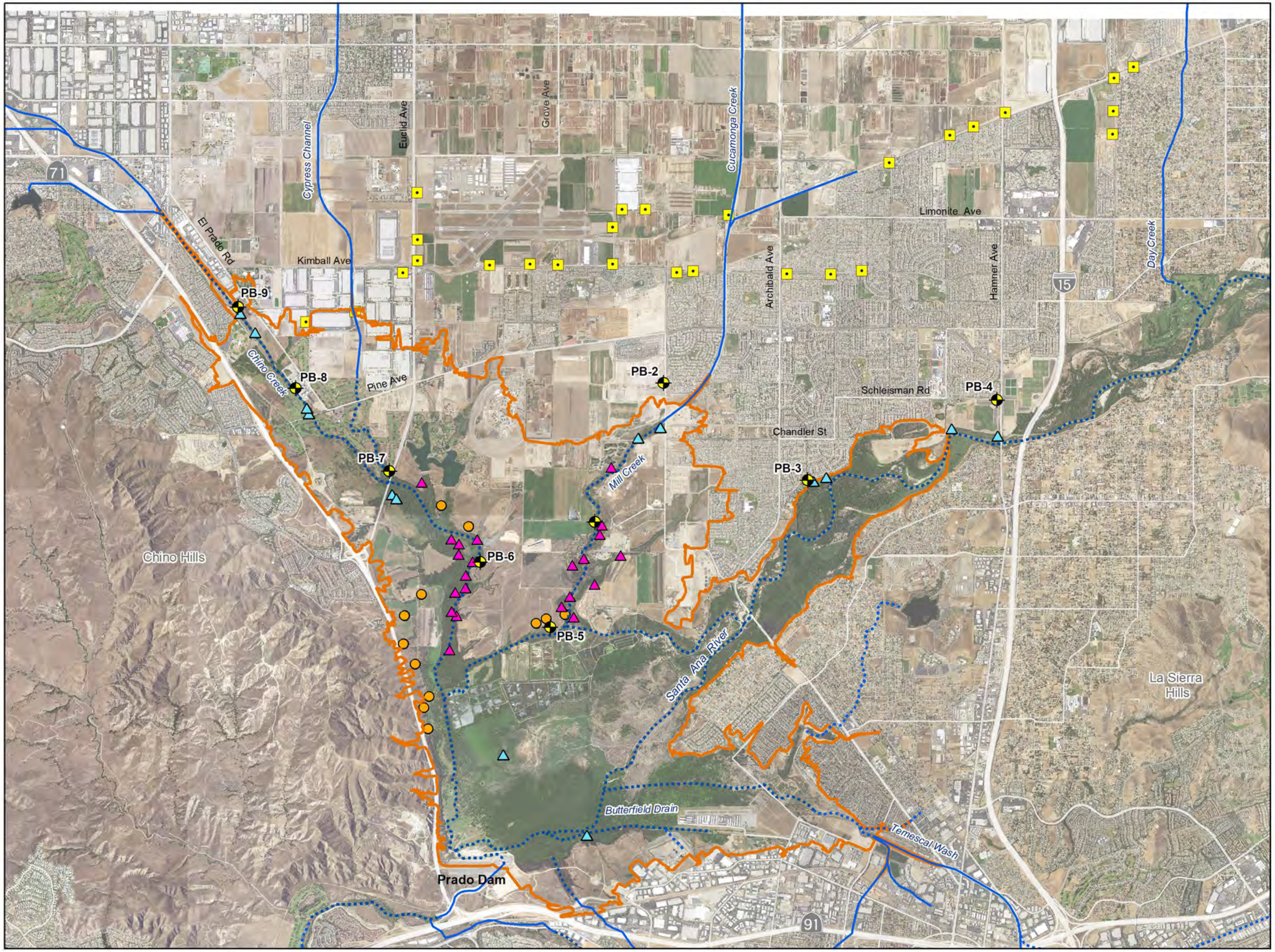

Riparian Habitata Monitoring Program

Site-Specific Monitoring

- USBR Vegetation Surveys 2007, 2013, and 2016
- USBR Vegetation Surveys 2016
- OCWD Photo Stations (2010 - 2016)

Regional Monitoring

- Prado Flood Control Basin (Prado Basin) - Area of Interest for Analysis of NDVI and Air Photos.
- Chino Basin Desalter Authority Well
- PBHSP Monitoring Well
- Concrete-Lined Channels
- Unlined Rivers and Streams

Aerial Photo: USDA, 2016. Mosaic of photos from June 2, 2016 to June14, 2016

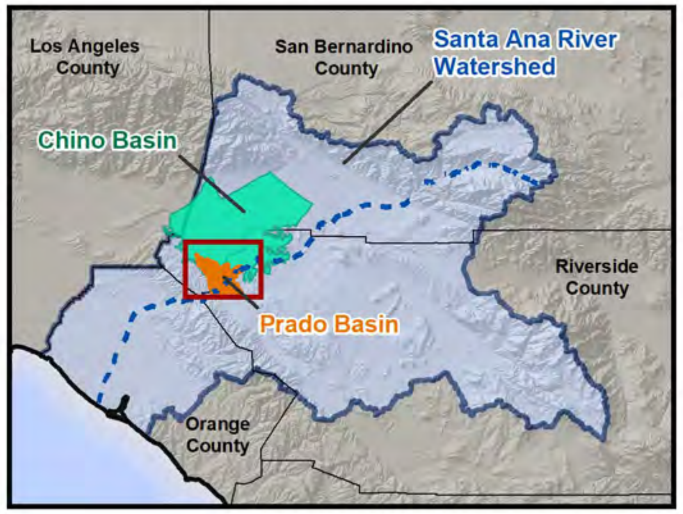

Prepared by:

WEI
WILDERMUTH ENVIRONMENTAL, INC.

Author: VMW
Date: 2/12/2018
File: 2017_Figure 2-1 Veg Monitoring

N

0 1 2 Miles

0 1 2 3 KM

2017 Annual Report

Prado Basin Habitat Sustainability Committee

Riparian Habitat Monitoring Program

Figure 2-1

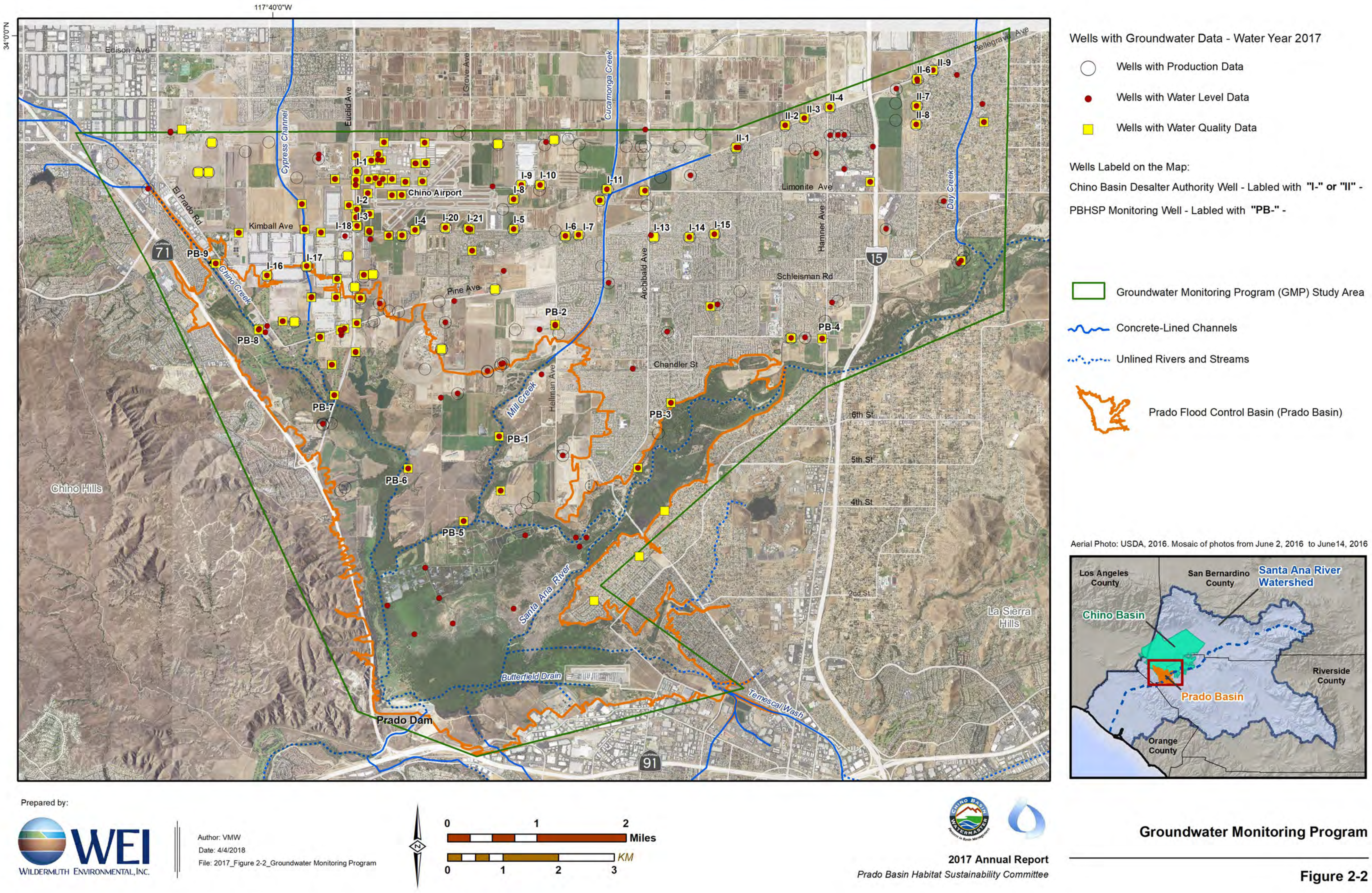

Prepared by:

WEI
Wildermuth Environmental, Inc.

Author: VMW
Date: 4/4/2018
File: 2017_Figure 2-2_Groundwater Monitoring Program

2017 Annual Report
Prado Basin Habitat Sustainability Committee

Groundwater Monitoring Program

Figure 2-2

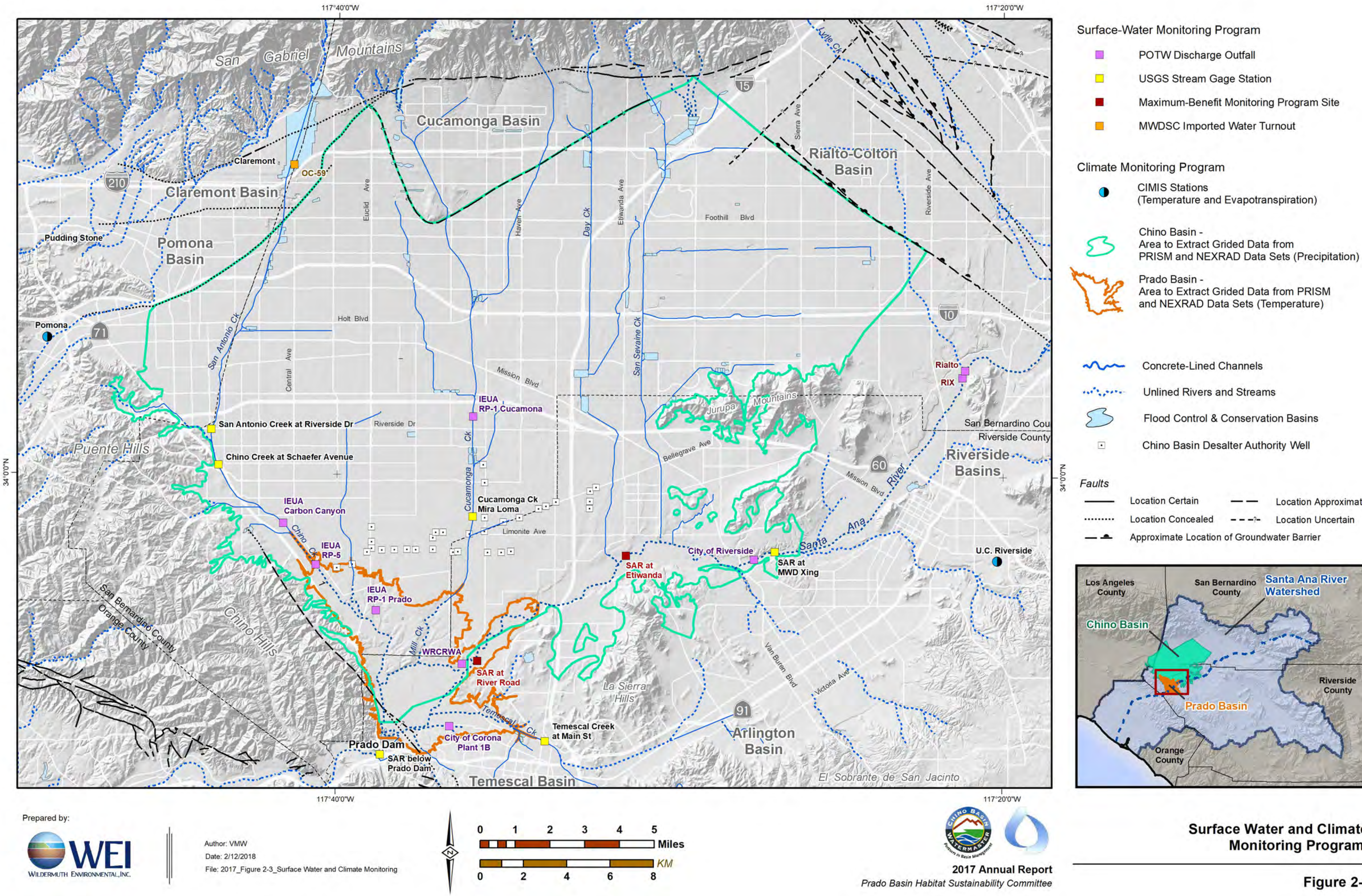

Prepared by:

WEI
Wildermuth Environmental, Inc.

Author: VMW
Date: 2/12/2018
File: 2017_Figure 2-3_Surface Water and Climate Monitoring

2017 Annual Report
Prado Basin Habitat Sustainability Committee

Surface Water and Climate Monitoring Programs

Figure 2-3

Section 3 – Results and Interpretations

This section describes the analysis and interpretation of the monitoring data and groundwater-modeling results for the PBHSP. The data analyzed span various historical periods, based on data availability, and include periods both pre- and post-Peace II implementation (2007).

The primary intent of this section is to identify trends in the extent and quality of riparian habitat and the factors that can impact the riparian habitat, and to understand cause-and-effect relationships, particularly cause-and-effect relationships that may be associated with Peace II implementation. This section begins with the analysis of trends in the extent and quality of the riparian habitat, and then describes the factors that could have potentially impacted the extent and quality of the riparian habitat, including changes in groundwater levels, surface-water discharge, climate, and other factors, such as pests and wildfires. Declining groundwater levels is the primary factor that is potentially related to Peace II implementation and could adversely impact the riparian habitat. This section also includes a review of the most recent results of Watermaster's predictive groundwater modeling of the Chino Basin to identify areas of future drawdown that could lead to prospective loss of riparian habitat.

3.1 Trends in Riparian Habitat Extent and Quality

The regional assessment of riparian habitat in the Prado Basin includes the analysis of air photos and NDVI to characterize trends in the extent and quality of the riparian habitat over time. The regional assessment techniques are two independent methods that are analyzed comparatively to complement and corroborate each other. The site-specific monitoring of riparian habitat in the field is used to ground truth the regional monitoring and assessment.

3.1.1 Extent of the Riparian Habitat

Figure 3-1a shows a times series of historical air photos compiled and digitized for the first annual report for 1960, 1977, 1985, 1999, 2006, and 2016 (WEI, 2017). The figure illustrates the changes in the extent and vegetated density of the riparian habitat in the Prado Basin from 1960 to 2016. From the 1930s to about 1960, large areas of the Prado Basin were managed to minimize the growth of riparian vegetation and its associated consumptive use of water in an effort to maximize flow in the SAR (Woodside, G., personal communication). In general, from 1960 to 1999, the mapped extent of the riparian habitat increased from about 1.8 to 6.7 square miles, and its vegetated density increased. Since 1999, the extent and vegetated density of the riparian habitat has remained relatively constant.

Figure 3-1b compares the 2016 and 2017 air photos that were acquired for the PBHSP. The air photo resolution increased from 2016 (60-cenimeter pixels) to 2017 (3-inch pixels), which enhanced the ability to map the extent and visually assess the riparian habitat. The mapped extent of the riparian habitat decreased by 0.01 squares miles from 2016 to 2017. This decrease is attributed the enhanced ability to digitize the extent of the riparian habitat with the higher-resolution 2017 air photo, and thus does not indicate an actual change in extent.

Figure 3-1c compares the 2017 air photo and the mapped extent of the riparian habitat to the NDVI estimates for the Prado Basin area on a date that corresponds to the maximum of the spatial average of NDVI during the growing season for 2017.[18] The same air-photo/NDVI comparison figures were prepared and analyzed in the first annual report for 1985, 1999, 2006, and 2016 (WEI, 2017). Four main observations and interpretations are derived from these figures:

1. Generally, the following ranges in NDVI during the growing season correspond to these land cover types:

NDVI	Land Cover During Growing Season
< 0	Water
0 - 0.2	Non-vegetated surfaces, such as urbanized land cover and barren land.
0.3 - 1.0	Vegetated land cover – the higher NDVI values indicate greater photosynthetic activity of the vegetation

2. Prado Basin riparian vegetation areas have NDVI estimates of about 0.4 to 0.9 during the growing season. Active agricultural lands in the Prado Basin region can also have NDVI values of about 0.3 to 0.7 during the growing season.
3. The NDVI estimates support the delineation of the extent of the riparian habitat as drawn from the air photos.
4. The processing and georeferencing of air photos and NDVI for this study were performed accurately, which supports subsequent analyses and interpretations.

3.1.2 Quality of the Riparian Habitat

As discussed and referenced in Section 2, the NDVI is a measure of the photosynthetic activity of vegetation and therefore can be used as an indicator of the health or "quality" of the riparian vegetation. In this section, the NDVI is spatially and temporally analyzed in maps and time-series charts for defined areas throughout Prado Basin to characterize changes in the quality of riparian habitat for the period 1984 to 2017. The defined areas of NDVI analyses are shown in Figure 3-2. These defined areas include: the entire 2017 extent of the riparian habitat which is about 6.8 square miles (19,520 30 x 30-meter NDVI pixels); one area in the lower Prado Basin, which is about 0.26 square miles (650 30 x 30-meter NDVI pixels); and multiple areas primarily located along the northern reaches of the riparian habitat in Prado Basin near the PBHSP monitoring wells—these areas are 6,500 square-meters (four 30 x 30-meter NDVI pixels).

Figure 3-3 compares the maps of NDVI across the entire Prado Basin area for 2016 and 2017 on the dates that correspond to the maximum of the spatial average NDVI for extent of the riparian vegetation in Prado Basin during the growing season. This figure is used to identify

[18] The growing season for the Prado Basin riparian vegetation in is from March through October (Merkel, 2007; USBR, 2008).

any areas of significant change in NDVI that may indicate a recent change in the quality of the riparian habitat.

Figures 3-4, 3-5, and 3-6a through 3-6k are time-series charts of the NDVI for each of the defined areas. These figures are used to identify trends in NDVI in specific areas that may indicate changes in the quality of the riparian habitat. There are three time-series curves shown on each chart that illustrate trends in the NDVI estimates:

1. The spatial average of the NDVI pixels within the defined area of analysis. This characterizes the seasonal and long-term trends in NDVI for the area. The NDVI time-series are typical for a deciduous forest, meaning that NDVI is higher in the growing season assumed to run from March through October, and lower in the dormant season running from November through February when plants shed their leaves and become dormant.
2. The annual average of the spatial average of the NDVI estimates for the growing season period of March through October ('average growing-season NDVI'). This curve shows the annual changes and long-term trends in the NDVI for growing-season. This metric is used to analyze the year-to-year and long-term trends in this annual report.
3. The annual maximum of the spatial average of NDVI estimates for the growing season period of March through October ('maximum growing-season NDVI'). This curve shows the trend in the annual maximum NDVI estimates. Maximum growing-season NDVI typically occurs during the summer months. This metric is used to analyze the year-to-year and long-term trends in this annual report.

NDVI maps and air photos are included on the time-series charts for spatial reference and as a visual check on the interpretations derived from the time-series charts. The air photos used on the figures include 1999, 2006, 2016, and 2017— showing pre- and post-Peace II Agreement periods and the last two years.

To statistically characterize the long-term trends in the NDVI time-series for each area in Figures 3-4, 3-5, and 3-6a through 3-6k, a Mann-Kendall trend test was performed on the average growing-season NDVI for the entire period of record from 1984 to 2017. The Mann-Kendall trend test is used to statistically analyze if there is a monotonic increasing or decreasing trend in data that does not have a normal distribution. Appendix B describes the Mann-Kendall test method and the test results. The final Mann-Kendall test result of the average growing-season NDVI ('increasing trend', 'decreasing trend', or 'no trend') is shown on each figure.

The following table summarizes the Mann-Kendall test result for each area, and the short-term variability for the average growing-season NDVI over the period of record (1984-2017) and recently (2015-2017):

Defined Area	Figure Number	Short-Term Changes from 1984 - 2015			Recent Short-Term Changes from 2015 - 2017			Long-Term Trend in NDVI 1984-2017 [1]
		Average Annual Change in NDVI	Largest Annual Increase in NDVI	Largest Annual Decrease in NDVI	2015 - 2016	2016 - 2017	2015 - 2017	
2017 Rip Veg Extent	3-4	0.02	0.06	-0.07	-0.02	0.02	0.00	No Trend
Lower Prado	3-5	0.03	0.10	-0.09	-0.01	0.00	-0.01	Increasing
CC-1	3-6a	0.03	0.09	-0.06	-0.03	-0.03	-0.05	Increasing
CC-2	3-6b	0.03	0.07	0.07	-0.01	-0.01	-0.02	Increasing
CC-3	3-6c	0.03	0.14	-0.08	-0.03	-0.01	-0.04	Increasing
CC-4	3-6d	0.04	0.10	0.12	-0.01	-0.03	-0.04	Increasing
MC-1	3-6e	0.03	0.08	-0.10	-0.06	-0.01	-0.07	Increasing
MC-2	3-6f	0.04	0.16	-0.18	-0.02	-0.04	-0.06	No Trend
MC-3	3-6g	0.04	0.13	-0.12	0.00	-0.05	0.05	No Trend
MC-4	3-6h	0.04	0.11	-0.10	-0.02	-0.03	-0.05	Increasing
SAR-1	3-6i	0.05	0.11	-0.21	-0.01	-0.21	-0.23	Increasing
SAR-2	3-6j	0.03	0.08	-0.11	0.00	0.08	0.08	Increasing
SAR-3	3-6k	0.03	0.09	-0.11	-0.02	0.00	-0.02	Increasing

1 -- See Appendix B for a description of the Mann-Kendall test.

3.1.2.1 Analysis of Prado Basin Riparian Habitat in Aggregate

Visual inspection of Figure 3-3 indicates:

1. Little to no change in NDVI across most of the extent of the riparian habitat from 2016 to 2017.
2. In the southeastern portion of lower Prado Basin, within an area that was burned by wildfire in 2015, the NDVI increased from 2016 to 2017, which indicates that the riparian vegetation is recovering in this area.

Figure 3-4 is a time-series chart from 1984-2017 of the spatial average of all 19,520 NDVI pixels that are within the 2017 extent of the riparian habitat in the Prado Basin. The intent of the chart is to characterize the trend in the NDVI for the Prado Basin as a whole. The trend is used as a basis of comparison to the trends in the NDVI for each of the smaller defined areas shown in subsequent figures. Figure 3-4 also includes NDVI maps for a year from each decade to visually compare the spatial NDVI to the NDVI time-series.

Figure 3-4 shows that average growing-season NDVI vary from year-to-year by no more than 0.07 and show no apparent long-term trend. The Mann-Kendall test result indicates that from 1984 to present there is no trend in the average growing-season NDVI. From 2016 to 2017 the average growing-season NDVI increased by about 0.02. These long-term trends in NDVI suggest that, the riparian habitat in Prado Basin analyzed as a whole, has not degraded since 1984.

3.1.2.2 Analysis of the Riparian Habitat in Lower Prado Basin

Figure 3-5 is a time-series chart from 1984-2017 of the spatial average of 650 NDVI pixels within a defined area in the southern portion of the Prado Basin (Lower Prado). The intent of the chart is to characterize NDVI trends in an area of the Prado Basin that is not expected to be impacted by the drawdown associated with Peace II implementation based on projections of groundwater levels from groundwater modeling. This analysis is used as a basis of comparison to trends in NDVI for each of the smaller defined areas located further to the north along Chino Creek, Mill Creek, and the SAR.

Figure 3-5 includes a series of air photos for spatial reference and as a visual check on the interpretations derived from the NDVI time-series charts. The air photos are for 1999, 2006, 2016 and 2017—showing periods of both pre-Peace and Peace II Agreements implementation, and the last two years.

Figure 3-5 shows that the maximum growing-season NDVI vary from year-to-year by no more than 0.1 and show no long-term declining trend. The Mann-Kendall test result indicates that from 1984 to 2017 there is an increasing trend in the average growing-season NDVI. From 2016 to 2017 the average growing-season NDVI shows no trend. These trends in the NDVI suggest that the riparian habitat in Lower Prado has not degraded since 1984.

3.1.2.3 Analysis of the Riparian Habitat along Chino Creek, Mill Creek, and the Santa Ana River

Figures 3-6a through 3-6k are time-series charts from 1984-2017 of the spatial average of four NDVI pixels for areas located along Chino Creek, Mill Creek, and the SAR. The intent of these charts is to characterize NDVI trends in smaller areas primarily located along the northern stream reaches of the riparian habitat in the Prado Basin—areas that are most susceptible to potential impacts from declining groundwater levels associated with Peace II implementation. These areas are located near the PBHSP monitoring well sites to facilitate the comparison of NDVI to shallow groundwater levels.

Figures 3-6a through 3-6k also include a series of air photos for spatial reference and as a visual check on the interpretations derived from the NDVI time-series charts. The air photos are for 1999[19], 2006, 2016 and 2017—showing periods of both pre-Peace and Peace II Agreements implementation, and the last two years.

[19] Figures 3-6i shows the 1994 air photo instead of the 1999 air photo.

Chino Creek **(Figures 3-6a to 3-6d)**. Four areas were analyzed along Chino Creek: CC-1, CC-2, CC-3, and CC-4 (see locations on Figure 3-2). These areas were selected to characterize NDVI trends in vegetated areas in the Prado Basin located just southwest of the CDA well field.

These figures show that the average growing-season NDVI vary by no more than 0.14 from year-to-year in all four areas and show no long-term declining trend along the entire reach of Chino Creek. The Mann-Kendall test results indicate that from 1984 to 2017 there is an 'increasing trend' in the average growing-season NDVI at all four areas.

From 2015 to 2017, the average growing-season NDVI decreased in all four areas. However, these two-year declines in NDVI are no more than 0.05, which is within the range of the long-term, year-to-year variability in these NDVI statistics. Visual inspection of the air photos on these figures do not show evidence of degradation of the riparian vegetation.

***Mill Creek*.** **(Figures 3-6e to 3-6h).** Four areas were analyzed along Mill Creek: MC-1, MC-2, MC-3, and MC-4 (see locations on Figure 3-2). These sites were selected to characterize NDVI trends in vegetated areas in the Prado Basin located just south of the CDA well field.

These figures show that the average growing-season NDVI vary by no more than 0.18 from year-to-year at all four areas, and that the long-term average growing-season NDVI show no declining trend along the entire reach of Mill Creek. The Mann-Kendall test results indicate that from 1984 to 2017 there is an 'increasing trend' in the average growing-season NDVI for the northern and southern most areas (MC-1 and MC-4), and 'no trend' for the two areas along the middle portion of Mill Creek (MC-2 and MC-3).

From 2015 to 2017, the average growing-season NDVI increased at MC-3 along the middle portion of Mill Creek and decreased at the three other areas (MC-1, MC-2, and MC-4) along the upper and lower portion on Mill Creek. These two-year declines in the NDVI are no more than 0.07, which is within the range of the long-term, year-to-year variability in these NDVI statistics. In addition, visual inspection of the air photos on these figures do not show evidence of degradation of the riparian vegetation.

Santa Ana River **(Figures 3-6i to 3-6k).** Three areas were analyzed along the floodplain of the Santa Ana River: SAR-1, SAR-2, and SAR-3 (see locations on Figure 3-2). These areas were selected to characterize NDVI trends in the Prado Basin located south of the CDA well field along the SAR.

These figures show that the average growing-season NDVI vary by no more than 0.21 from year-to-year at all three areas, and that the long-term average growing-season NDVI show no long-term declining trend along the entire reach of the SAR. The Mann-Kendall test results indicate that from 1984 to 2017 there is an 'increasing trend' in the average growing-season NDVI at all three areas.

From 2015 to 2017 the average growing-season NDVI increased by about .08 at SAR-2 and remained stable at SAR-3. From 2015 to 2017, the average growing-season NDVI decreased at SAR-1 by about 0.23, with most of the decrease occurring from 2016 to 2017 (0.21 decrease). Inspection of the air photos in Figure 3-6i (for SAR-1) confirm an isolated area of brown color throughout most of the area which contrasts with green colors in the prior 2016 air photo, indicating some degradation in the vegetation. This level of a decrease in the NDVI has occurred previously in this area in the early 1990s, followed by a gradual increase. Inspection of the air photo for 1994 in Figure 3-6i indicates that the meandering SAR channel was the likely cause of that NDVI decrease in the early 1990s.

3.1.2.4 Analysis of Trends in Riparian Habitat

Figures 3-7a through 3-7d are bar charts that further characterize long-term trends in the growing-season NDVI for the 13 defined areas shown on Figures 3-4, 3-5, and 3-6a through 3-6k. The bar charts show the annual departure of the average growing-season NDVI from the mean of the average growing-season NDVI for the 22-year period of 1984 to 2006 (referred to herein as 'NDVI baseline'). This 22-year period for the NDVI baseline was chosen because it is prior to implementation of the Peace II Agreement in 2007.

The bar charts demonstrate the magnitude and duration of the negative (decreasing) or positive (increasing) departure from the NDVI baseline. Included for reference with the bar charts are the time series of spatial average NDVI for the area being analyzed, the corresponding average growing-season NDVI, and the NDVI baseline. Also included on these figures are the results from the Mann-Kendall trend test of the average growing-season NDVI over the 1984-2017 period.

Figure 3-7a characterizes trends in the average growing-season NDVI compared to the NDVI baseline for the entire 2017 extent of riparian vegetation in Prado Basin. The bar chart demonstrates no increasing or decreasing trend for the growing-season NDVI which agrees with the Mann-Kendall test result of no trend. The majority of the annual departures of the average growing-season NDVI from the NDVI baseline are positive after the NDVI baseline period, indicating an increasing trend since 2007.

Figure 3-7b characterizes trends in the average growing-season NDVI compared to the NDVI baseline for the four areas along Chino Creek. The bar charts demonstrate an increasing trend in growing-season NDVI at all four areas which agrees with the Mann-Kendall test results of increasing trend' At all four areas the majority the annual departures of the average growing-season NDVI from the NDVI baseline are positive after the NDVI baseline period, indicating an increasing trend since 2007. This increasing trend is more prominent at the two areas along the northern reach of Chino Creek (CC-1 and CC-2).

Figure 3-7c characterizes trends in the average growing-season NDVI compared to the NDVI baseline for the four areas along Mill Creek. The bar charts demonstrate an increasing trend in growing-season NDVI at the northern most and southern most areas along Mill Creek (MC-1 and MC-4) which agrees with the Mann-Kendall test results of increasing trend. Additionally, these areas, the majority of the annual departures of the average growing-season NDVI from the NDVI baseline are positive after the NDVI baseline period, indicating an increasing trend since 2007. The bar charts demonstrate no trend in growing-season NDVI for the two areas along the middle portion of Mill Creek (MC-2 and MC-3) which agrees with the Mann-Kendall test results of no trend. However, all the average growing-season NDVI from the NDVI baseline are positive after 2009, indicating and increasing trend since then.

Figure 3-7d characterizes trends in the average growing-season NDVI compared to the NDVI baseline for the three areas along the SAR and the Lower Prado area. The bar charts demonstrate an increasing trend in growing-season NDVI at all four areas which agrees with the Mann-Kendall test results of increasing trend. The majority of the annual departures of the average growing-season NDVI from the NDVI baseline are positive after the NDVI baseline period, indicating an increasing trend since 2007.

3.1.3 Analysis of Vegetation Surveys

Vegetation field surveys were not performed for the PBHSP in 2017. Vegetation surveys are performed for the PBHSP once every three years. The most recent vegetation surveys were performed in 2016 by the USBR and were a continuation and expansion of the surveys performed in 2007 and 2013.

Table 3-1 summarizes the measured and calculated parameters for all areas surveyed in 2007, 2013, and 2016. The percent canopy cover measurements from the USBR vegetation surveys are the most appropriate information for ground-truthing the NDVI data. Where and when available, the average percent canopy cover for surveyed areas near the areas of NDVI analysis in Figures 3-6a through 3-6k are shown with the NDVI time-series data for comparison. Canopy cover is a measurement of the percentage of the ground surface area that is directly covered by the vertical projections of tree crowns (USDA, 1999). Although there is no direct quantitative relationship between percent canopy cover and NDVI, canopy cover is a metric of the areal density of the vegetation that is reflecting the visible and near-infrared light and, therefore can be used to validate field conditions to correlate with the NDVI analysis. Where percent canopy cover measurements are available for more than one year, they typically show stable or increasing trends, consistent with increasing trends in NDVI since 2007. Table 3-2 shows that overall, the percent canopy cover for all surveyed areas each year has increased—the average for percent canopy cover at all areas surveyed in 2007, 2013, and 2016 were 75%, 76%, and 86%, respectively.

3.1.4 Summary

This assessment of the riparian habitat in Prado Basin, through the analysis of historical air photos shows that the riparian habitat has increased in its extent since the 1960s.

The quality of riparian habitat, as characterized by the time series of average-growing season NDVI at the defined areas, shows no trend in degradation from 1984 to 2017, and may have improved since the implementation of the Peace II Agreement. For some areas, the average-growing season NDVI decreased during 2015 to 2017 period. These two-year declines in the NDVI are within the range of the long-term annual variability in these NDVI statistics. Continued monitoring and more information is required to determine if and how the riparian vegetation is changing in these specific areas. Strategies for continued monitoring and acquiring more information are described in Section 4.

The remainder of Section 3 describes the factors that can affect the riparian habitat, how these factors have changed over time, and compares trends in the NDVI to trends in these factors to explore cause-and-effect relationships.

3.2 Groundwater and Its Relationship to Riparian Habitat

The implementation of the Peace II Agreement was projected to change patterns of groundwater production and reduce artificial recharge through 2030, both of which change groundwater levels in the Chino Basin. Changes in groundwater levels caused by the implementation of the Peace II Agreement and other water management activities unrelated to Peace II[20] have the potential to impact the extent and quality of riparian habitat in the Prado Basin.

This section characterizes the history of groundwater production and the groundwater-level responses in the GMP study area in the southern Chino Basin and compares these trends to trends in the extent and quality of the riparian habitat.

3.2.1 Groundwater Production

Table 3-2 lists the annual estimates of groundwater production within the GMP study area for WY 1961 to 2017.[21] From the execution of the Judgment to the Peace Agreement (WY 1979 to 2000), groundwater production from this area occurred mainly from agricultural wells and averaged about 41,700 AFY. During the post-Peace Agreement period (WY 2001 to 2017), agricultural groundwater production progressively declined and by WY 2017 was about 6,000 AFY; CDA production commenced and increased to replace the declining agricultural groundwater production—as envisioned in the OBMP/Peace Agreement and Peace II Agreement—and by WY 2017 was about 28,200 AFY. Total groundwater production from the study area during WY 2001-2017 averaged about 35,500 AFY.

Figures 3-8a through 3-8c illustrate the spatial distribution of groundwater production within the GMP study area over the period of WY 1978 to 2017 and the extent of the riparian habitat. Each figure includes: a map that illustrates the spatial distribution and magnitude of production at wells for a single year based on the Watermaster's production records for WY 1978 (commencement of the Judgment), 1999 (commencement of the OBMP) and 2017 (current conditions); a bar chart of annual groundwater production in the GMP study area for WY 1961 through 2017[22]; an air photo for that period; and the extent of the riparian vegetation based on the air photo.

---

[20] Other water management activities unrelated to Peace II Agreement implementation include changes in wastewater discharge to the SAR due to conservation, recycling, and drought response; increases in storm water diverted and recharged; increases in recycled water recharge; and the implementation of the dry-year yield program with Metropolitan Water District of Southern California.

[21] Production for years prior to WY 2001 were estimated in the calibration of the 2013 Chino Basin groundwater model (WEI, 2015). Production estimates for WY 2001 and thereafter are based on metered production data and water-duty estimates compiled by the Watermaster.

[22] Ibid

***WY 1978* (*Figure 3-8a*).** Groundwater production was about 47,000 AF and occurred at wells distributed throughout the GMP study area that were mostly private domestic and agricultural wells. The extent of the riparian vegetation in Prado Basin at this time was about 2,780 acres.

***WY 1999* (*Figure 3-8b*).** Groundwater production was about 24,000 AF—50 percent less than WY 1978. The production occurred at wells distributed throughout the GMP study area that were mostly private domestic and agricultural wells for dairies. Production decreased primarily due to land use conversions from agricultural to urban uses. The extent of the riparian vegetation in the Prado Basin area expanded to about 4,280 acres—a 54 percent increase from 1978.

WY 2017 (Figure 3-8c). Groundwater production was about 34,000 AF—28 percent less than WY 1978 and 40 percent greater than 1999. The production occurred primarily at CDA wells located in the northern portion of the GMP study area. Even though total production from this area has increased since 1999, the domestic and agricultural production for dairies continued to decline and by WY 2017 was about 6,000 AFY. As articulated in the OBMP and subsequent Peace Agreements, CDA production was planned to replace the declining domestic and agricultural production. CDA production began in WY 2001 at about 9,000 AFY from 11 wells and increased to about 28,000 AFY from 26 wells by WY 2017. The extent of riparian vegetation in the Prado Basin was about 4,350 acres—a two percent increase from 1999.

3.2.2 Groundwater Levels

Figures 3-9a and 3-9b are groundwater-elevation contour maps of the GMP study area for the shallow aquifer system in September 2016 (prior year's annual report condition) and September 2017 (current condition).[23] The contours were drawn based on measured groundwater elevations at wells. These contours were used to create rasterized surfaces of groundwater elevation for September 2016 and September 2017. The raster for September 2016 was subtracted from the raster for September 2017 to create a raster of change in groundwater elevation over the past year and is shown on Figure 3-10. Groundwater levels changed by up to +/- five feet across the GMP study area and within the 2017 extent of the riparian habitat in the Prado Basin. Along Chino Creek, groundwater levels increased by up to five feet along its northern reach near well PB-8 and decreased by one to five feet along its southern reach. Along Mill Creek, groundwater levels slightly increased or remained the same. Along most of the SAR, groundwater levels generally remained unchanged since the prior year.

The raster of groundwater elevation for September 2017 was subtracted from a 1-meter horizontal resolution digital elevation model of the ground surface (Associated Engineers, 2007) to create a raster of depth-to-groundwater in September 2017 and is shown in Figure 3-11. The outline of the 2017 extent of the riparian habitat in the Prado Basin is superimposed on the raster of depth-to-groundwater in 2017. With the exception of the Temescal Wash area, the

[23] Historical groundwater-elevation data in Prado Basin are scarce due to a lack of wells and/or monitoring. Therefore, discussion and interpretation of measured depth-to-groundwater is focused on last year's condition and current condition.

riparian habitat overlies areas where the depth-to-groundwater is less than 15 feet below the ground surface.

Figures 3-12a through 3-12c are time-series charts that compare long-term trends in groundwater production and groundwater elevations to the NDVI for three areas in the Prado Basin: Chino Creek, Mill Creek, and the SAR. These figures show the average growing-season NDVI for the 12 defined areas of riparian habitat discussed in Section 3.1 and shown in Figures 3-5 and 3-6a through 3-6k.

The groundwater-elevation estimates for the period 1960 to 2011 were extracted from Watermaster's most recent calibration of its groundwater-flow model at monitoring well locations (WEI, 2015). The more recent groundwater-elevation data shown on these charts were measured at monitoring wells that were constructed by Watermaster and IEUA to support the Hydraulic Control Monitoring Program (HCMP) (beginning in 2005) and the PBHSP (beginning in 2015). Where the measured and model-estimated groundwater elevations overlap in time, the model-estimated elevations mimic the seasonal fluctuations and the longer-term trends of the measured elevations, and the model-estimated elevations are typically no more than 10 feet different than the measured elevations.

Chino Creek (Figure 3-12a). The upper chart on Figure 3-12a compares changes in groundwater-levels along Chino Creek to long-term trends in groundwater production within the study area. In the long-term, groundwater levels appear to have changed only slightly in response to the long-term changes in groundwater production—typically by less than +/- five feet. The chart shows that groundwater levels have remained steady since 1961 despite the decline in groundwater production that started in late 1980s and continued until 2000, when the CDA began production, and have remained relatively stable through WY 2017.

Groundwater-level monitoring at the PBHSP monitoring wells along Chino Creek indicates that groundwater levels fluctuate each year, in some cases by more than 15 feet, under the seasonal stresses of production and recharge. During the winter months of WY 2017, groundwater levels at the PBHSP monitoring wells increased to their highest recorded levels, likely in response to the recharge of stormwater discharge in unlined creeks and the associated surface-water reservoir that ponds behind Prado Dam. From September 2015 to September 2017, groundwater levels increased by up to one foot along the north portion of Chino Creek (PB-9/1, RP2-MW3, and PB-8), and decreased by up to one foot along the southern portion of Chino Creek (PB-7/1 and PB-6/1).

The lower chart on Figure 3-12a shows the time series of the average growing-season NDVI from 1984 to present for the four areas along Chino Creek. The NDVI estimates show a long-term increasing trend from 1984 to 2017 indicating an improvement in the quality of the riparian vegetation, while shallow groundwater levels along Chino Creek remained relatively stable. From 2015 to 2017, NDVI decreased at all four areas along Chino Creek. These decreases in NDVI are within the historical range of annual and short-term variability of NDVI at these areas and therefore do not necessarily represent a degradation of the riparian habitat. In addition, the analysis of air photos does not illustrate signs of degradation of the riparian habitat (see Section 3.1). Declines in groundwater levels are not a likely the cause of the recent declines in NDVI considering that the declines in groundwater levels, if any, are less than one foot and appear to be within the historical range of short-term variability.

Mill Creek*. *(Figure 3-12b). The upper chart on Figure 3-12b compares changes in groundwater-levels along Mill Creek to long-term trends in groundwater production within the study area. In the long-term, groundwater levels appear to respond to the long-term changes in groundwater production —typically by less than +/- 10 feet. These responses were greatest along the northern portion of Mill Creek near the MC-1 area (at the HCMP-5 and PB-2 wells) where groundwater levels declined by about 10 feet when groundwater production increased to its maximum in 1986, increased by a similar amount when production decreased to its minimum in 1998, and declined again by a similar amount after CDA production began in 2000. Downstream from the MC-1 area, groundwater levels along Mill Creek have remained relatively stable from 1961 through WY 2017.

Groundwater-level monitoring at the PBHSP monitoring wells along Mill Creek indicates that groundwater levels fluctuate each year, in some cases by more than 10 feet, under the seasonal stresses of production and recharge. During the winter months of WY 2017, groundwater levels at the PBHSP monitoring wells increased to their highest recorded levels, likely in response to the recharge of stormwater discharge in unlined creeks and the associated surface-water reservoir that ponds behind Prado Dam. From September 2015 to September 2017, groundwater levels at the monitoring wells along Mill Creek increased by up to two feet.

The lower chart on Figure 3-12b shows the time series of the average growing-season NDVI from 1984 to present for the four areas along Mill Creek. There is a long-term increasing trend in average growing-season NDVI at the northern and southern areas along Mill Creek (MC-1 and MC-4) and no long-term trend in the average growing-season NDVI along the middle reach of Mill Creek (MC-2 and MC-3). From 1984 to 2017, groundwater levels along the northern reach of Mill Creek increased and decreased by up to 10 feet and remained relatively stable along the southern reach. There does not appear to be a clear relationship between the long-term changes in groundwater levels and the NDVI. From 2015 to 2017, NDVI decreased at three of four areas along Mill Creek. These decreases in NDVI are within the historical range of annual and short-term variability of NDVI at these areas and therefore do not necessarily represent a degradation of the riparian habitat. In addition, the analysis of air photos does not illustrate signs of degradation of the riparian habitat (see Section 3.1). Changes in groundwater levels are not a likely the cause of the recent declines in NDVI given that groundwater levels increased by up to one foot along Mill Creek.

Santa Ana River (***Figure 3-12c***). The upper chart on Figure 3-12c compares changes in groundwater-levels along the SAR to long-term trends in groundwater production within the study area. In the long-term, groundwater levels appear to respond to changes in groundwater production—typically by less than +/- 10 feet. These responses are greatest along the northern portion of the SAR near the SAR-1 area (PB-4 well) where groundwater levels declined by about 10 feet when groundwater production increased to its maximum in 1986, increased by a similar amount when production decreased to its minimum in 1998, and declined again by a similar amount after CDA production began in 2000. Downstream from the SAR-1 area, groundwater levels along the SAR have remained relatively stable from 1961 through WY 2017.

Groundwater-level monitoring at the PBHSP monitoring wells along the SAR indicates that groundwater levels fluctuate each year by up to three feet, under the seasonal stresses of production and recharge. During the winter months of WY 2017, groundwater levels at the PBHSP monitoring wells increased to their highest recorded levels, likely in response to the recharge of stormwater discharge in the SAR and the associated surface-water reservoir that ponds behind Prado Dam. From September 2015 to September 2017, groundwater levels at the monitoring wells along the SAR increased by up to one feet.

The lower chart on Figure 3-12c shows the time series of the average growing-season NDVI from 1984 to present for four areas along the SAR. There is a long-term increasing trend in the average growing-season NDVI from 1984 to 2017 at all four areas along the SAR indicating an improvement in the quality of the riparian vegetation. From 1984 to 2017, groundwater levels along the northern upstream reach of the SAR increased and decreased by up to 10 feet, and along the southern downstream portion groundwater levels gradually increased. There is no clear relationship between the long-term changes in groundwater levels and the NDVI. From 2015 to 2017, NDVI remained relatively stable along the SAR except for a decrease of 0.21 at SAR-1 from 2016 to 2017. Analysis of the 2017 air photo indicates that the decrease in NDVI at SAR-1 from 2016 to 2017 is due to a change in the riparian vegetation at SAR-1 (see Section 3.1). During this time groundwater levels increased by up to one foot along the SAR near SAR-1.

3.2.3 Summary

The following observations and interpretations are derived from the analysis of groundwater production, groundwater levels, and NDVI:

- Depth to groundwater in the Prado Basin area is relatively shallow—typically less than 15 feet below the ground surface where the riparian habitat exists. The shallow groundwater contributes to rising groundwater discharge to the SAR and its tributaries and evapotranspiration by the riparian vegetation in the Prado Basin.
- With two exceptions, groundwater levels across the GMP study area have remained stable since 1961 and appear to have been unaffected by the implementation of the Peace Agreements (starting in 2000). The two exceptions are along the northern reaches of Mill Creek and the SAR where groundwater levels have fluctuated by up to +/- 10 feet, likely in response to decreased groundwater production within the GMP area in the 1990s (which coincided with increases in groundwater levels) and increased production after about 2000 with the commencement of CDA pumping (which coincided with decreases in groundwater levels).
- During WY 2017, groundwater levels fluctuated, in some cases by more than 15 feet, under the seasonal stresses of production and recharge. During the winter months of WY 2017, groundwater levels at the PBHSP monitoring wells increased to their highest

recorded levels, likely in response to the recharge of stormwater discharge in unlined creeks and the associated surface-water reservoir that ponds behind Prado Dam. These short-term increases in groundwater levels are temporary, and groundwater levels declined during the growing season under the stresses of groundwater production and evapotranspiration.

- From September 2015 to September 2017, groundwater levels increased by up to two feet at all PBHSP monitoring well locations except along the southern portion of Chino Creek (PB-7/1 and PB-6/1) where groundwater levels declined by up to one foot. The NDVI also showed a decline from September 2015 to September 2017 along the southern portion of Chino Creek. The declines in groundwater levels are not a likely cause of the recent declines in NDVI at these locations because the declines in groundwater levels are less than one foot and appear to be within the historical range of short-term variability.

- From 2015 to 2017, the average growing-season NDVI decreased in several areas of riparian habitat in Prado Basin. With the exception of the SAR-1 area, the decreases in NDVI were minor and within the historical range of short-term variability of NDVI, and hence, may not be indicative of riparian habitat degradation. Most of the areas where NDVI decreased from 2015 to 2017 occurred in areas where groundwater levels remained the same or increased by up to two feet.

- Analysis of the 2017 air photo indicates that the decrease in NDVI at the SAR-1 area from 2016 to 2017 is due to a change in the riparian vegetation at SAR-1 (see Section 3.1). Groundwater levels have been stable in this area, which indicates that a decrease in groundwater levels was not a factor in the observed change in NDVI. Additional investigations are required to understand the cause of the change to the riparian habitat at SAR-1.

3.3 Analysis of Groundwater and Surface Water Interactions

One of the objectives of the PBHSP is to identify factors that contribute to the long-term sustainability of the riparian habitat in Prado Basin. The depth to groundwater analysis shown on Figure 3-11 indicates that the riparian vegetation exists in areas of shallow groundwater that is typically 15 feet below ground surface (ft-bgs) or less, and that the riparian vegetation is likely dependent upon the shallow groundwater, at least in part.

This section describes the results of an analysis of surface-water discharge and quality, groundwater quality, groundwater levels, and groundwater model results that was performed to understand the sources of the shallow groundwater in the Prado Basin and the groundwater/surface-water interactions that may be important to the long-term sustainability of the riparian habitat in Prado Basin.

The nine PBHSP monitoring wells were strategically located along the fringes of the riparian habitat adjacent to Chino Creek, Mill Creek, and SAR, and were constructed to sample the shallow groundwater. Figures 3-13a through 3-13i display groundwater data, surface-water data, and model results at and near the nine PBHSP monitoring well sites. Each figure includes the following data graphics:

- *A map of model-simmulated groundwater-flow directions for 2017*. The map shows the location of the PBHSP monitoring well site. The simulated groundwater-flow directions are output information from the Chino Basin groundwater-flow model for layer 1 for June 30, 2017, and are shown with arrow symbols. Model-simulated groundwater-flow directions can corroborate an understanding of the groundwater/surface-water interactions derived from the measured data. Groundwater-flow directions (arrows) that converge on a stream segment indicate a gaining reach (i.e. groundwater discharge). Groundwater-flow directions that diverge from a stream segment indicate a losing reach (i.e. streambed recharge).

- *A time-series chart of the surface-water discharge in the stream adjacent to the PBHSP monitoring wells, groundwater-elevation at the PBHSP monitoring wells, and the thalweg elevation in the adjacent stream*. The groundwater elevation time-series for the shallow and deep PBHSP monitoring wells are charted with the thalweg elevation of the adjacent creek or river. The thalweg elevation was determined from a 1-meter horizontal resolution digital elevation model of the ground surface (Associated Engineers, 2007)[24]. The thalweg elevations are compared to the groundwater elevations to determine the potential for groundwater discharge or streambed recharge along the specific stream reaches. The relationship between the groundwater elevations in the shallow and deep PBHSP wells are compared to identify downward or upward vertical hydraulic gradients at the well site, which are additional information that can be used to characterize groundwater/surface-water interactions. Daily surface-water discharge data are also charted and compared with groundwater elevations to characterize the relationship between surface-water discharge and groundwater levels.

- *A time-series chart of TDS concentrations in groundwater and surface water.* On these charts, TDS concentrations for groundwater and surface water are compared to help determine the source of the shallow groundwater at the PBHSP monitoring wells. In the southern portion of Chino Basin, shallow groundwater quality is impacted by return flows from applied water and can have TDS concentrations ranging from about 500-4,800 mg/L. The TDS concentration in deeper groundwater is typically lower, generally ranging from 200-500 mg/L. The TDS concentrations of surface-water discharge typically range from 500-750 mg/L depending on the source.

- *A Piper diagram of general-mineral chemistry for groundwater and surface water.* Groundwater in the Chino Basin typically has a different general mineral chemistry than that of surface-water discharge, which is predominantly tertiary-treated discharge from POTWs and

[24] The 1-meter resolution digital elevation model of the ground surface uses the Ayala Park datum, which is the same datum that was used to establish the reference-point elevations at the PBHSP wells. This allows for an accurate comparison between the thalweg elevation and the measured groundwater elevations at the PBHSP wells.

stormwater discharge. Piper diagrams compare groundwater and surface-water via a graphical display of the ratio of the major cations and anions. Water from similar or related sources will generally plot in similar locations on a piper diagram. The data plotted on the Piper diagrams are from the last five years (2013-2017), except for the surface-water quality data for Mill Creek and Chino Creek, which is from a sampling program conducted during 2008-2012.[25] Each Piper diagram indicates the general area of the diagram where typical groundwater and surface water chemistry plot for the Prado Basin region of interest (SAR, Chino Creek, and Mill Creek) based on the available data; this can be used to characterize the source of water that is sampled at the PBSHP monitoring wells.

Table 3-3 summarizes the analysis of the groundwater and surface water interactions and interpretations on the source(s) of the shallow groundwater based on the data presented in Figures 3-13a through 3-13i. In general, the analysis concludes that the SAR from PB-4 to PB-3 and Mill Creek near PB-2 are losing reaches characterized by streambed recharge. Most other areas along Chino Creek and Mill Creek, are gaining reaches characterized by groundwater discharge. That said, at most locations in Prado Basin, there appears to be multiple and transient sources that feed the shallow groundwater and the groundwater/surface-water interactions are complex. Additional monitoring and testing are needed to better characterize the source waters and the groundwater/surface-water interactions.

3.4 Climate and Its Relationship to the Riparian Habitat

Precipitation and temperature are climatic factors that can affect the extent and quality of the riparian habitat. Precipitation can provide a source of water for consumptive use by the riparian vegetation via direct infiltration of precipitation and runoff which increases soil moisture that can be directly used by the vegetation or by maintaining groundwater levels underlying the vegetation for subsequent use by the vegetation. Temperatures affect the rate of plant growth and productivity. Both factors are unrelated to the implementation of the Peace II Agreement.

This section characterizes the time series of precipitation and temperature in the Prado Basin area, and compares that time series to trends in the quality of the riparian habitat, as indicated by NDVI, to analyze if these factors have influenced the riparian habitat in the Prado Basin.

3.4.1 Precipitation

Figure 3-14 is a time-series chart that shows annual precipitation estimates within the Chino Basin for WY 1896 to 2017. These estimates were computed as a spatial average across the Chino Basin using rasterized data from the PRISM Climatic Group (an 800-meter by 800-meter grid). The long-term average annual precipitation in the Chino Basin is 16.47 inches per year

[25] Surface water quality sampling for the Chino Basin Maximum-Benefit monitoring program ended in December 2012. There has been no other surface water quality sampling along Mill and Chino Creeks since. It is a recommendation for the PBSHP monitoring program next year to initiate water quality sampling in Mill Creek and Chino Creek.

(in/yr). The chart includes a cumulative departure from the mean (CDFM) precipitation curve, which characterizes the occurrence and magnitude of wet and dry periods: positive sloping segments (trending upward to the right) indicate wet periods, and negative sloping segments (trending downward to the right) indicate dry periods.

Review of the CDFM precipitation curve indicates that the Chino Basin has experienced several prolonged wet and dry periods from WY 1896 to 2017. Typically, dry periods are longer in duration than wet periods. The longest dry period occurred between 1946 through 1977 (32 years). The Peace and Peace II Agreements period (2001 through 2017) has been a dry period punctuated by three wet years: 2005, 2011, and 2017. Over the 122-year record, about 39 percent of the years had precipitation greater than the average and 61 percent had below average precipitation. In the 17-year period since the Peace Agreement was implemented, 29 percent of the years had precipitation greater than the average and 71 percent had below average precipitation. During the last five years (2013-2017) of the current 18-year dry period the average precipitation was 10.21 in/yr—about 40 percent less than the long-term annual average.

3.4.2 Temperature

Maximum and minimum temperatures during the growing season are the temperature metrics used in this analysis because they can influence NDVI since plant growth and development are dependent upon the temperatures surrounding the plant (Hatfield and Prueger, 2015). Maximum temperatures during the growing season directly influence photosynthesis, evapotranspiration, and breaking of the dormancy of vegetation (Pettorelli, 2015). Minimum temperatures affect nighttime plant respiration rates and can potentially can have an effect on plant growth that occurs during the day (Hatfiled et. al, 2011). All species of plants have a range of maximum and minimum temperatures necessary for growth (Hatfield and Prueger, 2015). Climate change is more likely to increase minimum temperatures, while maximum temperatures are affected more by local conditions (Knowles et al., 2006; Alfaro et al., 2006).

Figure 3-15a is a time-series chart that shows the average maximum and minimum temperatures for the growing season months (March – October) in the Prado Basin from 1896 to 2017 (referred to as growing-season maximum and minimum temperatures). The data used to generate this chart are based on observed daily maximum and minimum temperature converted to monthly statistics and interpolated by the PRISM Climate Group to produce a gridded monthly maximum and minimum temperature estimates (an 800-meter by 800-meter grid). These estimates were computed as a spatial average across the Prado Basin from rasterized data from the PRISM Climatic Group. This chart also shows the five-year moving average of the growing-season maximum and minimum temperatures for the Prado Basin. The five-year moving average is a smoothing technique used to analyze trends over time.

Also shown on this chart is a complete record of atmospheric carbon dioxide (CO2) concentrations assembled from multiple sources:

- Values prior to 1959 are estimated from an analysis of the Law Dome DE08 and DE08-2 ice cores in Antarctica. (Acquired from the Carbon Dioxide Information Analysis Center --http://cdiac.ornl.gov/trends/co2/lawdome.html; Accessed on June 6, 2017).

- Values after 1959 are from measured CO2 concentration data at the Mauna Loa Observatory in Hawaii. (Acquired from the National Oceanic and Atmospheric Association's Earth Systems Research Laboratory -- https://www.esrl.noaa.gov/gmd/ccgg/trends/full.html; Accessed on June 5, 2017).

The time history of atmospheric CO2 concentration shows a monotonic increasing trend ranging from about 290 parts per million (ppm) in the late 1890s to about 310 ppm in 1950 after which the CO2 concentration increases at an increasing rate and exceeds 400 ppm by 2015.

From 1896 to 2017 the growing-season maximum temperatures fluctuate from 80° F to 89° F and do not appear to have a long-term increasing or decreasing trend, until 1950 where there is a slight increasing trend of about one-degree Fahrenheit through 2016. From 2016 to 2017 the average maximum temperature increases by three degrees Fahrenheit and is the all-time maximum recorded temperature for this data set. From 1896 to 2017 the growing-season minimum temperatures fluctuates from about 49° F to 58° F and do not appear to have an increasing or decreasing trend till about 1950 where there is a clear increasing trend of about five degrees Fahrenheit through 2017. These increasing trends in growing-season maximum and minimum temperatures since 1950 appear to correlate with the increase in atmospheric CO2 concentrations. The rate of increase in the minimum growing-season temperature is greater than the rate of increase in the maximum growing-season temperature. The five-year moving average of the both the growing-season minimum and maximum temperatures demonstrate and increasing trend for the last five years.

Figures 3-15b and 3-15c are bar charts that characterize long-term trends of the growing-season maximum and minimum temperatures, respectively, in Prado Basin. The bar charts show the departure of the average growing-season temperatures for each year from the growing-season mean for the thirty-year period of 1921 to 1950. This thirty-year period is prior to the break in curvature of atmospheric CO2 concentration time series, and prior to any observed trends in the maximum and minimum temperatures shown in Figure 3-15a. The five-year moving average for the growing-season temperatures is also show on these figures to compare the trend with these bar charts.

Figure 3-15b demonstrates that there is no prominent long-term increasing or decreasing trend in the average growing-season maximum temperature from the 1921-1950 mean, until the last few years which show an increasing positive departure trend and an increasing five-year moving average to the highest the highest observed values in the period of record.

Figure 3-15c demonstrates that there is a prominent increasing trend in the departure from the 1921-1950 mean for the growing-season minimum temperature. All but two of the annual departures from the 1921- 1950 mean are positive since 1950 and show an increasing trend since 1950. In the last six years the average departure was about positive five degrees Fahrenheit, and the five-year moving average of the minimum growing-season temperature has increased over this time.

Figures 3-16a through 3-16c are time-series charts that compare long-term trends in precipitation and temperature to the NDVI for three areas in Prado Basin: Chino Creek, Mill

Creek, and the SAR. These figures plot the average growing-season NDVI for the 12 defined areas of riparian habitat, as discussed in Section 3.1 and shown in Figures 3-5 and 3-6a through 3-6k. The period of analysis for these charts is 1984-2017—the period of NDVI data availability.

The upper chart on Figures 3-16a through 3-16c area time-series charts that show the annual precipitation in Chino Basin, the CDFM precipitation curve, and the five-year moving average for the growing-season maximum and minimum temperatures in the Prado Basin. The lower charts on Figures 3-16a through 3-16c shows the time series of the average growing-season NDVI along each respective area from 1984 to the present.

Chino Creek (Figure 3-16a) The NDVI estimates show a long-term increasing trend from 1984 to 2017 indicating an improvement in the quality of the riparian vegetation. These increases occurred over both the wet period in the early 1990's and the prolonged dry period since 1999. The NDVI show no long-term correlation to the fluctuating maximum and minimum temperatures in Prado Basin. The recent decreases in NDVI from 2015 to 2017 at all four areas along Chino Creek are within the year-to-year variability of the NDVI estimates for these areas and occurred during the recent warming trend in the minimum and maximum temperatures in Prado Basin and at the end of the current 18-year dry period.

Mill Creek (Figure 3-16b) The NDVI estimates show a long-term increasing trend in average growing-season NDVI at the northern most and southern most areas along Mill Creek (MC-1 and MC-4) and no long-term trend in the average growing-season NDVI at the two middle areas along Mill Creek (MC-2 and MC-3). There is an increasing trend observed at all four areas during the onset of the early 1990s wet period, and no long-term trend or an increasing trend over the prolonged dry period since 1999. The NDVI show no long-term correlation to the fluctuating maximum and minimum temperatures. The recent decreases in NDVI from 2015 to 2017 at three of areas along Mill Creek are within the year-to-year variability of the NDVI estimates for these areas, and occurred during the recent warming trend in the minimum and maximum temperatures in Prado Basin and at the end of the current 18-year dry period.

Santa Ana River (Figure 3-16c) The NDVI estimates show a long-term increasing trend in average growing-season NDVI at all four areas. There is an increasing trend observed at three of the four areas during the onset of the early 1990s wet period, and no long-term trend or increasing trend at all four areas over the prolonged dry period since 1999. The NDVI show no long-term correlation to the fluctuating maximum and minimum temperatures. From 2015 to 2017, NDVI remained relatively stable or increased along the SAR except for a decrease of 0.23 at SAR-1. This large decrease at SAR-1 and occurred during the recent warming trend in the minimum and maximum temperatures in Prado Basin and at the end of the current 18-year dry period.

3.4.3 Summary

The following observations and interpretations are derived from the analysis of precipitation, temperature, and NDVI:

- The current 18-year dry period includes the period of implementation of both Peace and Peace II Agreements. During the last five years (2013-2017) of the current 18-year dry period the average precipitation was 10.21 in/yr—about 40 percent less than the long-term annual average, although during WY 2017 precipitation was above average.
- The quality of riparian habitat, as characterized by the time series of NDVI at the 12 defined areas, has shown no consistent long-term relationship to precipitation or growing-season temperatures, and may have improved slightly during the relatively dry Peace Agreements period along the northern reaches of Chino Creek, Mill Creek, and the SAR within the study area.
- The early portion of the wet period in the 1990s coincides with a short-term increase in NDVI at most areas along Chino Creek, Mill Creek and the SAR. This observation suggests that the wet period may have had a positive influence on the riparian vegetation in Prado Basin and resulted in increasing NDVI.
- The NDVI at the areas analyzed did not display a declining trend during the extended dry period from 1999 to 2017. This observation suggests the availability of water, other than precipitation and runoff, such as surface water and shallow groundwater for consumptive use by the riparian vegetation.
- There is a warming trend observed in the Prado Basin as indicated by the increases in the five-year moving average for the growing-season maximum and minimum temperatures. In addition, in 2017 the maximum and minimum temperatures and the five-year moving average were the highest for the entire period of record (1895-2017).
- Visual comparison of the trends in five-year moving average for the growing-season maximum and minimum temperatures versus trends in average growing-season NDVI from 1984 to 2017 reveal no obvious correlation at any of the areas analyzed.
- From 2015 to 2017, the average growing-season NDVI decreased in several areas of riparian habitat in Prado Basin. With the exception of the SAR-1 area, the decreases in NDVI were minor and within the historical range of short-term variability of NDVI, and may not be indicative of riparian habitat degradation. These decreases in NDVI occurred during the recent warming trend in the minimum and maximum temperatures in Prado Basin and at the end of the current 18-year dry period. Continued monitoring and analysis is required to determine the relationship between recent trends in temperature with the recent trends in the quality of the riparian habitat characterized by NDVI at the defined study areas.

3.5 Stream Discharge and Its Relationship to the Riparian Habitat

SAR stream discharge and its tributaries that flow through the Prado Basin is a factor that can affect the extent and quality of the riparian habitat in Prado Basin. Stream discharge can recharge the groundwater system along losing stream reaches and supply water through the groundwater system to riparian vegetation. Stream discharge is also important to fauna living within the stream system. Flooding events and flood-control/water-conservation operations at Prado Dam can scour and inundate areas of the riparian habitat and potentially cause adverse impacts.

This section characterizes the time series of stream discharge within the Prado Basin, and compares that time series to trends in the extent and quality of the riparian habitat, as indicated by the NDVI, to determine whether changes in stream discharge have resulted in impacts to riparian habitat in the Prado Basin.

3.5.1 Stream Discharge

There are three primary components of stream discharge in the SAR and its tributaries: storm discharge, non-tributary discharge, and base-flow discharge. Storm discharge is rainfall runoff. Non-tributary discharge typically originates from outside the watershed, such as imported water discharge from the OC-59 turnout on San Antonio Creek. Base-flow discharge, as used herein (and by the Santa Ana River Watermaster), includes tertiary-treated wastewater discharge from POTWs (Publicly-Owned Treatment Works), rising groundwater, and dry-weather runoff.

Figure 3-17 includes time-series charts that summarize important annual discharges within the upper SAR watershed that are tributary to Prado Dam from water years 1971 to 2017 (SARW, 2018). The upper chart in Figure 3-17 characterizes the annual outflow from Prado Basin as total measured SAR discharge at the USGS gage *SAR at below Prado Dam*. The upper chart also shows the base-flow component of total measured discharge as estimated by the Santa Ana River Watermaster. This chart shows that base-flow discharge declined from about 154,000 AFY in 2005 to about 63,000 AFY by 2014, and slightly increased and leveled off to about 70,000 AFY in 2017.

The decline in base-flow discharge is primarily related to declines in POTW effluent discharge that is tributary to Prado Dam. The lower chart in Figure 3-17 shows that the combined POTW discharges that are tributary, at least in part, to Prado Dam declined from about 192,000 AFY in 2005 to about 89,000 AFY by 2014 and increased to about 96,000 AFY in 2017. This decrease is mostly attributed to decreases in effluent discharge from IEUA and the POTWs that discharge to Temescal Creek. The post-2005 decrease in POTW effluent discharge was caused by increased recycled-water reuse, decreased water use due to the economic recession that began in 2008 and the implementation of emergency water-conservation measures during the recent drought.

Figures 3-18a through 3-18c are time-series charts that compare long-term trends in stream discharge to the NDVI for three areas in Prado Basin: Chino Creek, Mill Creek, and the SAR. The figures display the annual volumes of measured discharge to each stream during the growing season (March-October), including: measurements at USGS gaging stations located upstream of Prado Basin, and POTW discharges.[26] These figures show the average growing-

[26] These charts do not describe other hydrologic processes that affect surface-water discharge within the Prado Basin, including evaporation, evapotranspiration, the infiltration of water along unlined stream segments, and rising groundwater discharge.

season NDVI for the 12 defined areas of riparian habitat discussed in Section 3.1 and shown in Figures 3-5 and 3-6a through 3-6k.

Chino Creek (Figure 3-18a). Chino Creek is a concrete-lined flood-control channel that transitions into an unlined stream channel at the Prado Basin boundary and flows south to merge with Mill Creek and the SAR behind Prado Dam (see Figure 2-3). The upper chart on Figure 3-18 shows the growing-season discharge to Chino Creek, including: imported water discharged from the OC-59 turnout, measured discharge at the USGS gage *Chino Creek at Schaefer*, and POTW discharges at locations downstream of the USGS gage from IEUA's Carbon Canyon, RP-2, RP-5, and RP-1 plants. Measured discharge at *Chino Creek at Schaefer*, is representative of storm-water and dry-weather runoff in the concrete-lined channel upstream of the IEUA discharge locations and the imported water discharge from OC-59 turnout. Discharges not characterized in this figure are storm-water runoff, dry-weather runoff, and rising-groundwater discharge downstream of *Chino Creek at Schaefer* gage. During 1984-1999, the stream discharge in Chino Creek during the growing season averaged about 31,000 AFY. From 1999-2017, discharge in Chino Creek during the growing season averaged about 17,000 AFY. The recent five-year average (2013-2017) of the growing-season discharge is about 7,800 AF, and in 2017 was about 4,500 AF. This decreasing trend is attributed to dry climatic conditions since 1999, water conservation in response to drought and the decrease in effluent discharge from the IEUA plants along Chino Creek.

The lower chart on Figure 3-18a shows the time series of the average growing-season NDVI from 1984 to present for four areas along Chino Creek. The NDVI estimates show a long-term increasing trend from 1984 to 2017 indicating an improvement in the quality of the riparian vegetation. As discharge in Chino Creek gradually declined from 1999 through the present, there is no clear declining trends in NDVI estimates at any of the locations along Chino Creek during that time. From 2015 to 2017, NDVI decreased at all four areas along Chino Creek. These decreases in NDVI are within the historical range of annual and short-term variability of NDVI at these areas and therefore do not necessarily represent a degradation of the riparian habitat. In addition, the analysis of air photos does not illustrate signs of degradation of the riparian habitat (see Section 3.1). These recent changes in NDVI occurred when growing-season discharge was above the five-year average in 2016 (16,600 AF) due to discharge from OC-59, and when growing-season discharge was below the five-year average in 2017 (4,500 AF). From 2015 to 2017 the growing-season discharge decreased by 1,500 AF which is about twenty percent of the five-year average of the growing-season discharge in Chino Creek.

Mill Creek (Figure 3-18b). Cucamonga Creek is a concrete-lined flood-control channel and transitions into an unlined stream channel at the Prado Basin boundary, and at that point, its name changes to Mill Creek (see Figure 2-3). The upper chart on Figure 3-14b shows the annual discharge to Mill Creek, including: POTW effluent discharge from IEUA's RP-1 plant to Cucamonga Creek, and measured discharge at the downstream USGS gage *Cucamonga Creek near Mira Loma* (less the RP-1 discharge). The measured discharge of *Cucamonga Creek near Mira Loma* (less the RP-1 discharge) is representative of storm-water and dry-weather runoff in Cucamonga Creek upstream of this gaging station. Discharges not characterized on this figure are storm-water runoff, dry-weather runoff, and rising-groundwater discharge downstream of *Cucamonga*

Creek near Mira Loma gage. The upper chart shows that from 1984 to 2012 discharge during the growing season in Mill Creek averaged about 20,000 AF. The recent five-year average (2013-2017) of the growing-season discharge is about 10,000 AF, and in 2017 was about 6,400 AF. This decline in growing season discharge is attributed to dry climatic conditions, water conservation in response to drought and the decrease in effluent discharge from IEUA's RP-1 plant to Cucamonga Creek.

The lower chart on Figure 3-12b shows the time series of the average growing-season NDVI from 1984 to present for the four areas along Mill Creek. There is a long-term increasing trend in average growing-season NDVI at the northern and southern areas along Mill Creek (MC-1 and MC-4) and no long-term trend in the average growing-season NDVI along the middle reach of Mill Creek (MC-2 and MC-3). As the discharge in Mill Creek gradually declined from 2012 through the present, there is no clear declining trends in NDVI estimates at any of the locations along Mill Creek during that time. From 2015 to 2017, NDVI decreased at three areas along Mill Creek. These decreases in NDVI are within the historical range of annual and short-term variability of NDVI at these areas and therefore do not necessarily represent a degradation of the riparian habitat. In addition, the analysis of air photos does not illustrate signs of degradation of the riparian habitat (see Section 3.1). These recent discharges in NDVI occurred when growing-season discharge was above average in 2016 (13,000 AF), and when growing-season discharge was below average in 2017 (6,400 AF). From 2015 to 2017 the growing-season discharge decreased by 7,000 AF which is about fifty percent of the five-year average growing-season discharge in Mill Creek.

Santa Ana River (Figure 3-18c). The SAR is an unlined stream channel from the Riverside Narrows to Prado Dam—its entire reach across the Chino Basin (see Figure 2-3). The upper chart on Figure 3-14c shows the annual discharge at the USGS gage *Santa Ana River at MWD Crossing* (Riverside Narrows) and discharges to the SAR downstream of the MWD crossing, including wastewater effluent from the City of Riverside's Regional Water Quality Control Plant and from Western Riverside County Regional Wastewater Authority (WRCRWA) plant that is conveyed in an unlined channel (along with a portion of SAR discharge) to the OCWD Prado Wetlands. The measured discharge at *Santa Ana River at MWD Crossing* gage includes storm flow and base flow in the SAR upstream of the gaging station at the Riverside Narrows. The base-flow discharge includes wastewater discharge from the RIX and Rialto treatment plants, dry-weather runoff and rising groundwater. Discharges not characterized on this figure are storm-water runoff, dry-weather runoff, and rising-groundwater discharge downstream of *Santa Ana River at MWD Crossing*. From 1984 to 2012, discharge during the growing-season in the SAR was generally steady, with episodic increases in storm-water discharge during wet years, and averaged about 79,000 AFY. The recent five-year average (2013-2017) of the growing-season discharge is about 47,000 AF, and in 2017 was about 44,900 AF. This decrease in growing-season discharge is mainly attributed to dry climatic conditions, water conservation in response to drought., and decrease in the baseflow at the Riverside Narrows.

The lower chart on Figure 3-18c shows the time series of average growing-season NDVI from 1984 to present for four areas along the SAR. There is a long-term increasing trend in the average growing-season NDVI from 1984 to 2017 at all locations along the SAR indicating an improvement in the quality of the riparian vegetation. With the exception of SAR-1, there is no clear declining trend in NDVI estimates at any of the locations along the SAR from 2012 to present, even though surface-water discharge has declined over this period. From 2015 to 2017, NDVI remained relatively stable or increased along the SAR except for a decrease of 0.21 at SAR-1 from 2016 to 2017. The large decrease in NDVI from 2016 to 2017 of 0.21 at SAR-1 occurred when the total discharge in the SAR remained stable.

3.5.2 Summary

The following observations and interpretations are derived from the analysis of surface discharge, and NDVI:

- Discharge in the SAR and its tributaries to Prado Dam has declined significantly since 2005. The declining trend in discharge is attributed to dry climatic conditions from 1999-2017, decreases in wastewater discharge because of increased recycled-water reuse, decreased wastewater discharge due to the economic recession that began in 2008, and the implementation of emergency water-conservation measures during the recent drought.

- The quality of riparian habitat, as characterized by the time series of average growing-season NDVI in the 12 defined areas along Chino Creek, Mill Creek, and the SAR, has shown no consistent relationship or declining trend that coincides with declines in growing-season stream discharge, and may have improved slightly during the Peace II Agreement period.

- With the exception of the area SAR-1, the decreases in the average growing-season NDVI were minor and within the historical range of short-term variability of NDVI, and hence, may not be indicative of riparian habitat degradation. These decreases in NDVI occurred when the growing-season discharge for both Chino Creek and Mill Creek decreased from 2015 to 2017, and the growing-season discharge remained stable in the SAR. Continued monitoring and analysis is required to determine the relationship between recent trends in stream discharge with the recent trends in the quality of the riparian habitat characterized by NDVI at the defined study areas.

- Analysis of the 2017 air photo indicates that the decrease in NDVI at SAR-1 from 2016 to 2017 is due to a change in the riparian vegetation at SAR-1 (see Section 3.1). This decrease in NDVI occurred when the growing-season discharge in the SAR remained stable, which indicates that discharge in the SAR were likely not a factor in the observed change in NDVI.

3.6 Other Factors and Their Relationship to the Riparian Habitat

Other factors that can affect the extent and quality of riparian habitat in the Prado Basin analyzed in this annual report are wildfire and pests. These factors are unrelated to the implementation of the Peace II Agreement.

This section characterizes the time series of what is known about these two factors, and compares time series of other factors to trends in the extent and quality of the riparian habitat to determine whether these factors resulted in impacts to the quality of riparian habitat as characterized by the NDVI.

3.6.1 Wildfire

Available wildfire perimeter data from the FRAP database[27] were compiled within the Prado Basin extent for the period 1950-2016.[28] Beginning in the early 1980s, wildfires occurred in the Prado Basin in 1985, 1989, 2007, and 2015. Figure 3-19 shows the spatial extent of these wildfires mapped on the 2017 air photo. Portions of the extent of the 2015 wildfire is still identifiable in the air photo by a brownish color compared to the dark green color of the surrounding unburned areas.

Figures 3-20a through 3-20c are time-series charts that explore the relationship between wildfire and the NDVI for three areas in Prado Basin: Chino Creek, Mill Creek, and the SAR. The figures show the average growing-season NDVI for the 12 defined areas of riparian habitat, as discussed in Section 3.1 and shown in Figures 3-5 and 3-6a through 3-6k. Wildfire occurrences, annotated by date, are shown on the charts if the wildfire extent intersects with the extent of the defined area of NDVI analysis.

The 2007 wildfire burned portions of Chino Creek in the CC-3 area and portions of Mill Creek in the MC-2 area. As Figures 3-20a and 3-20b show, the NDVI at CC-3 decreases by about 0.05 after the 2007 wildfire, and the NDVI at MC-2 decreases by about 0.08 after the 2007 wildfire. However, decreases in NDVI of similar magnitude year-to-year occur at all other sites analyzed along Chino Creek and Mill Creek, suggesting that the effects of the 2007 wildfire are not reflected in the NDVI at CC-3 and MC-2.

The 1985 wildfire burned portions of SAR floodplain in the SAR-1 and SAR-2 areas. As Figure 3-16c shows, the NDVI at SAR-1 and SAR-2 increase slightly by about 0.05 and 0.02, respectively, after the 1985 wildfire, suggesting that the effects of the 1985 wildfire are not reflected in the NDVI for the SAR-1 and SAR-2 areas.

---

[27] http://frap.fire.ca.gov/index (Website for California Department of Forestry and Fire Protection's Fire and Resource Assessment Program).

[28] Data is updated in late April for the previous year, so 2017 data was not available for this annual report

3.6.2 Polyphagous Shot Hole Borer

The PSHB, from the group known as ambrosia beetles, is a relatively new pest in Southern California. The PSHB bores into trees and brings with it fungi that assists in establishing colonies. Infection caused by the fungi can cause a dark stain surrounding the entry holes, discolored bark, leaf discoloration and wilting, and dieback of entire branches. The PSHB attacks many species of trees, but some trees are resistant to the fungi it carries.

Figure 3-19 shows the locations where the presence of the PSHB has been documented within the Prado Basin from 2016 to 2016. The University of California, Department of Agriculture on their Natural Resources PSHB/FD Distribution Map[29] noted the presence of the PSHB in the Prado Basin riparian habitat at four locations from 2016-2017. During the USBR site-specific vegetation surveys performed in 2016, the presence of the PSHB was identified at 29 of the 37 sites surveyed. At these sites, all of the trees identified with the presence of the PSHB were noted as stressed except one which was noted as dead. There were no USBR site-specific vegetation surveys performed during 2017.

OCWD biologists in the Prado Basin have been working with the University of California, Riverside, the USFWS, and the Santa Ana Watershed Association (SAWA) to actively monitor the occurrence and impact of PSHB within Prado Basin riparian habitat. These agencies have noted that the presence of the PSHB is widespread through the Prado Basin, and has significantly reduced tree canopy cover throughout the region (Zembal, R., personal communication, 2018). But thus far, tree mortality is confined to small local patches. These agencies are conducting studies on how to potentially protect certain areas of the Prado Basin from the PSHB using attractants and deterrents, however and there are too many trees to effectively protect the entire forest (Zembal, R., personal communication, 2018). Figure 3-19 shows the locations of 12 PSHB traps in the Prado Basin deployed by the OCWD and SAWA between August 2016 and April 2017. The trap locations are placed throughout the lower portion of Prado Basin and along the SAR. The total number of PBHB beetles trapped at each location during August 2016 and April 2017 ranged from seven to 2,092.

Figures 3-20a through 3-20c are time-series charts that explore the relationship between the PSHB and NDVI for three areas in Prado Basin: Chino Creek, Mill Creek, and the SAR. These figures show the average growing-season NDVI for the 12 defined areas of riparian habitat discussed in Section 3.1 and shown in Figures 3-5 and 3-6a through 3-6k. The percentage of infected trees with PBSB to the total of all trees within each site ranged from three to 100 percent (see Table 3-1). The percentage of infected trees relative to the total of all trees within the surveyed areas are plotted on these charts as the secondary y-axis value. For the 12 defined areas shown on Figures 3-20a through 3-20c, ten of them are near vegetation survey sites where PSHB was noted in 2016. Of those ten, eight of them show decreases in the average growing-season NDVI from 2015 to 2017; these include all sites along Chino Creek, three sites along Mill Creek (MC-1, MC-2, MC-4), and one site along the SAR (SAR-1). At the remaining two

---

[29] http://ucanr.maps.arcgis.com/apps/Viewer/index.html?appid=3446e311c5bd434eabae98937f085c80

areas where the PSHB was noted nearby in 2016, the average growing-season NDVI increased from 2015 to 2017 (MC-3 and SAR-2).

The 2016 USBR surveys were the first site-specific surveys that documented the presence and abundance of the PSHB for the PBHSP, and it is too early to suggest that the PSHB has caused a decrease in NDVI. It is recommended that future vegetation surveys include measurement of the presence, abundance, and effect of the PSHB on trees within the riparian habitat.

3.7 Analysis of Prospective Loss of Riparian Habitat

The meaning of "prospective loss" of riparian habitat in this context is "future potential loss" of riparian habitat. Watermaster's recent predictive modeling results[30] were used to identify areas of prospective loss of riparian habitat that may be attributable to the Peace II Agreement by projecting future groundwater level conditions in the Prado Basin area through 2030. To perform this evaluation, the predictive model results were mapped and charted to identify areas, if any, where groundwater levels are projected to decline to depths that may negatively impact riparian habitat in the Prado Basin.

Figure 3-21 is a map that shows the predicted change in groundwater levels in the Prado Basin area over the period of 2017-2030. In this scenario, groundwater levels are predicted to remain steady across most of the Prado Basin area through 2030, including the areas along Chino Creek and Mill Creek. The stability in groundwater levels is explained by projected declines in groundwater production from private wells in the area; IEUA's delivery of treated recycled water to this area for direct uses, such as outdoor irrigation, and the fact that most of the CDA production will occur to the north and north east.

Figure 3-21 shows that groundwater levels are projected by 2030 to increase by less than five feet along the eastern reach of the SAR within the study area. This area is located directly south of the main production centers of the CDA.

Figure 3-22 is a time-series chart of projected groundwater levels at the PBHSP monitoring wells for the period 2017-2030. These wells are strategically located adjacent to the riparian habitat south of the CDA well field to best understand the potential impacts of Peace II implementation on groundwater levels and riparian habitat. The chart shows:

- Groundwater levels are projected to fluctuate seasonally at the PBHSP monitoring wells by about one to two feet.

---

[30] The predicted groundwater level changes through 2030 were made with the 2017 Chino Basin Groundwater Model for Scenario 1A developed in Watermaster's Storage Framework investigation (WEI, to be published in 2018). Scenario 1A represents the Chino Basin parties' best estimates of how future supplies would be used to meet demands. Scenario 1A serves as the baseline for the storage programs evaluated in the Storage Framework investigation

- Groundwater levels are projected to remain stable at most of the PBHSP monitoring wells through the duration of the Peace II Agreement through 2030 with no significant periods of increasing or decreasing groundwater levels.
- Two of the PBHSP monitoring wells are projected to experience declines in groundwater levels of about one foot by 2030: PB-9 along the northern portion of Chino Creek; and PB-2 along northern portion Mill Creek.
- One of the PBHSP monitoring wells is projected to experience an increase in groundwater levels of about two feet by 2030: PB-4 along the eastern portion of the SAR.

With regard to prospective loss of riparian habitat:

- Across the Prado Basin where the riparian habitat exists, there are no projected declines in groundwater levels through 2030 that would indicate a threat for prospective loss of riparian habitat. And along the eastern portion of the SAR groundwater levels are projected to rise by about two feet.
- There are two areas within Prado Basin where groundwater levels are projected to decline by 2030—the northernmost reaches of Chino Creek and Mill Creek. Figure 3-11 shows the current depth-to-groundwater (Fall 2017) for The Prado Basin. Where the riparian vegetation is growing along the northernmost reaches of Chino Creek and Mill Creek, the depth to water is about zero to 13 feet-bgs. In these areas, the model-projected decline in groundwater levels from 2017-2030 is about one foot. This suggests that the depth-to-groundwater in these areas will be about one to 14 feet by 2030. Figure 3-11 shows that the riparian vegetation in the Prado Basin grows in areas where depth-to-groundwater is up to 15 feet-bgs. Hence the projected declines in groundwater levels along Chino Creek and Mill Creek are minor, and it is not likely that they will result in adverse impacts to the riparian habitat in Prado Basin.
- The projected changes in groundwater level under the Prado Basin study area are predicated on the Chino Basin parties pumping groundwater and conducting recharge operations consistent with their planning that was incorporated into the model projections.

Table 3-1
Summary of USBR Vegetation Surveys in 2007, 2013, and 2016 in Prado Basin

Site	Canopy Cover (%) [1]				Tree Condition (% surveyed per plot) [2]												Polyphagous Shot-Hole Borer [3]		Basal Area (m^2/ha) [4]			Density per plot (trees/ha) [5]			Crown Ratio [6]		
					Live				Stressed				Dead														
	2007	2013	2016	Change - 2007 to 2016	2007	2013	2016	Change - 2013 to 2016	2007	2013	2016	Change - 2013 to 2016	2007	2013	2016	Change - 2013 to 2016	Present in 2016	% of Trees	2007	2013	2016	2007	2013	2016	2007	2013	2016
Chino Creek Sites																											
Chino 3	59%	NM	NM	-	NM	NM	NM	-	NM		NM	-	NM		NM	-	NM	NM	36	NM	NM	127	NM	NM	NM	NM	NM
Chino 3B	NM	97%	96%	-	NM	100%	0%	-100%	NM	0%	100%	100%	NM	0%	0%	0%	no	0%	NM	6	30	NM	318	1019	NM	0.66	0.67
Chino 4	80%	94%	98%	18%	NM	100%	7%	-93%	NM	0%	80%	80%	NM	0%	13%	13%	no	0%	29	34	43	255	318	477	NM	0.71	0.84
Chino 9	92%	96%	95%	4%	NM	100%	0%	-100%	NM	0%	100%	100%	NM	0%	0%	0%	no	0%	32	39	33	382	318	318	NM	0.82	0.76
Chino 11	94%	96%	96%	2%	NM	100%	50%	-50%	NM	0%	42%	42%	NM	0%	8%	8%	no	0%	5	118	185	64	1146	1528	NM	0.75	0.75
Chino 16	46%	61%	81%	35%	NM	NM	27%	-	NM	NM	64%	-	NM	NM	9%	-	no	0%	23	34	28	127	318	350	NM	0.77	0.82
Chino 18	38%	87%	90%	52%	NM	100%	7%	-93%	NM	0%	67%	67%	NM	0%	27%	27%	yes	40%	26	21	94	127	605	1910	NM	0.86	0.68
Chino 21	98%	94%	88%	-10%	NM	100%	0%	-100%	NM	0%	100%	100%	NM	0%	0%	0%	yes	17%	73	103	83	414	1019	764	NM	0.72	0.63
Chino 24	93%	93%	98%	4%	NM	100%	6%	-94%	NM	0%	94%	94%	NM	0%	0%	0%	yes	6%	17	32	30	223	318	573	NM	0.72	0.75
Chino 30	79%	88%	NM	-	NM	NM	NM	-	NM	NM	NM	-	NM	NM	NM	-	NM	NM	60	8	NM	382	255	NM	NM	0.76	NM
Chino 30B	NM	NM	89%	-	NM		0%	0%	NM	NM	89%	-	NM	NM	11%	-	yes	100%	NM	NM	63	NM	NM	1146	NM	NM	0.74
Chino 31	82%	93%	97%	14%	NM	100%	7%	-93%	NM	0%	93%	93%	NM	0%	0%	0%	yes	7%	31	34	57	350	318	446	NM	0.78	0.82
Chino 34	96%	97%	89%	-7%	NM	100%	0%	-100%	NM	0%	67%	67%	NM	0%	33%	33%	no	0%	22	76	60	255	1019	764	NM	0.66	0.70
Chino 78	95%	98%	87%	-8%	NM	100%	0%	-100%	NM	0%	80%	80%	NM	0%	20%	20%	yes	80%	51	40	27	318	350	318	NM	0.74	0.87
Chino 81	92%	0%	NM	-	NM	NM	NM	-	NM	NM	NM	-	NM	NM	NM	-	NM	NM	6	NM	NM	72	NM	NM	NM	NM	NM
Chino 85	89%	0%	NM	-	NM	NM	NM	-	NM	NM	NM	-	NM	NM	NM	-	NM	NM	3	NM	NM	28	NM	NM	NM	NM	NM
Chino X3	NM	NM	93%	-	NM	NM	25%	-	NM	NM	75%	-	NM	NM	0%	-	no	0%	NM	NM	81	NM	NM	509	NM	NM	0.76
Chino X4	NM	NM	92%	-	NM	NM	0%	-	NM	NM	100%	-	NM	NM	0%	-	yes	100%	NM	NM	15	NM	NM	891	NM	NM	0.61
Chino X5	NM	NM	96%	-	NM	NM	75%	-	NM	NM	25%	-	NM	NM	0%	-	yes	25%	NM	NM	122	NM	NM	1019	NM	NM	0.82
Chino X6	NM	NM	98%	-	NM	NM	87%	-	NM	NM	13%	-	NM	NM	0%	-	yes	13%	NM	NM	69	NM	NM	1910	NM	NM	0.68
Chino X7	NM	NM	88%	-	NM	NM	0%	-	NM	NM	70%	-	NM	NM	30%	-	yes	70%	NM	NM	30	NM	NM	318	NM	NM	0.85
Chino X8	NM	NM	85%	-	NM	NM	0%	-	NM	NM	62%	-	NM	NM	38%	-	yes	46%	NM	NM	68	NM	NM	1655	NM	NM	0.82
Average	**81%**	**78%**	**92%**	**11%**	**-**	**100%**	**16%**	**-84%**	**-**	**0%**	**73%**	**82%**	**-**	**0%**	**11%**	**10%**	**yes**	**28%**	**30**	**45**	**62**	**223**	**525**	**884**	**-**	**0.75**	**0.75**
Mill Creek Sites																											
Mill 1	40%	0%	NM	-	NM	NM	NM	-	NM	NM	NM	-	NM	NM	NM	-	NM	NM	4	NM	NM	80	NM	NM	NM	NM	NM
Mill 3	8%	13%	NM	-	NM	NM	NM	-	NM	NM	NM	-	NM	NM	NM	-	NM	NM	NM	NM	NM	NM	NM	NM	NM	NM	NM
Mill 4	38%	6%	0%	-38%	NM	0%	0%	0%	NM	63%	50%	-13%	NM	37%	50%	13%	yes	50%	6	NM	0	350	605	191	NM	0.63	0.73
Mill 8	66%	88%	82%	16%	NM	33%	33%	0%	NM	67%	0%	-67%	NM	0%	67%	67%	yes	33%	NM	3	4	NM	764	764	NM	0.00	0.91
Mill 11	75%	80%	NM	-	NM	90%	NM	-	NM	0%	NM	-	NM	10%	NM	-	NM	NM	10	24	NM	318	318	NM	NM	0.75	NM
Mill 18	62%	68%	78%	16%	NM	100%	38%	-63%	NM	0%	38%	38%	NM	0%	25%	25%	yes	38%	34	22	21	318	223	255	NM	0.92	0.91
Mill 22	89%	93%	96%	7%	NM	86%	0%	-86%	NM	0%	79%	79%	NM	14%	21%	7%	yes	64%	16	NM	80	382	1783	1910	NM	0.65	0.77
Mill 30	63%	63%	NM	-	NM	NM	NM	-	NM	NM	NM	-	NM	NM	NM	-	NM	NM	12	35	NM	286	732	NM	NM	0.41	NM
Mill 35	81%	95%	NM	-	NM	100%	NM	-	NM	0%	NM	-	NM	0%	NM	-	NM	NM	4	40	NM	80	1401	NM	NM	0.78	NM
Mill 39	94%	87%	96%	2%	NM	92%	0%	-92%	NM	0%	67%	67%	NM	8%	33%	25%	yes	44%	18	23	21	350	382	286	NM	0.82	0.88
Mill 60	76%	90%	83%	6%	NM	86%	0%	-86%	NM	0%	93%	93%	NM	14%	7%	-7%	yes	29%	4	NM	22	103	1783	446	NM	0.72	0.85
Mill 62	66%	96%	96%	30%	NM	100%	0%	-100%	NM	0%	94%	94%	NM	0%	6%	6%	yes	94%	2	121	124	35	2165	2037	NM	0.76	0.72
Mill 63	70%	97%	78%	8%	NM	100%	0%	-100%	NM	0%	68%	68%	NM	0%	32%	32%	yes	41%	3	33	22	72	668	700	NM	0.70	0.82
Mill 67	75%	95%	NM	-	NM	100%	NM	-	NM	0%	NM	-	NM	0%	NM	-	NM	NM	6	105	NM	88	1655	NM	NM	0.77	NM
Mill 69	92%	84%	75%	-17%	NM	90%	0%	-90%	NM	0%	64%	64%	NM	10%	36%	26%	yes	64%	21	16	22	446	605	446	NM	0.87	0.92
Mill 82	92%	96%	56%	-36%	NM	100%	0%	-100%	NM	0%	75%	75%	NM	0%	25%	25%	yes	25%	6	30	29	95	382	382	NM	0.71	0.78
Mill 101	90%	94%	83%	-7%	NM	96%	0%	-96%	NM	0%	87%	87%	NM	4%	13%	9%	yes	83%	3	40	50	39	764	955	NM	0.72	0.79
Mill X9	NM	NM	94%	-	NM	NM	70%	-	NM	NM	30%	-	NM	NM	0%	-	yes	10%	NM	NM	47	NM	NM	1273	NM	NM	0.76
Mill X10	NM	NM	89%	-	NM	NM	0%	-	NM	NM	50%	-	NM	NM	50%	-	yes	50%	NM	NM	94	NM	NM	2037	NM	NM	0.82
Average	**69%**	**73%**	**77%**	**-1%**	**-**	**84%**	**11%**	**-74%**	**-**	**9%**	**61%**	**53%**	**-**	**7%**	**28%**	**21%**	**yes**	**48%**	**10**	**41**	**41**	**203**	**949**	**899**	**-**	**0.68**	**0.82**
Santa Ana River Sites																											
SAR X1	NM	NM	58%	-	NM	NM	76%	-	NM	NM	5%	-	NM	NM	19%	-	yes	3%	NM	NM	28	NM	NM	1178	NM	NM	0.76
SAR X2	NM	NM	93%	-	NM	NM	11%	-	NM	NM	89%	-	NM	NM	0%	-	yes	17%	NM	NM	51	NM	NM	573	NM	NM	0.63
SAR X11	NM	NM	88%	-	NM	NM	27%	-	NM	NM	64%	-	NM	NM	9%	-	yes	82%	NM	NM	129	NM	NM	1401	NM	NM	0.91
SAR X12	NM	NM	96%	-	NM	NM	9%	-	NM	NM	91%	-	NM	NM	0%	-	yes	91%	NM	NM	45	NM	NM	2801	NM	NM	0.81
SAR X13	NM	NM	87%	-	NM	NM	0%	-	NM	NM	67%	-	NM	NM	33%	-	yes	67%	NM	NM	75	NM	NM	1146	NM	NM	0.69
SAR X14	NM	NM	88%	-	NM	NM	0%	-	NM	NM	100%	-	NM	NM	0%	-	yes	100%	NM	NM	63	NM	NM	1019	NM	NM	0.90
Average	**-**	**-**	**85%**	**-**	**-**	**-**	**21%**		**-**	**-**	**69%**		**-**	**-**	**10%**		**yes**	**60%**	**-**	**-**	**65**	**-**	**-**	**1353**	**-**	**-**	**0.78**
Average all Sites	**75%**	**76%**	**86%**	**11%**	**-**	**91%**	**15%**	**-76%**	**-**	**5%**	**68%**	**63%**	**-**	**4%**	**17%**	**13%**	**yes**	**40%**	**20**	**43**	**55**	**213**	**760**	**965**	**-**	**0.71**	**0.78**

Notes:

NM - Not Measured

1- Canopy cover is a measurement of the percentage of the ground area directly covered by vertical projections of tree crowns. In the field, canopy cover is measured using a spherical densiometer standing five meters from the center of the plot in the four cardinal directions (north, south, east, west). Canopy Cover percent herein is the average of the four measurements.

2- Tree condition is a qualitative measurement of the health of the tree. Trees were assessed and classified as "live", "stressed", or "dead". The percentage of each classification per plot is shown here.

3- In 2016 trees were assessed for the presence of polyphagous shot-hole borer. If a tree showed signs of the beetle it was noted. The percent of trees in each plot that showed signs of beetle infestation was then calculated.

4- Basal area is a measurement of the amount of land occupied by the cross sectional area of tree stems. It is determined by measuring tree diameter at breast height (DBH). DBH is used to calculate the cross sectional areas of each tree stem in a plot, which are summed and divided by the total plot area.

5-Tree density is calculated by dividing the number of trees counted per plot by the plot area.

6-Crown ratio is the ratio of living crown height to total tree height. Living crown height was determined by subtracting the distance to the canopy bottom from the total height of the tree.

Table 3-2
Annual Groundwater Production in the Groundwater Monitoring Program Study Area

Water Year	Non-CDA Production (AFY) [1]	CDA Production (AFY)	Total (AFY) [1]
1961	48,577	0	48,577
1962	43,811	0	43,811
1963	43,293	0	43,293
1964	45,170	0	45,170
1965	43,294	0	43,294
1966	46,891	0	46,891
1967	42,709	0	42,709
1968	47,180	0	47,180
1969	37,754	0	37,754
1970	45,849	0	45,849
1971	45,492	0	45,492
1972	47,541	0	47,541
1973	38,427	0	38,427
1974	47,014	0	47,014
1975	44,606	0	44,606
1976	44,847	0	44,847
1977	45,710	0	45,710
1978	46,881	0	46,881
1979	48,829	0	48,829
1980	46,402	0	46,402
1981	53,326	0	53,326
1982	41,719	0	41,719
1983	42,200	0	42,200
1984	52,877	0	52,877
1985	46,876	0	46,876
1986	54,501	0	54,501
1987	46,875	0	46,875
1988	46,277	0	46,277
1989	46,835	0	46,835
1990	45,732	0	45,732
1991	42,266	0	42,266
1992	44,617	0	44,617
1993	43,186	0	43,186
1994	37,390	0	37,390
1995	32,604	0	32,604
1996	35,200	0	35,200
1997	33,340	0	33,340
1998	22,366	0	22,366
1999	23,632	0	23,632
2000	24,299	523	24,822
2001	21,249	9,470	30,719
2002	20,271	10,173	30,445
2003	18,600	10,322	28,922
2004	18,606	10,480	29,086
2005	13,695	10,595	24,290
2006	14,261	19,819	34,079
2007	12,988	28,529	41,517
2008	12,293	30,116	42,409
2009	11,694	28,456	40,150
2010	10,452	28,964	39,416
2011	10,460	28,941	39,401
2012	11,193	28,230	39,423
2013	11,433	27,380	38,813
2014	9,059	29,626	38,685
2015	6,985	29,877	36,862
2016	5,900	28,249	34,148
2017	5,899	28,351	34,250
Average: 1979-2000	41,662	23	41,685
Average: 2001-2017	12,649	22,799	35,448

1- Prior to water year 2001 production is estimated with the calibrated 2013 Chino Basin groundwater model (WEI, 2015).

Table 3-3
Analysis of Groundwater/Surface-Water Interactions in the Prado Basin and Sources of Shallow Groundwater

Location *Figure No.*	Lines of Evidence					Interpretations
	Model-Simulated Groundwater-Flow Directions	Groundwater Elevations	Surface-Water Discharge vs. Groundwater Levels	TDS in Surface Water and Groundwater	Piper Diagrams	
Chino Creek @ PB-9 *Figure 3-13a*	The simulated groundwater-flow directions (arrow symbols on the map) converge on Chino Creek, which indicates that this is an area of shallow groundwater discharge to Chino Creek.	Groundwater elevations at both PB-9 wells are typically at or above the thalweg elevation, which indicates that this is an area of groundwater discharge during these periods. There are periods when nearby pumping causes groundwater elevations in PB-9/2 to decline below the thalweg elevation, which may cause streambed recharge under these conditions. The shallow well PB-9/1 may be screened across a perched aquifer as indicated by a lack of water-level response to nearby pumping and a downward vertical gradient between the monitoring wells.	Water levels in both monitoring wells increase during and immediately after periods of stormwater discharge in Chino Creek, which suggests that stormwater discharge is a source of recharge to shallow groundwater.	TDS concentrations at both PB-9 wells are generally about 900-1,000 mg/L, similar to or slightly higher than the TDS concentrations of shallow groundwater at other nearby wells (HCMP-3/1), which suggests that the source of groundwater sampled at the PB-9 wells is primarily the shallow regional aquifer system and local concentrated return flows from precipitation and applied water. For a period of time during 2015 and 2016, the TDS concentrations at PB-9/2 (deeper wells) decreased to about 500 mg/L, similar to the TDS concentrations of the surface water. This was also a period when groundwater levels at PB-9/2 were below the thalweg, which indicates conditions of streambed recharge during this period.	Both PB-9 wells have chemistry that is similar to the regional shallow aquifer system, and is different than the surface water chemistry, which is primarily composed of effluent from IEUA's Carbon Canyon plant. This indicates that the source of water at the PB-9 wells is the shallow regional aquifer system. There were instances during 2015-2016 when the chemistry of samples from PB-9/2 were similar to the chemistry of Carbon Canyon effluent. These instances correspond to periods when groundwater levels at PB-9/2 were below the thalweg and TDS concentrations at PB-9/2 had decreased to about 500 mg/L, which suggests conditions of streambed recharge during these periods.	Chino Creek at PB-9 appears to be an area of groundwater discharge with instances of streambed recharge when groundwater levels decline below the thalweg. The likely primary sources of the shallow groundwater in this area are a perched aquifer, the shallow regional aquifer system, and local return flows from precipitation and applied water. There are some indications that streambed recharge contributes to the shallow groundwater, especially during stormwater discharge events and when groundwater levels in the shallow regional aquifer system decline below the thalweg.
Chino Creek @ PB-8 *Figure 3-13b*	The simulated groundwater-flow directions (arrow symbols on the map) converge on Chino Creek, which indicates that this is an area of shallow groundwater discharge to Chino Creek.	Groundwater elevations at both PB-8 wells are always above the thalweg elevation and show an upward vertical hydraulic gradient, both of which indicate that this is an area of groundwater discharge during the period of record.	Water levels in both monitoring wells increase during and immediately after periods of stormwater discharge in Chino Creek, which suggests that stormwater discharge is a source of recharge to shallow groundwater.	TDS concentrations at both PB-8 wells are generally about 800-900 mg/L, similar to or slightly higher than the TDS concentrations of shallow groundwater at other nearby wells, which suggests that the source of groundwater sampled at the PB-8 wells is primarily the shallow regional aquifer system and local concentrated return flows from precipitation and applied water.	Both PB-8 wells have chemistry that is similar to the regional shallow aquifer system, and is different than the surface water chemistry of Chino Creek, which is primarily composed of effluent from IEUA's Carbon Canyon and RP-5 plants. This indicates that the source of water at the PB-8 wells is the shallow regional aquifer system.	Chino Creek at PB-8 appears to be an area of groundwater discharge. The likely primary sources of the shallow groundwater in this area are the shallow regional aquifer system and local return flows from precipitation and applied water. There are some indications that streambed recharge contributes to the shallow groundwater, especially during stormwater discharge events.
Chino Creek @ PB-7 *Figure 3-13c*	The simulated groundwater-flow directions (arrow symbols on the map) converge on Chino Creek, which indicates that this is an area of shallow groundwater discharge to Chino Creek.	Groundwater elevations at both PB-7 wells are typically above the thalweg elevation and show an upward vertical hydraulic gradient, both of which indicate that this is an area of groundwater discharge during the period of record.	Water levels in both monitoring wells increase during and immediately after periods of stormwater discharge in Chino Creek and the formation of a reservoir behind Prado Dam, which suggests that stormwater discharge is a source of recharge to shallow groundwater.	TDS concentrations at the PB-7/1 (shallow well) range between 800-1,300 mg/L, similar to the TDS concentrations of shallow groundwater at other nearby wells, which suggests that the source of groundwater sampled at the PB-7/1 well is primarily the shallow regional aquifer system. The TDS concentrations at PB-7/2 (deeper well) display a decreasing trend with concentrations as low as 270 mg/L that are typically associated with stormwater.	The general-mineral chemistry for the PB-7 wells do not cluster on the piper diagram--not with each other or from sample to sample. This indicates: multiple and different sources of water for each well and complex and transient groundwater/surface-water interactions. The general-mineral chemistry for PB-7/1 (shallow well) plots on the piper diagram closest to the chemistry of groundwater sampled from other nearby wells that are screened across the regional shallow aquifer system. The chemistry for PB-7/2 plots in a different location on the piper diagram and migrates away from the chemistry of shallow groundwater and surface water (primarily effluent and dry-weather flow). This may indicate a stormwater source for PB-7/2.	Chino Creek at PB-7 appears to be an area of groundwater discharge. The likely primary source of the shallow groundwater in this area is the shallow regional aquifer system. However, the groundwater/surface-water interactions in this area appear to be complex with multiple and transient sources of water that are tributary to the PB-7 wells. Additional monitoring and testing are needed to better characterize the source waters and the groundwater/surface-water interactions.

Table 3-3
Analysis of Groundwater/Surface-Water Interactions in the Prado Basin and Sources of Shallow Groundwater

Location *Figure No.*	Lines of Evidence					Interpretations
	Model-Simulated Groundwater-Flow Directions	Groundwater Elevations	Surface-Water Discharge vs. Groundwater Levels	TDS in Surface Water and Groundwater	Piper Diagrams	
Chino Creek @ PB-6 *Figure 3-13d*	The simulated groundwater-flow directions (arrow symbols on the map) converge on Chino Creek, which indicates that this is an area of shallow groundwater discharge to Chino Creek.	Groundwater elevations at both PB-6 wells are at or near the thalweg elevation and show no vertical gradient, which indicates that this can be an area of groundwater discharge and/or streambed recharge.	Water levels in both monitoring wells increase during and immediately after periods of stormwater discharge in Chino Creek and the formation of a reservoir behind Prado Dam, which suggests that stormwater discharge is a source of recharge to shallow groundwater.	TDS concentrations at the PB-6/1 (shallow well) range between 420-1,200 mg/L, which is similar to the TDS concentrations of shallow groundwater at nearby wells when the TDS is higher, and is similar to the surface-water discharge or stormwater when the TDS is lower. This suggests a transient mixture of sources of groundwater sampled at the PB-6/1 well. The TDS concentrations at PB-6/2 (deeper well) range between 320-410 mg/L, which is slightly lower than the surface-water discharge, which suggest that the source of groundwater sampled at PB-6/2 is influenced by stormwater recharge.	The general-mineral chemistry for PB-6/1 (shallow well) plots on the piper diagram similar to the chemistry of groundwater sampled from nearby wells that are screened across the regional shallow aquifer system; and other times the chemistry for PB-6/1 plots in different locations away from the chemistry of shallow groundwater and surface water. This indicates that the source of water at the PB-6/1 is sometimes influenced by the shallow regional aquifer system, and at other times by other sources (possibly stormwater). The chemistry for PB-6/2 plots on the Piper diagram in a location away from the general-mineral chemistry of shallow groundwater and surface water. This indicates another source water for PB-6/2, possibly stormwater.	Chino Creek at PB-6 appears to be an area of both groundwater discharge and streambed recharge. The likely sources of the shallow groundwater in this area are the shallow regional aquifer system and streambed recharge. However, the groundwater/surface-water interactions in this area appear to be complex with multiple and transient sources of water that are tributary to the PB-6 wells. Additional monitoring and testing are needed to better characterize the source waters and the groundwater/surface-water interactions.
Mill Creek @ PB-2 *Figure 3-13e*	The simulated groundwater-flow directions (arrow symbols on the map) diverge from Mill Creek, which indicates that this is an area of streambed recharge.	Groundwater elevations at PB-2 (shallow well) are typically at or above the thalweg elevation which indicates that this is an area of groundwater discharge. Groundwater elevations at HCMP-5/1 (deeper well) are below the thalweg elevation which indicates the potential for streambed recharge. The shallow well PB-2 may be screened across a perched aquifer as indicated by a downward vertical gradient between the monitoring wells, and that the groundwater elevations in the regional aquifer system (HCMP-5/1) are below the thalweg.	Water levels in both monitoring wells increase during and immediately after periods of stormwater discharge in Mill Creek, which suggests that stormwater discharge is a source of recharge to shallow groundwater.	TDS concentrations at both PB-2 wells (PB-2 and HCMP-5/1) are generally about 2,500-4,500 mg/L, which is higher than the TDS concentrations of shallow groundwater at nearby wells and the surface water in Mill Creek. This observation suggests that the source of groundwater sampled at the PB-2 wells is influenced by local concentrated return flows of precipitation and applied water.	Both PB-2 wells (PB-2 and HCMP-5/1) have general-mineral chemistry that is similar to the regional shallow aquifer system, and is different than the surface water chemistry of Mill Creek. This indicates that the source of water at the PB-2 wells is influenced by the shallow regional aquifer system.	Mill Creek to the south of PB-2 appears to be an area of streambed recharge at the location were the lined Cucamonga Creek ends and the unlined Mill Creek begins. However the primary sources of the shallow groundwater near PB-2 is the shallow regional aquifer system and/or perched groundwater recharged by local return flows from precipitation and applied water.
Mill Creek @ PB-1 *Figure 3-13f*	Directly upstream of this area, the groundwater-flow directions diverge from Mill Creek, which indicates an area of streambed recharge to Mill Creek. The simulated groundwater-flow directions then converge on Mill Creek near PB-1, which indicates that the streambed recharge upstream in Mill Creek then becomes shallow groundwater discharge to Mill Creek near PB-1.	Groundwater elevations at both PB-1 wells are always at or above the thalweg elevation and show an upward vertical hydraulic gradient, both of which indicate that this is an area of groundwater discharge during the period of record.	Water levels in both monitoring wells increase during and immediately after periods of stormwater discharge in Mill Creek, which suggests that stormwater discharge is a source of recharge to shallow groundwater.	TDS concentrations at PB-1/1 (shallow well) are about 2,500-3,000 mg/L, similar to the TDS concentrations of shallow groundwater at nearby wells (HCMP-6/1), which suggests that the source of groundwater sampled at the PB-1/1 is primarily the shallow regional aquifer system and/or local concentrated return flows from precipitation and applied water. TDS concentrations at PB-1/2 (deeper well) range from 440-590 mg/L, similar to the surface-water discharge in Mill Creek, which suggest that the source of groundwater sampled at the PB-1/2 is streambed recharge that occurs upstream from PB-1.	The general-mineral chemistry for PB-1/1 (shallow well) plots on the Piper diagram closest to the chemistry of groundwater sampled from nearby wells that are screened across the regional shallow aquifer system. The general-mineral chemistry for PB-1/2 plots near the chemistry of the surface water (primarily effluent), which indicates a surface water source for PB-1/2.	Mill Creek at PB-1 appears to be an area of groundwater discharge. The primary source of the shallow groundwater at PB-1 appears to be a complex mixture of the shallow regional aquifer system that is fed, in part, by streambed recharge in upstream areas of Mill Creek. The groundwater/surface-water interactions in this area appear to be complex with multiple sources of water that are tributary to the PB-5 wells. Additional monitoring and testing are needed to better characterize the source waters and the groundwater/surface-water interactions.

Table 3-3
Analysis of Groundwater/Surface-Water Interactions in the Prado Basin and Sources of Shallow Groundwater

Location *Figure No.*	Lines of Evidence: Model-Simulated Groundwater-Flow Directions	Lines of Evidence: Groundwater Elevations	Lines of Evidence: Surface-Water Discharge vs. Groundwater Levels	Lines of Evidence: TDS in Surface Water and Groundwater	Lines of Evidence: Piper Diagrams	Interpretations
Mill Creek @ PB-5 *Figure 3-13g*	The simulated groundwater-flow directions (arrow symbols on the map) converge on Mill Creek, which indicates that this is an area of groundwater discharge to Mill Creek.	Groundwater elevations at both PB-5 wells are always above the thalweg elevation on Mill Creek, which indicates that this is an area of groundwater discharge during the period of record.	Water levels in both monitoring wells increase during and immediately after periods of stormwater discharge in Mill Creek, which suggests that stormwater discharge is a source of recharge to shallow groundwater.	TDS concentrations at PB-5/1 (shallow well) ranges from 590-690 mg/L which is slightly higher than the TDS concentrations in surface water discharge, and much lower than TDS concentrations of shallow groundwater of 3,000 mg/L. TDS concentrations at PB-5/2 (deeper well) ranges from 350-440 mg/L, which is slightly lower than the surface water discharge and slightly higher than deeper groundwater. The TDS concentrations at both wells suggests that the source of groundwater sampled at the PB-5 wells is likely multiple sources: primarily deeper rising groundwatrer and shallow groundwater influence by nearby streambed recharge of effluent from WRCRWTP and IEUA's RP-1 plant to Cucamonga Creek. The lower TDS concentrations at PB-5/2 suggest some influence of deeper groundwater.	The general-mineral chemistry for both PB-5 wells plots on the Piper diagram between the chemistry of the surface water (primarily effluent), shallow groundwater, and deeper groundwater, which suggest that the sources of shallow groundwater at PB-5 are a complex mixture of nearby streambed recharge and rising groundwater.	Mill Creek at PB-5 appears to be an area of groundwater discharge. The likely source of shallow groundwater at PB-5 is a complex mixture of: (i) streambed recharge of effluent discharge in upstream areas of Mill Creek, the SAR, and the diversion channel that conveys WRCRWTP effluent to the OCWD Wetlands and (ii) rising groundwater discharge. Additional monitoring and testing are needed to better characterize the source waters and the groundwater/surface-water interactions.
SAR @ PB-4 *Figure 3-13h*	The simulated groundwater-flow directions (arrow symbols on the map) diverge from the SAR, which indicates that this is an area of streambed recharge of the SAR.	Groundwater elevations at both PB-4 wells are below the thalweg elevation, which indicates that this is an area of streambed recharge during the period of record.	Water levels in both monitoring wells increase slightly during and immediately after periods of stormwater discharge in the SAR, which suggests that stormwater discharge is a source of recharge to shallow groundwater.	TDS concentrations at PB-4/1 (shallow well) fluctuate between 730-1,500 mg/L; the lower range of TDS concentrations are similar to the TDS concentrations in baseflow of the SAR, while the higher TDS concentrations are similar to the TDS concentrations of shallow groundwater at other nearby wells. This suggests that the source of groundwater sampled at PB-4/1 well is influenced by streambed recharge of the SAR, the shallow regional aquifer system, and/or local return flows of precipitation and applied water. TDS concentrations at PB-4/2 (deeper well) range from 650-810 mg/L which is similar to the TDS concentrations in SAR baseflow, which suggests that the source of groundwater sampled at PB-4/2 is streambed recharge.	The general-mineral chemistry for both PB-4 wells plot on the Piper diagram between the chemistry of the surface water (baseflow of the SAR) and nearby wells, which indicates that the source of the shallow groundwater at PB-4 is streambed recharge of the SAR, the shallow regional aquifer system, and/or local return flows of precipitation and applied water.	The SAR at PB-4 is primarily an area of streambed recharge. The primary source of shallow groundwater at PB-4 is streambed recharge of the SAR, and at times there appears to be some influence of the shallow regional aquifer system and/or local return flows of precipitation and applied water.
SAR @ PB-3 *Figure 3-13i*	The simulated groundwater-flow directions (arrow symbols on the map) diverge from the SAR, which indicates that this is an area of streambed recharge of the SAR.	Groundwater elevations at both PB-3 wells are below the thalweg elevation, which indicates that this is an area of streambed recharge during the period of record.	Water levels in both monitoring wells increase slightly during and immediately after periods of stormwater discharge in the SAR, which suggests that stormwater discharge is a source of recharge to shallow groundwater.	TDS concentrations at both PB-9 wells are generally about 500-700 mg/L, which are similar to the baseflow of the SAR and suggests that the source of groundwater sampled at the PB-3 wells is streambed recharge of the SAR.	The general-mineral chemistry for both PB-3 wells plots on the Piper diagram near the general-mineral chemistry of the baseflow of the SAR, which indicates the source of groundwater sampled at the PB-3 wells is streambed recharge of the SAR.	The SAR at PB-3 is an area of streambed recharge. The primary source of shallow groundwater at PB-3 is streambed recharge of the SAR.

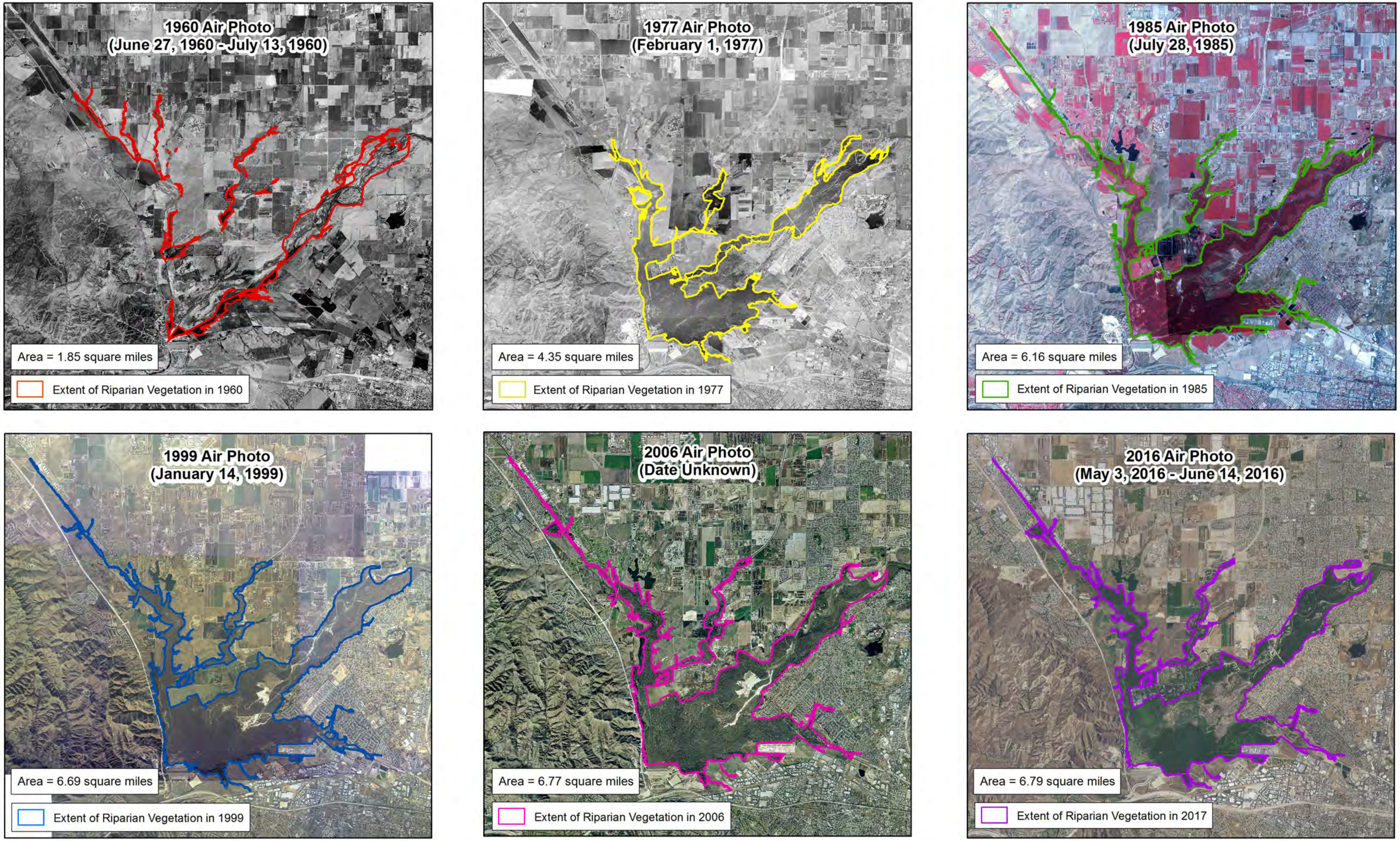

Prepared by:

WEI
Wildermuth Environmental, Inc.

Author: VMW
Date: 3/16/2018
File: 2017_Figure 3-1a_AirPhotos_VegExtent

0 1 2 Miles
0 1 2 3 KM

2017 Annual Report
Prado Basin Habitat Sustainability Committee

Historical Air Photos and Extent of Riparian Vegetation
1960 to 2016

Figure 3-1a

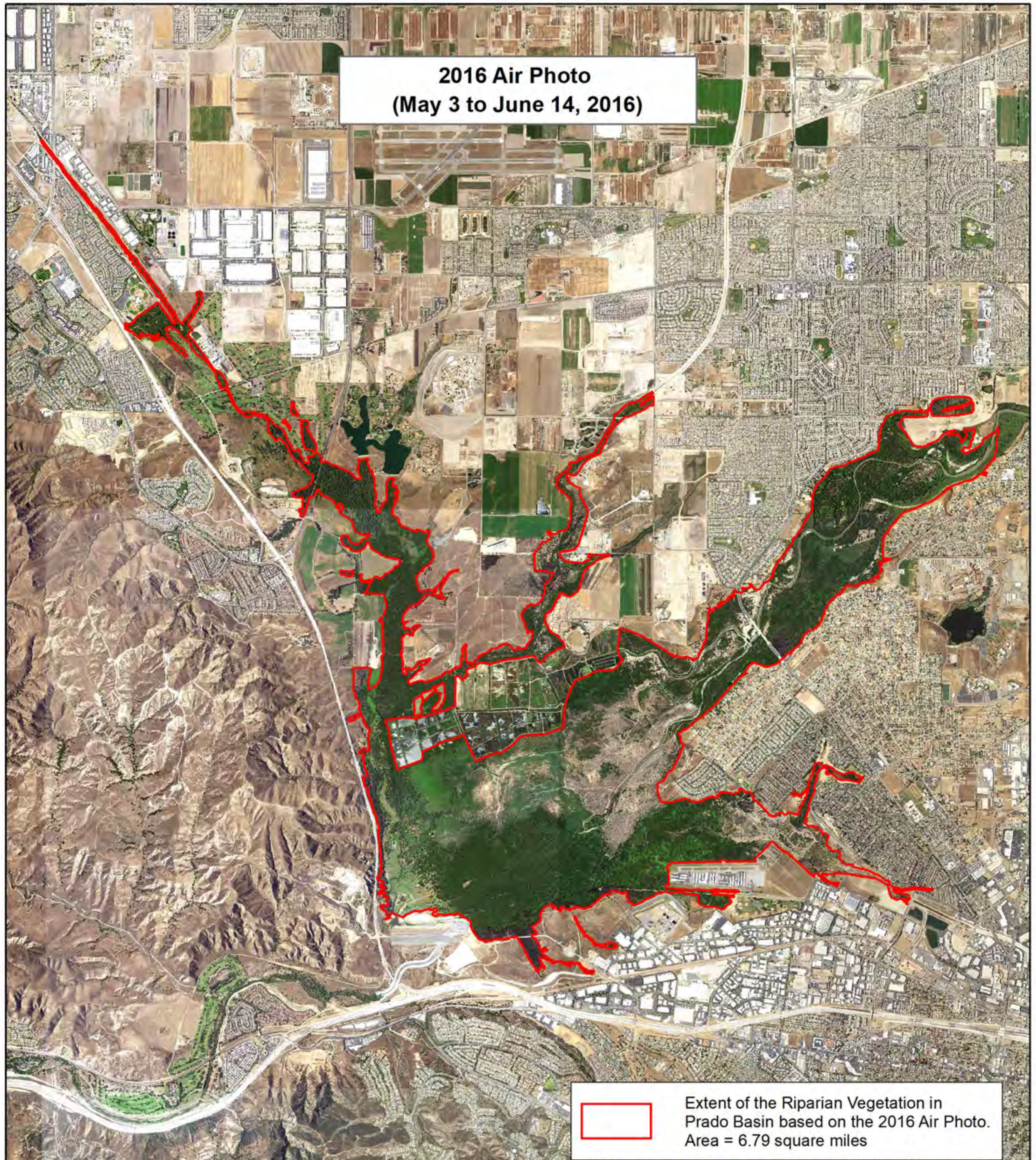

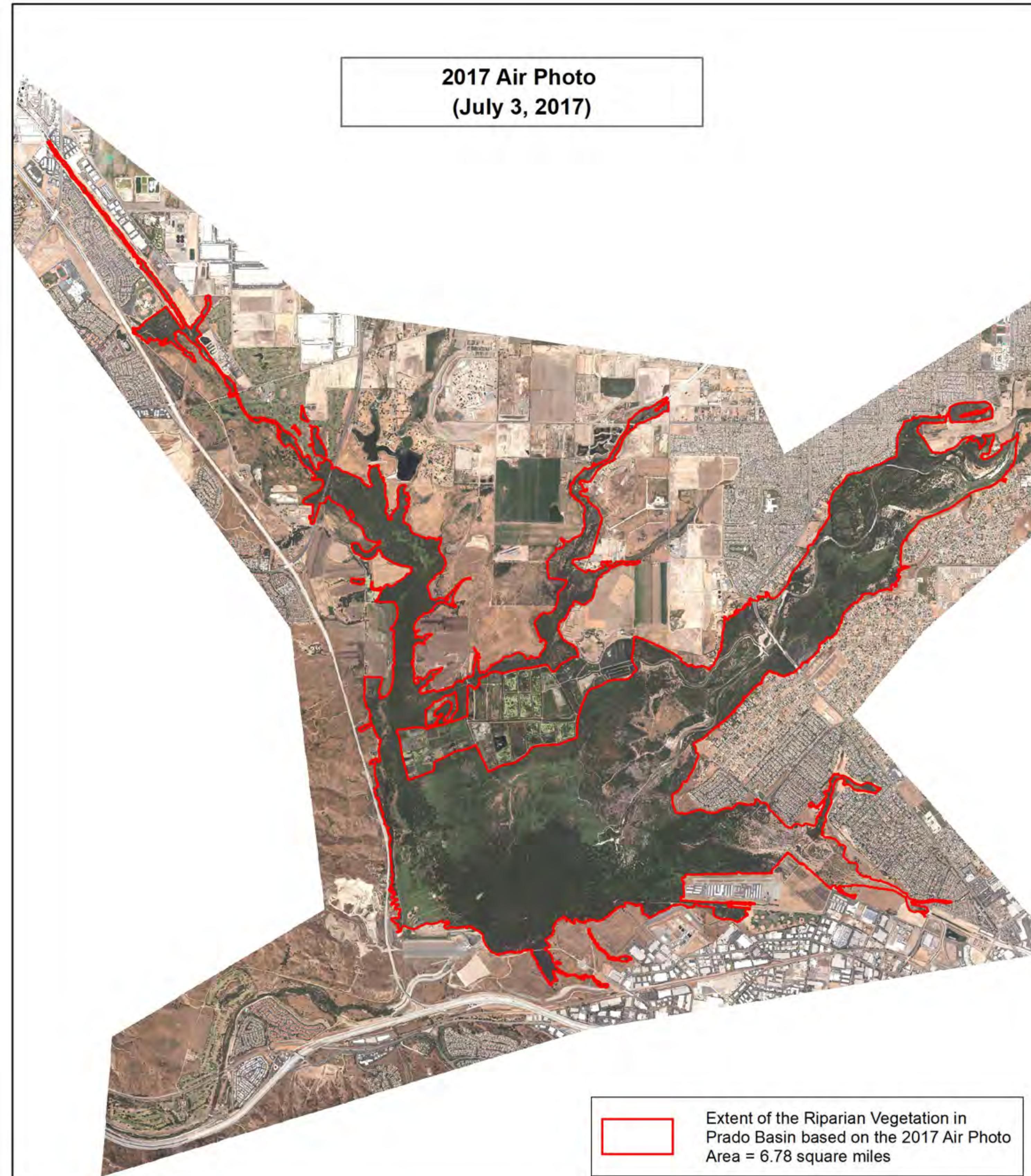

Prepared by:

WEI
WILDERMUTH ENVIRONMENTAL, INC.

Author: SO
Date: 4/5/2018
File: 2017_Figure 3-1b_2016 and 2017 Air Photos

0 1 2 Miles
0 1 2 3 KM

2017 Annual Report
Prado Basin Habitat Sustainability Committee

Air Photos and Extent of the Riparian Vegetation
2016 and 2017

Figure 3-1b

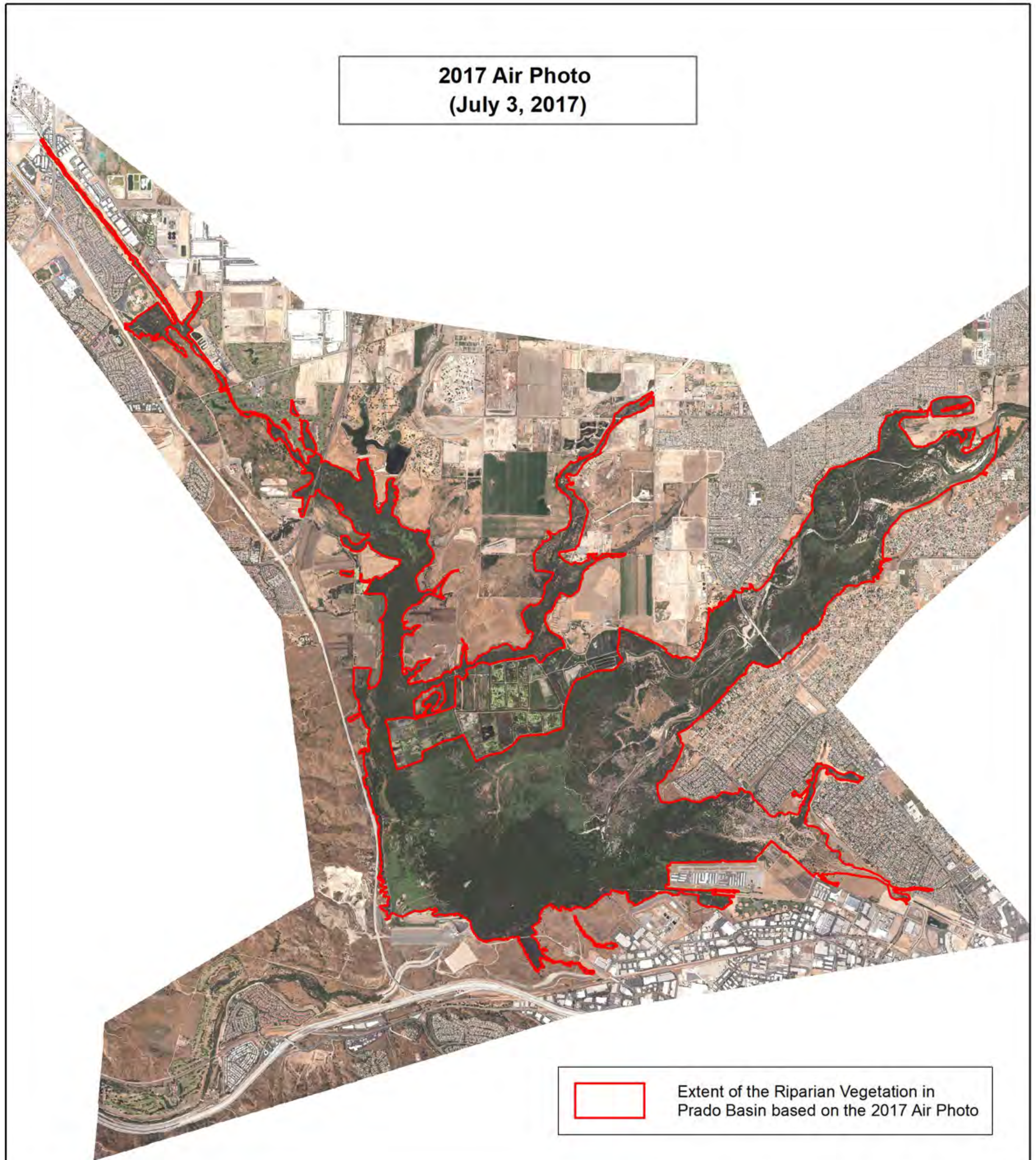

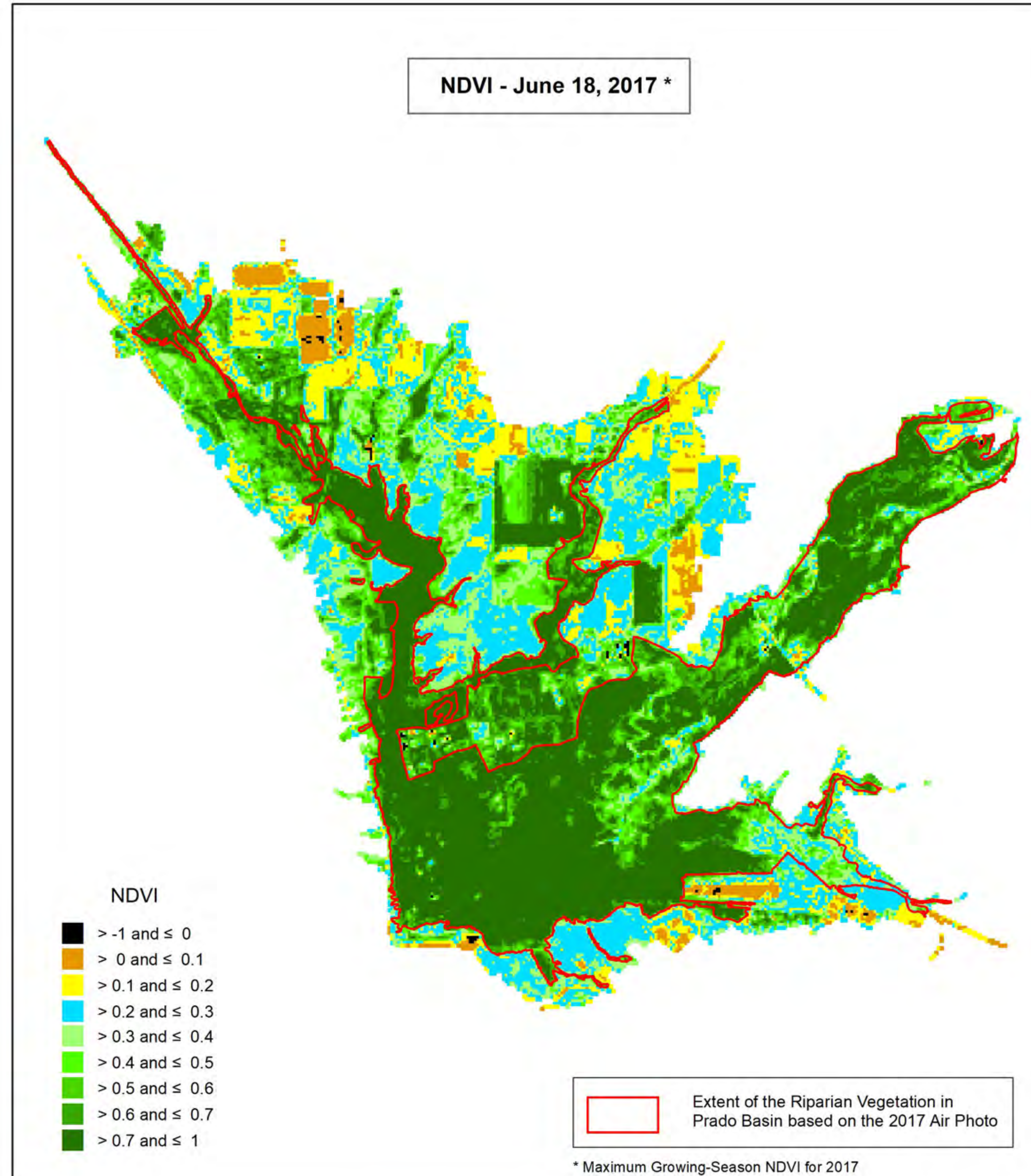

Prepared by:

WEI
WILDERMUTH ENVIRONMENTAL, INC.

Author: RT
Date: 4/18/2018
File: 2017_Figure 3-1c_2017_Prado_AirP_NDVI

0 1 2 Miles
0 1 2 3 KM

2017 Annual Report
Prado Basin Habitat Sustainability Committee

2017 Air Photo and Spatial NDVI for the Prado Basin Area

Figure 3-1c

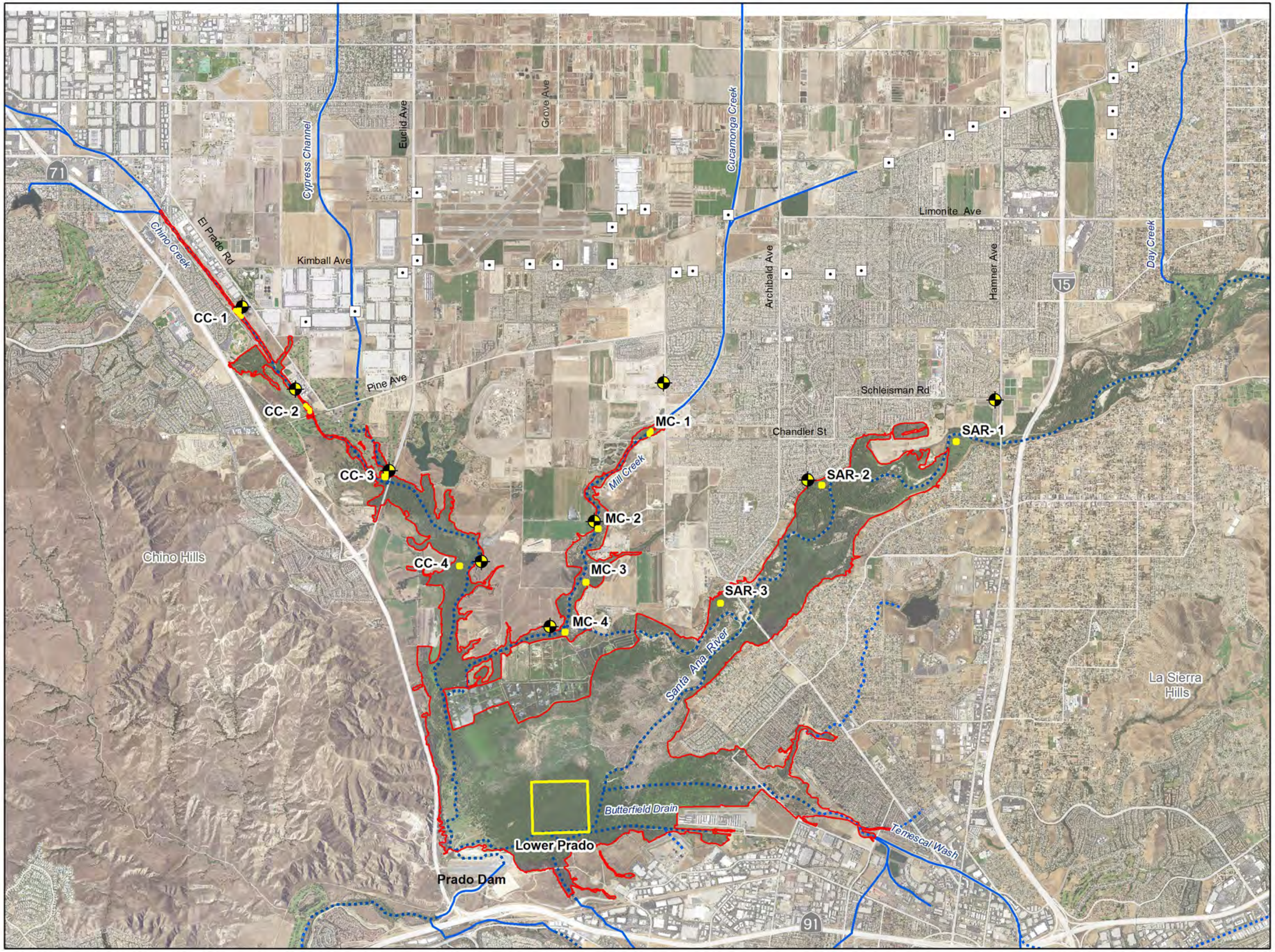

Defined Areas Analyzed for NDVI Temporally in Time-Series Charts

- 2017 Extent of Riparian Vegetation in Prado Basin (Figure 3-4)
- 0.26 square mile area (650 NDVI pixels) in Lower Prado (Figure 3-5)
- 3,600 square-meter area (four NDVI pixels) (Figures 3-6a through 3-6k)
- PBHSP Monitoring Well Site
- Chino Basin Desalter Authority Well
- Concrete-Lined Channels
- Unlined Rivers and Streams

Aerial Photo: USDA, 2016. Mosaic of photos from June 2, 2016 to June14, 2016

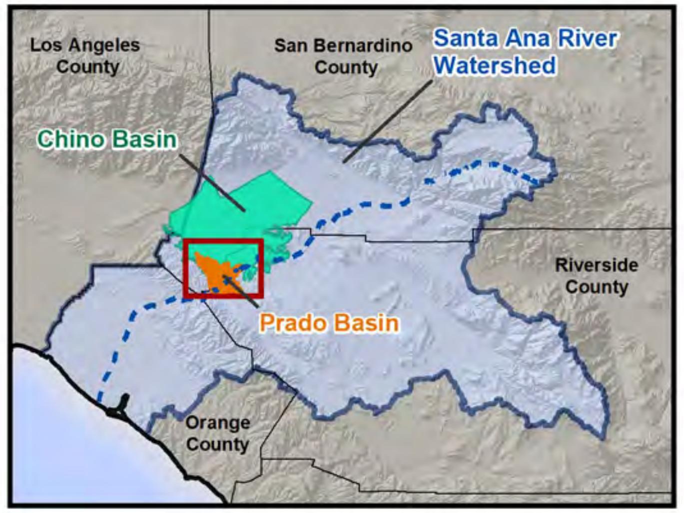

Prepared by:

WEI
Wildermuth Environmental, Inc.

Author: VMW
Date: 4/4/2018
File: 2017_Figure 3-2 Veg Monitoring_NDVI_Sites

0 1 2 Miles
0 1 2 3 KM

2017 Annual Report
Prado Basin Habitat Sustainability Committee

Areas for Analysis of NDVI Time Series

Figure 3-2

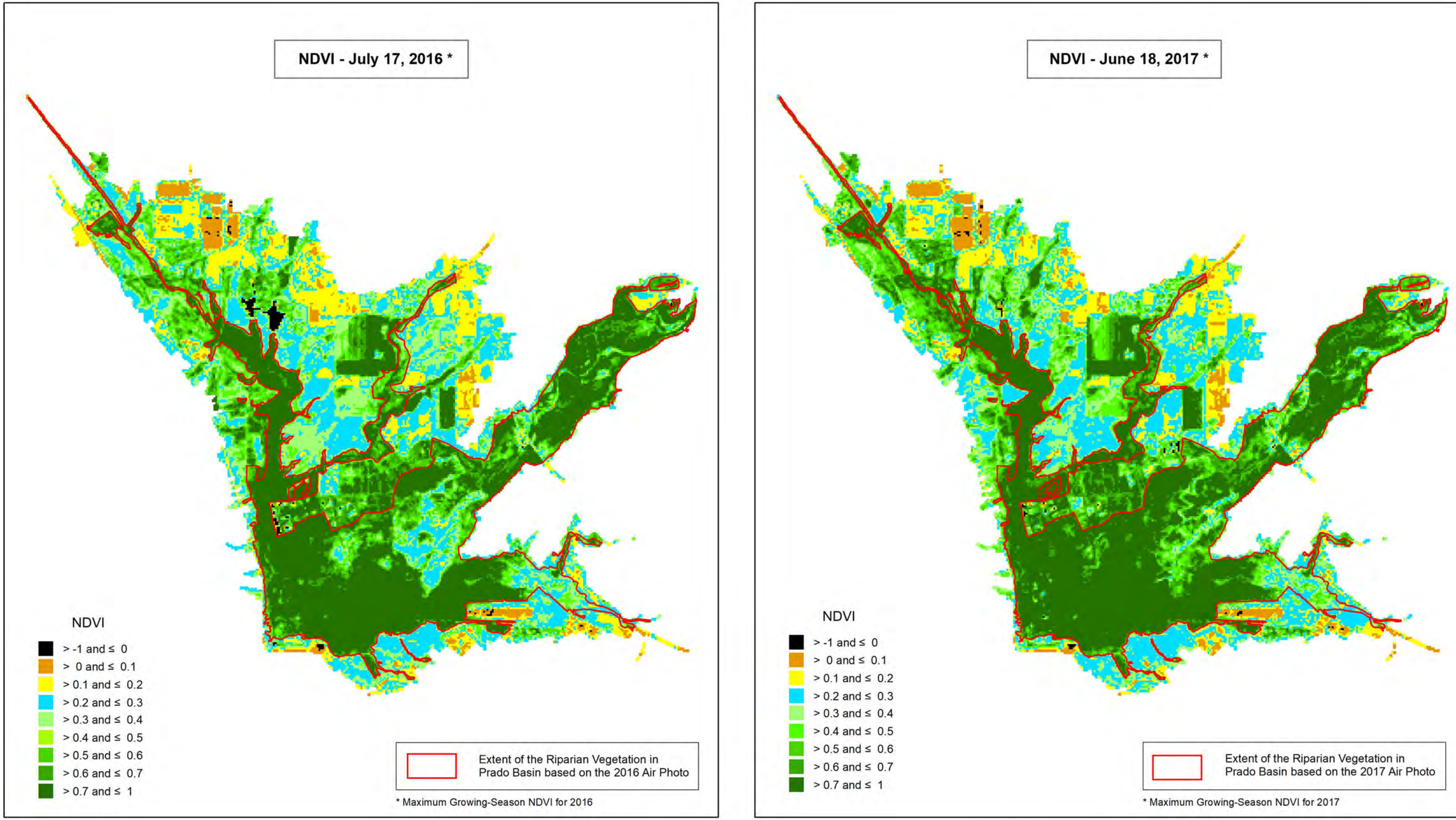

Prepared by:

WEI
WILDERMUTH ENVIRONMENTAL, INC.

Author: RT
Date: 4/18/2018
File: 2017_Figure 3-3_2016_2017_NDVI

0 1 2 Miles
0 1 2 3 KM

2017 Annual Report
Prado Basin Habitat Sustainability Committee

Spatial NDVI of the Prado Basin
2016 and 2017

Figure 3-3

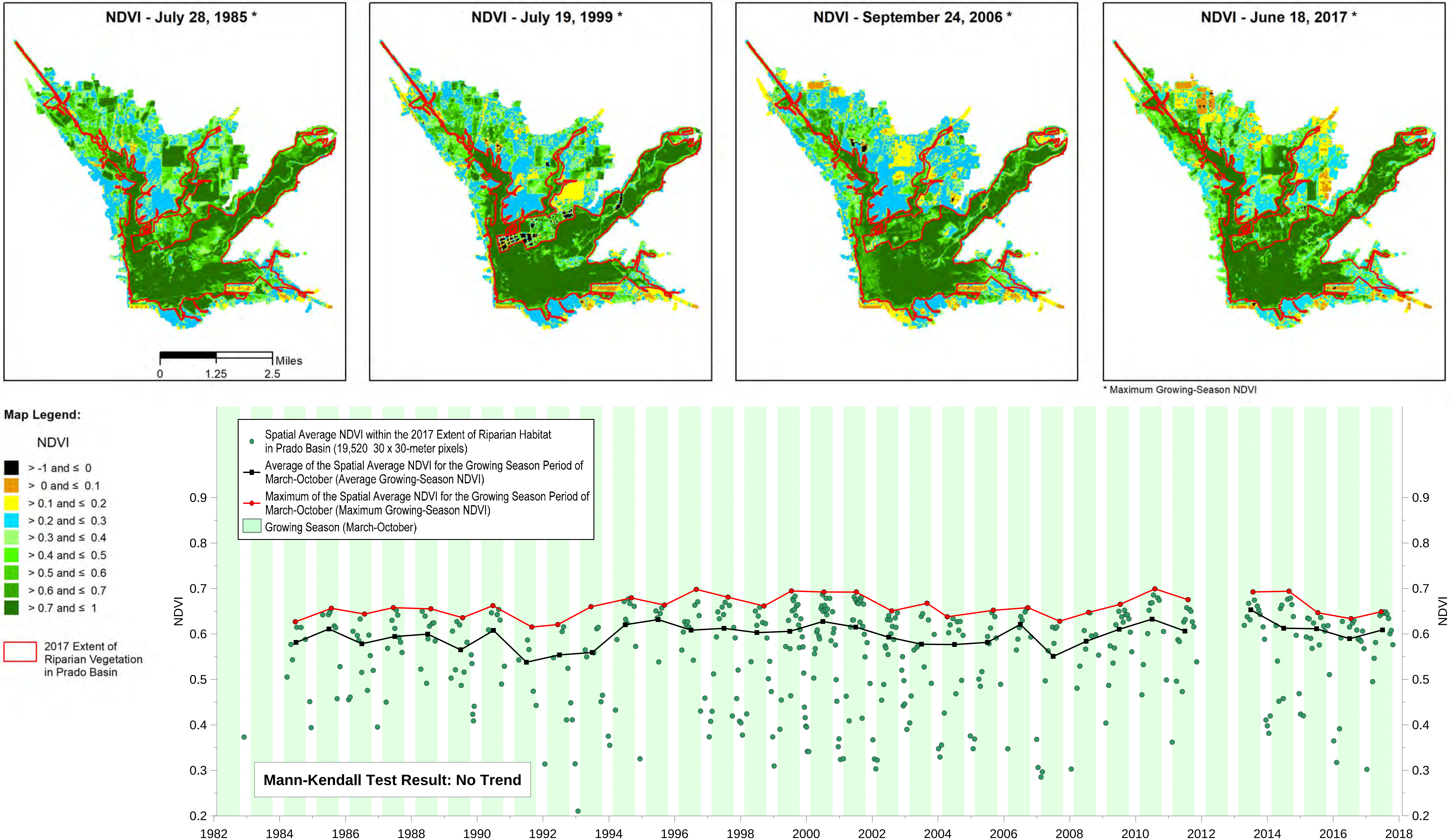

Prepared by:

WEI
Wildermuth Environmental, Inc.

Author: RT
Date: 20180129
Filename: NDVI_Prado Regional.grf

2017 Annual Report
Prado Basin Habitat Sustainability Committee

Time Series of NDVI for the 2017 Riparian Vegetaion Extent - *1984 to 2017*

Figure 3-4

1999 Air Photo (January 14, 1999)

2006 Air Photo (Date Unknown)

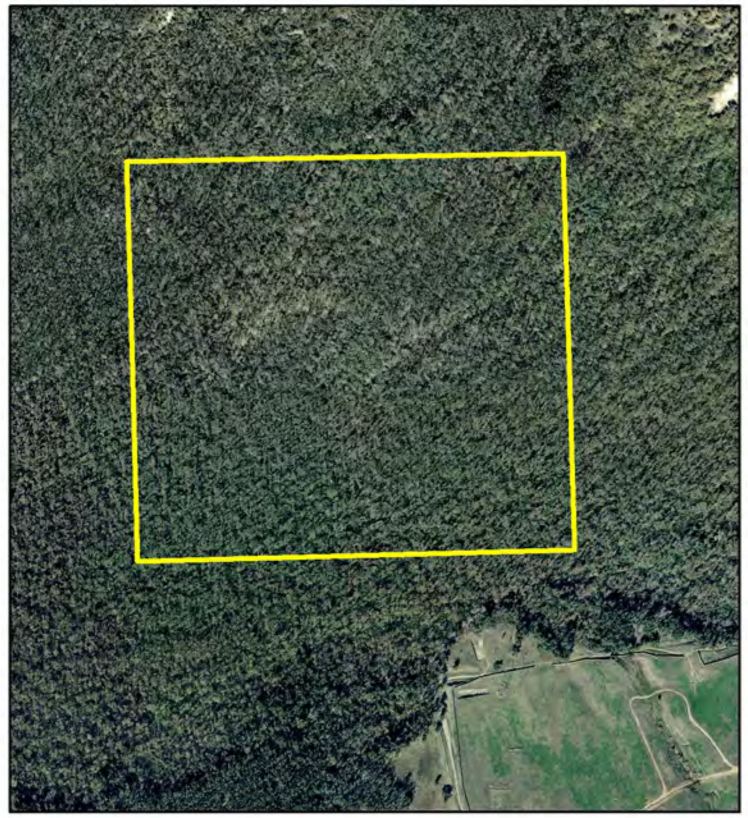

2016 Air Photo (May 3 to June 14, 2016)

2017 Air Photo (July 3, 2017)

0.26-Square Mile Area
(650 30 x 30 meter pixels)

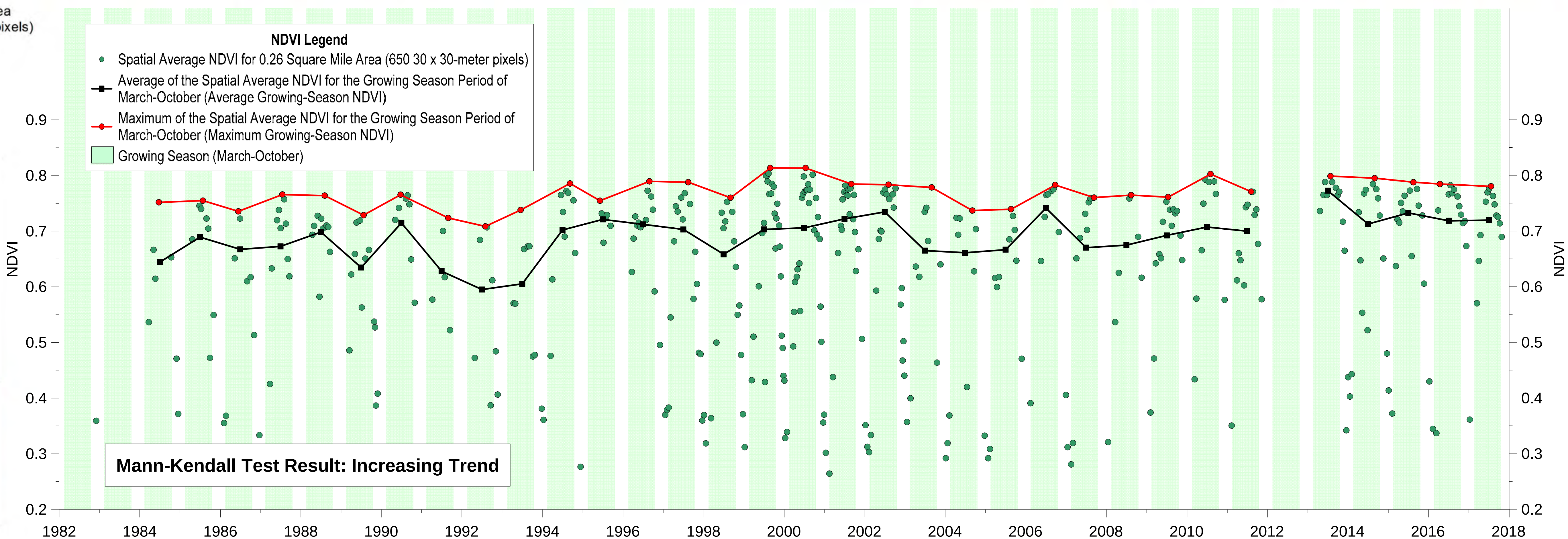

Location Along Lower Prado

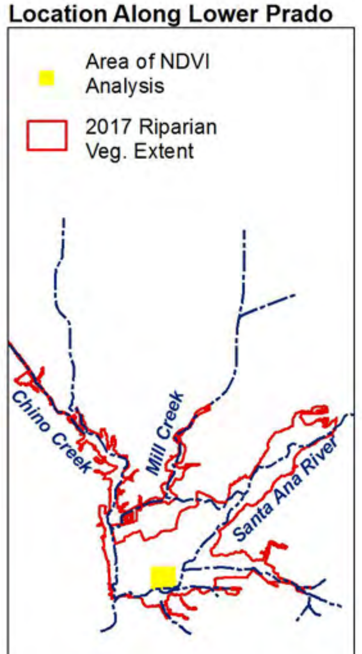

Prepared by:
WEI
Wildermuth Environmental, Inc.

Author: RT
Date: 20171122
Filename: NDVI_Lower Prado_AirPhotos.grf

2017 Annual Report
Prado Basin Habitat Sustainability Committee

Time Series of NDVI and Air Photos
Lower Prado Area for 1984 to 2017

Figure 3-5

1999 Air Photo (January 14, 1999)

2006 Air Photo (Date Unknown)

2016 Air Photo (May 3 to June 14, 2016)

2017 Air Photo (July 3, 2017)

NDVI 30 x 30 Meter Pixel

Location Along Chino Creek

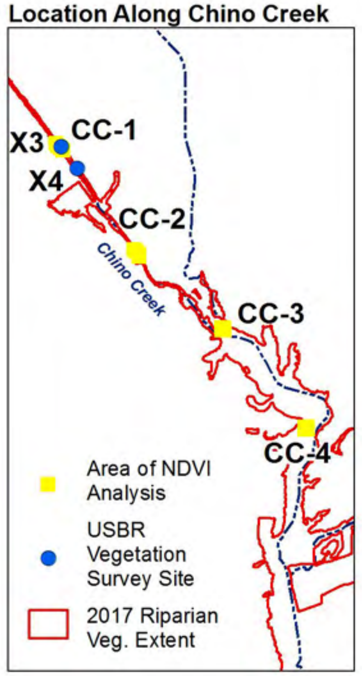

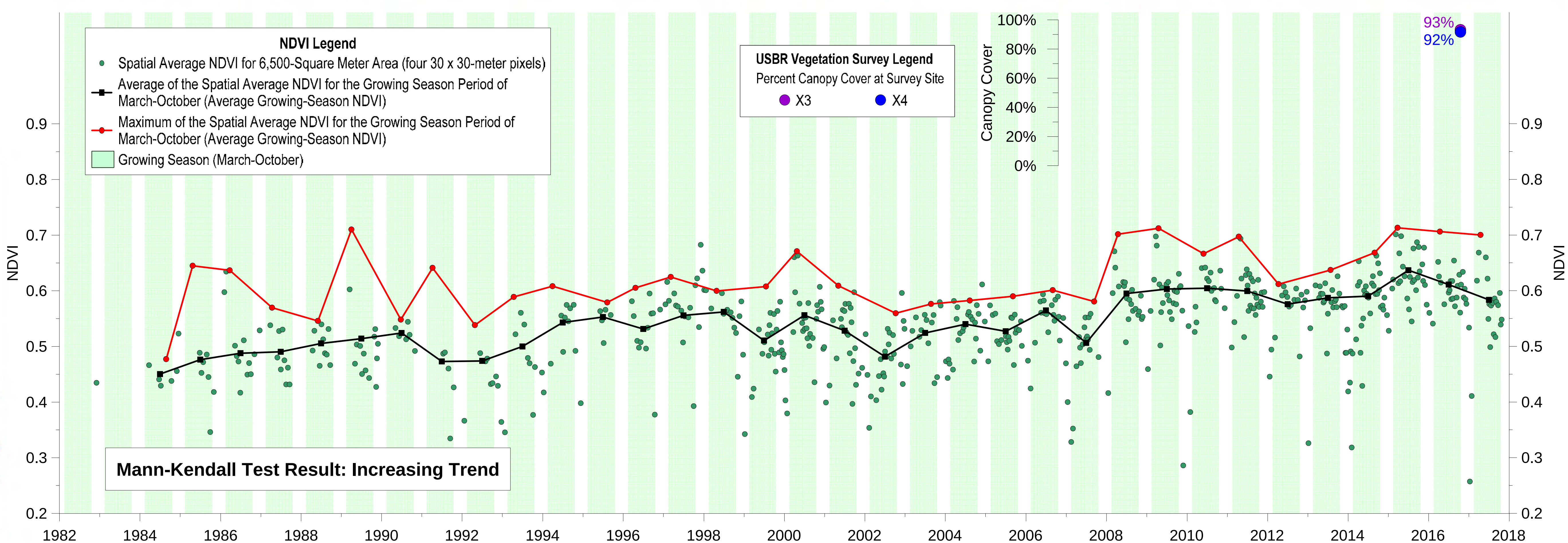

Prepared by:

WEI Wildermuth Environmental, Inc.

Author: RT
Date: 20171122
Filename: NDVI_CC-1_Airphoto.grf

2017 Annual Report
Prado Basin Habitat Sustainability Committee

Time Series of NDVI and Air Photos
CC-1 Area for 1984 to 2017

Figure 3-6a

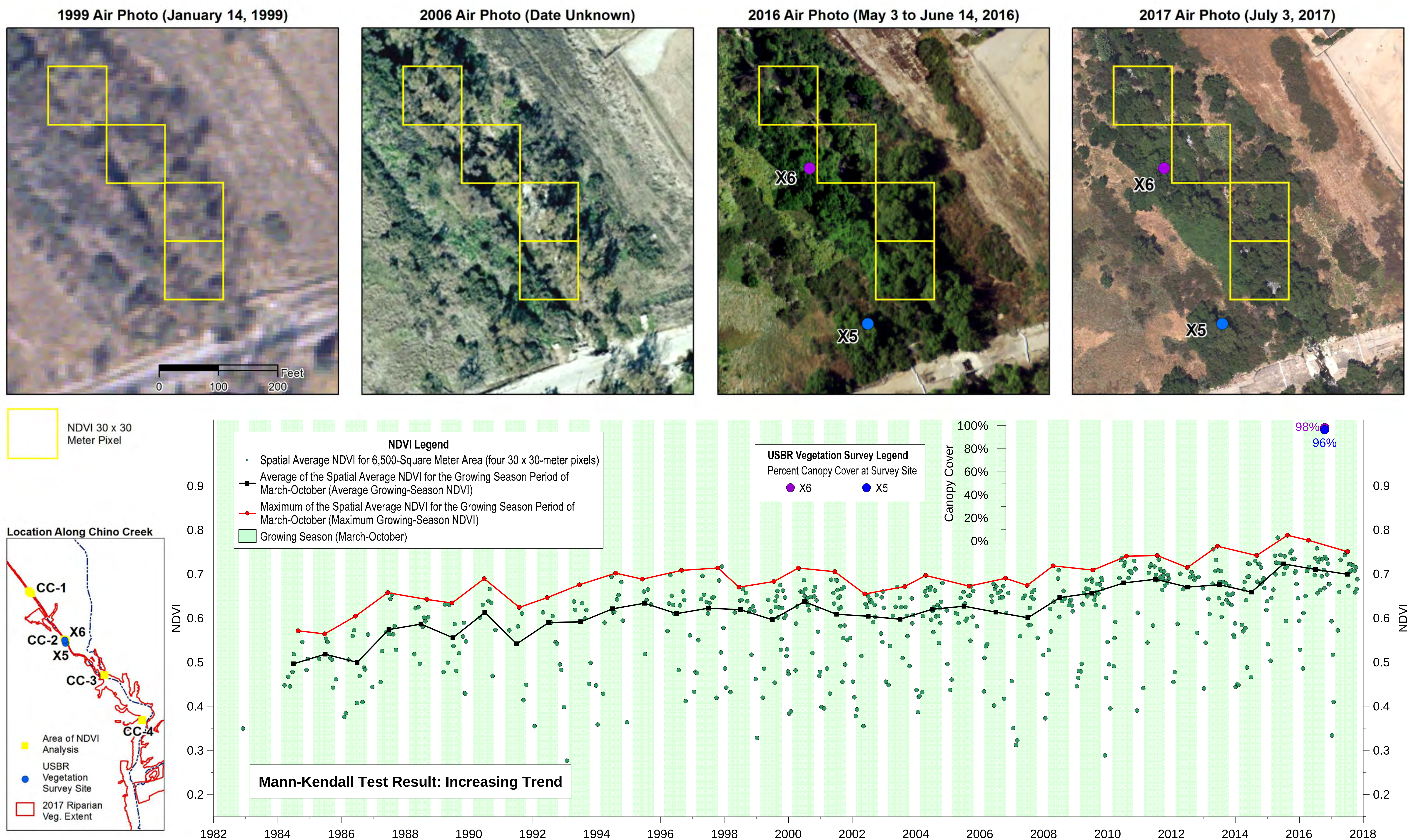

Prepared by:

WEI
WILDERMUTH ENVIRONMENTAL, INC.

Author: RT
Date: 20171122
Filename: NDVI_CC-2_Airphoto.grf

2017 Annual Report
Prado Basin Habitat Sustainability Committee

Time Series of NDVI and Air Photos
CC-2 Area for 1984 to 2017

Figure 3-6b

1999 Air Photo (January 14, 1999)

2006 Air Photo (Date Unknown)

2016 Air Photo (May 3 to June 14, 2016)

2017 Air Photo (July 3, 2017)

NDVI 30 x 30 Meter Pixel

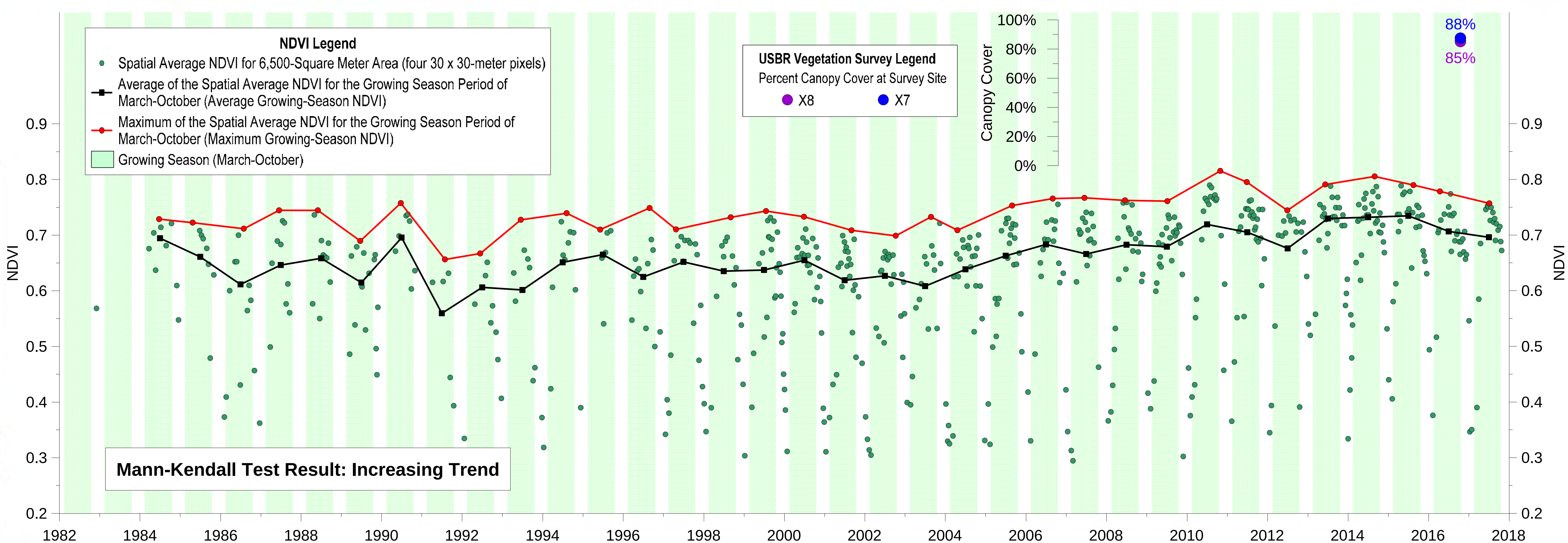

Location Along Chino Creek

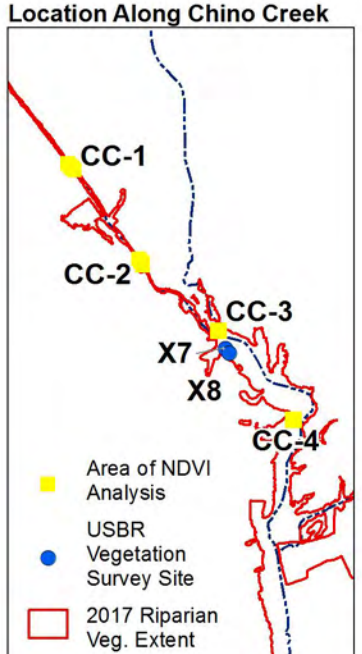

Prepared by:

WEI
Wildermuth Environmental, Inc.

Author: RT
Date: 20171122
Filename: NDVI_CC-3_AirPhoto.grf

2017 Annual Report
Prado Basin Habitat Sustainability Committee

Time Series of NDVI and Air Photos
CC-3 Area for 1984 to 2017

Figure 3-6c

1999 Air Photo (January 14, 1999)

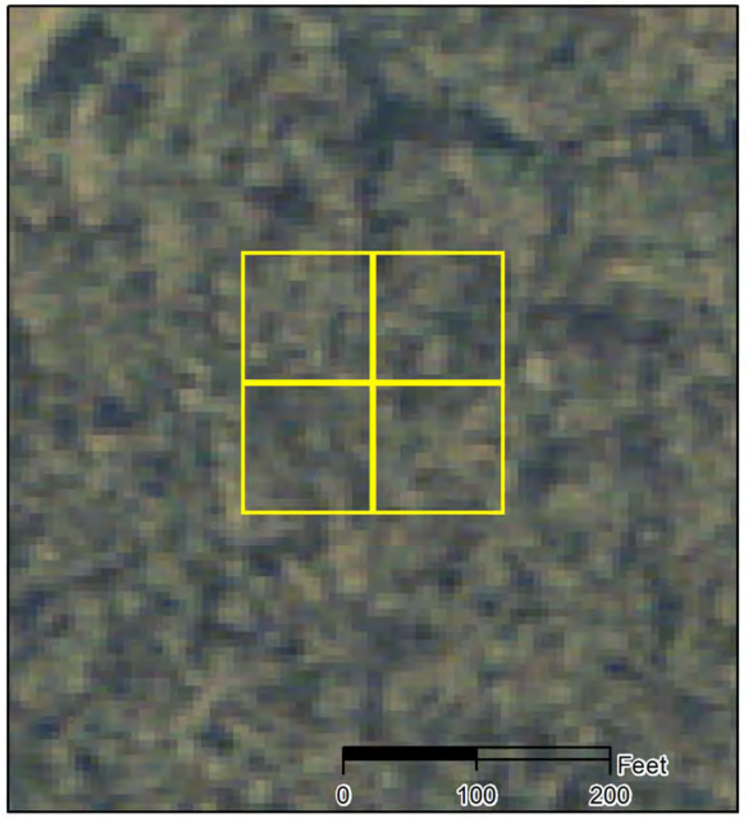

2006 Air Photo (Date Unknown)

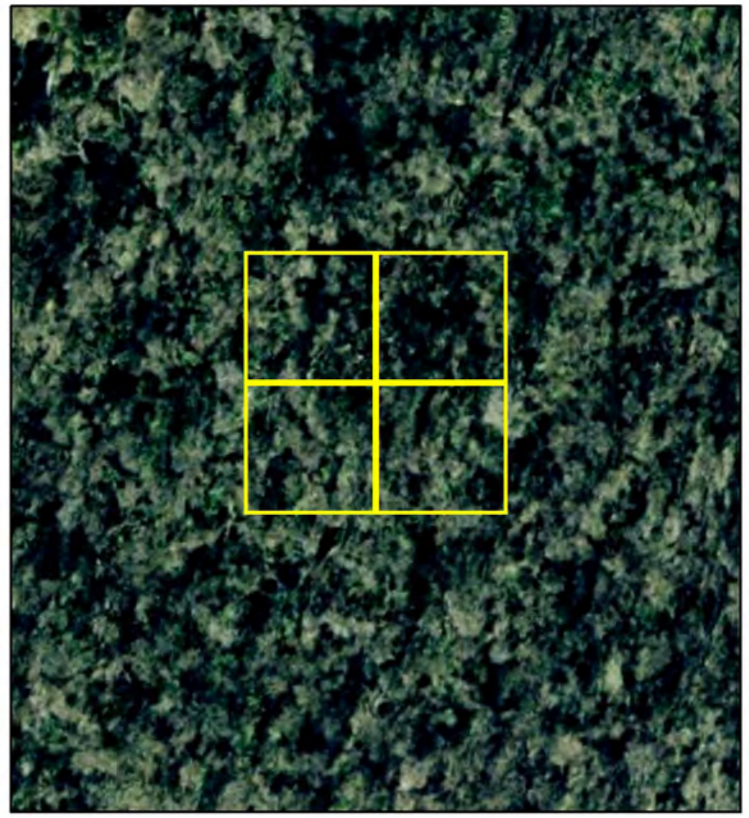

2016 Air Photo (May 3 to June 14, 2016)

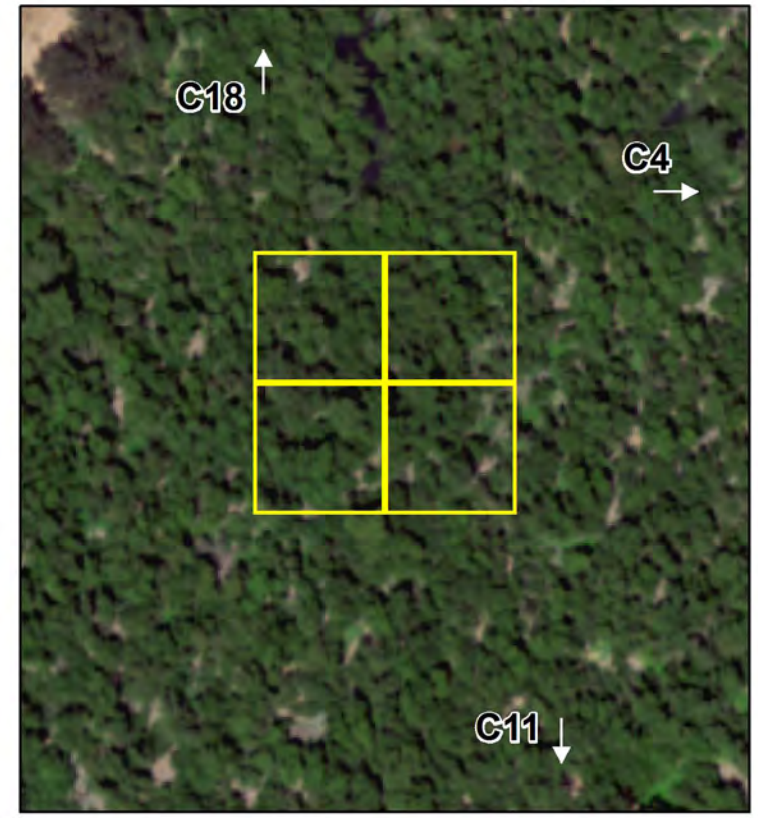

2017 Air Photo (July 3, 2017)

NDVI 30 x 30 Meter Pixel

Location Along Chino Creek

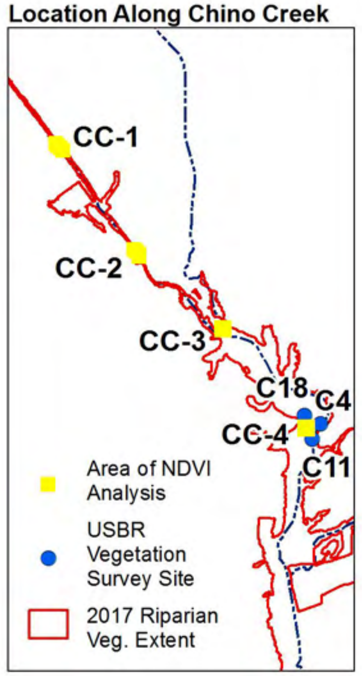

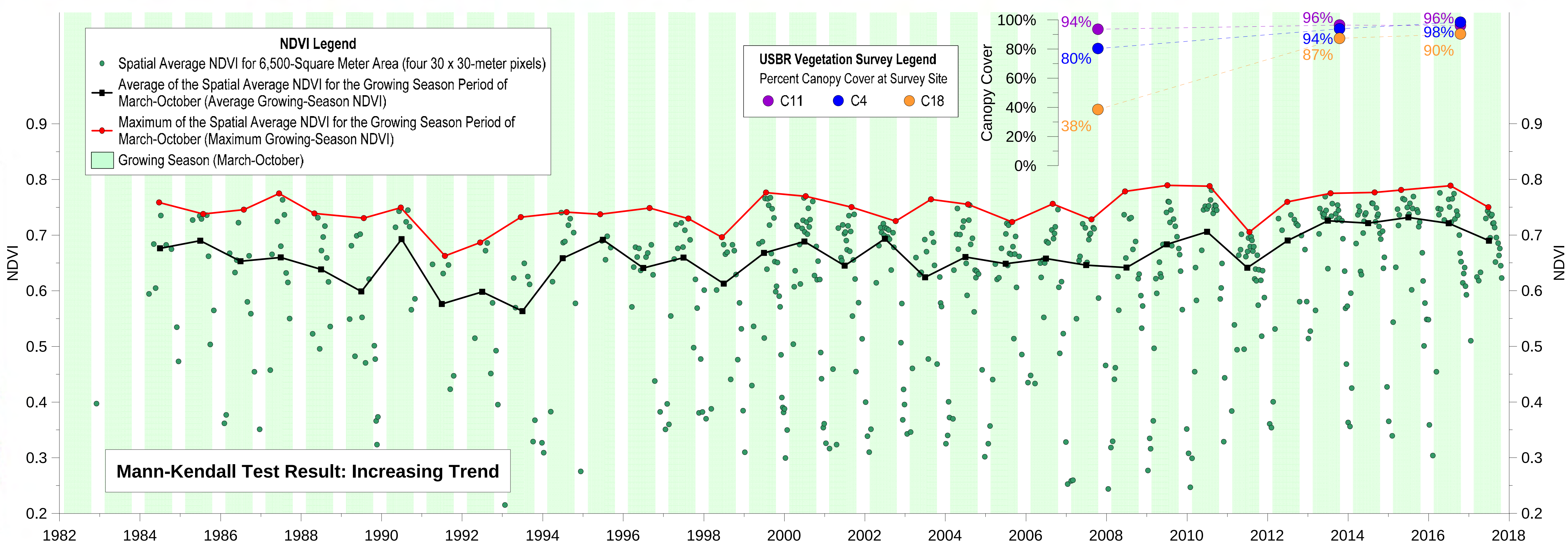

Prepared by:

WEI
Wildermuth Environmental, Inc.

Author: RT
Date: 20171122
Filename: NDVI_CC-4_AirPhoto.grf

2017 Annual report
Prado Basin Habitat Sustainability Committee

Time Series of NDVI and Air Photos
CC-4 Area for 1984 to 2017

Figure 3-6d

1999 Air Photo (January 14, 1999)

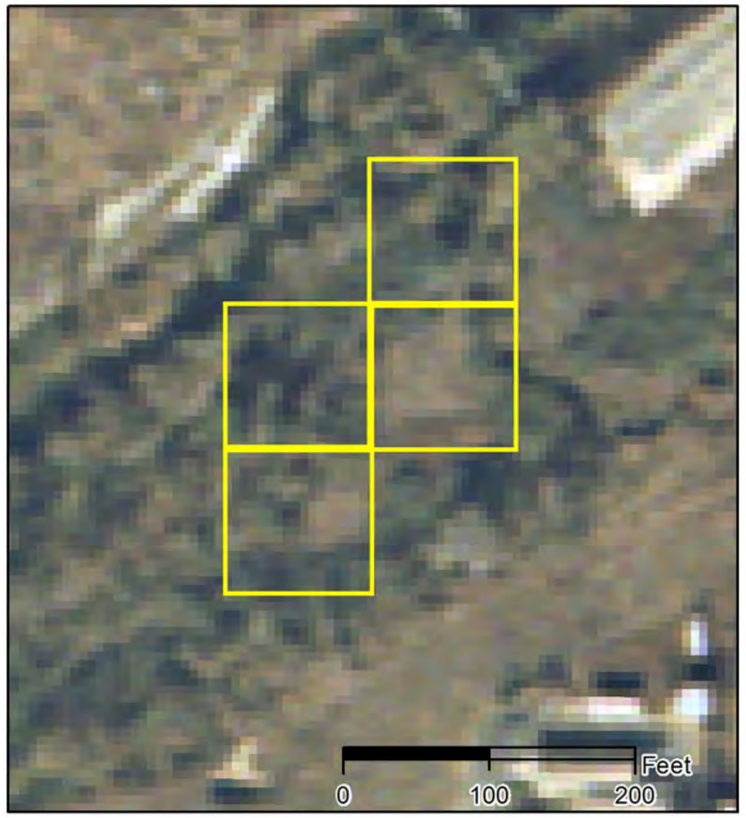

2006 Air Photo (Date Unknown)

2016 Air Photo (May 3 to June 14, 2016)

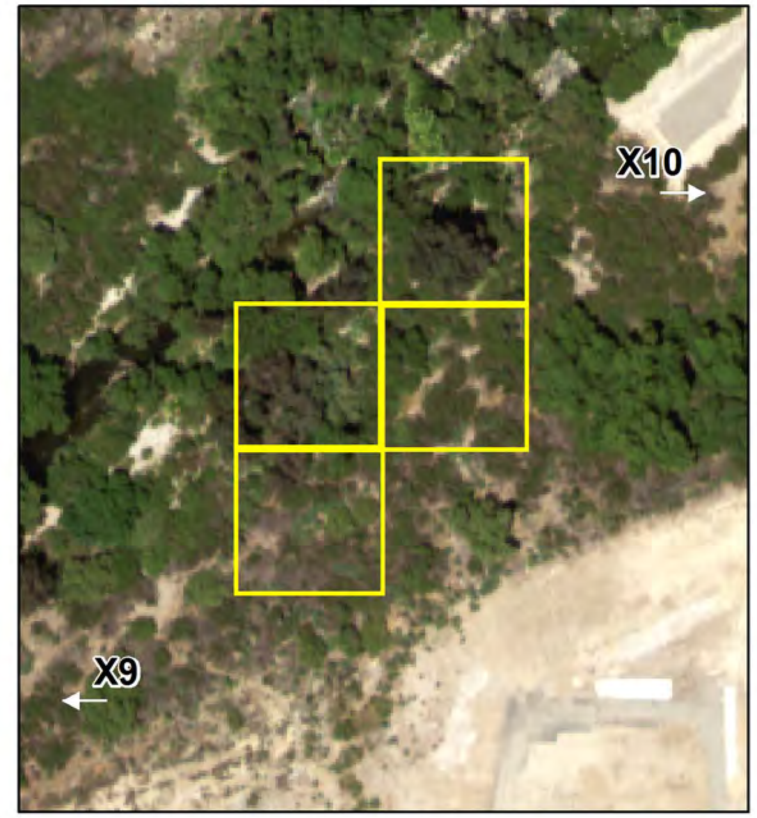

2017 Air Photo (July 3, 2017)

NDVI 30 x 30 Meter Pixel

Location Along Mill Creek

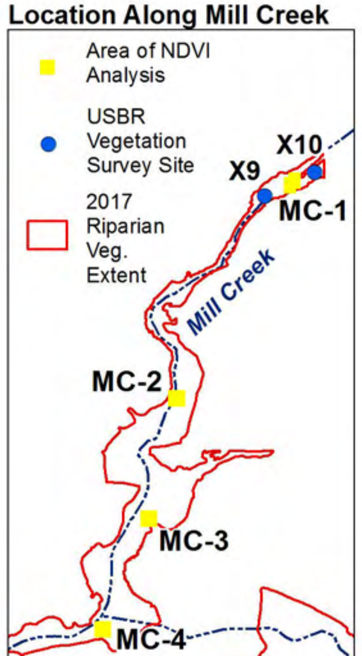

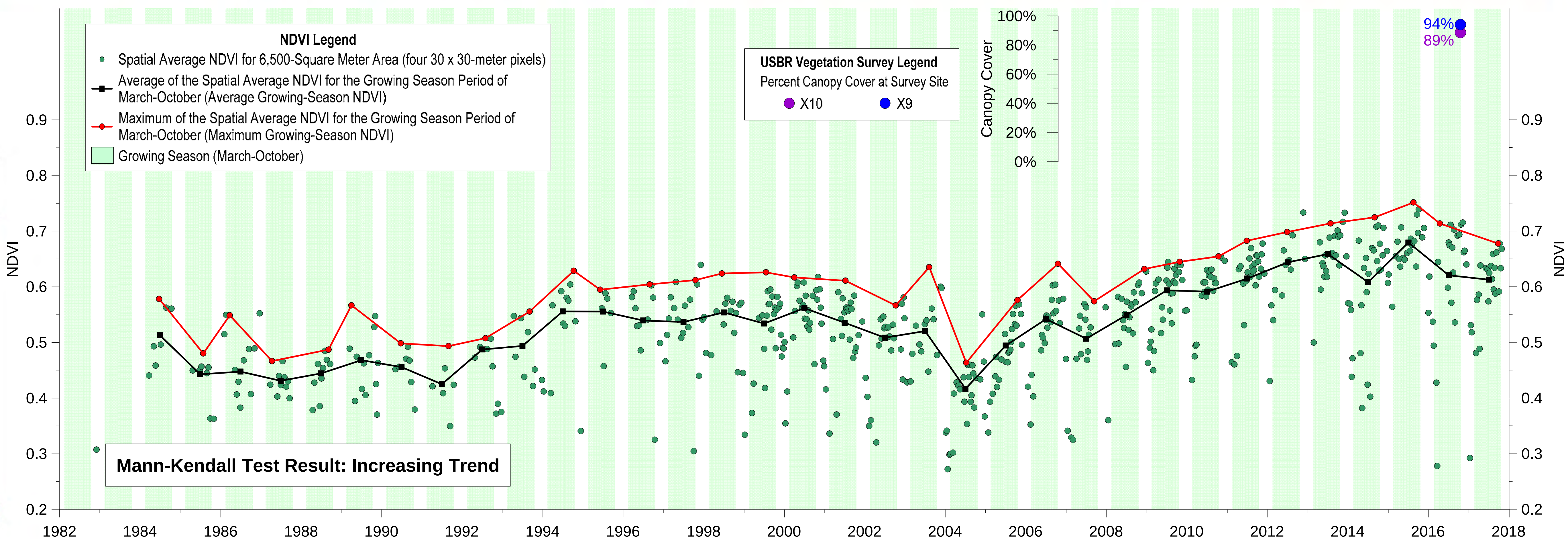

Prepared by:

Author: RT
Date: 20171122
Filename: NDVI_MC-1_AirPhoto.grf

2017 Annual Report
Prado Basin Habitat Sustainability Committee

Time Series of NDVI and Air Photos
MC-1 Area for 1984-2017

Figure 3-6e

1999 Air Photo (January 14, 1999)

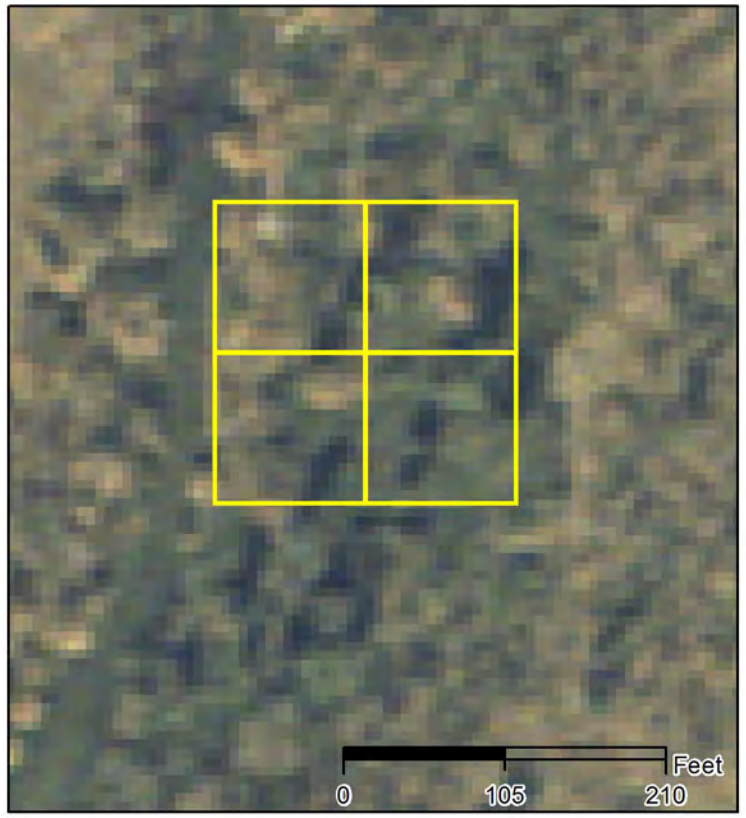

2006 Air Photo (Date Unknown)

2016 Air Photo (May 3 to June 14, 2016)

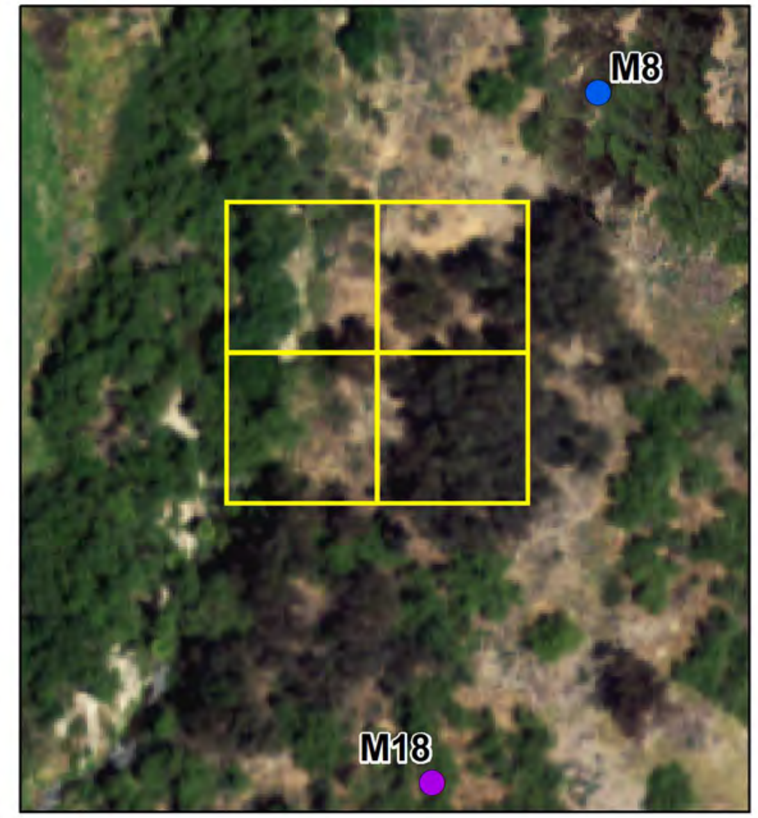

2017 Air Photo (July 3, 2017)

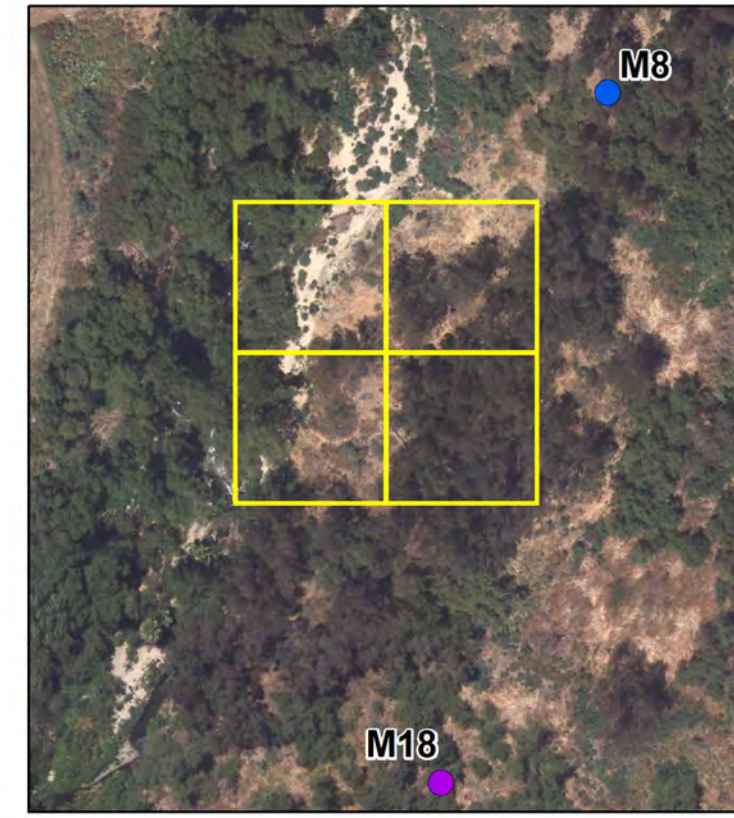

NDVI 30 x 30 Meter Pixel

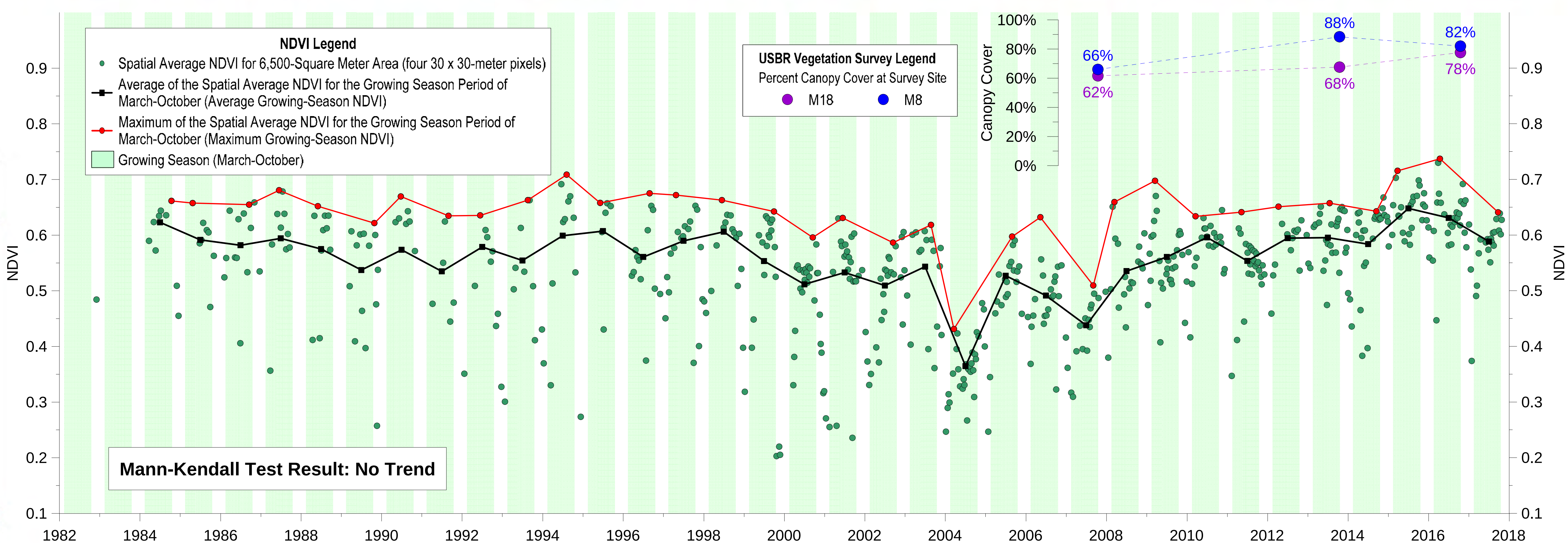

Location Along Mill Creek

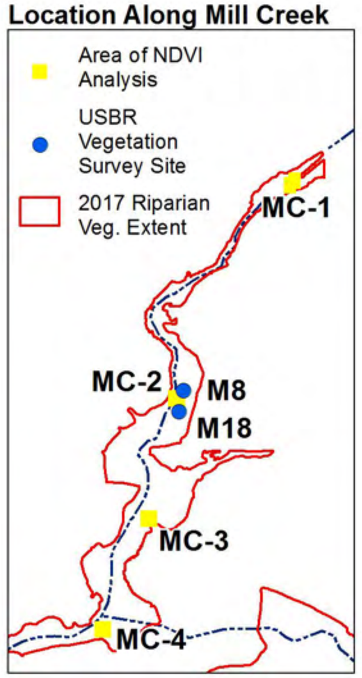

Prepared by:

WEI
Wildermuth Environmental, Inc.

Author: RT
Date: 20171122
Filename: NDVI_MC-2_AirPhoto.grf

2017 Annual report
Prado Basin Habitat Sustainability Committee

Time Series of NDVI and Air Photos
MC-2 Area for 1984 to 2017

Figure 3-6f

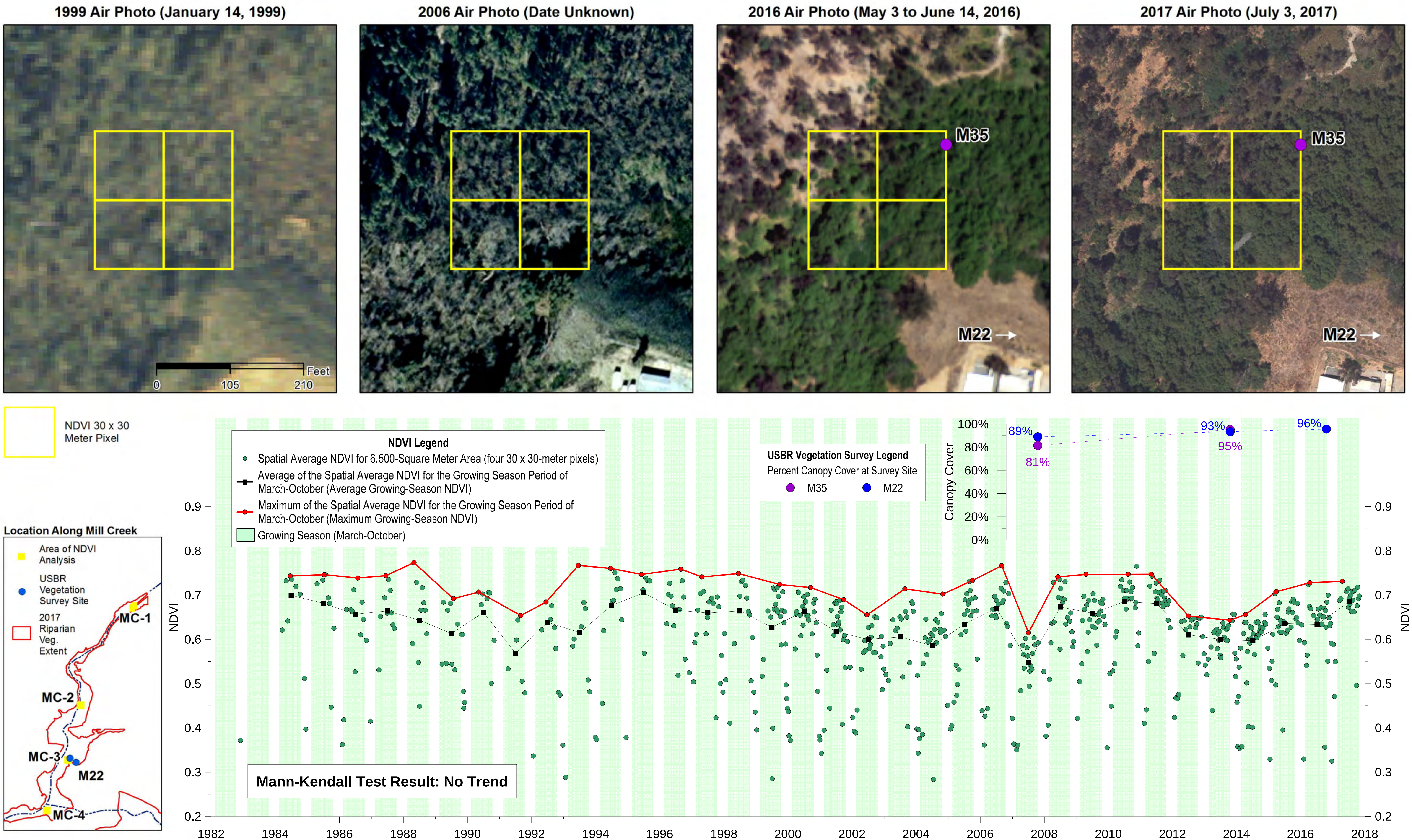

Prepared by:

WEI
Wildermuth Environmental, Inc.

Author: RT
Date: 20171122
Filename: NDVI_MC-3_Airphoto.grf

2017 Annual Report
Prado Basin Habitat Sustainability Committee

Time Series of NDVI and Air Photos
MC-3 Area for 1984 to 2017

Figure 3-6g

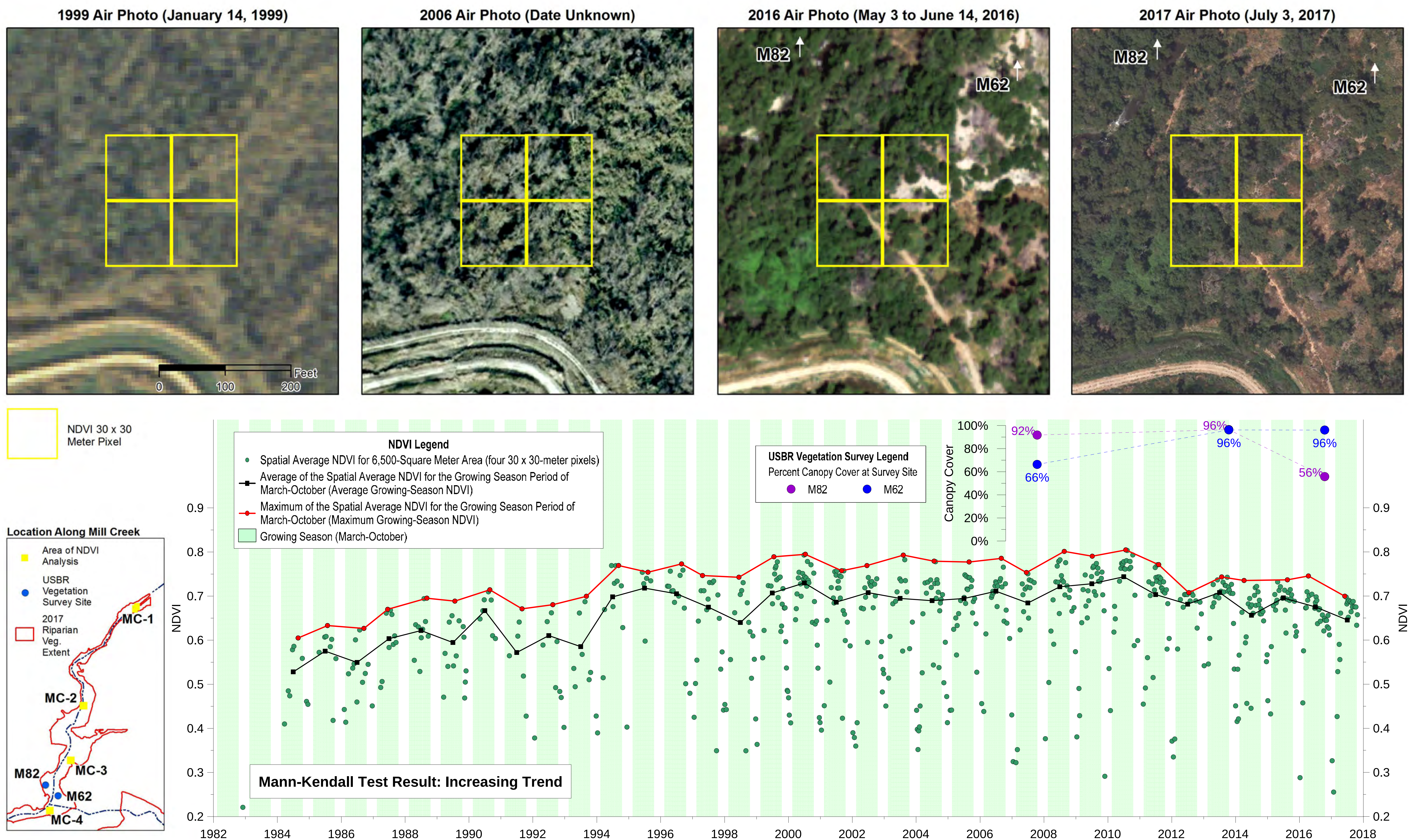

Prepared by:

WEI
Wildermuth Environmental, Inc.

Author: RT
Date: 20171122
Filename: NDVI_MC-4_AirPhoto.grf

2017 Annual Report
Prado Basin Habitat Sustainability Committee

Time Series of NDVI and Air Photos
MC-4 Area for 1984 to 2017

Figure 3-6h

1994 Air Photo (June 1, 1994)

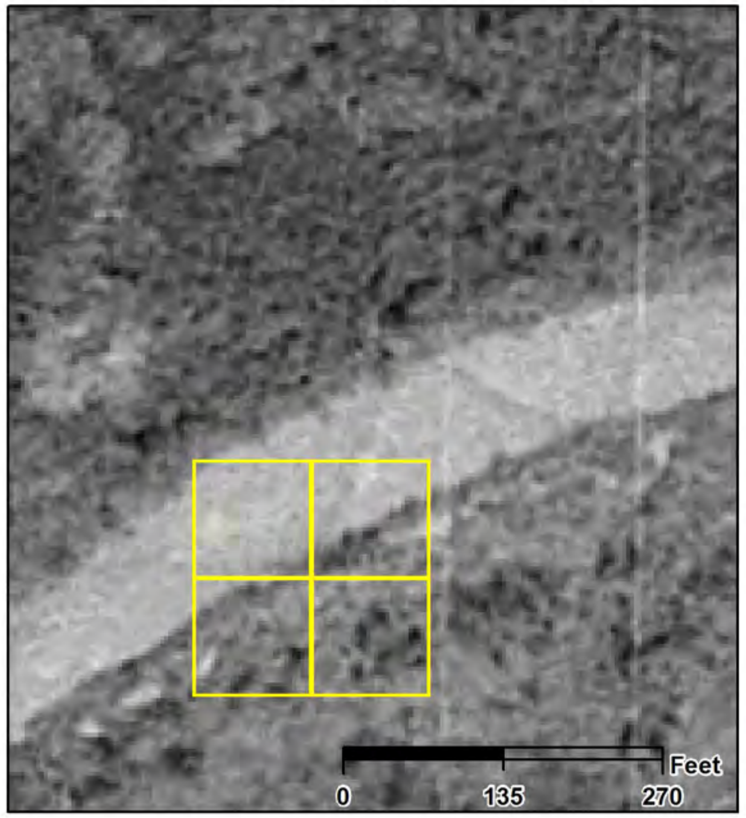

2006 Air Photo (Date Unknown)

2016 Air Photo (May 3 to June 14, 2016)

2017 Air Photo (July 3, 2017)

NDVI 30 x 30 Meter Pixel

Location Along SAR

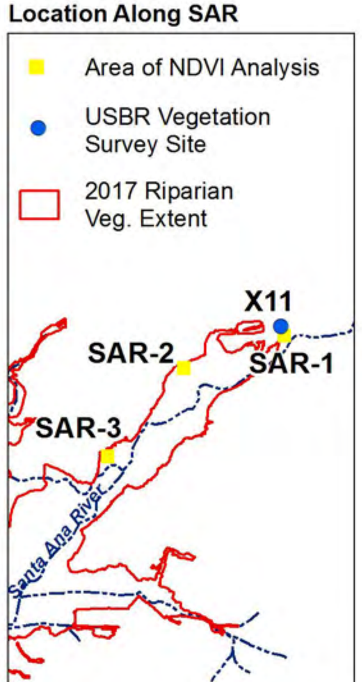

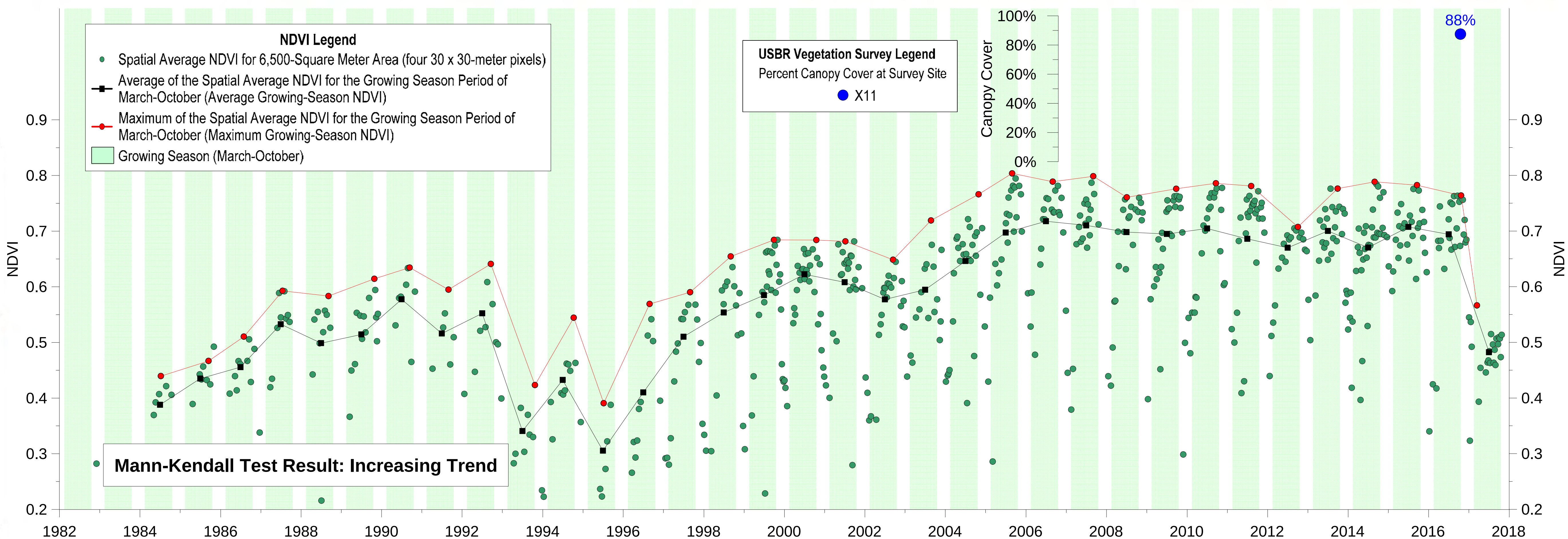

Prepared by:

WEI
Wildermuth Environmental, Inc.

Author: RT
Date: 20171122
Filename: NDVI_SAR-1_AirPhoto.grf

2017 Annual Report
Prado Basin Habitat Sustainability Committee

Time Series of NDVI and Air Photos
SAR-1 Area for 1984 to 2017

Figure 3-6i

1999 Air Photo (January 14, 1999)

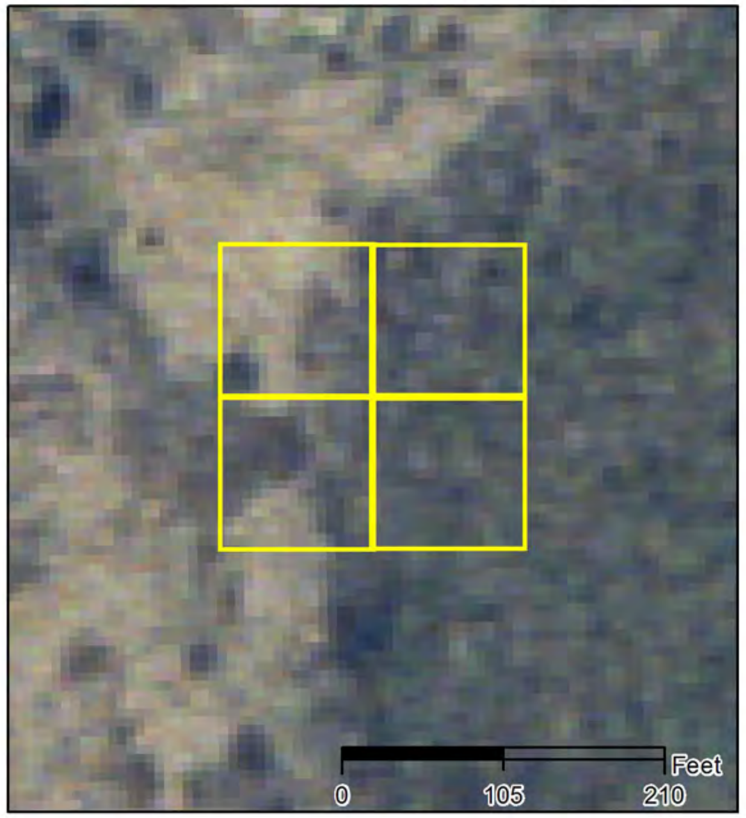

2006 Air Photo (Date Unknown)

2016 Air Photo (May 3 to June 14, 2016)

2017 Air Photo (July 3, 2017)

NDVI 30 x 30 Meter Pixel

Location Along SAR

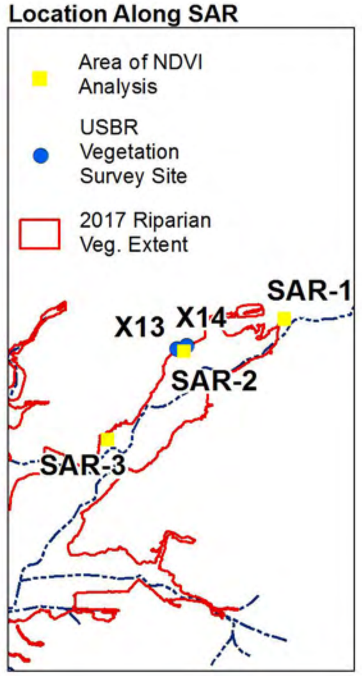

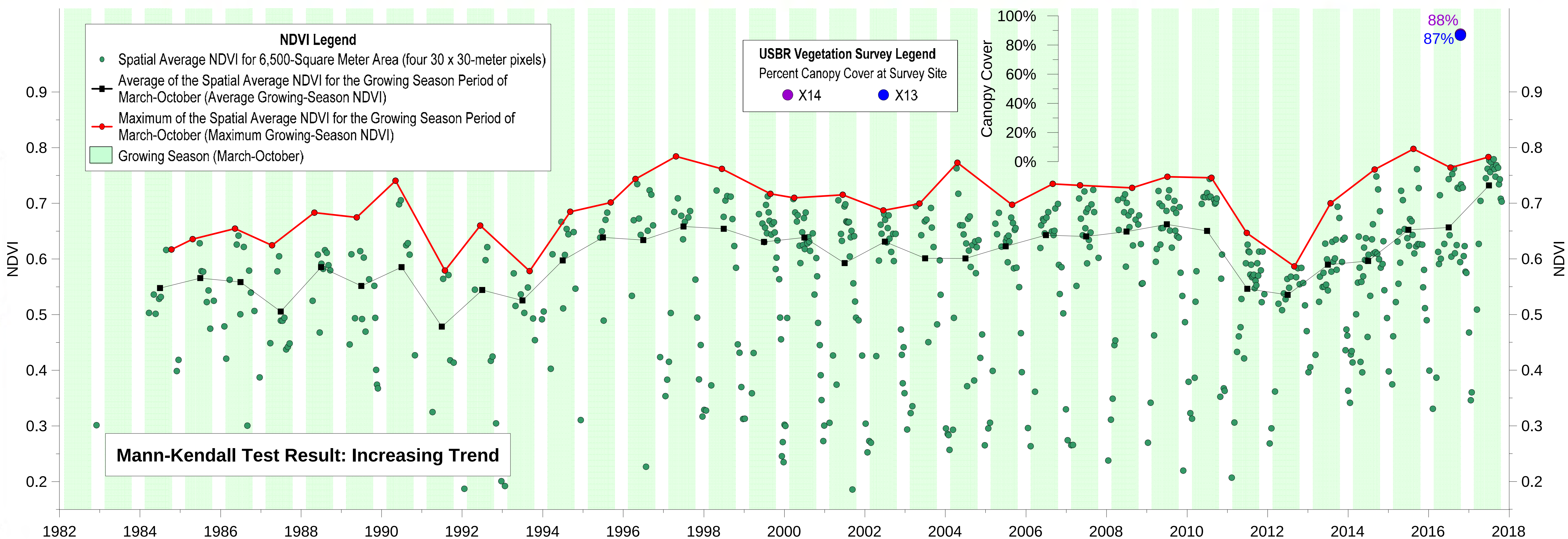

Prepared by:

WEI

Wildermuth Environmental, Inc.

Author: RT
Date: 20171122
Filename: NDVI_SAR-2_AirPhoto.grf

2017 Annual Report
Prado Basin Habitat Sustainability Committee

Time Series of NDVI and Air Photos
SAR-2 Area for 1984-2017

Figure 3-6j

1999 Air Photo (January 14, 1999)

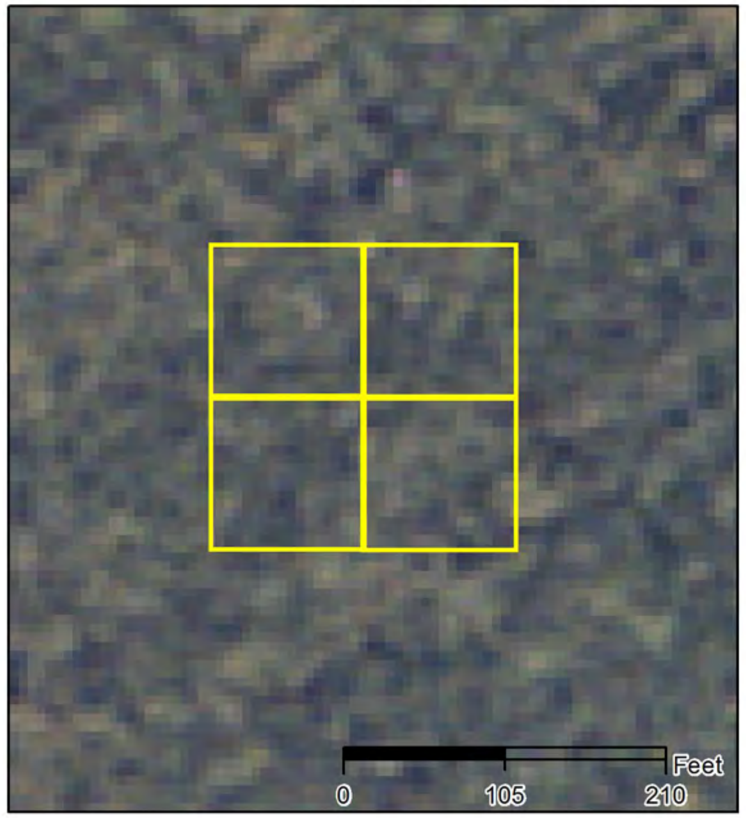

2006 Air Photo (Date Unknown)

2016 Air Photo (May 3 to June 14, 2016)

2017 Air Photo (July 3, 2017)

NDVI 30 x 30 Meter Pixel

Location Along SAR

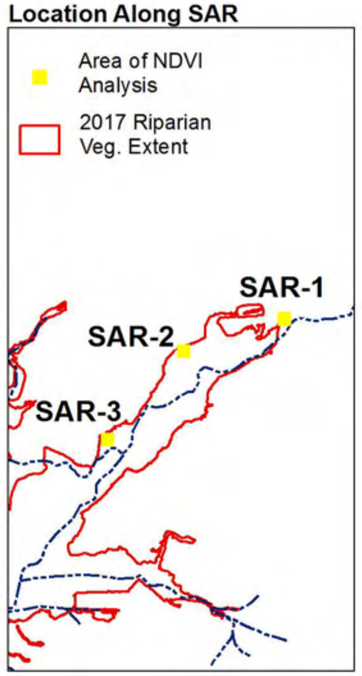

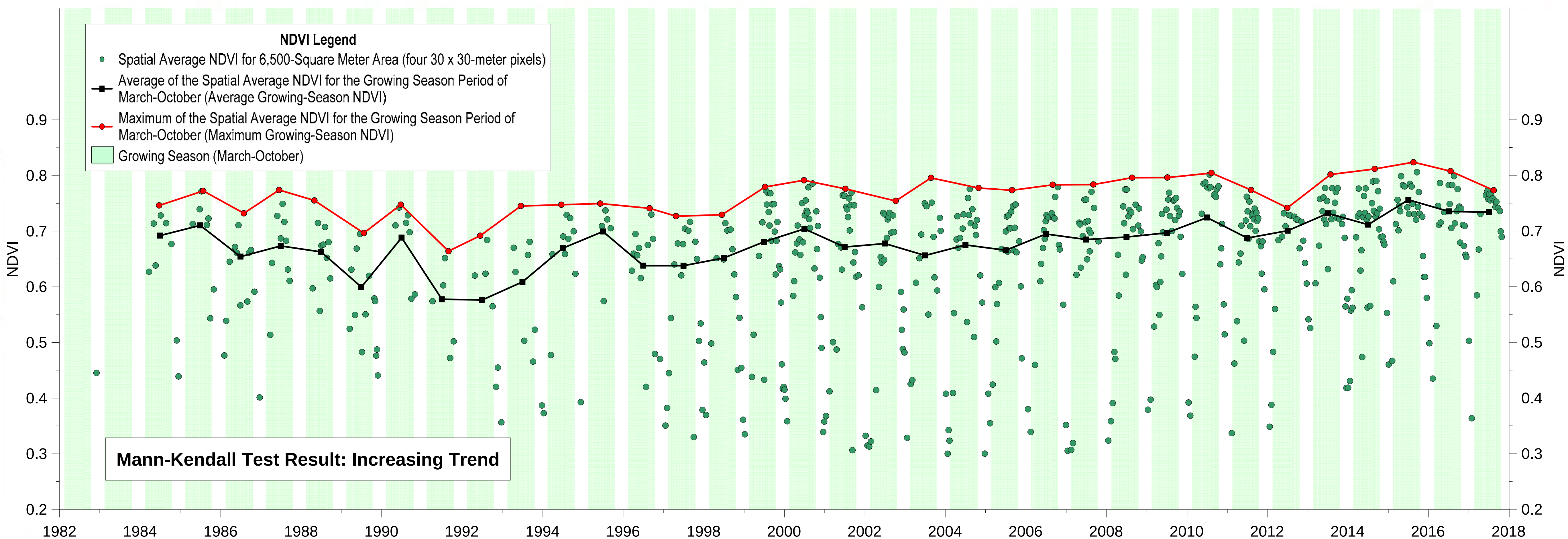

Prepared by:

WEI
WILDERMUTH ENVIRONMENTAL, INC.

Author: RT
Date: 20171122
Filename: NDVI_SAR-3_Airphoto.grf

2017 Annual Report
Prado Basin Habitat Sustainability Committee

Time Series of NDVI and Air Photos
SAR-3 Area for 1984 to 2017

Figure 3-6k

Figure 3-7a

Trend Analysis of Growing Season NDVI for the 2017 Extent of the Riparian Vegetation - 1984-2017

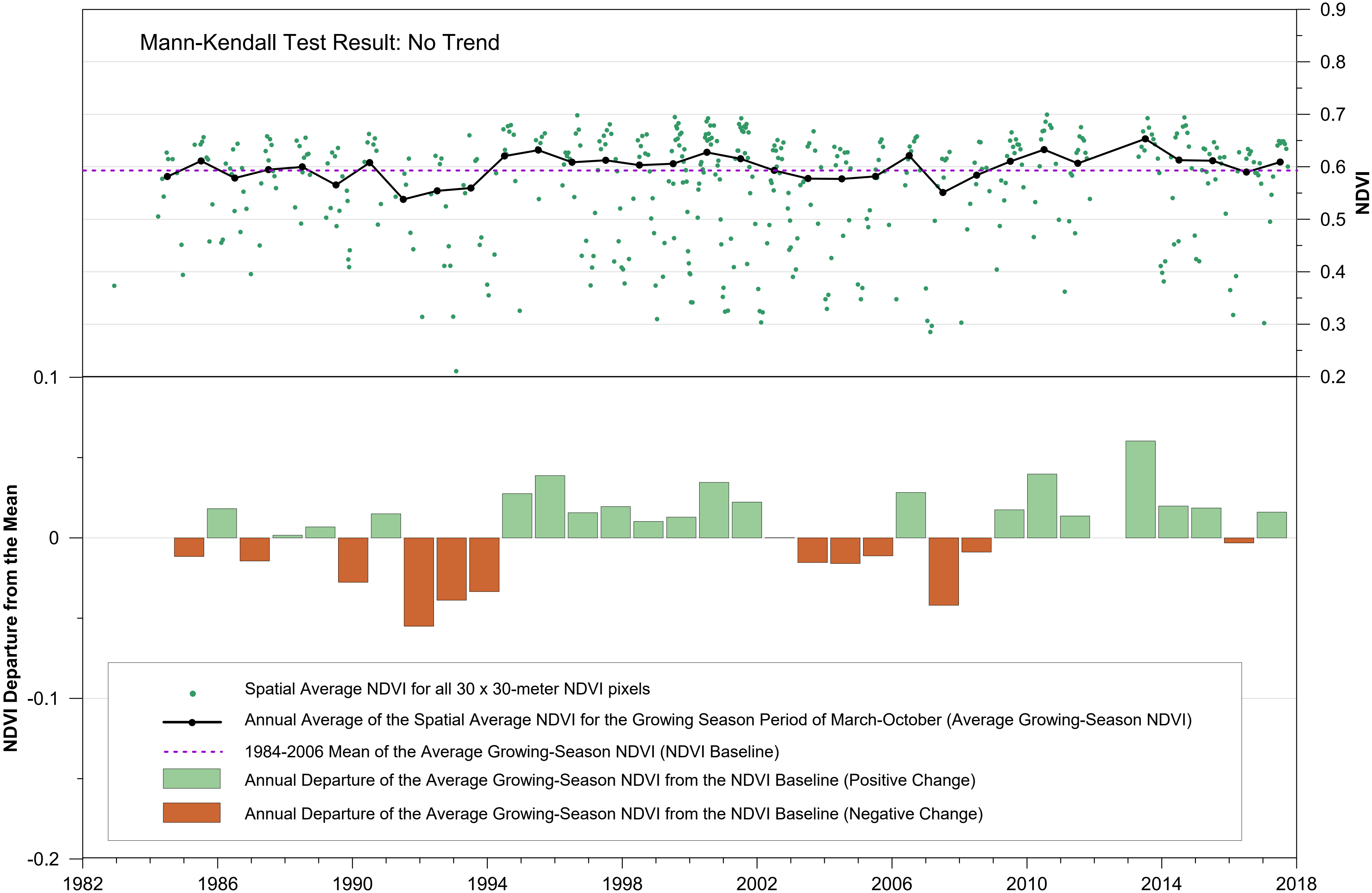

WEI

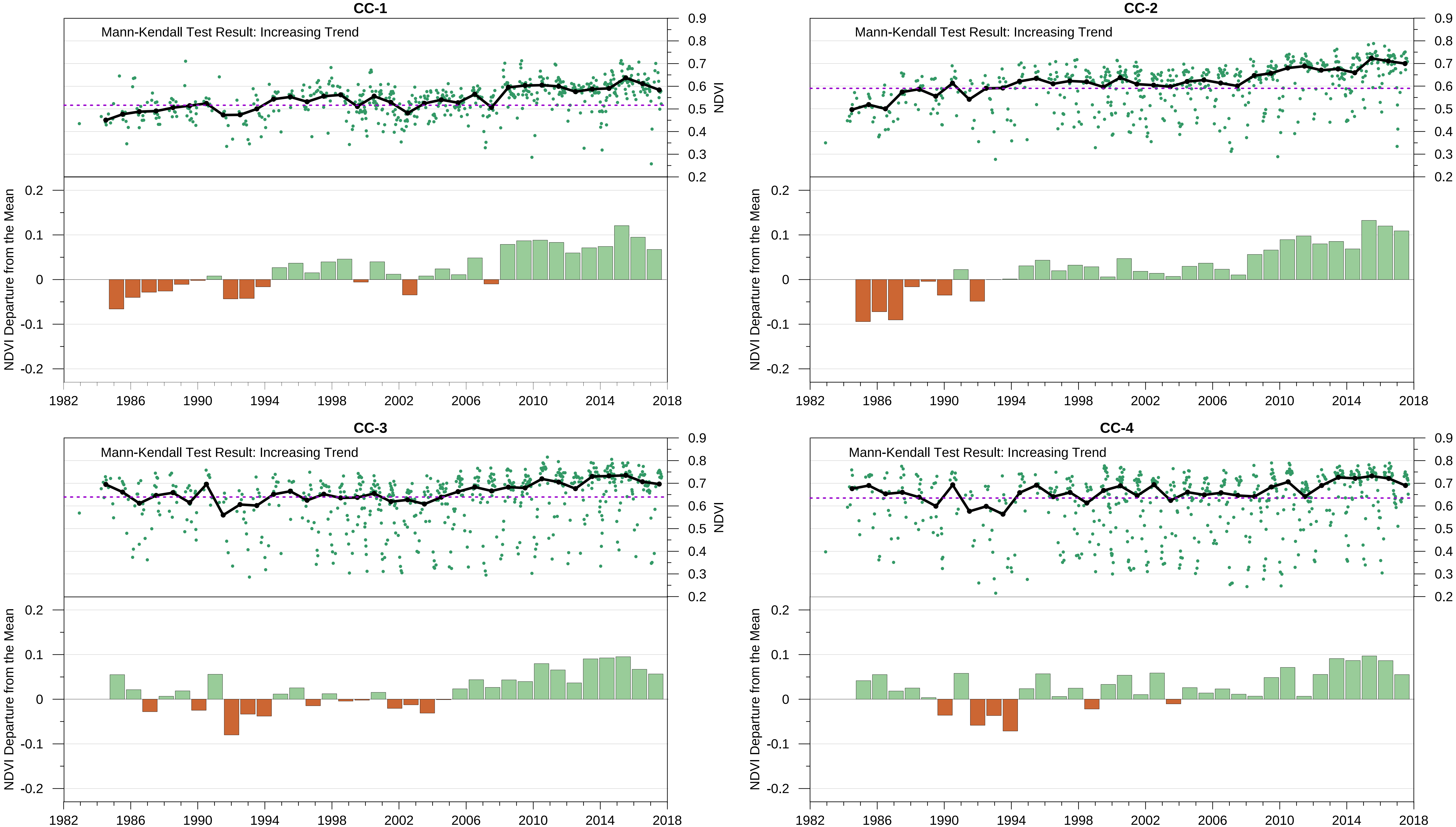

Spatial Average of NDVI for all 30 x 30-meter NDVI pixels

Annual Average of the Spatial Average NDVI for the Growing Season Period of March-October (Average Growing-Season NDVI)

1984-2006 Mean of the Average Growing-Season NDVI (Baseline NDVI)

Annual Depature from the Average Growing-Season NDVI from the Baseline NDVI (Positive Change)

Annual Depature from the Average Growing-Season NDVI from the Baseline NDVI (Negative Change

WEI
WILDERMUTH ENVIRONMENTAL, INC.

2017 Annual Report
Prado Basin Habitat Sustainability Committee

Trend Analysis of Growing Season NDVI
Chino Creek Area for 1984-2017

Figure 3-7b

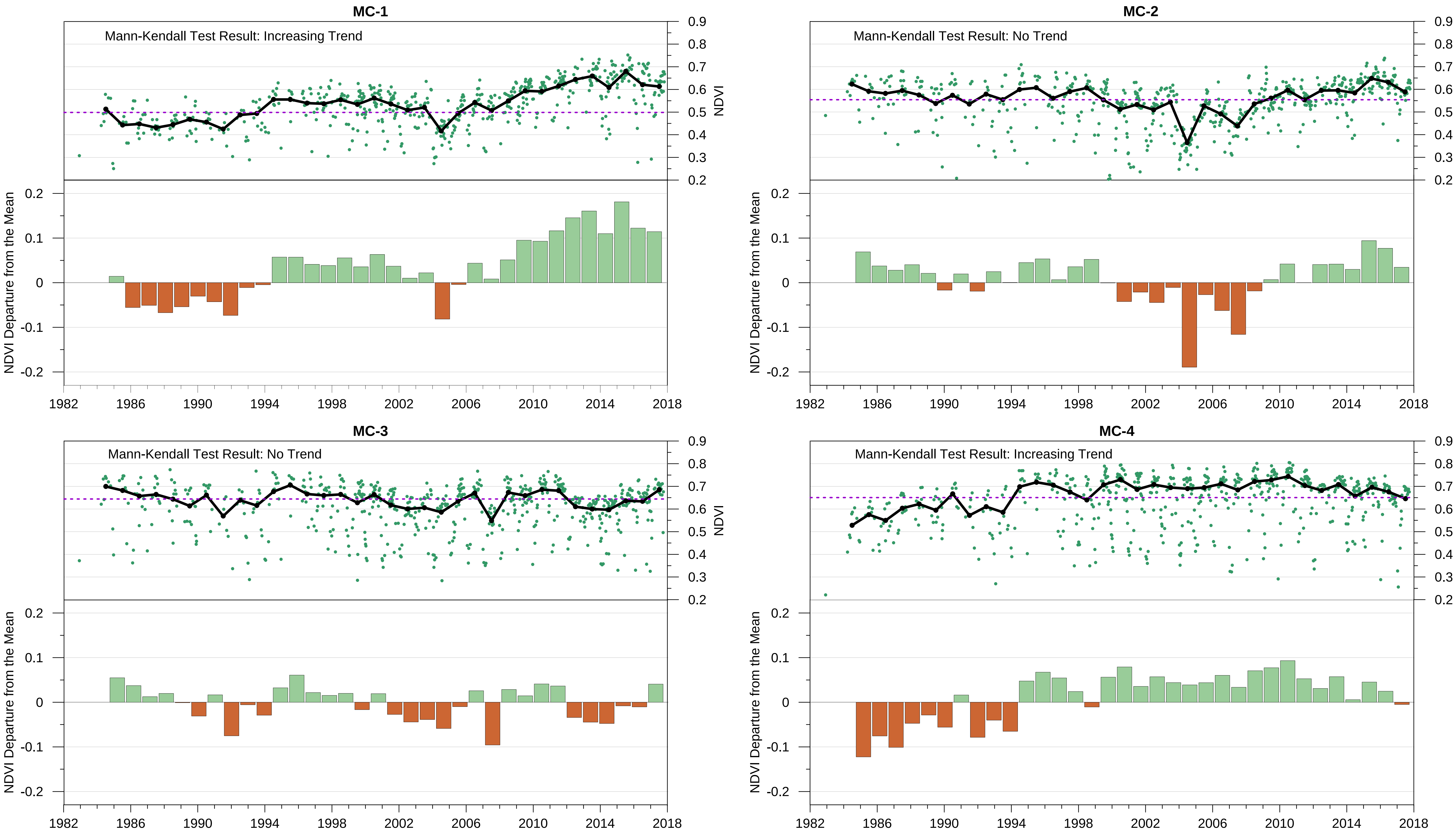

Spatial Average of NDVI for all 30 x 30-meter NDVI pixels

Annual Average of the Spatial Average NDVI for the Growing Season Period of March-October (Average Growing-Season NDVI)

1984-2006 Mean of the Average Growing-Season NDVI (NDVI Baseline)

Annual Depature from the Average Growing-Season NDVI from the Baseline NDVI (Positive Change)

Annual Depature from the Average Growing-Season NDVI from the Baseline NDVI (Positive Change)

WEI
WILDERMUTH ENVIRONMENTAL, INC.

2017 Annual Report
Prado Basin Habitat Sustainability Committee

Trend Analysis of Growing-Season NDVI
Mill Creek Area for 1984-2017

Figure 3-7c

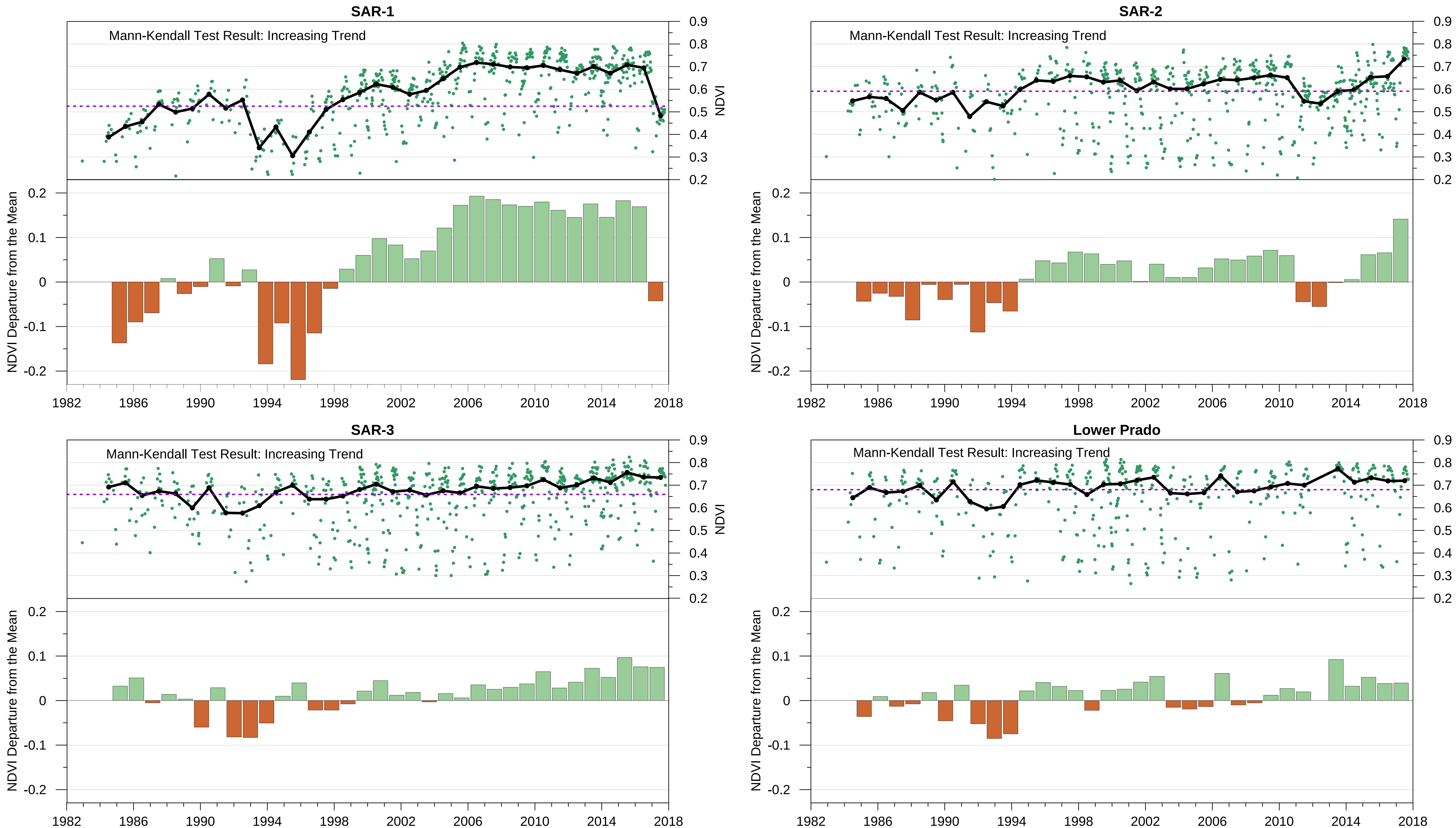

Spatial Average of NDVI for all 30 x 30-meter NDVI pixels

Annual Average of the Spatial Average NDVI for the Growing Season Period of March-October (Average Growing-Season NDVI)

1984-2006 Mean of the Average Growing-Season NDVI (NDVI Baseline)

Annual Depature from the Average Growing-Season NDVI from the Baseline NDVI (Positive Change)

Annual Depature from the Average Growing-Season NDVI from the Baseline NDVI (Positive Change)

WEI
WILDERMUTH ENVIRONMENTAL, INC.

2017 Annual Report
Prado Basin Habitat Sustainability Committee

Trend Analysis of Growing-Season NDVI
Santa Ana River Area for 1984-2017

Figure 3-7d

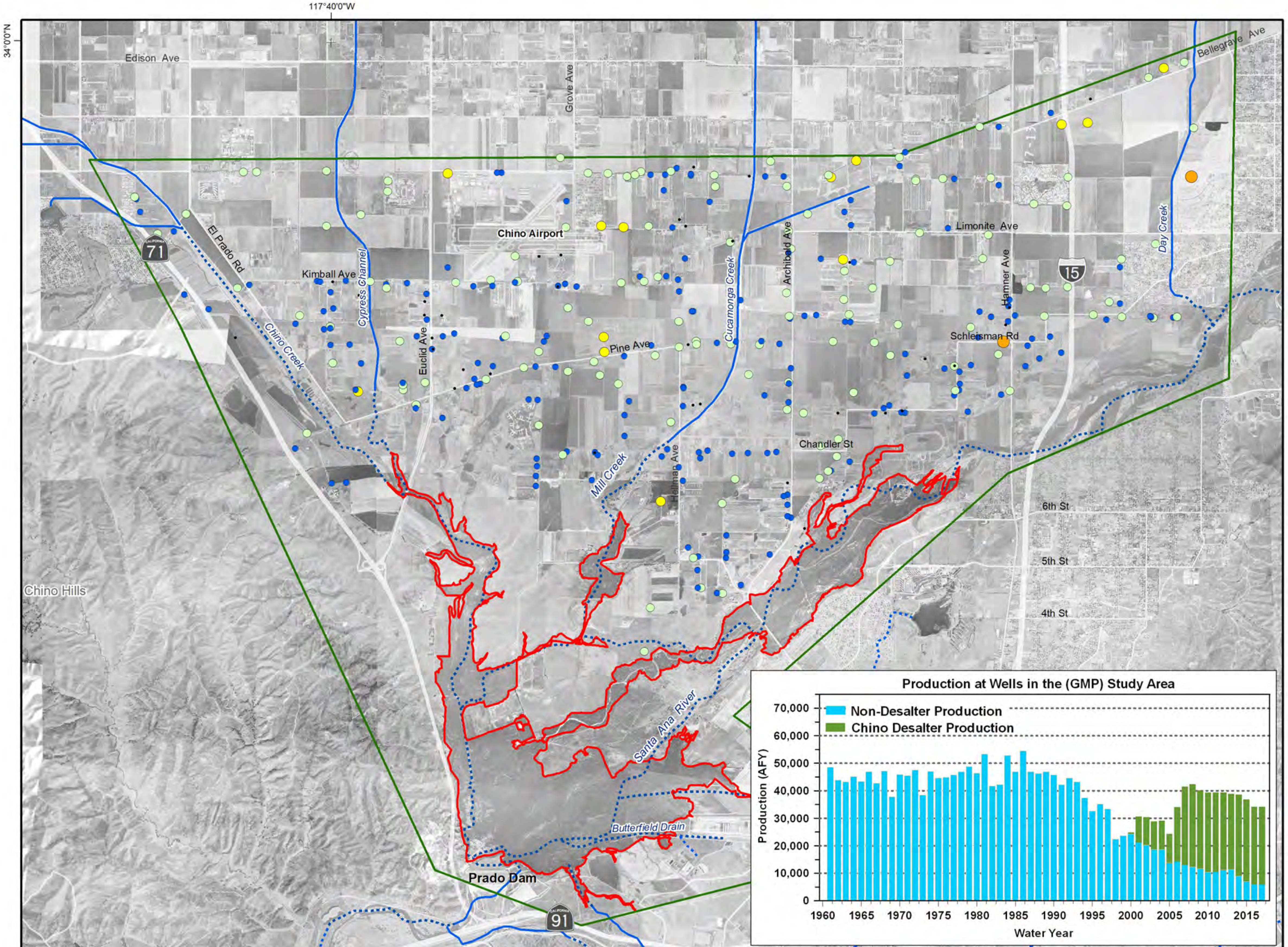

Groundwater Production
Water Year 1978 (AF) *

- < 10
- 10 - 100
- 100 - 500
- 500 - 1,000
- 1,000 - 2,500
- 2,500 - 5,000
- > 5,000

* Data shown spatially are estimates from Watermaster production records, and are representative of the spatial distribution of the production. Data shown on bar chart and in Table 3-2 are estimates from the calibrated 2013 Chino Basin groundwater-flow model.

Groundwater Monitoring Program (GMP) Study Area

Extent of Riparian Vegetation in Prado Basin based on the1977 Air Photo

Concrete-Lined Channels

Unlined Rivers and Streams

Aerial Photo: UCSB, 1977. February 2, 1977

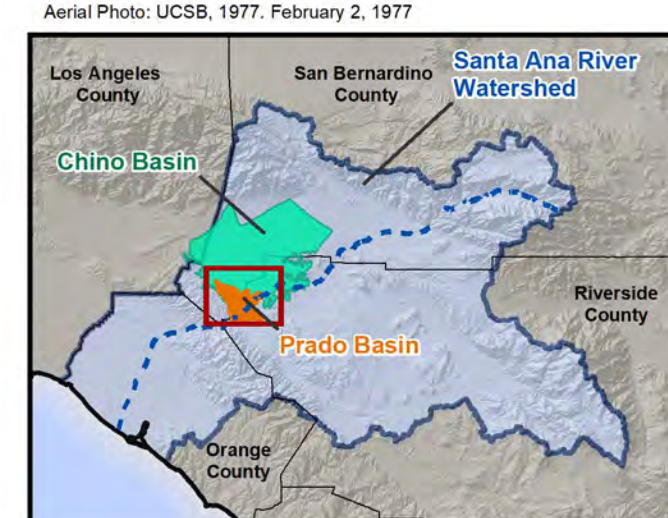

Prepared by:

WEI
WILDERMUTH ENVIRONMENTAL, INC.

Author: VMW
Date: 4/5/2018
File: 2017_Figure 3-8a_Production_WY_1977

0 1 2 Miles

0 1 2 3 KM

2017 Annual Report
Prado Basin Habitat Sustainability Committee

Groundwater Production in Water Year 1978

Figure 3-8a

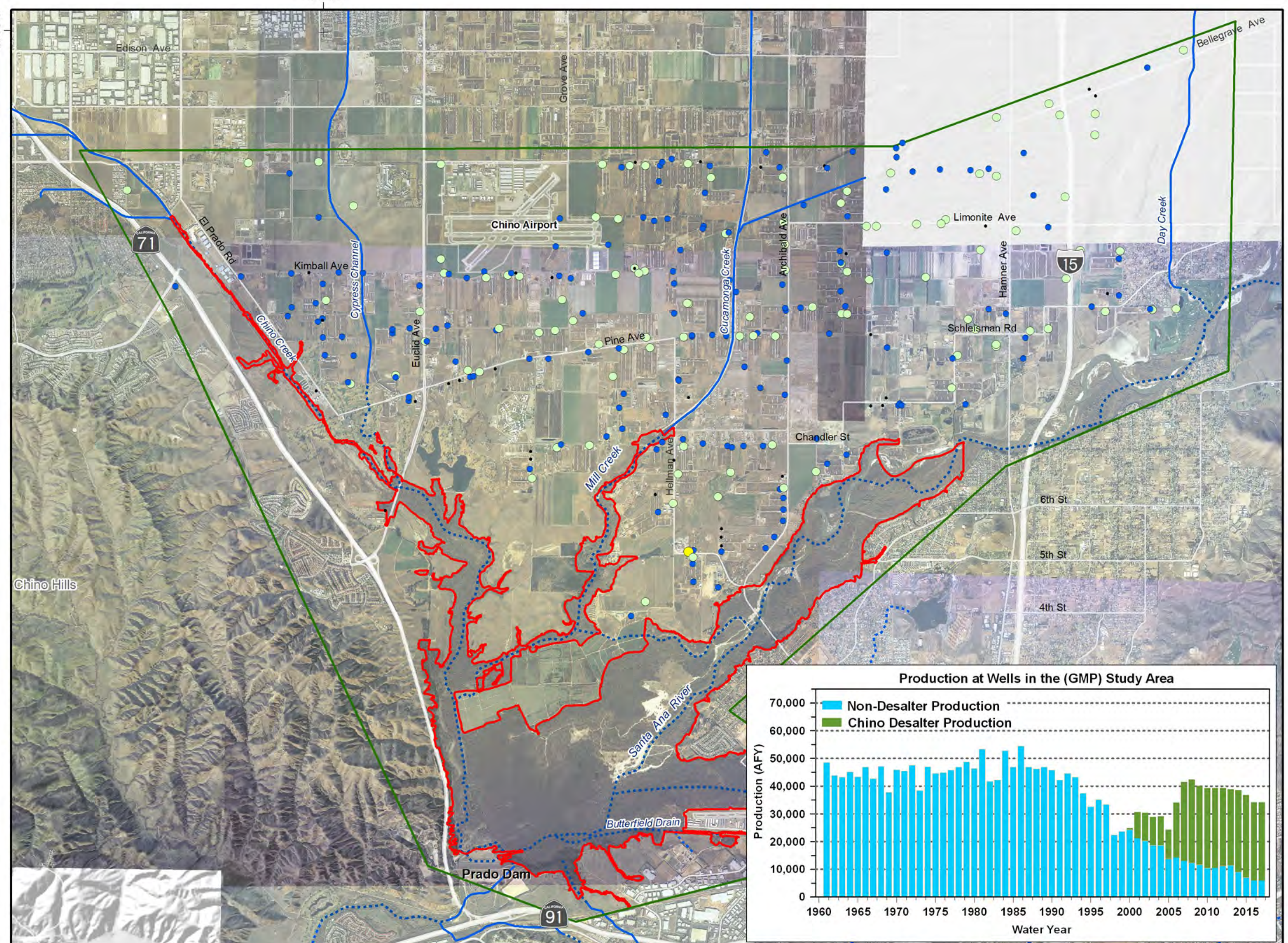

Groundwater Production
Water Year 1999 (AF) *

- < 10
- 10 - 100
- 100 - 500
- 500 - 1,000
- 1,000 - 2,500
- 2,500 - 5,000
- > 5,000

* Data shown spatially are estimates from Watermaster production records, and are representative of the spatial distribution of the production. Data shown on bar chart and in Table 3-2 are estimates from the calibrated 2013 Chino Basin groundwater-flow model.

Groundwater Monitoring Program (GMP) Study Area

Extent of Riparian Vegetation in Prado Basin based on the 1999 Air Photo

Concrete-Lined Channels

Unlined Rivers and Streams

Aerial Photo: UCSB, 1999. January 14,1999

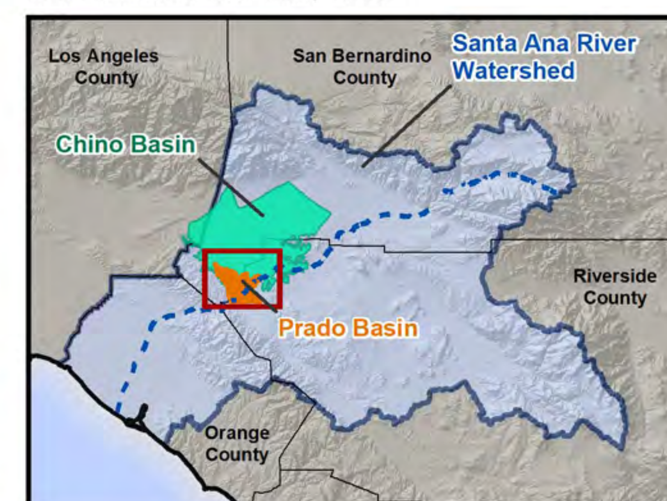

Prepared by:

WEI
WILDERMUTH ENVIRONMENTAL, INC.

Author: VMW
Date: 4/5/2018
File: 2017_Figure 3-8b_Production_WY_1999

0 1 2 Miles
0 1 2 3 KM

2017 Annual Report
Prado Basin Habitat Sustainability Committee

Groundwater Production in Water Year 1999

Figure 3-8b

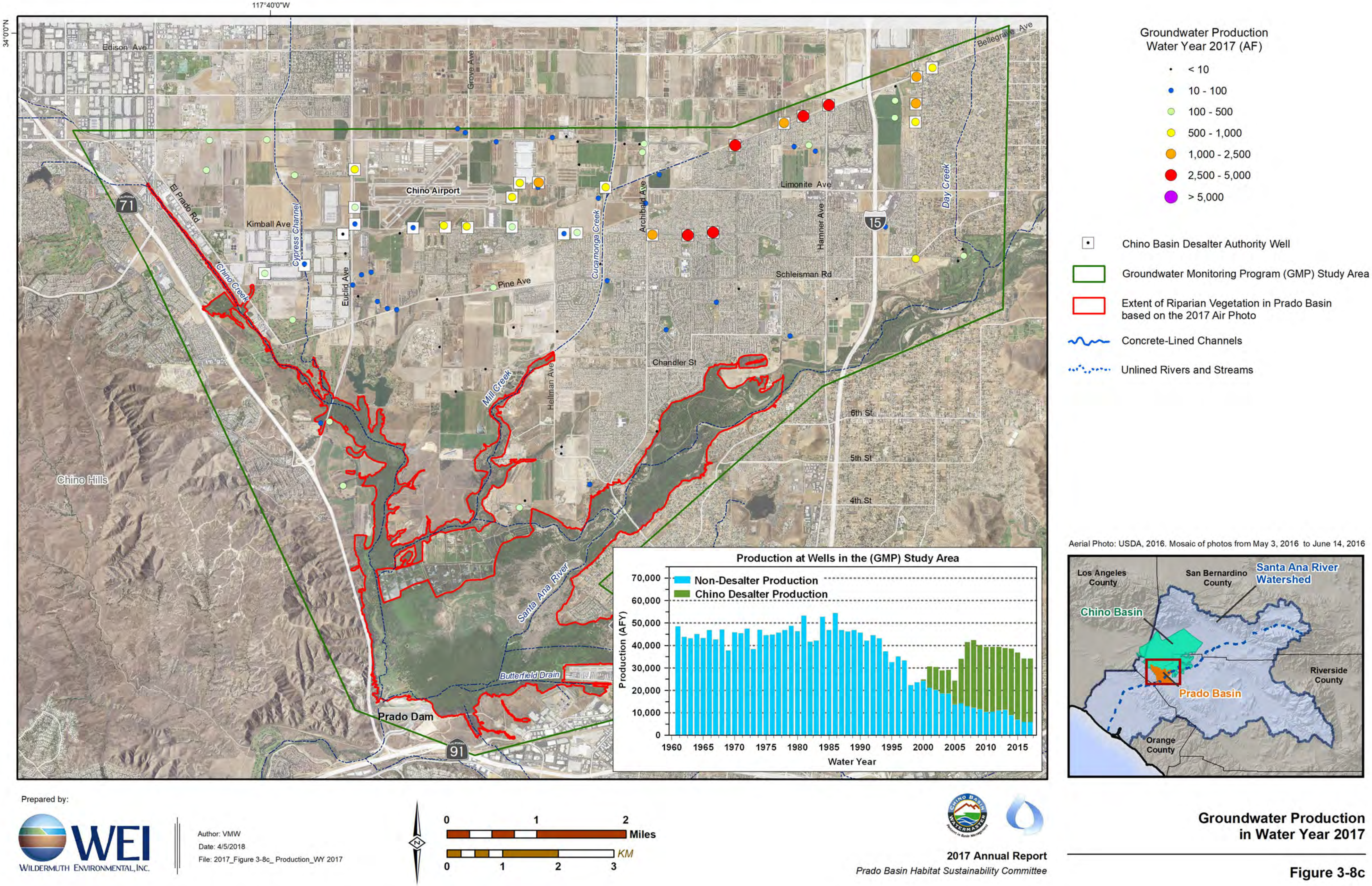

Prepared by:

WEI
Wildermuth Environmental, Inc.

Author: VMW
Date: 4/5/2018
File: 2017_Figure 3-8c_ Production_WY 2017

2017 Annual Report
Prado Basin Habitat Sustainability Committee

Groundwater Production in Water Year 2017

Figure 3-8c

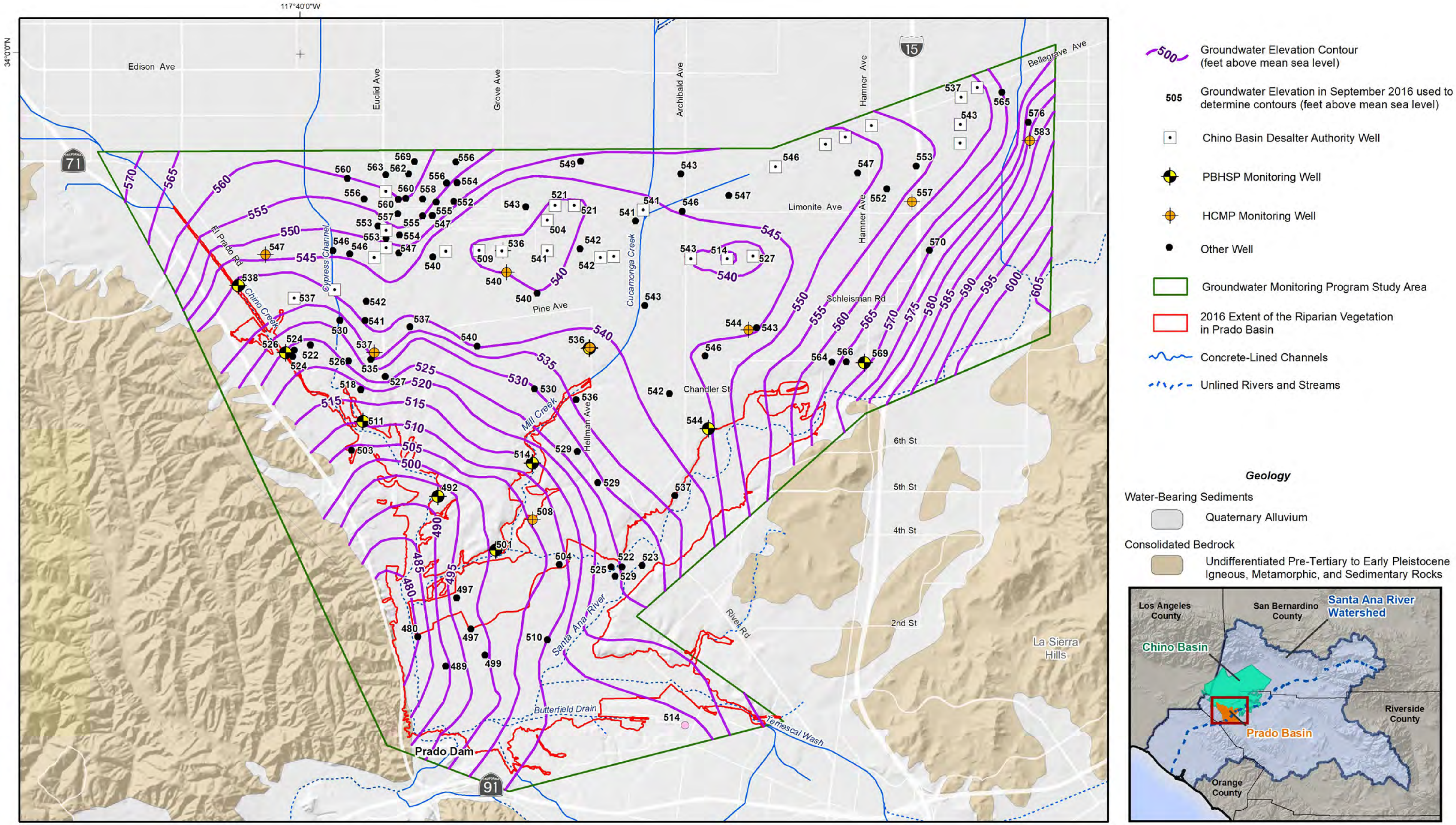

Prepared by:

WEI
WILDERMUTH ENVIRONMENTAL, INC.

Author: EM
Date: 3/7/2018
File: 2017_Figure 3-9a_f2016_GWLE_Contours

2017 Annual Report
Prado Basin Habitat Sustainability Committee

Map of Groundwater Elevation
September 2016 - Shallow Aquifer System

Figure 3-9a

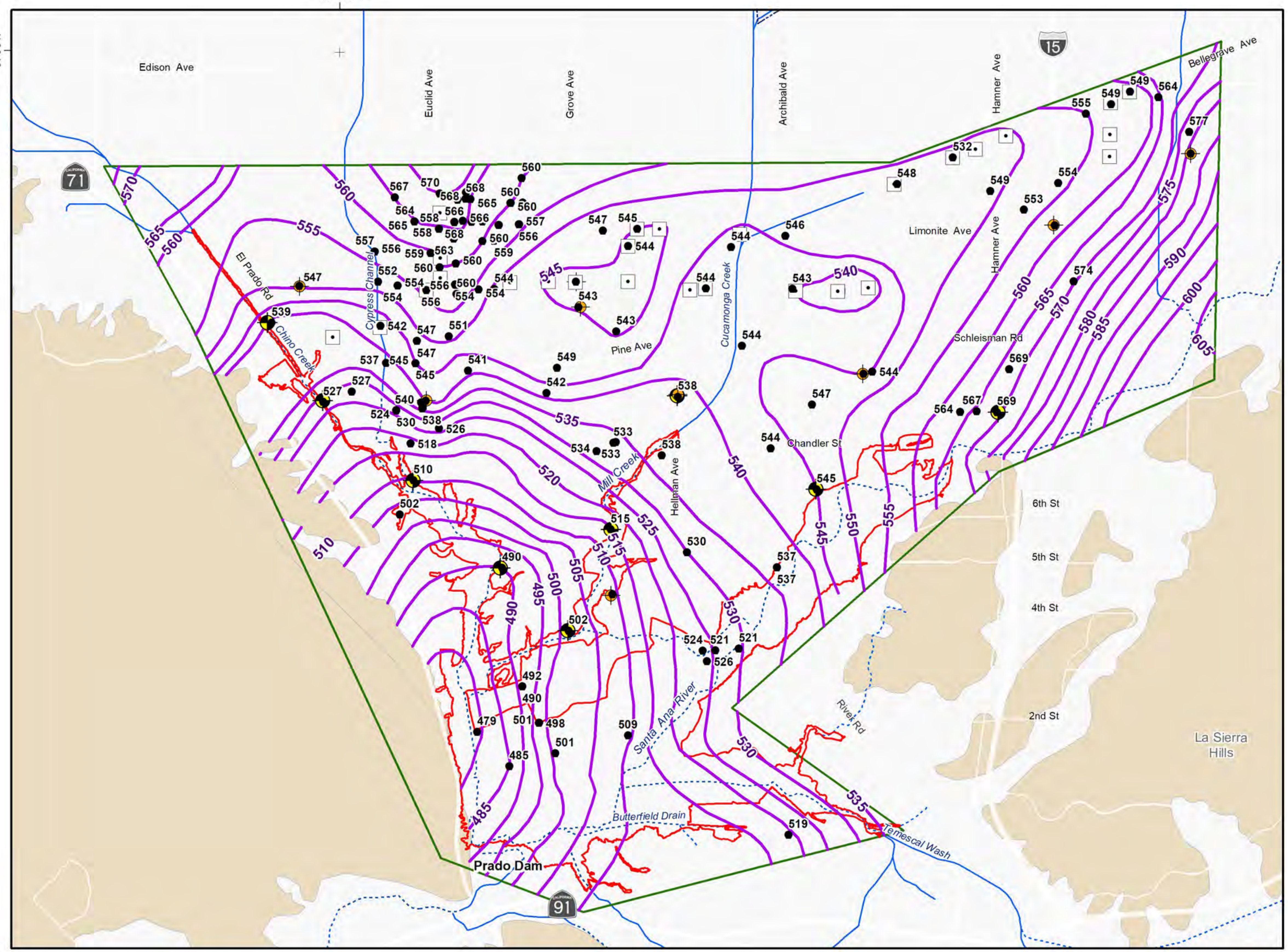

Groundwater Elevation Contour (feet above mean sea level)

505 Groundwater Elevation in September 2017 used to determine contours (feet above mean sea level)

Chino Basin Desalter Authority Well

PBHSP Monitoring Well

HCMP Monitoring Well

Other Well

Groundwater Monitoring Program Study Area

2017 Extent of the Riparian Vegetation in Prado Basin

Concrete-Lined Channels

Unlined Rivers and Streams

Geology

Water-Bearing Sediments

Quaternary Alluvium

Consolidated Bedrock

Undifferentiated Pre-Tertiary to Early Pleistocene Igneous, Metamorphic, and Sedimentary Rocks

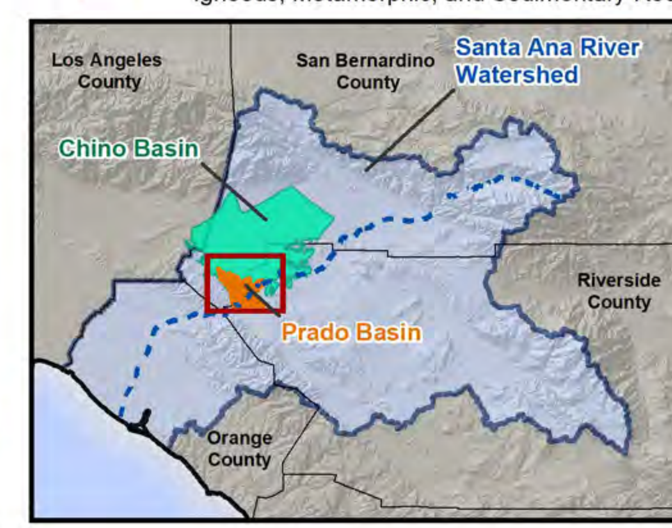

Prepared by:

WEI
Wildermuth Environmental, Inc.

Author: EM
Date: 3/7/2018
File: 2017_Figure 3-9b_f2017_GWLE_Contours

0 1 2 Miles

0 1 2 3 KM

2017 Annual Report
Prado Basin Habitat Sustainability Committee

Map of Groundwater Elevation

September 2017 - Shallow Aquifer System

Figure 3-9b

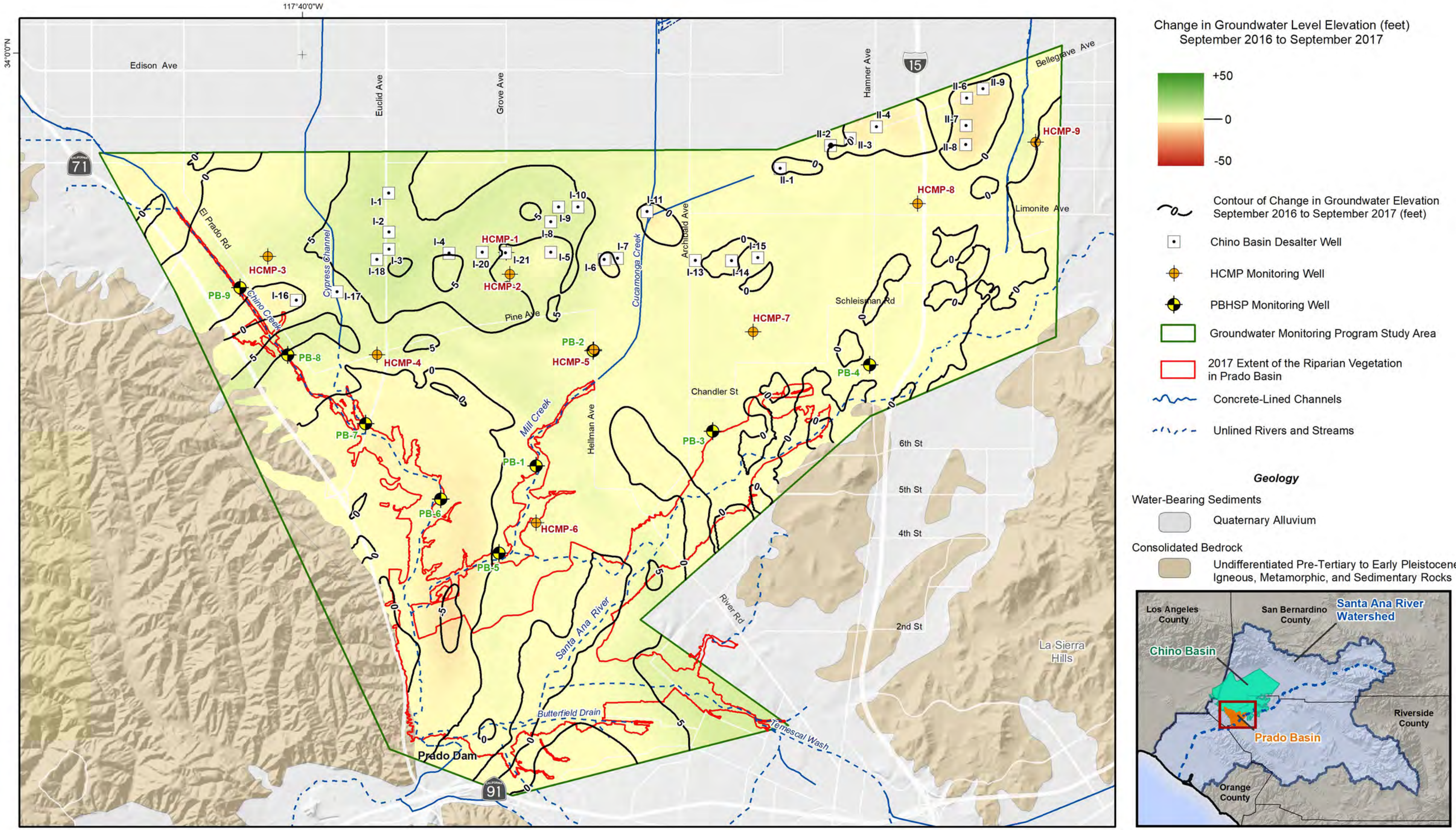

Prepared by:

WEI
WILDERMUTH ENVIRONMENTAL, INC.

Author: EM
Date: 3/6/2018
File: 2017_Figure 3-10_f16-f17_GWLE_change_map

2017 Annual Report
Prado Basin Habitat Sustainability Committee

Change in Groundwater Elevation September 2016 to September 2017

Figure 3-10

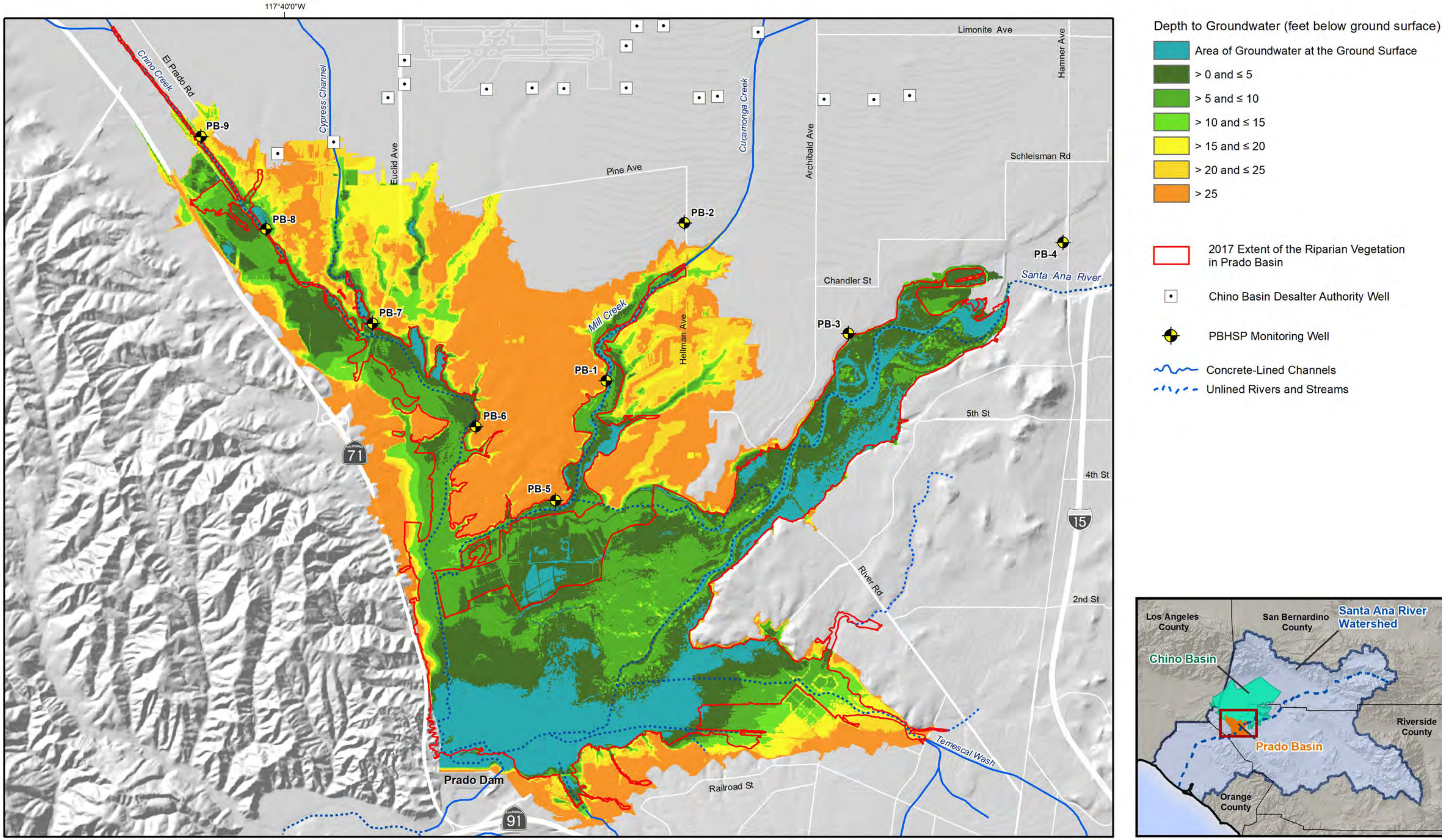

Prepared by:

WEI
Wildermuth Environmental, Inc.

Author: EM
Date: 3/5/2018
File: 2017_Figure 3-11_f2017_DTW

0 1 2 Miles
0 1 2 3 KM

2017 Annual Report
Prado Basin Habitat Sustainability Committee

Depth to Groundwater
September 2017

Figure 3-11

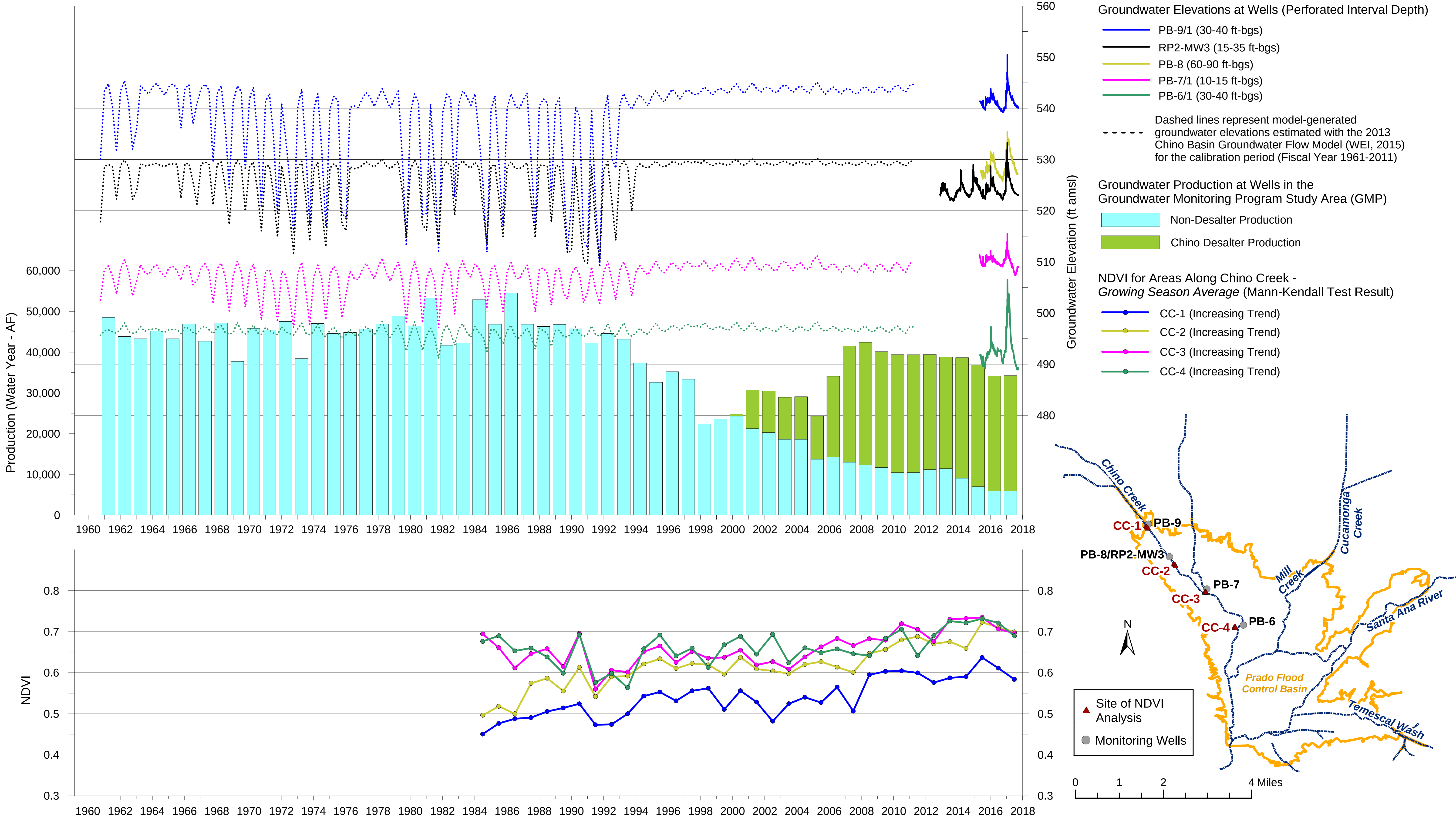

Prepared by:

WEI
Wildermuth Environmental, Inc.

Author: RT
Date: 20170404
Filename: Prod_GWLs_ChinoCreek.grf

2017 Annual Report
Prado Basin Habitat Sustainability Committee

Groundwater Production and Groundwater Levels versus NDVI
Chino Creek Area for 1960-2017

Figure 3-12a

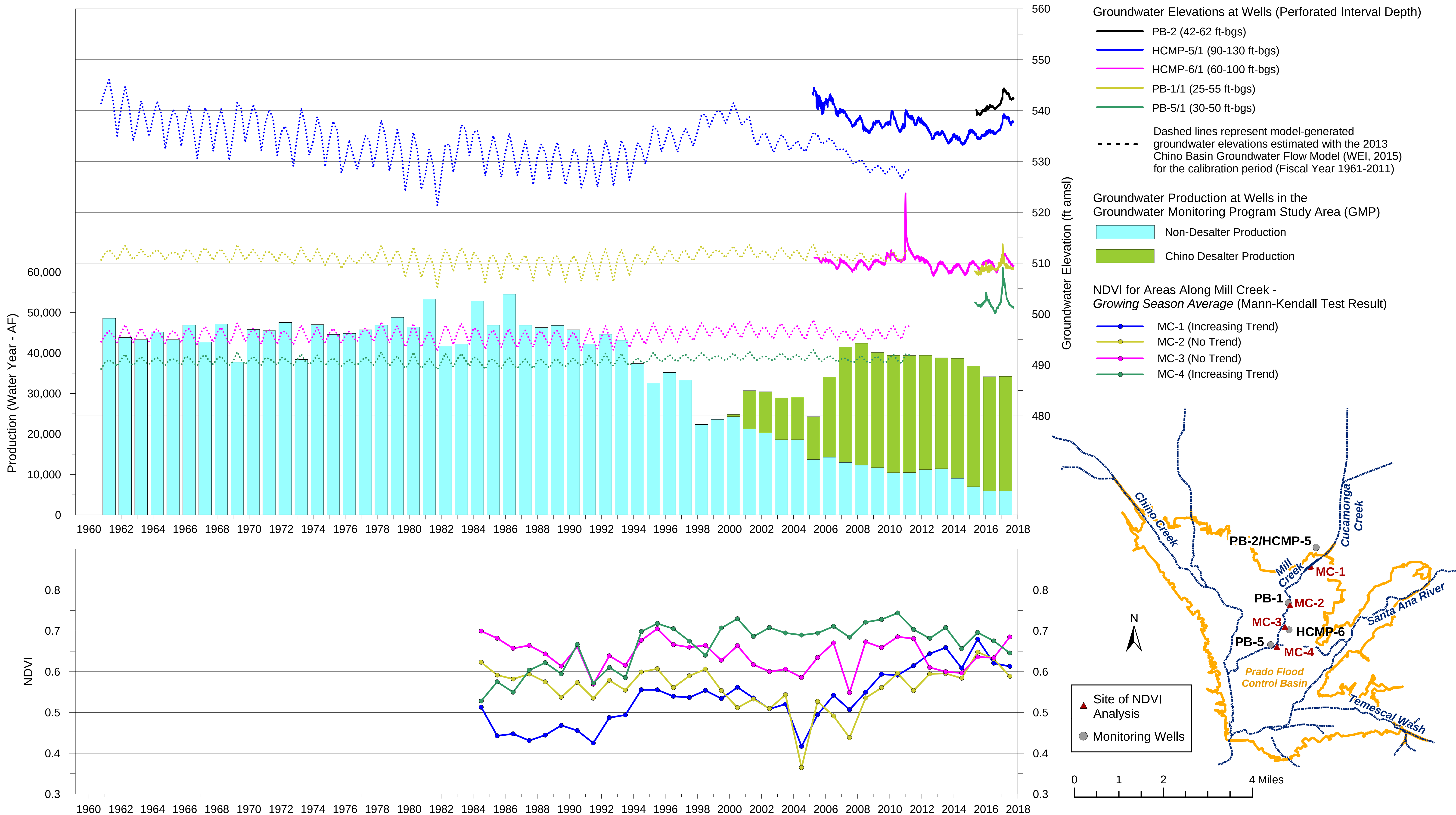

Prepared by:

WEI
Wildermuth Environmental, Inc.

Author: RT
Date: 20170329
Filename: Flows_WLs_MillCreek.grf

2017 Annual Report
Prado Basin Habitat Sustainability Committee

Groundwater Production and Groundwater Levels versus NDVI
Mill Creek Area for 1960-2017

Figure 3-12b

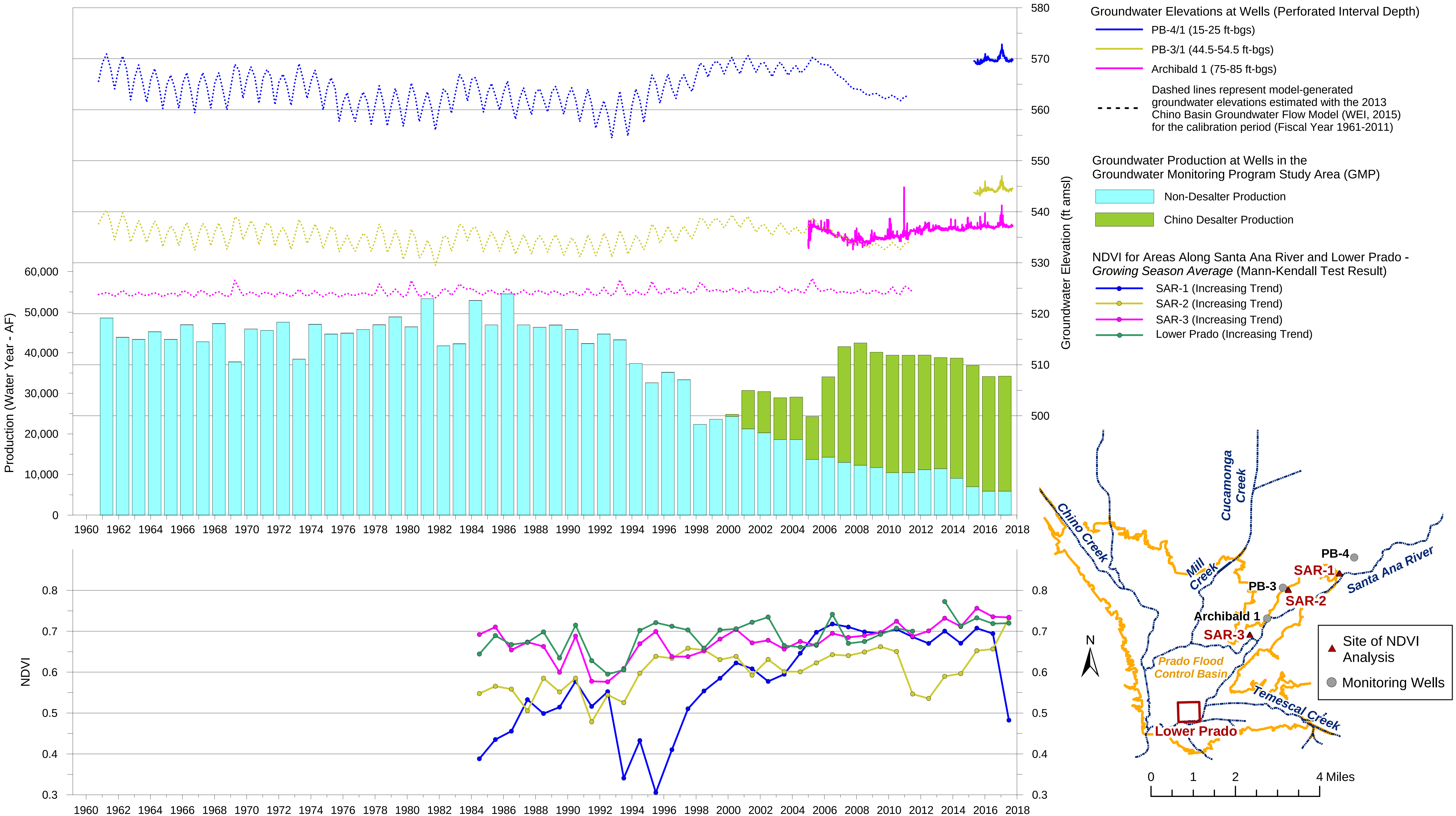

Prepared by:

WEI Wildermuth Environmental, Inc.

Author: RT
Date: 20170404
Filename: Prod_GWLs_SAR.grf

2017 Annual Report
Prado Basin Habitat Sustainability Committee

Groundwater Production and Groundwater Levels versus NDVI
Santa Ana River and Lower Prado Area for 1960-2017

Figure 3-12c

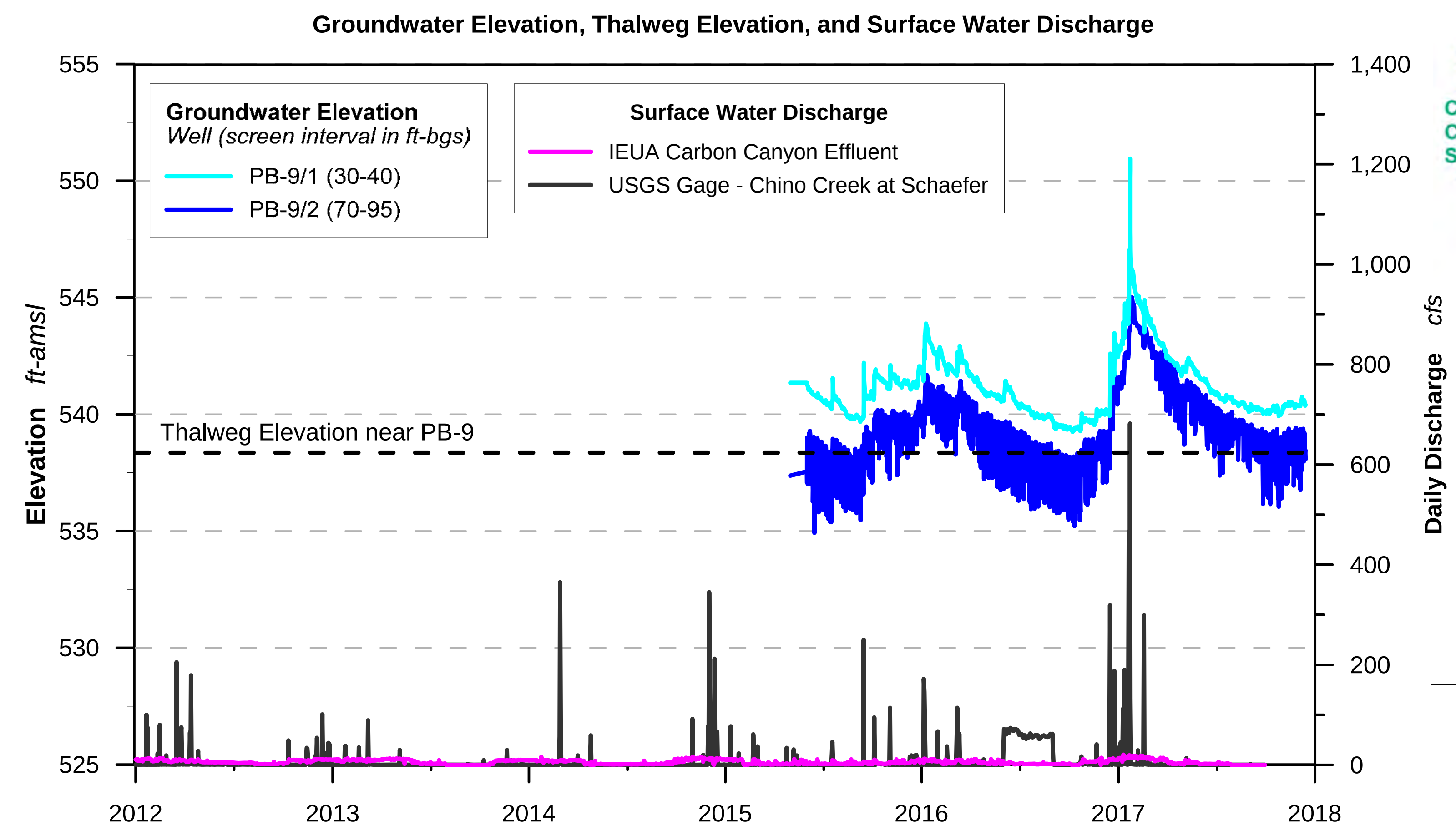

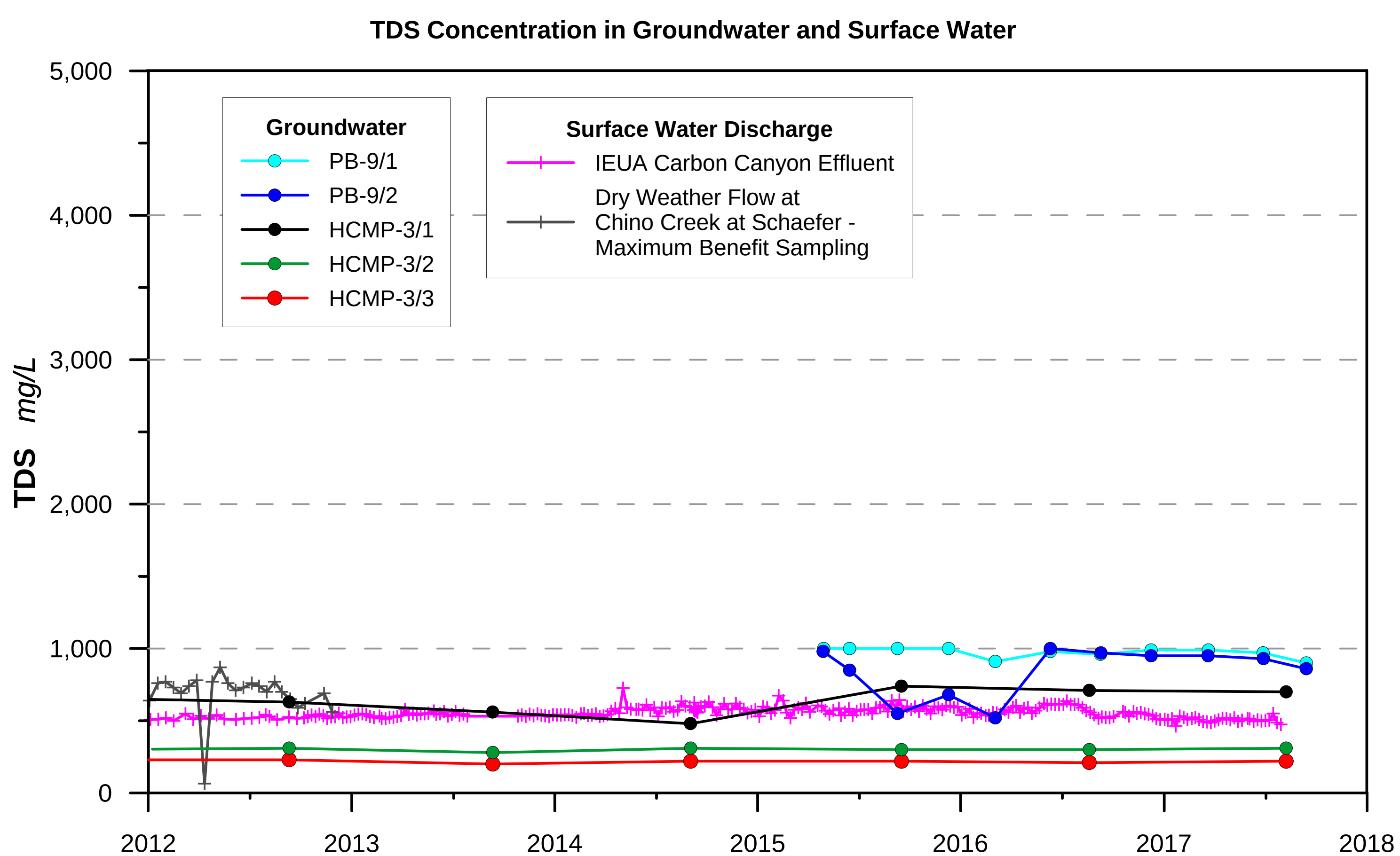

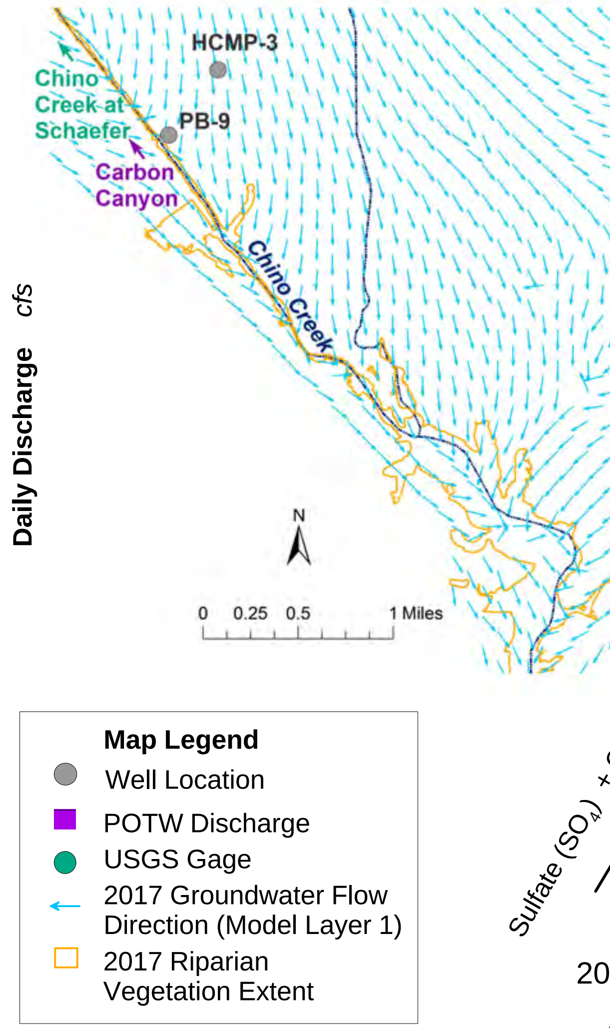

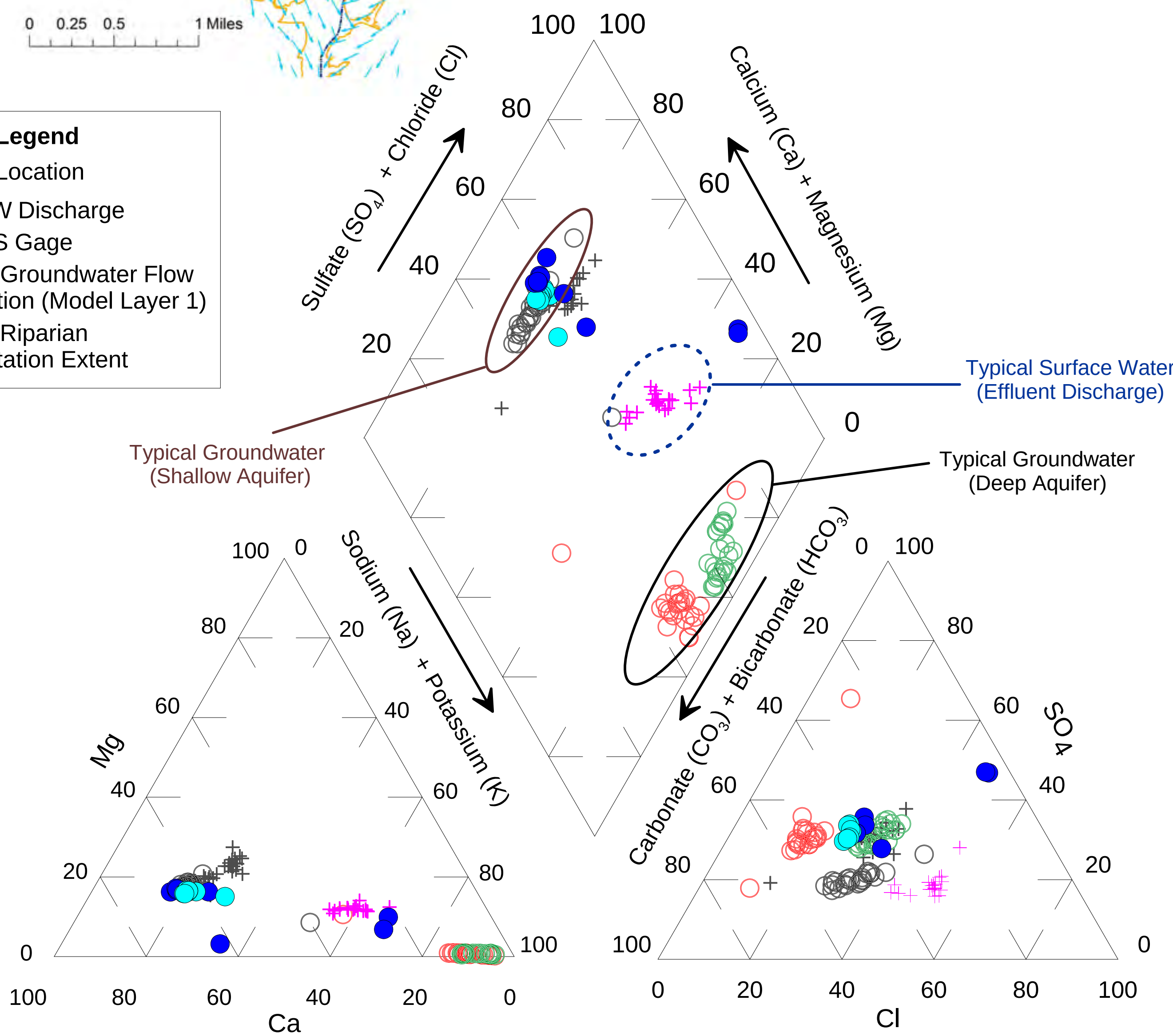

Prado Basin Habitat Sustainability Committee
2017 Annual Report

Groundwater and Surface Water Interactions
Chino Creek Near PB-9

Figure 3-13a

Groundwater Elevation, Thalweg Elevation, and Surface Water Discharge

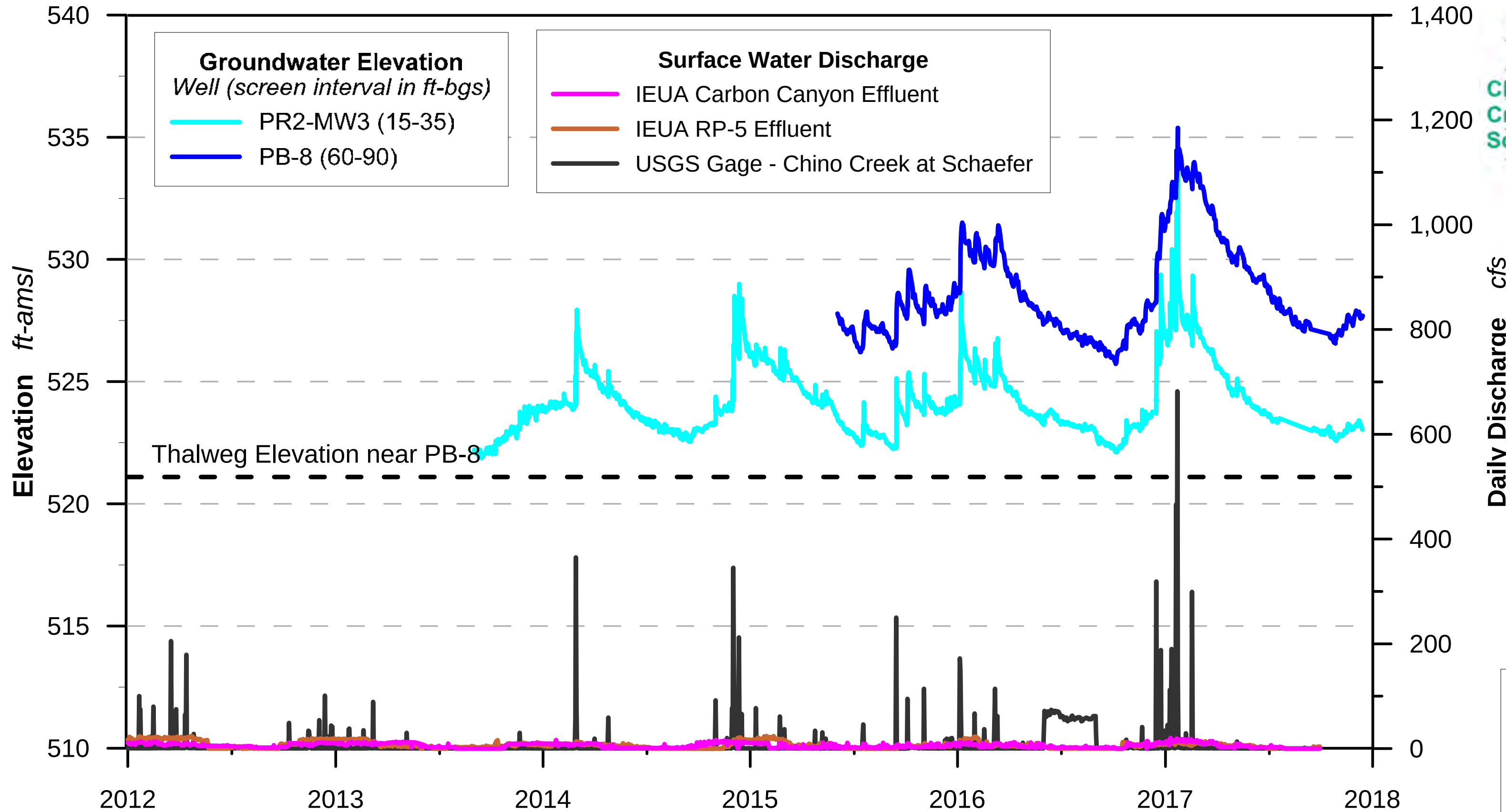

TDS Concentration in Groundwater and Surface Water

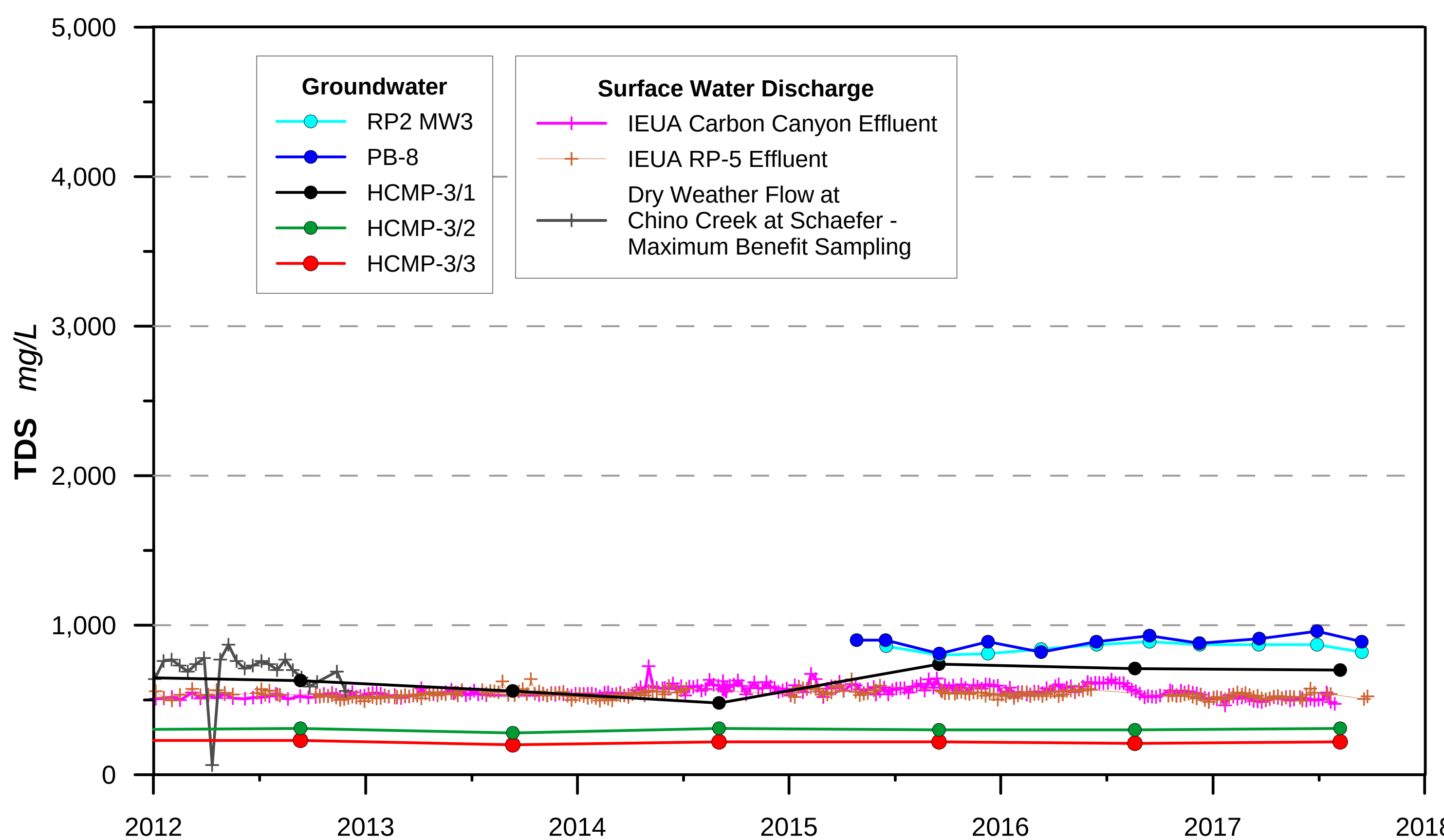

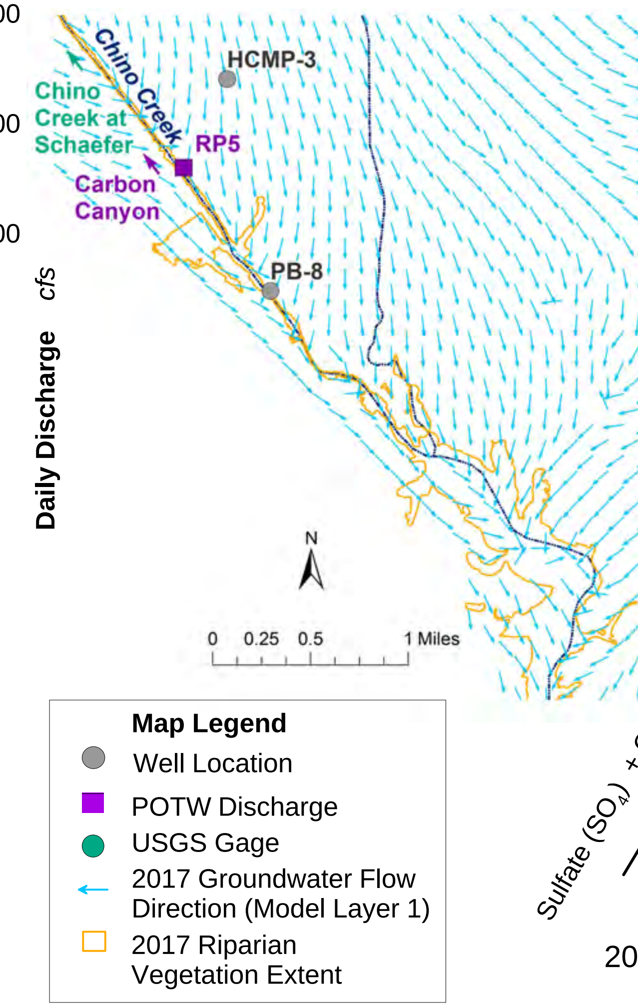

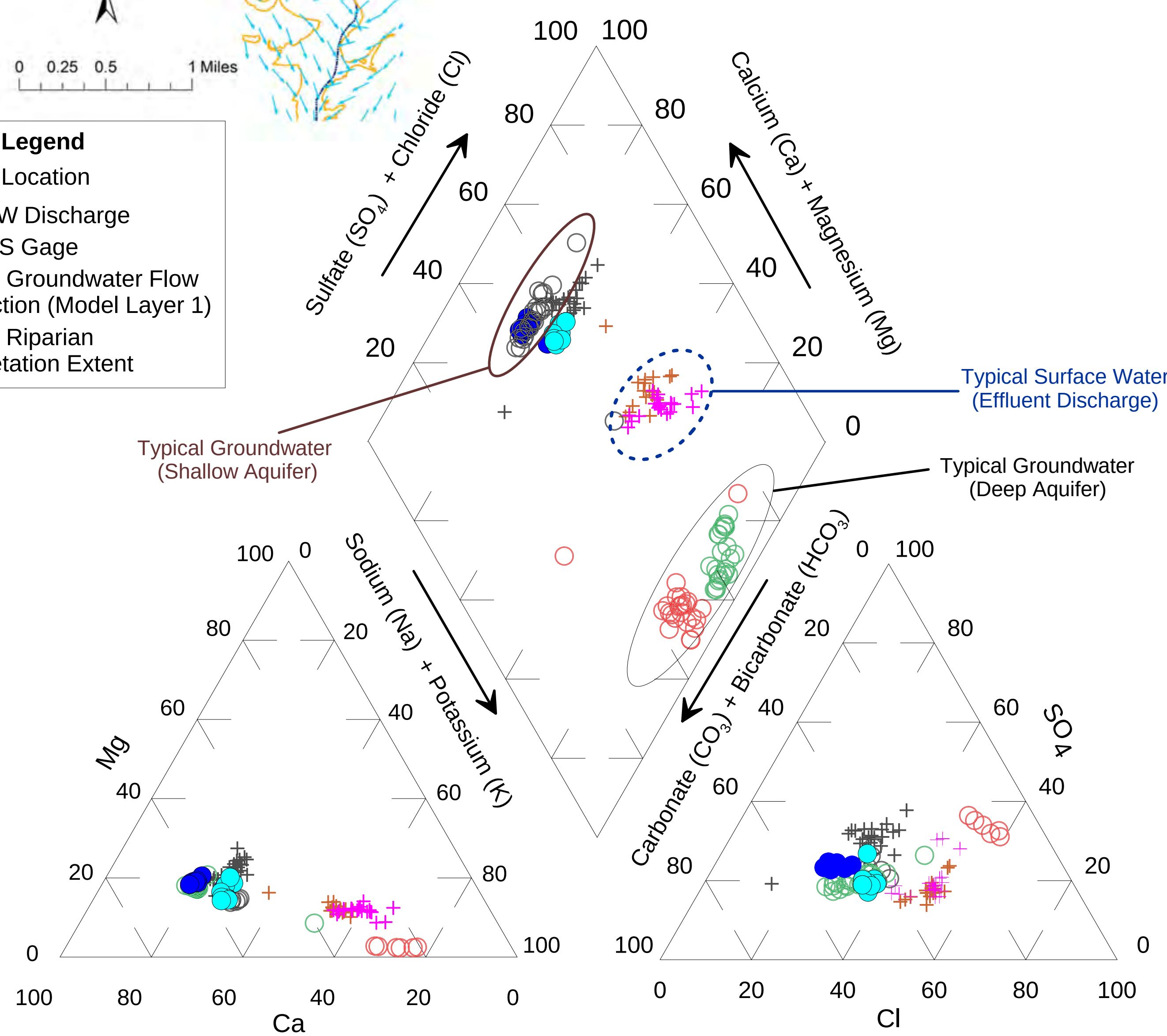

Prado Basin Habitat Sustainability Committee
2017 Annual Report

Groundwater and Surface Water Interactions
Chino Creek Near PB-8

Figure 3-13b

Groundwater Elevation, Thalweg Elevation, and Surface Water Discharge

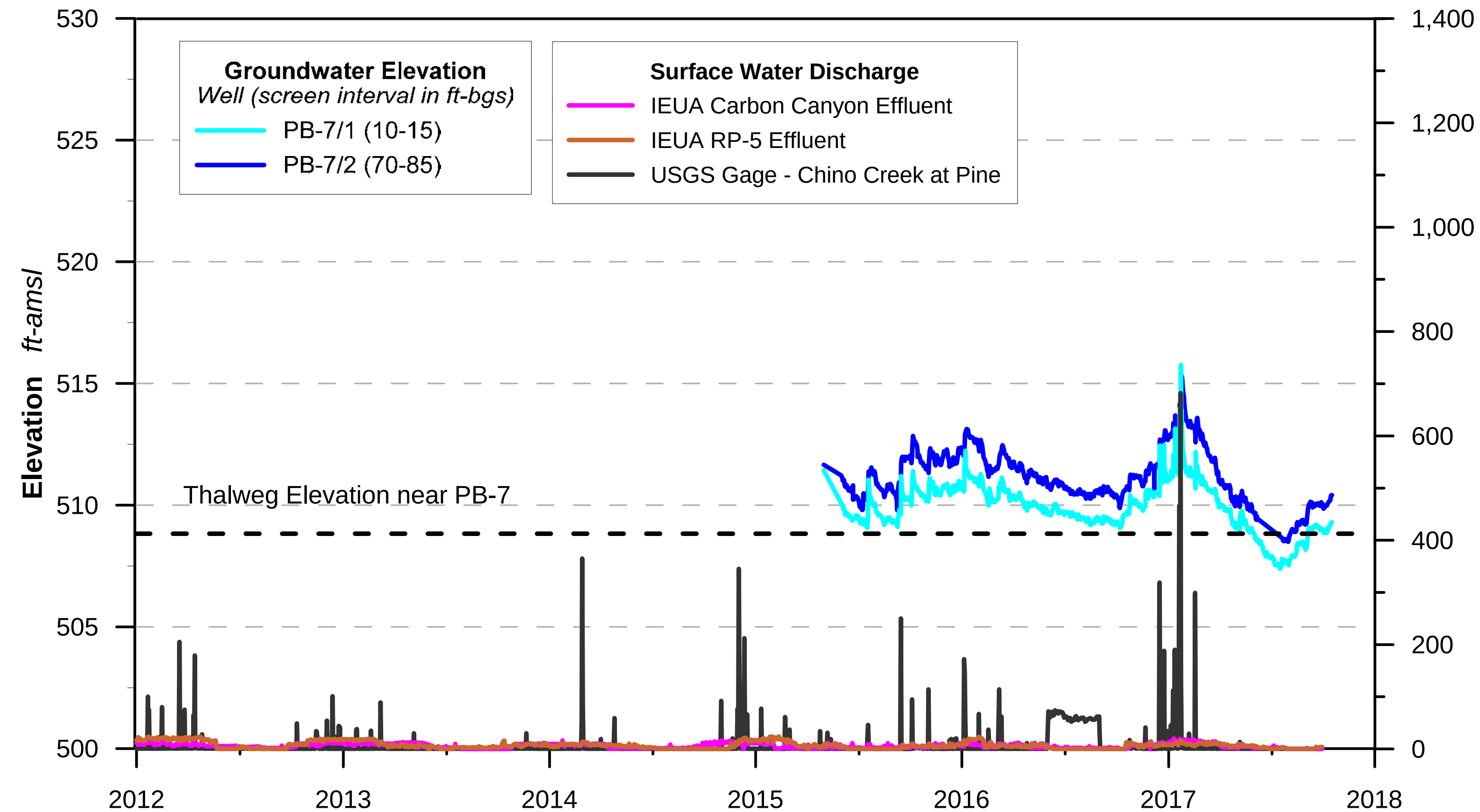

TDS Concentration in Groundwater and Surface Water

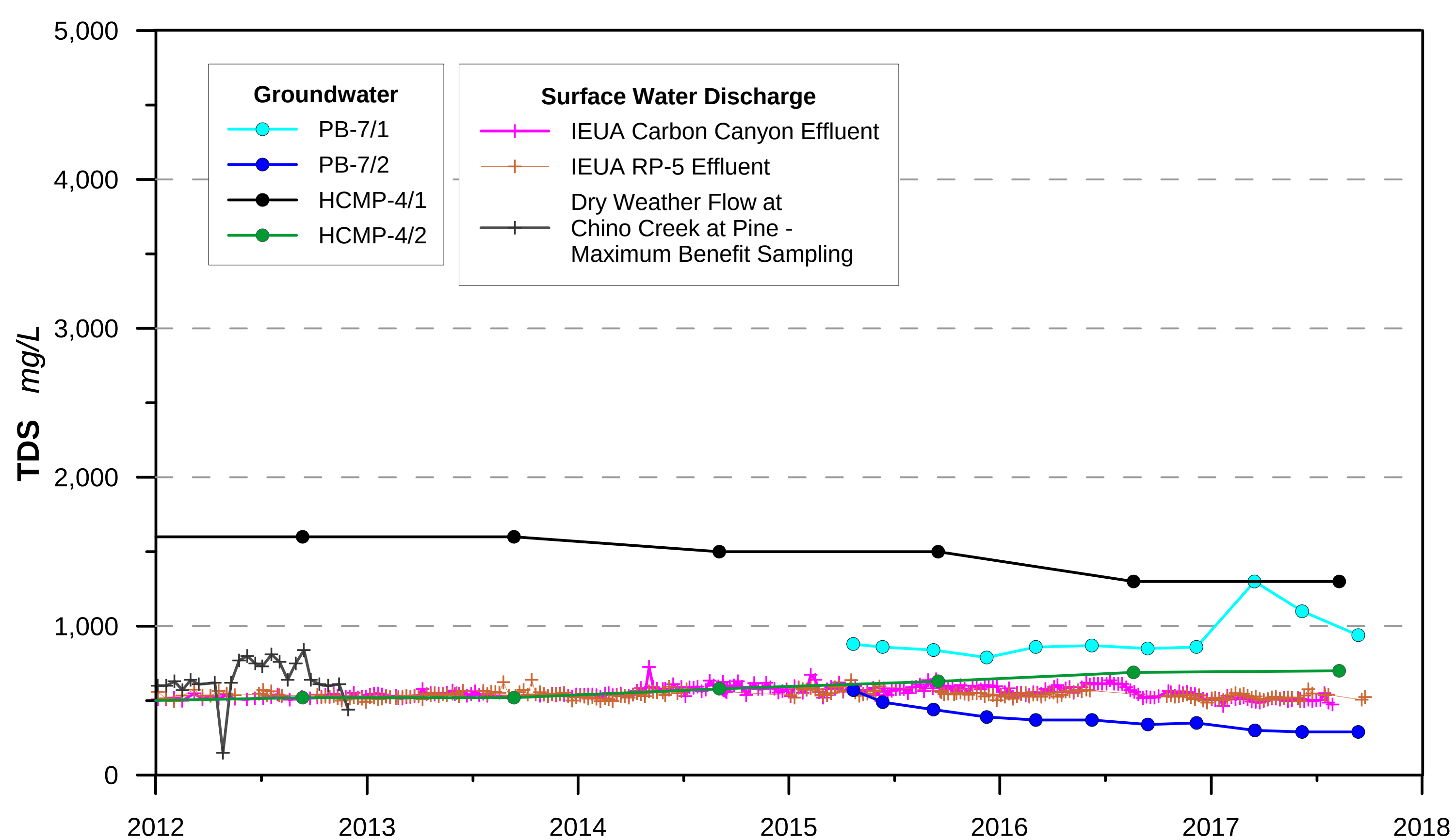

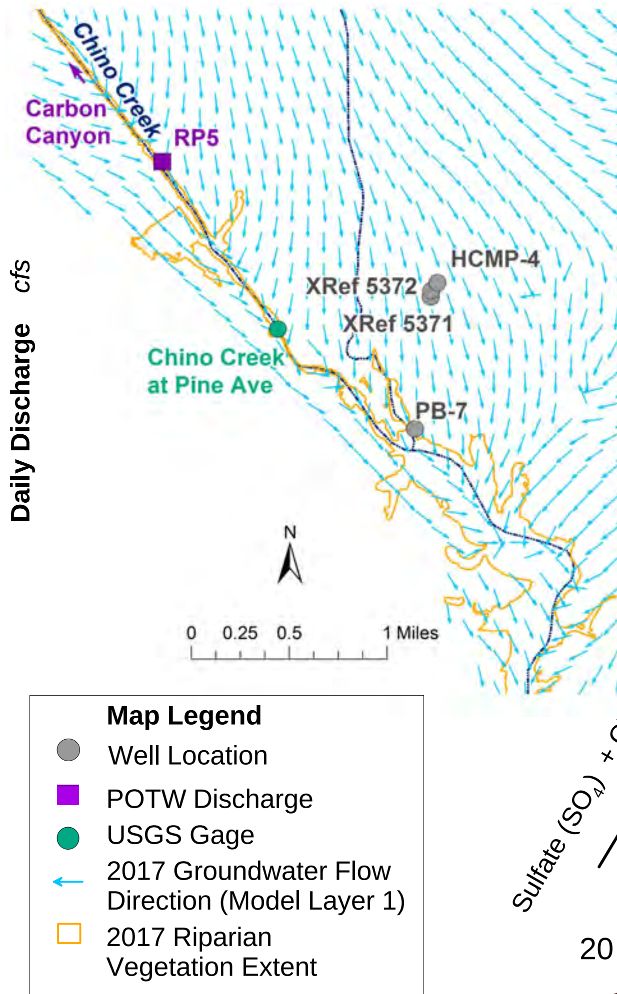

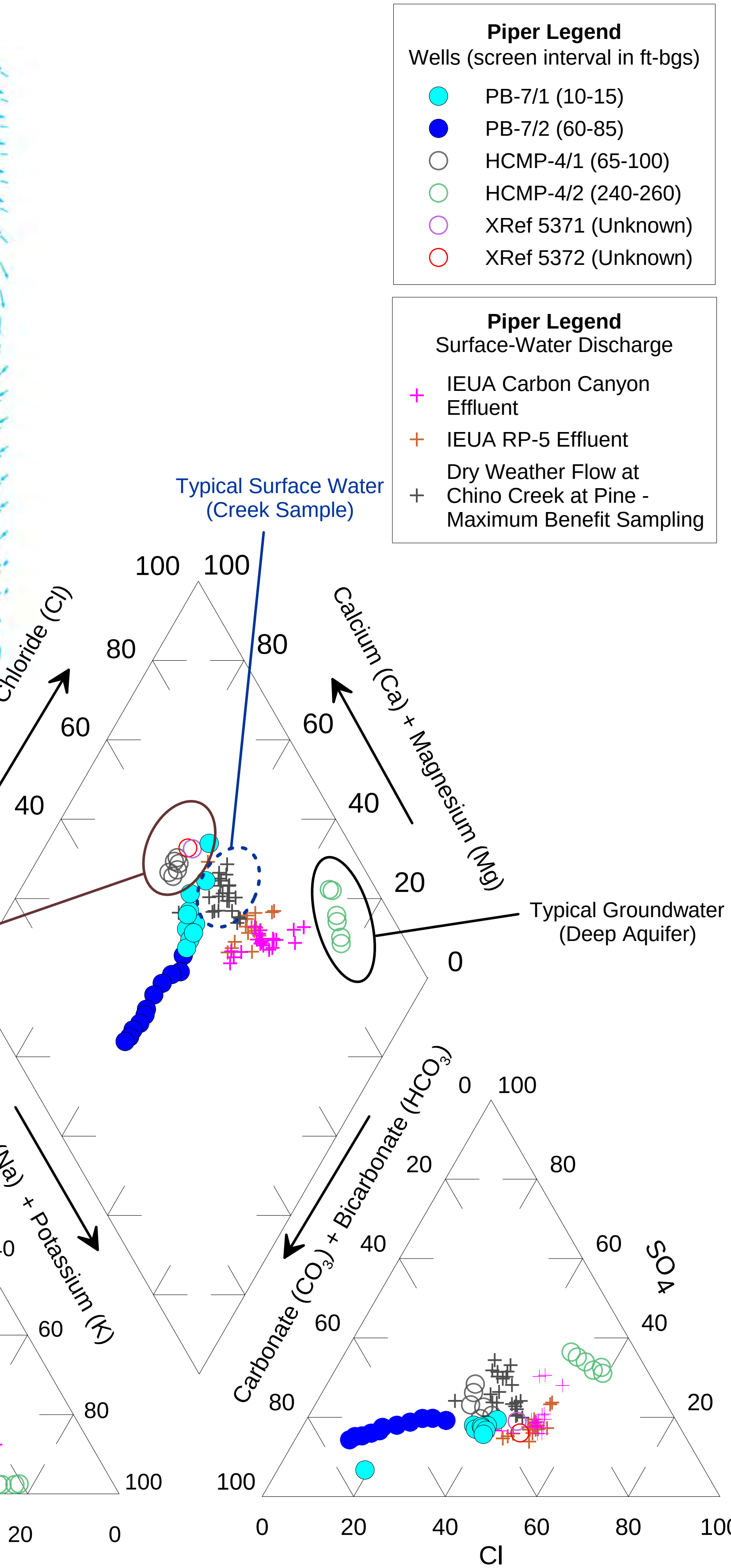

Prado Basin Habitat Sustainability Committee
2017 Annual Report

Groundwater and Surface Water Interactions
Chino Creek Near PB-7

Figure 3-13c

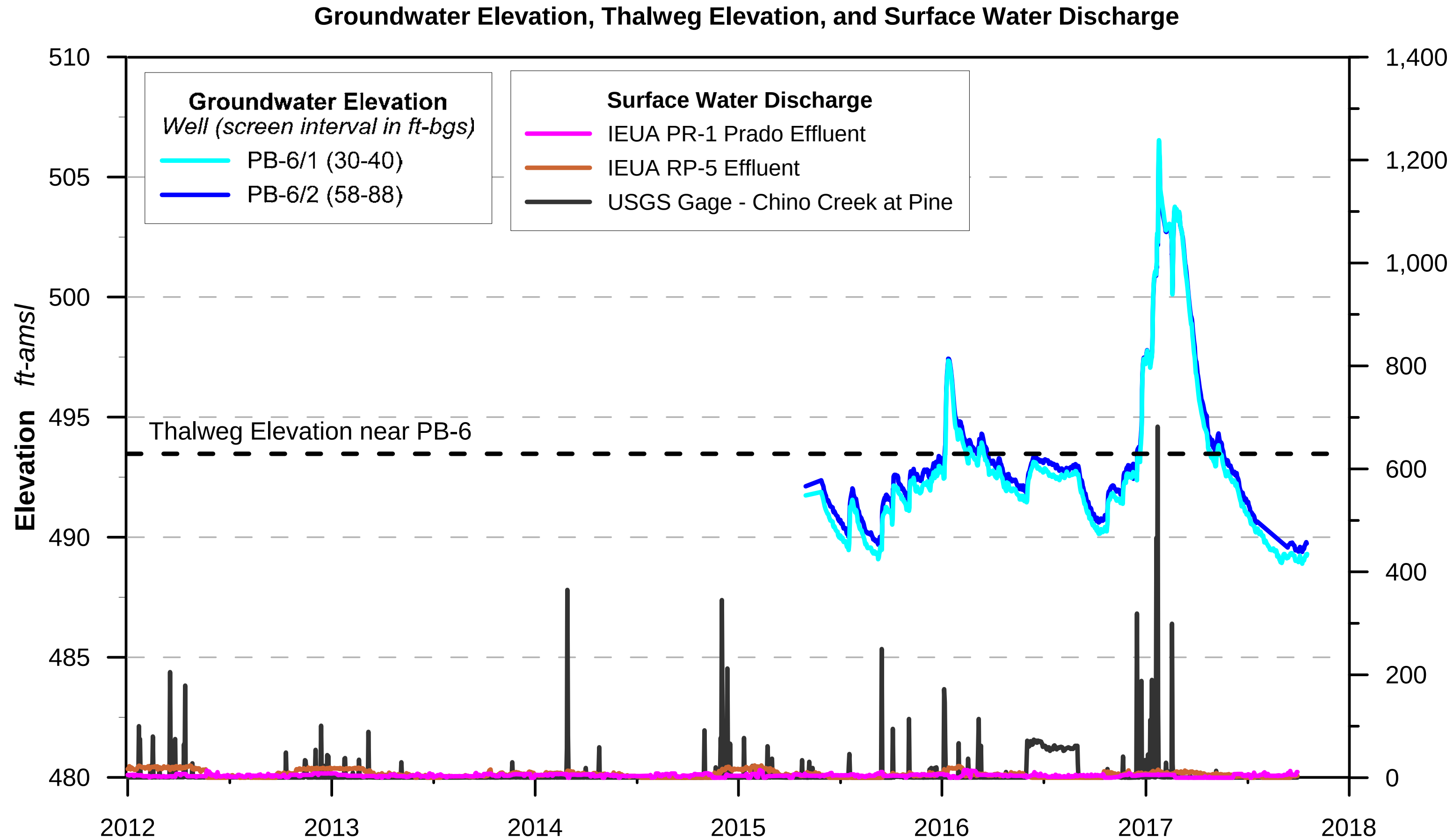

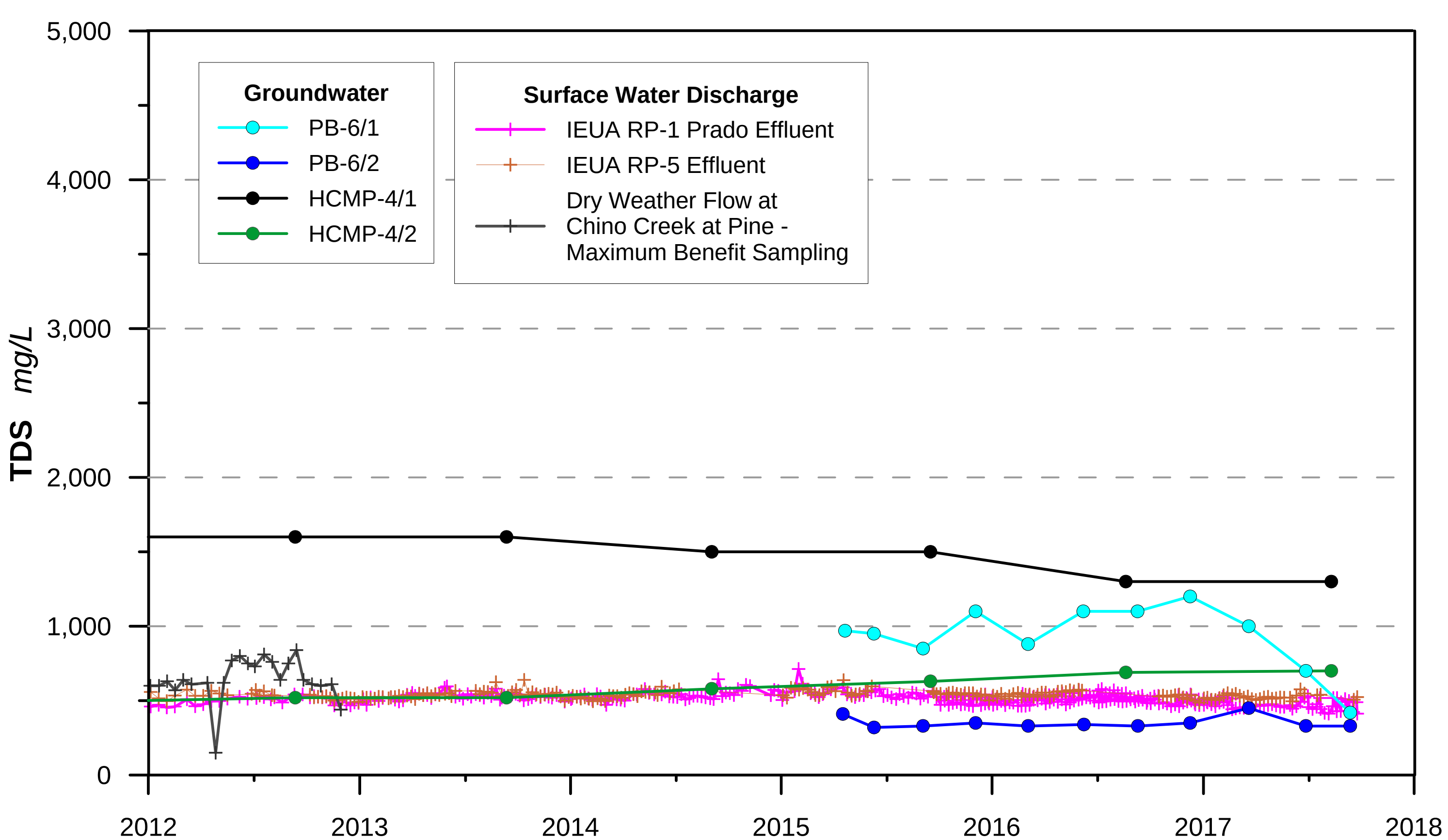

TDS Concentration in Groundwater and Surface Water

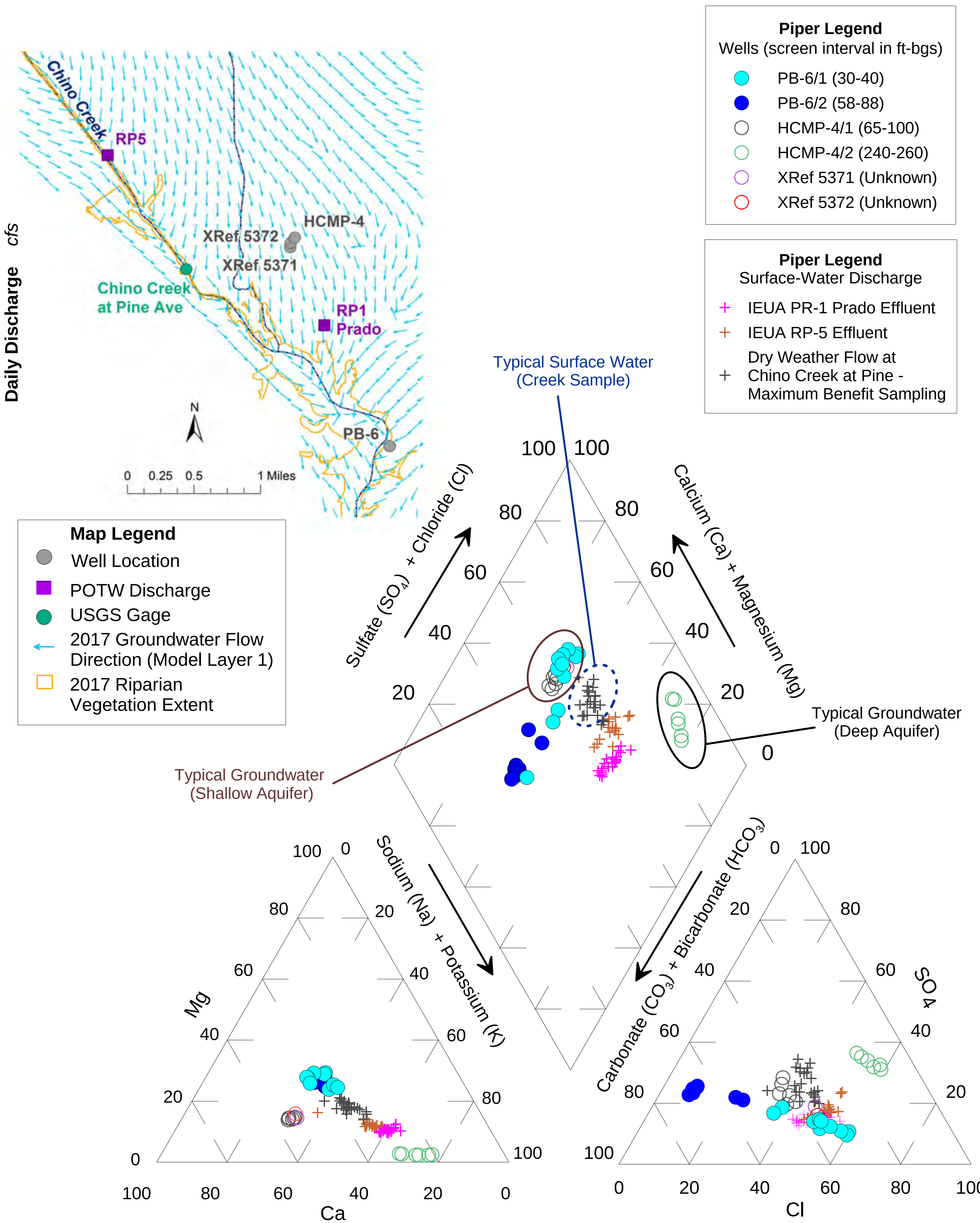

Prado Basin Habitat Sustainability Committee
2017 Annual Report

Groundwater and Surface Water Interactions
Chino Creek Near PB-6

Figure 3-13d

Groundwater Elevation, Thalweg Elevation, and Surface Water Discharge

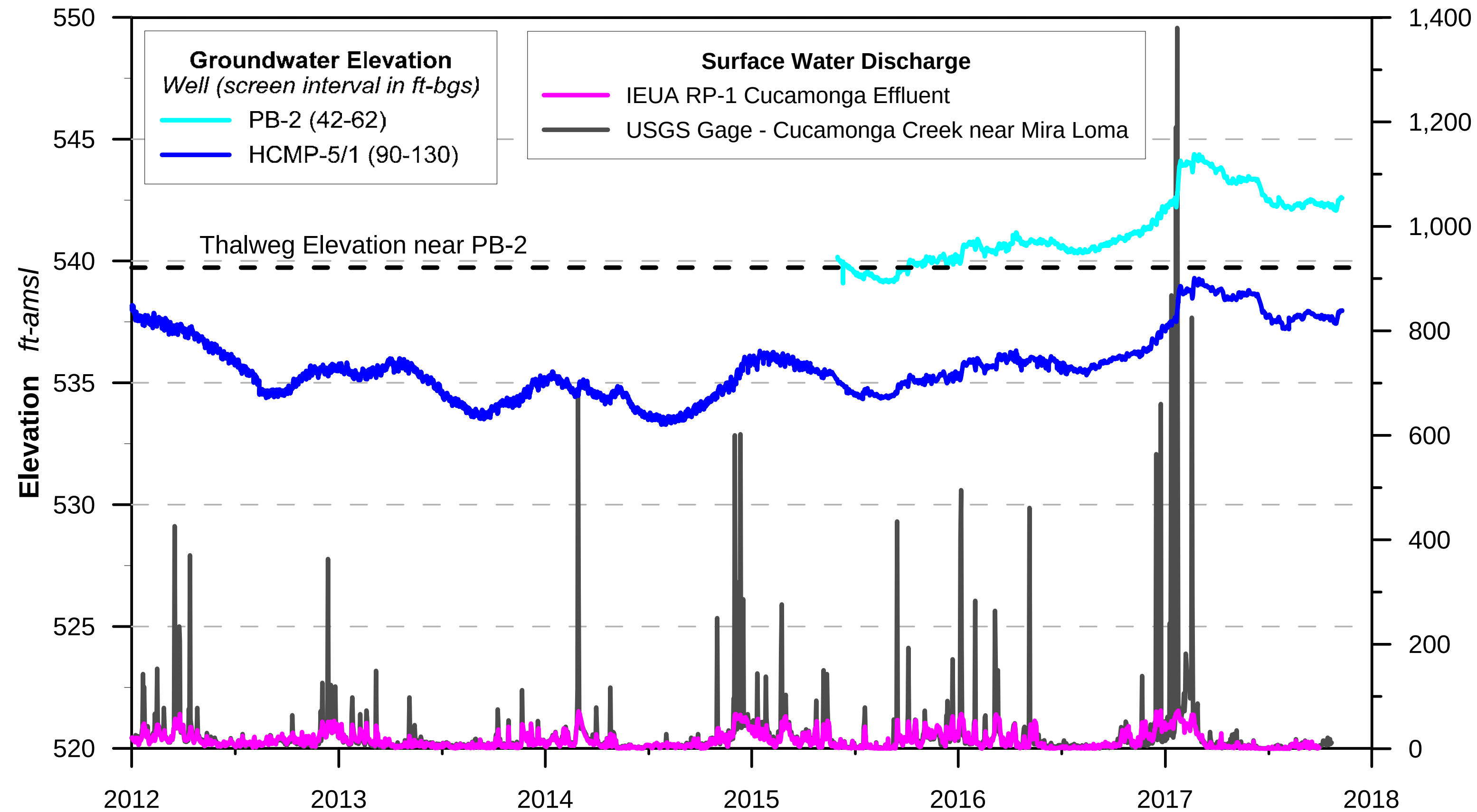

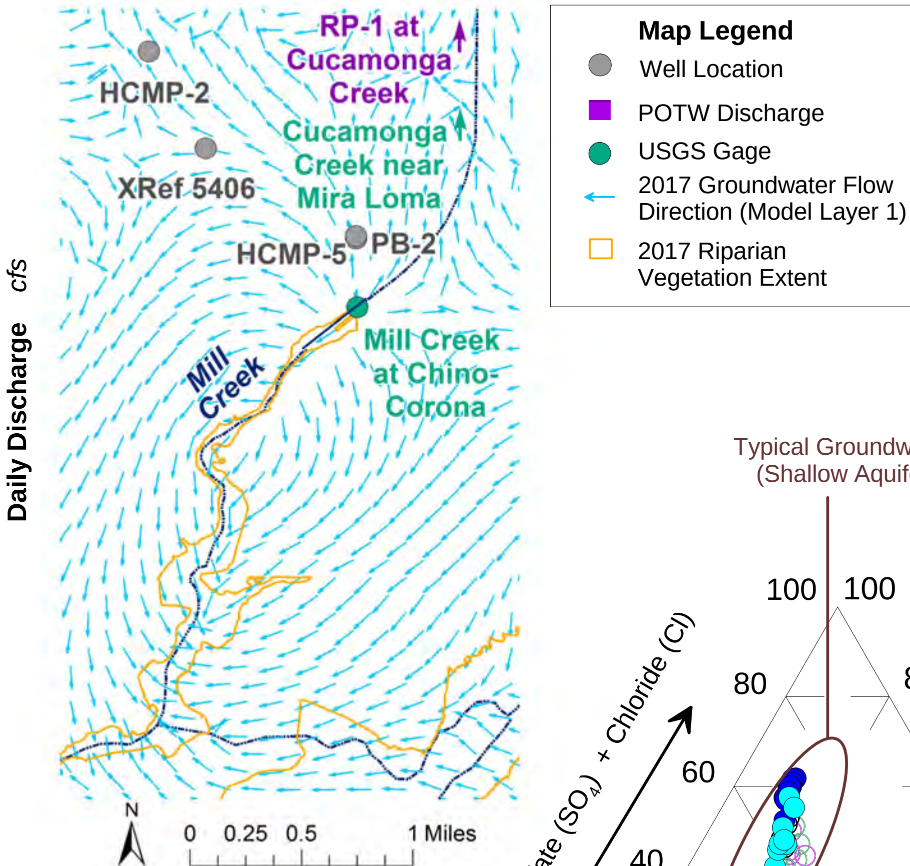

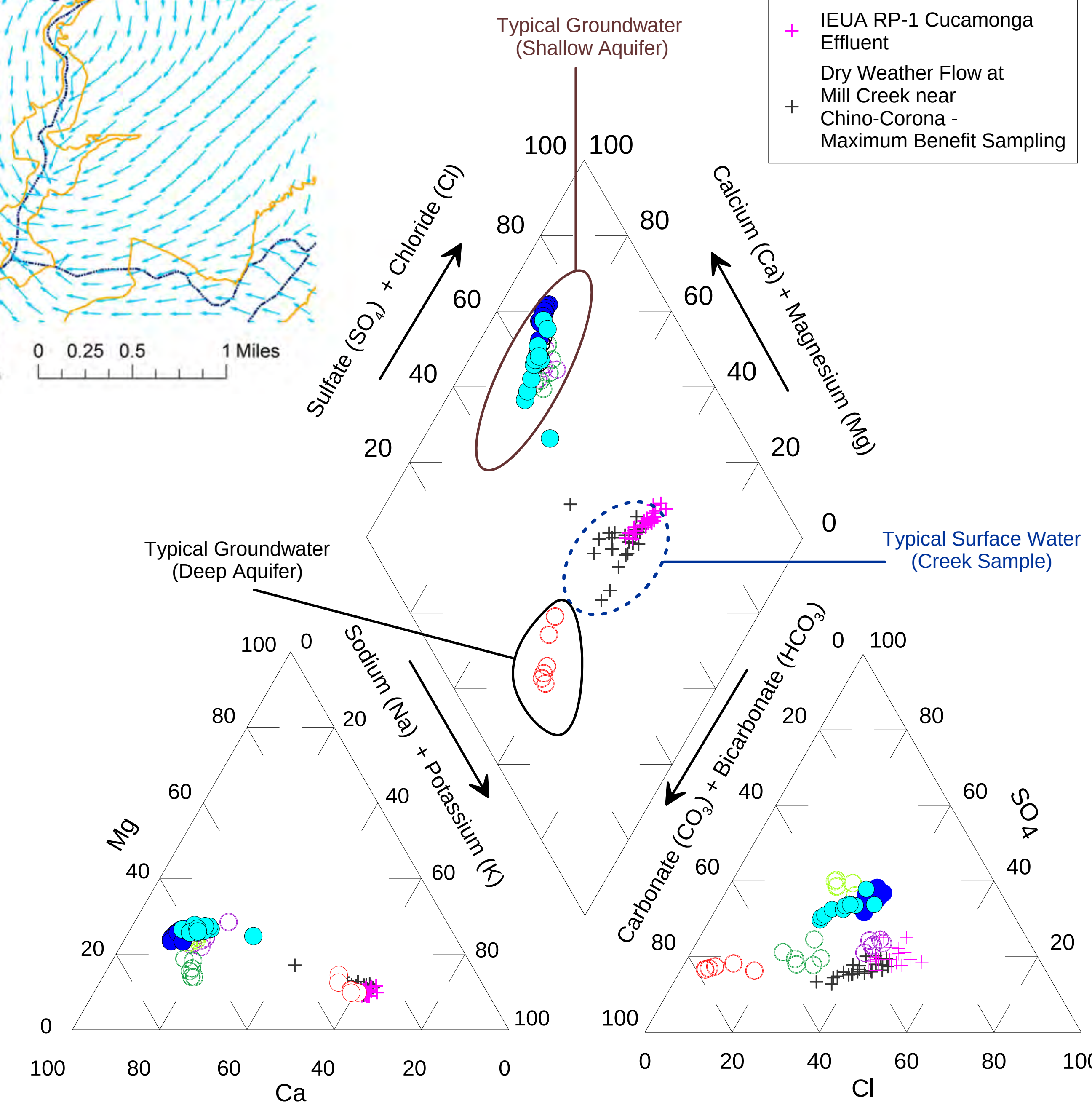

TDS Concentration in Groundwater and Surface Water

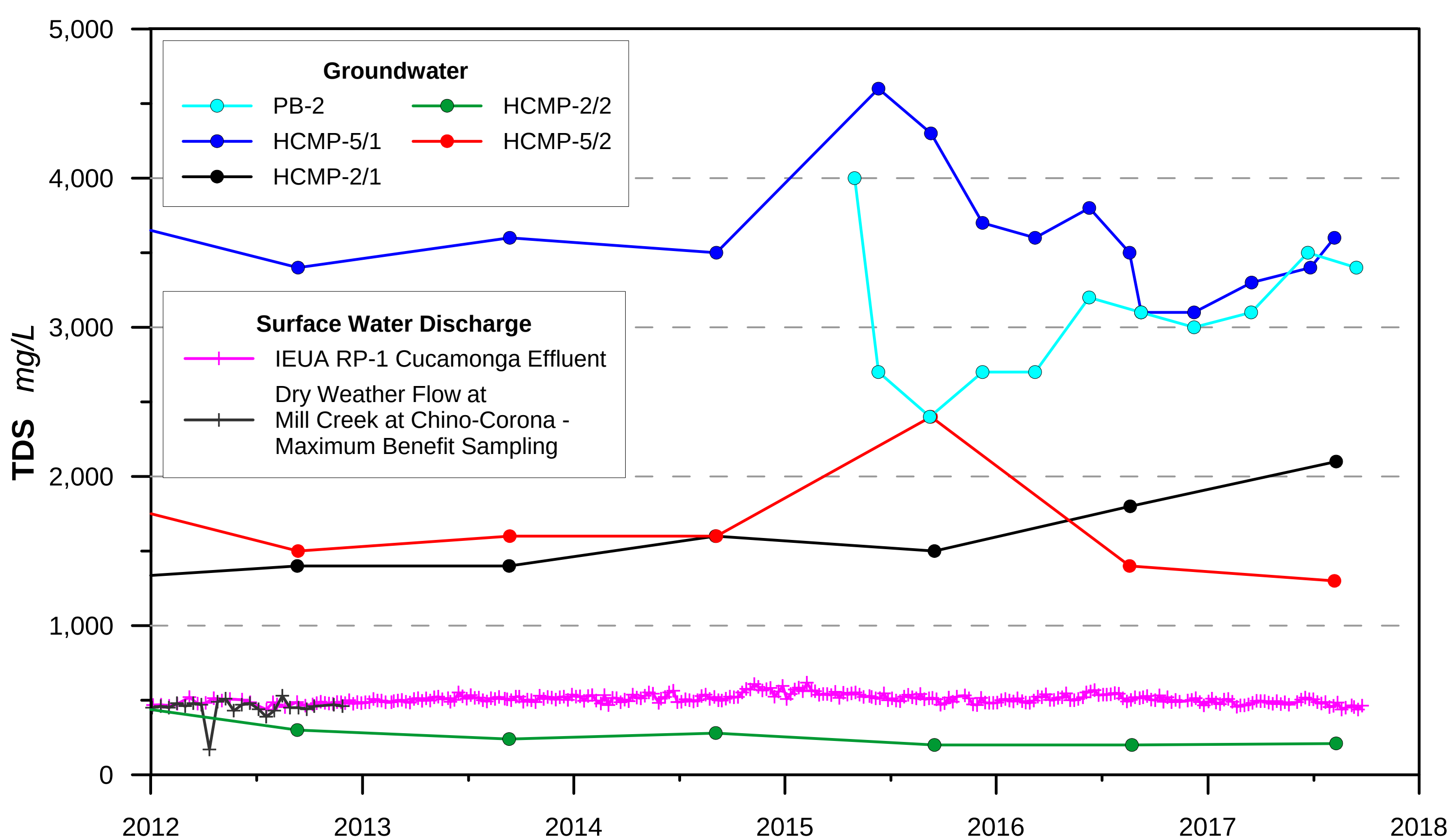

Groundwater and Surface Water Interactions
Mill Creek Near PB-2

Figure 3-13e

Groundwater Elevation, Thalweg Elevation, and Surface Water Discharge

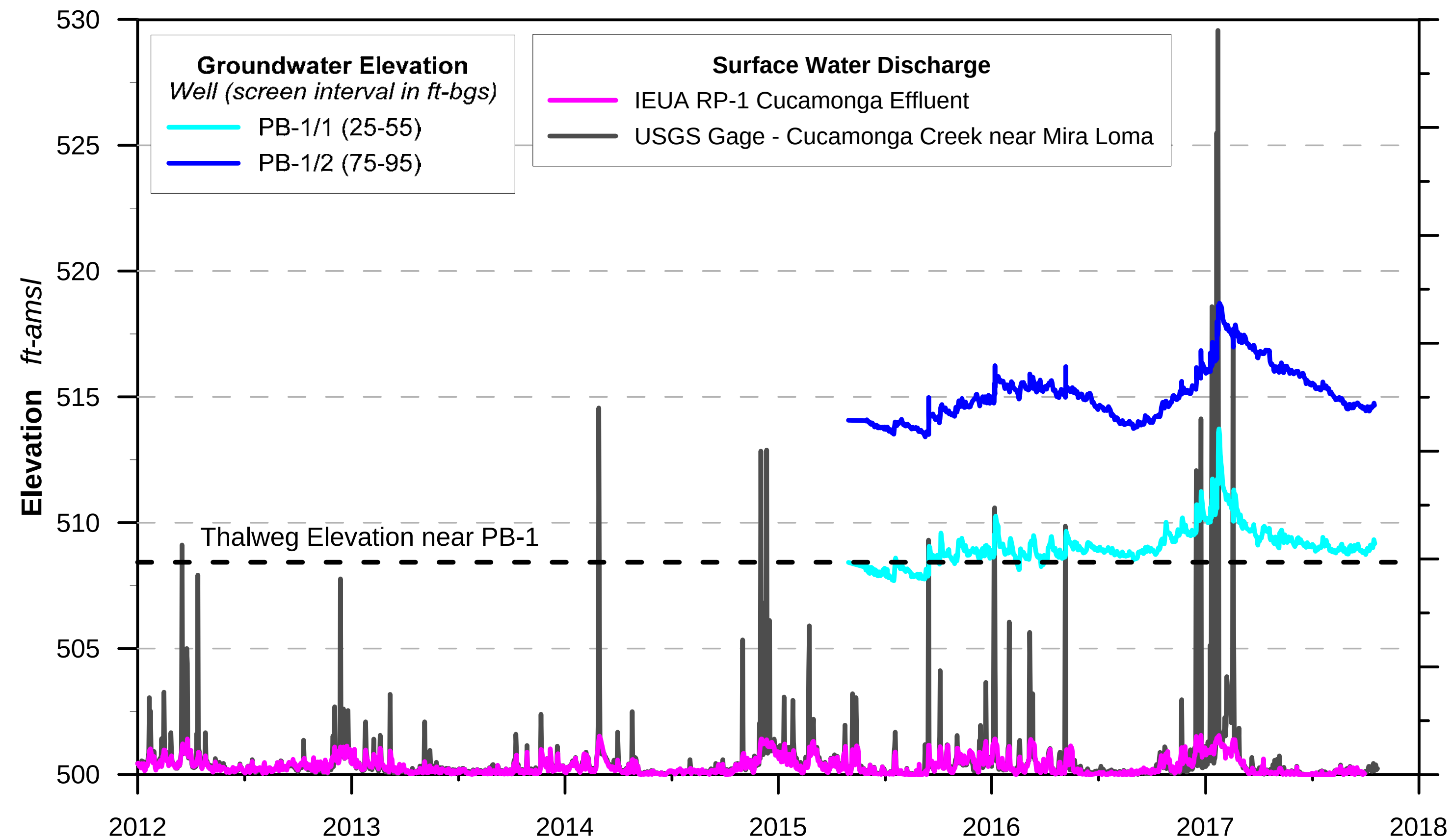

TDS Concentration in Groundwater and Surface Water

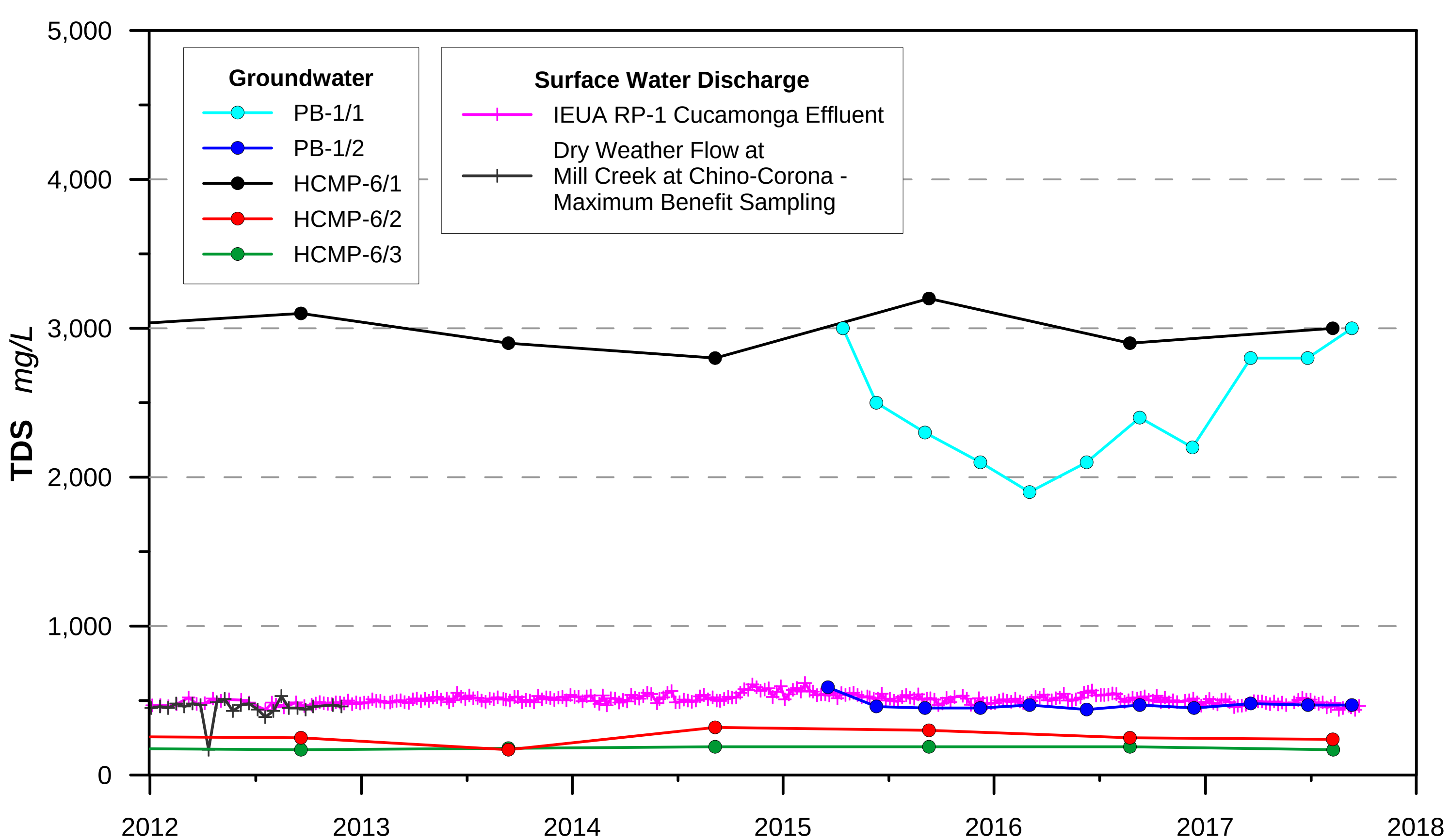

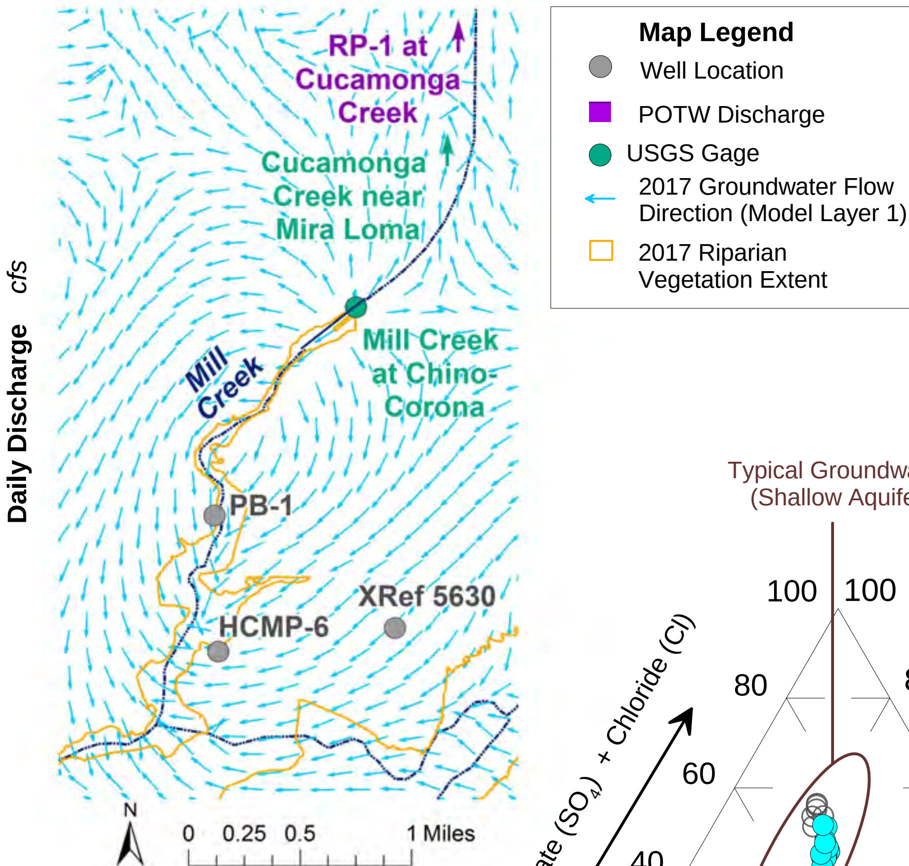

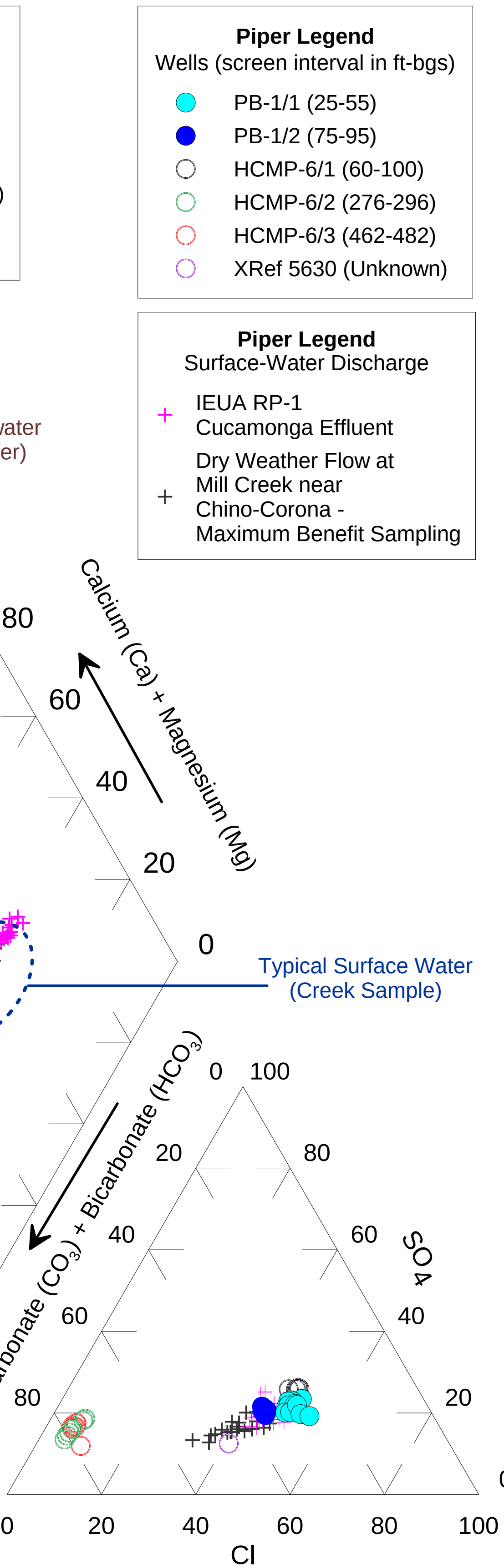

Prado Basin Habitat Sustainability Committee
2017 Annual Report

Groundwater and Surface Water Interactions
Mill Creek Near PB-1

Figure 3-13f

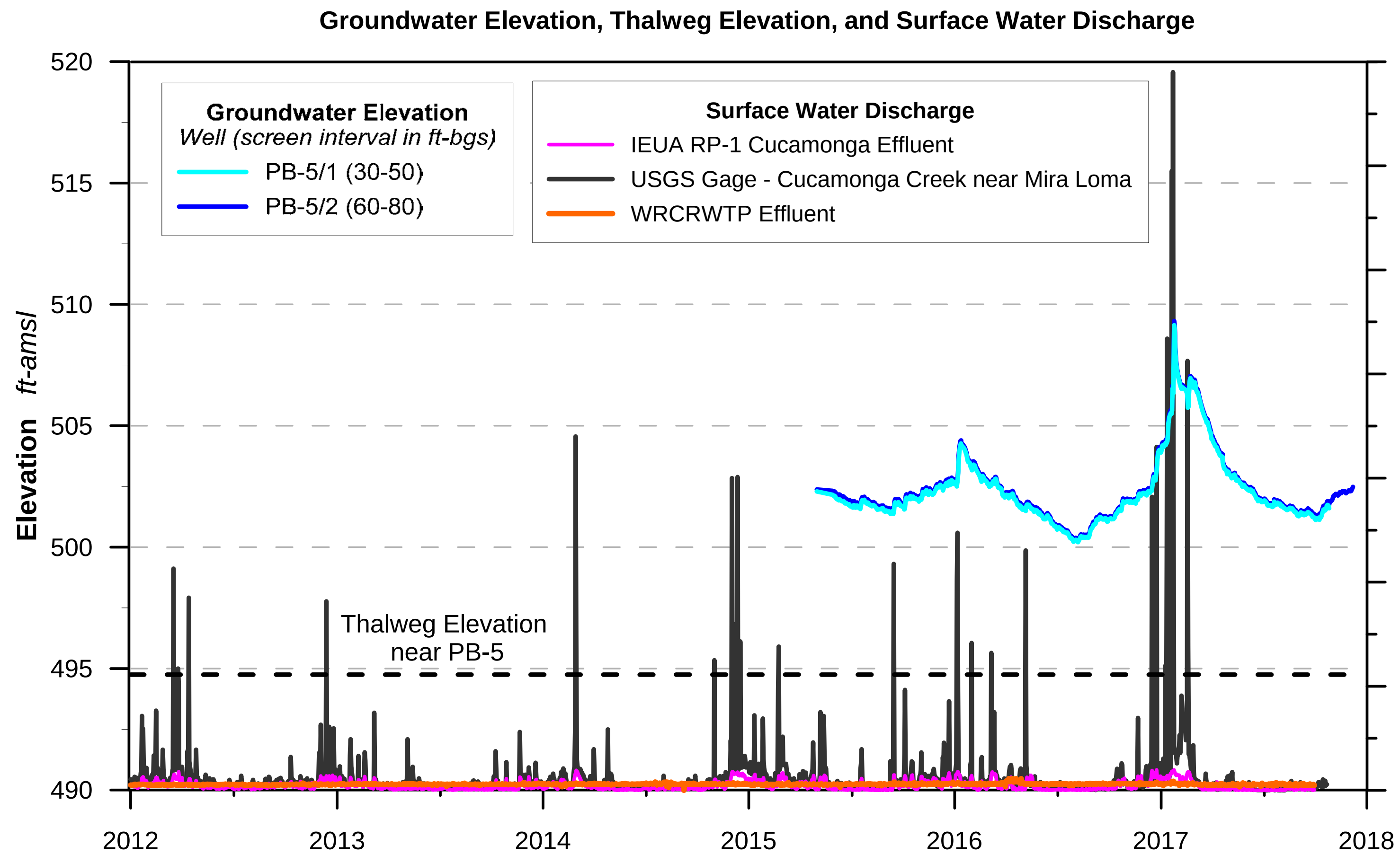

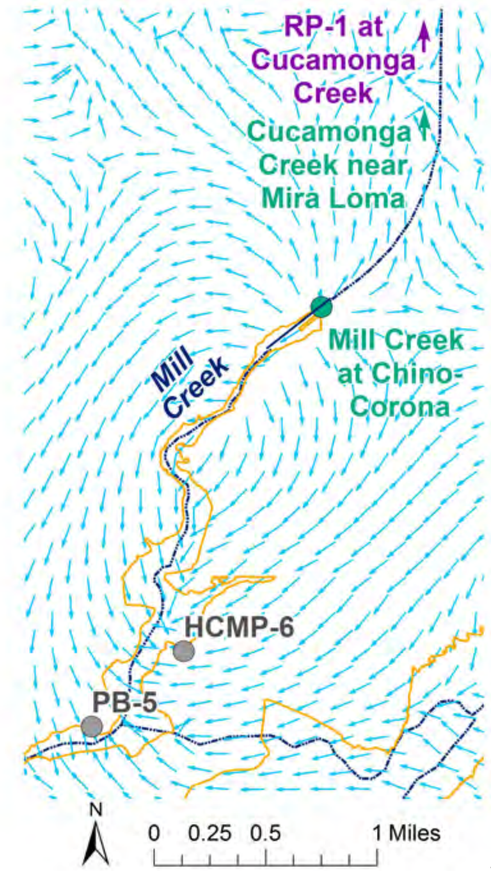

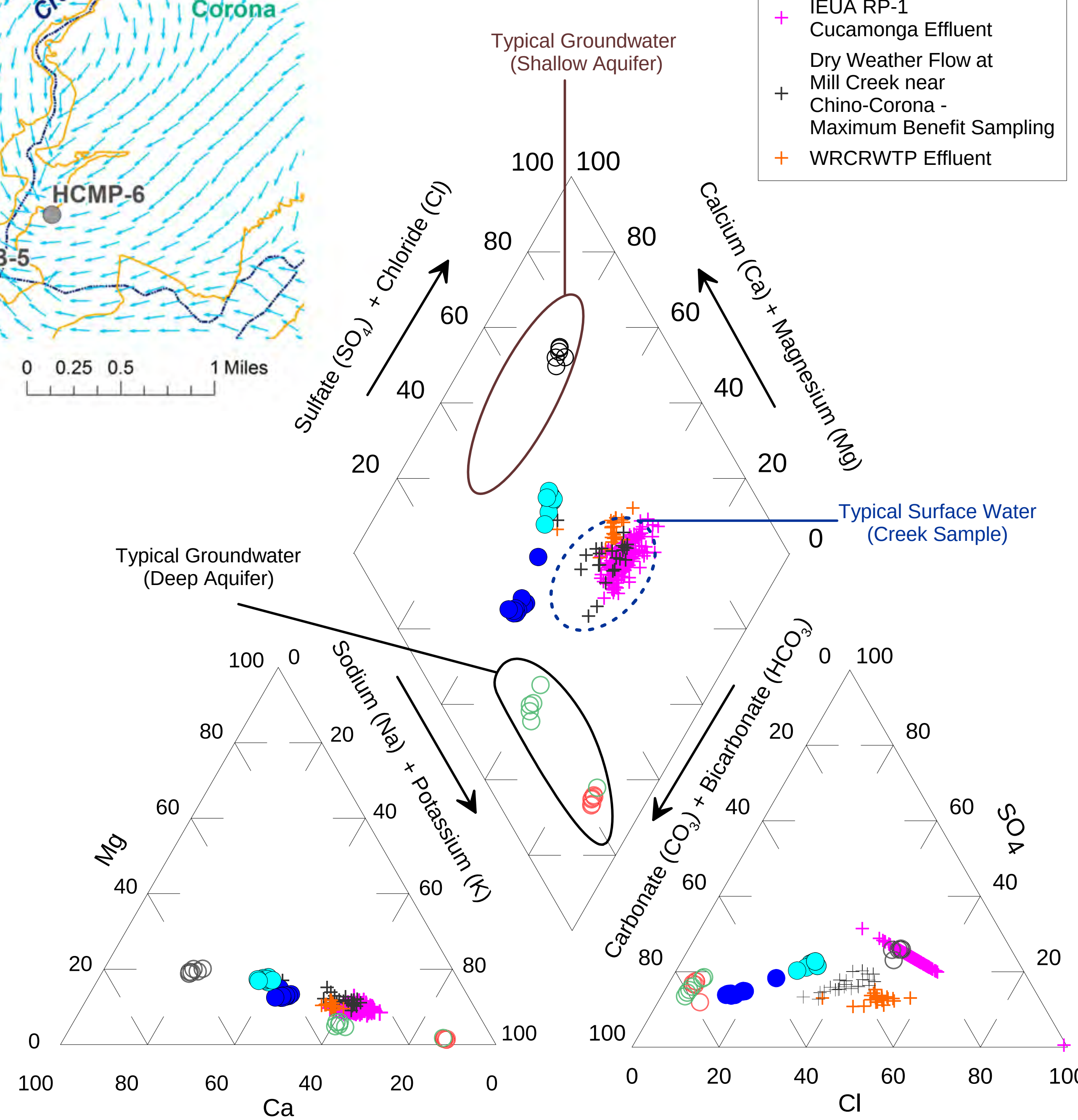

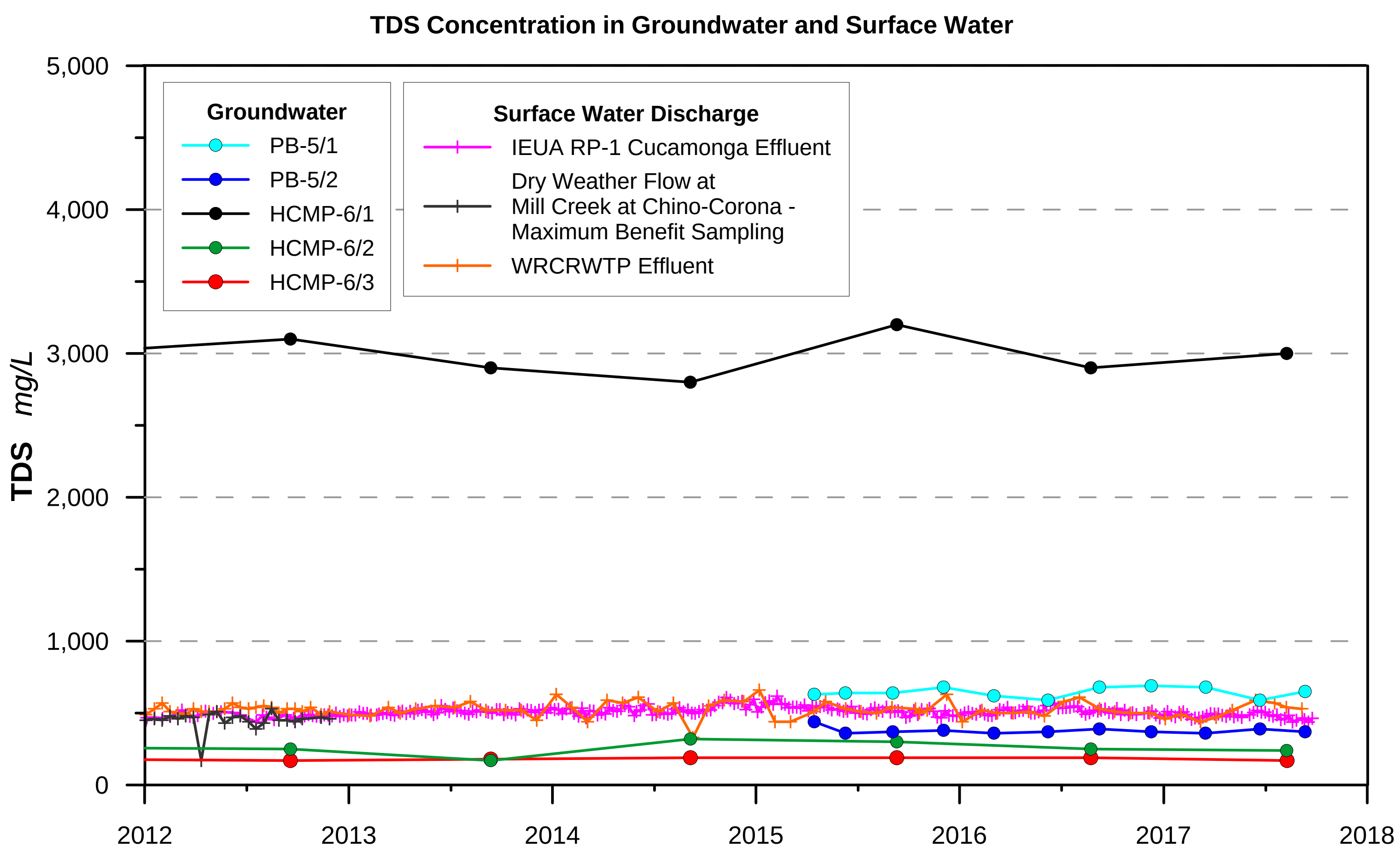

Prado Basin Habitat Sustainability Committee
2017 Annual Report

Groundwater and Surface Water Interactions
Mill Creek Near PB-5

Figure 3-13g

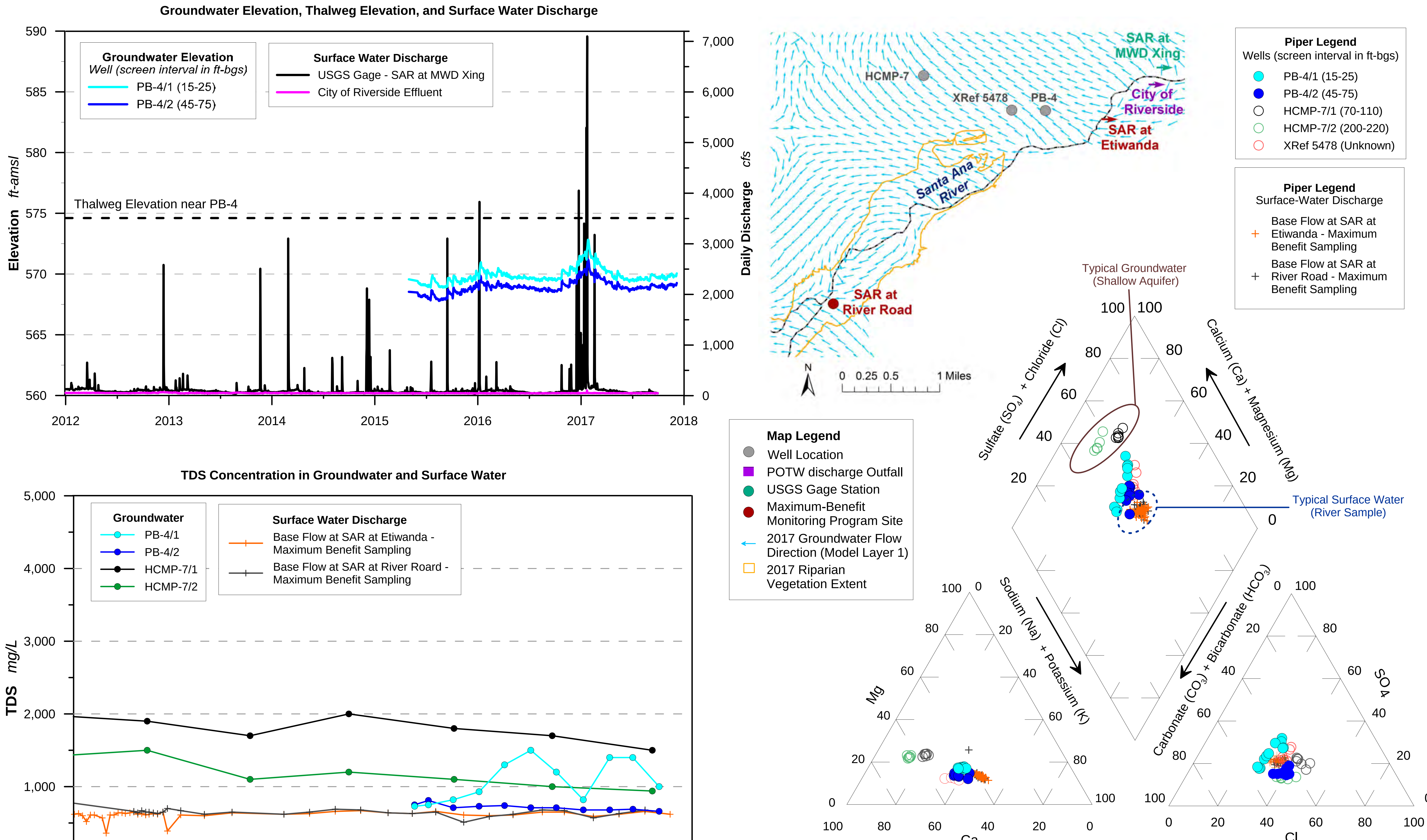

Prado Basin Habitat Sustainability Committee
2017 Annual Report

Groundwater and Surface Water Interactions
Santa Ana River Near PB-4

Figure 3-13h

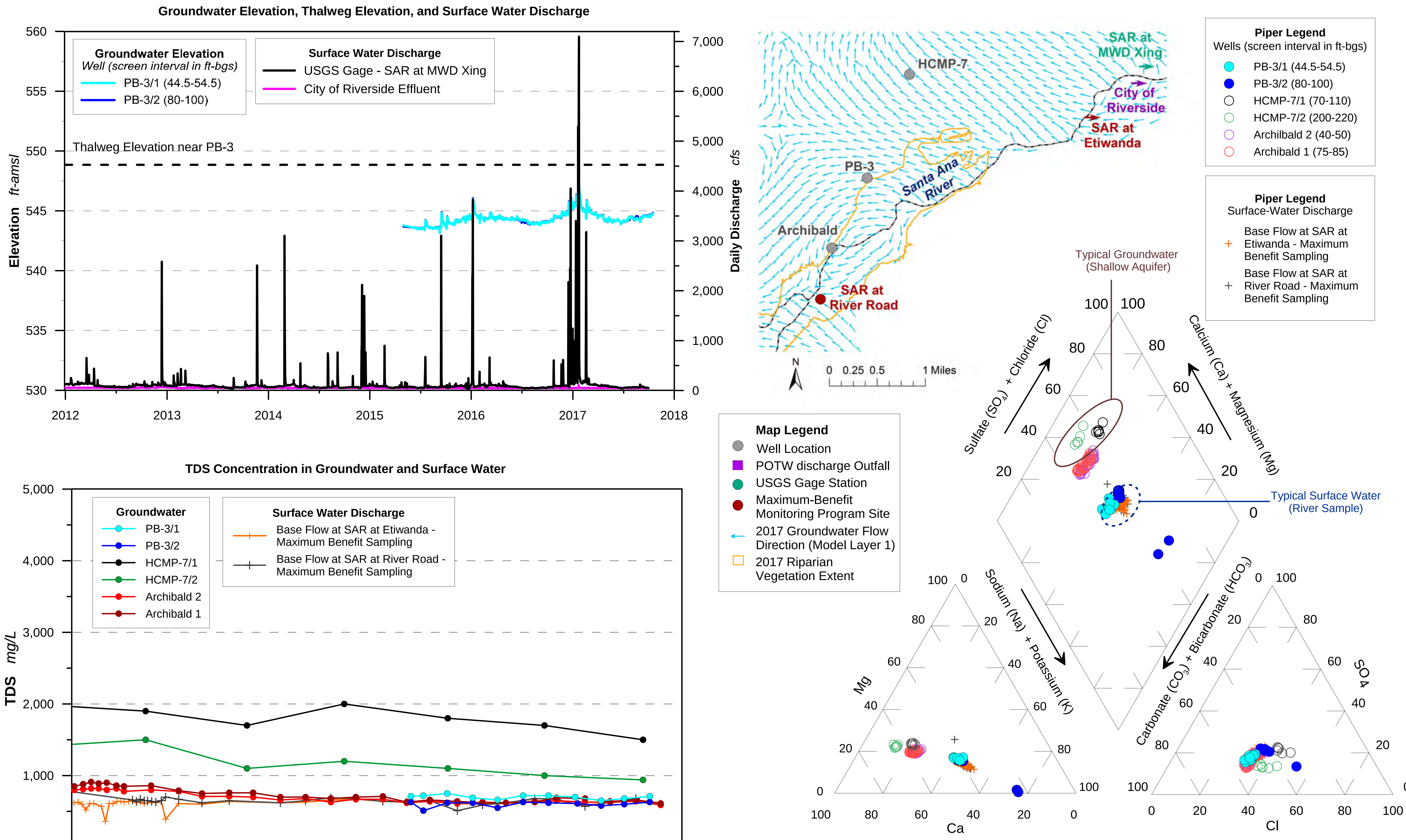

Prado Basin Habitat Sustainability Committee
2017 Annual Report

Groundwater and Surface Water Interactions
Santa Ana River Near PB-3

Figure 3-13i

Figure 3-14
Annual Precipitation in the Chino Basin - Water Years 1896-2017

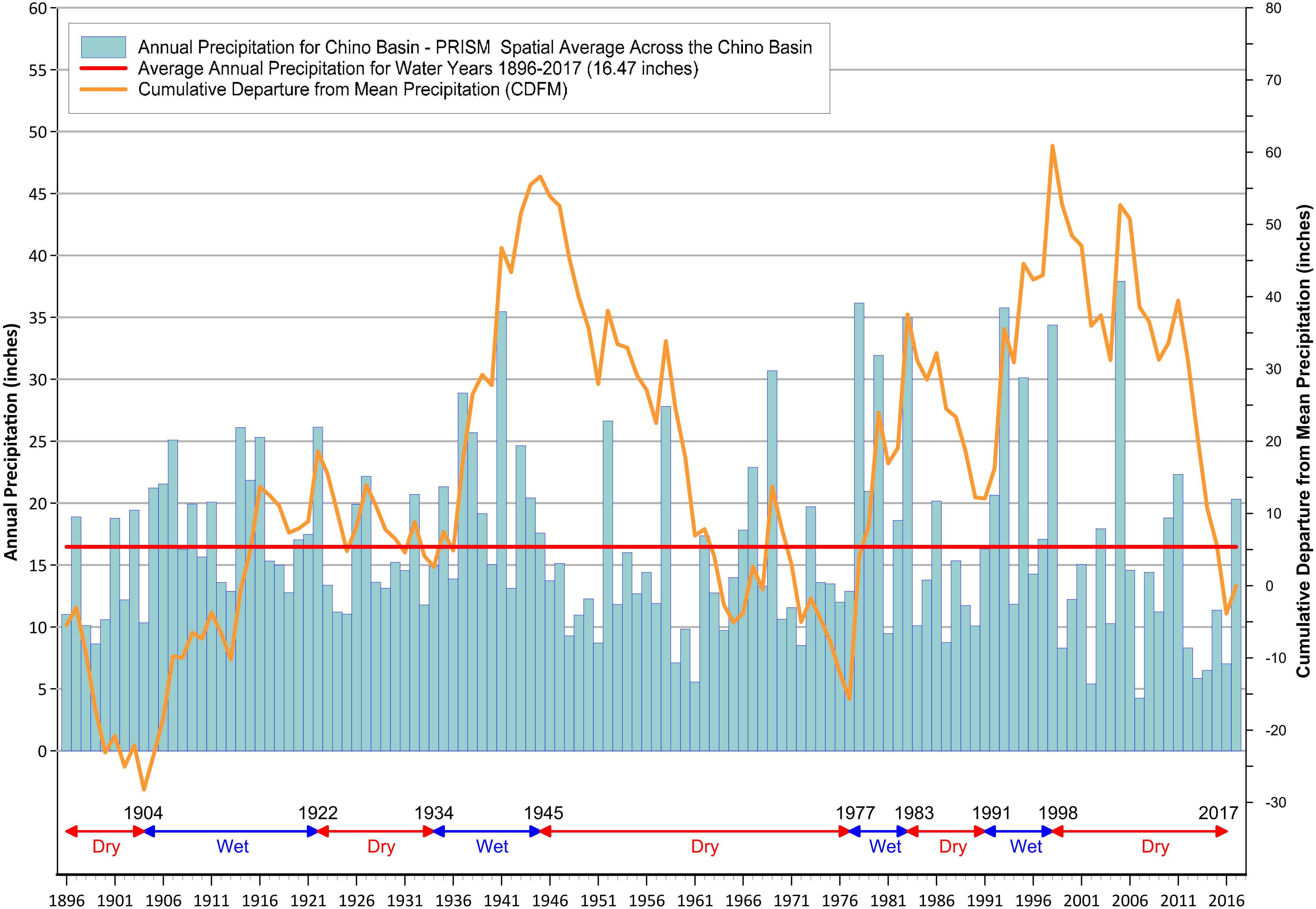

Figure 3-15a
Maximum and Minimum Temperature in Prado Basin - 1895-2017

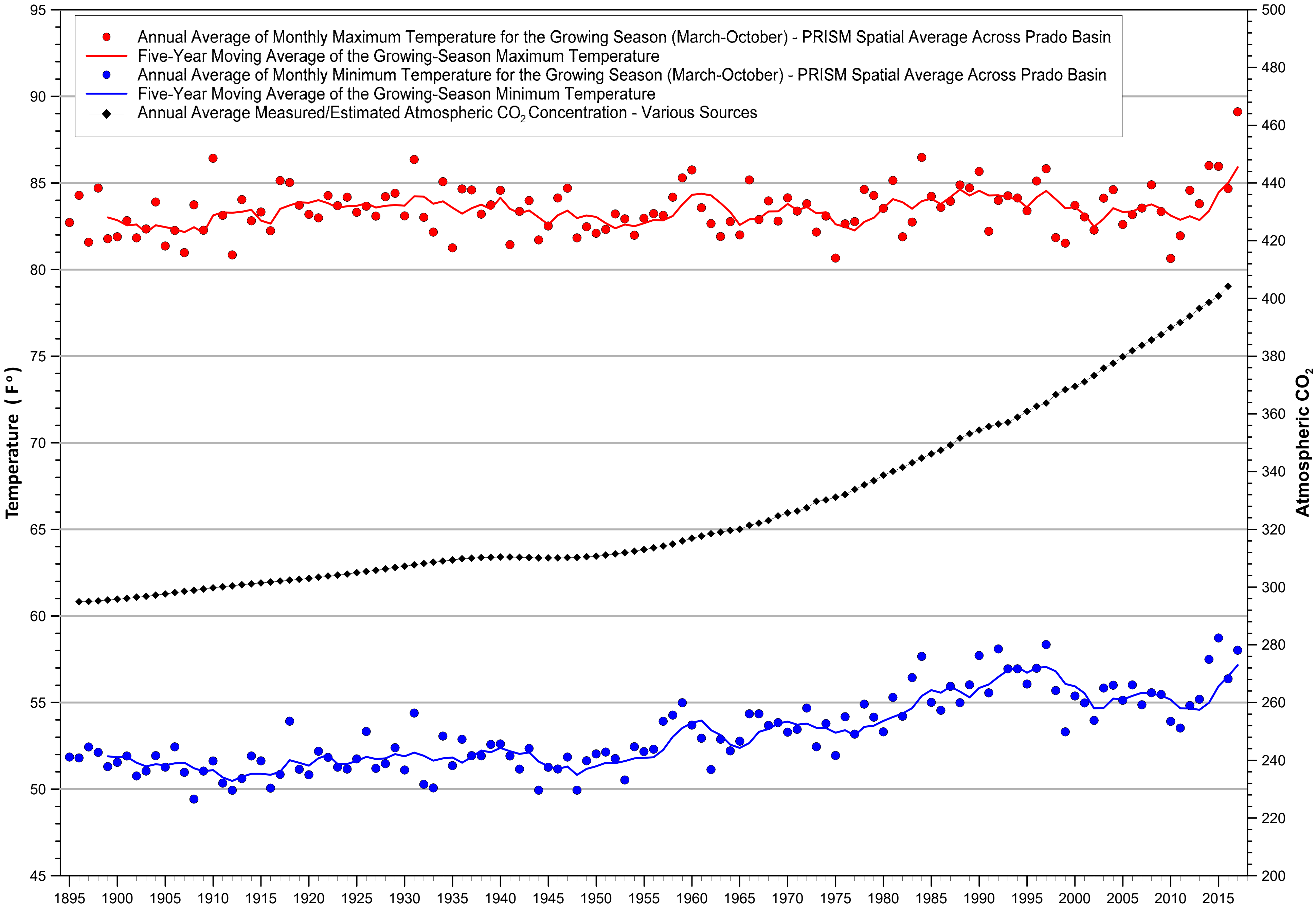

WEI
Wildermuth Environmental, Inc.

Figure 3-15b

Annual Departure of the Average Growing-Season Maximum Temperature in Prado Basin from the Growing-Season Mean for 1921-1950

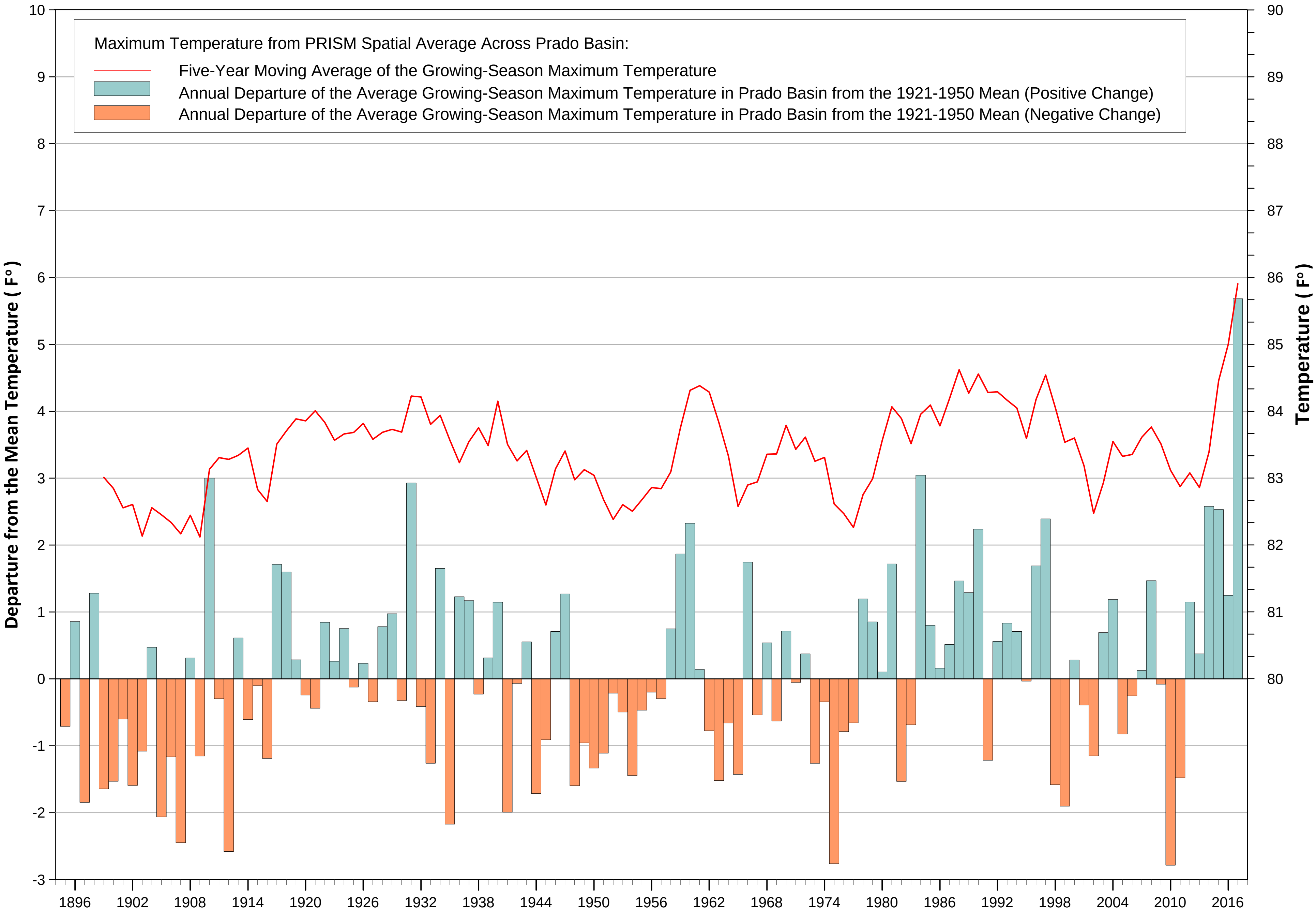

WEI
WILDERMUTH ENVIRONMENTAL, INC

Figure 3-15c

Annual Departure of the Average Growing-Season Minimum Temperature in Prado Basin from the Growing-Season Mean for 1921-1950

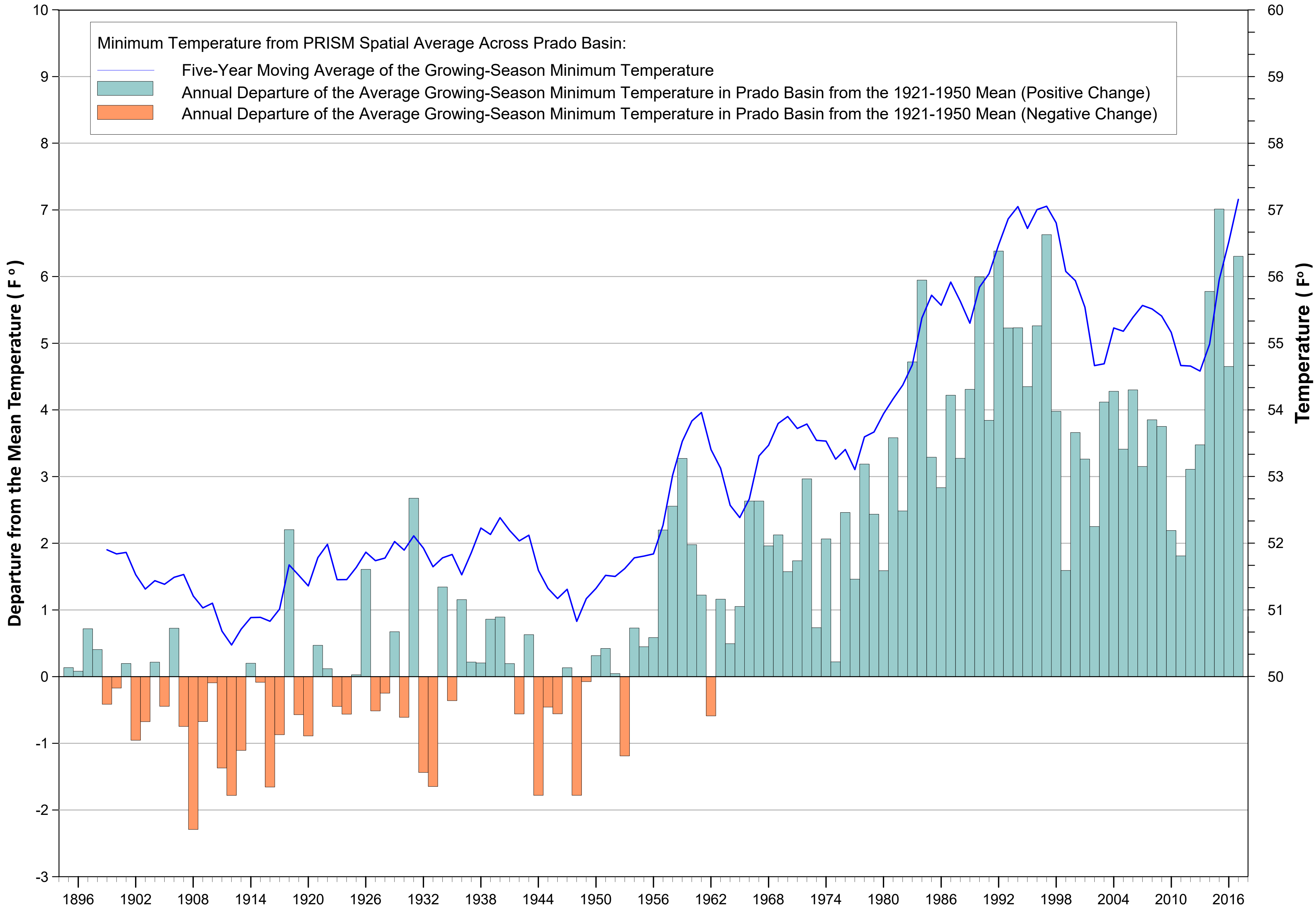

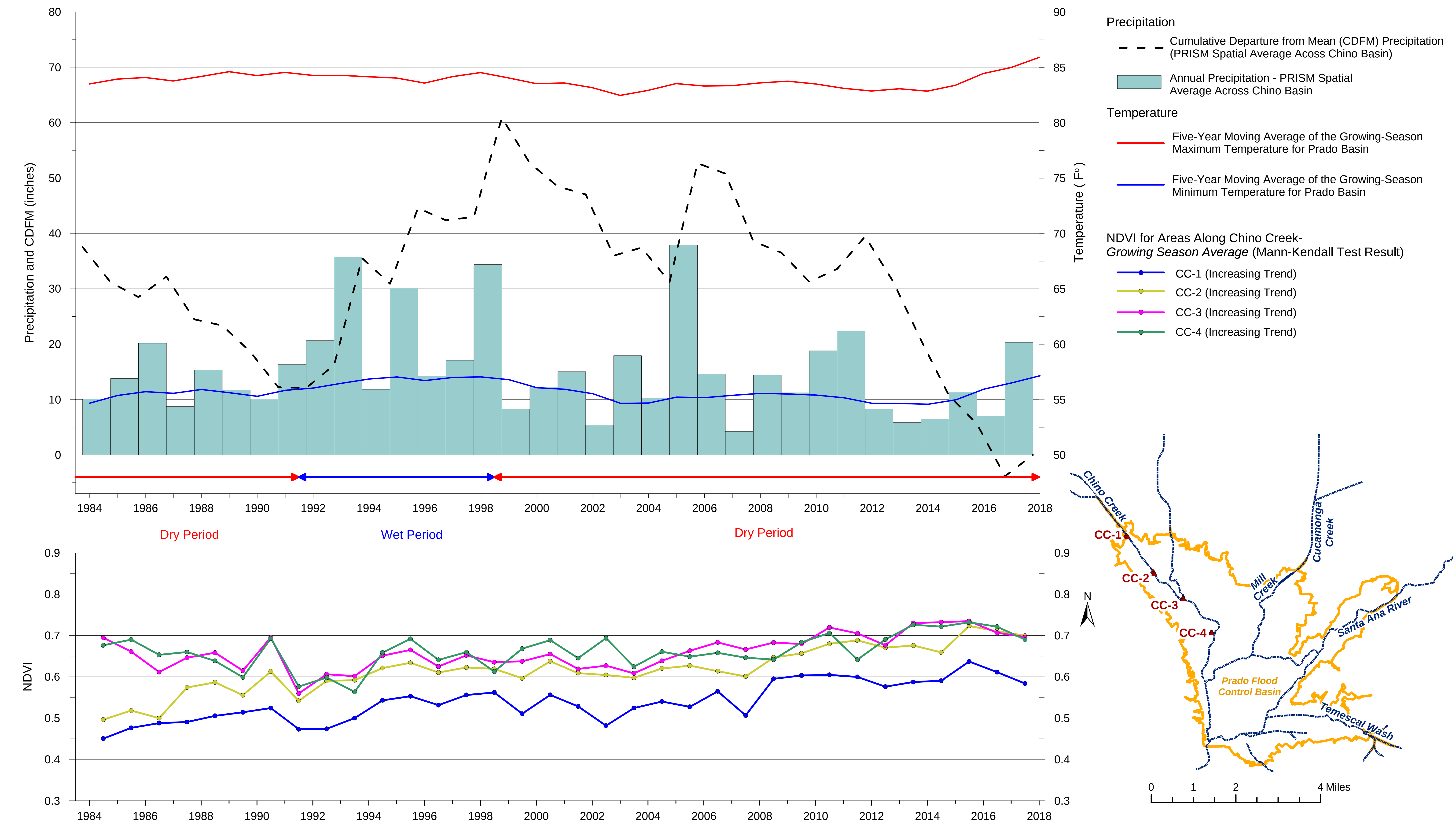

Prepared by:

WEI
Wildermuth Environmental, Inc.

Author: RT
Date: 20180110
Filename: CDFM_Temp_NDVI_ChinoCreek.grf

2017 Annual Report
Prado Basin Habitat Sustainability Committee

Climate versus NDVI
Chino Creek Area for 1984-2017

Figure 3-16a

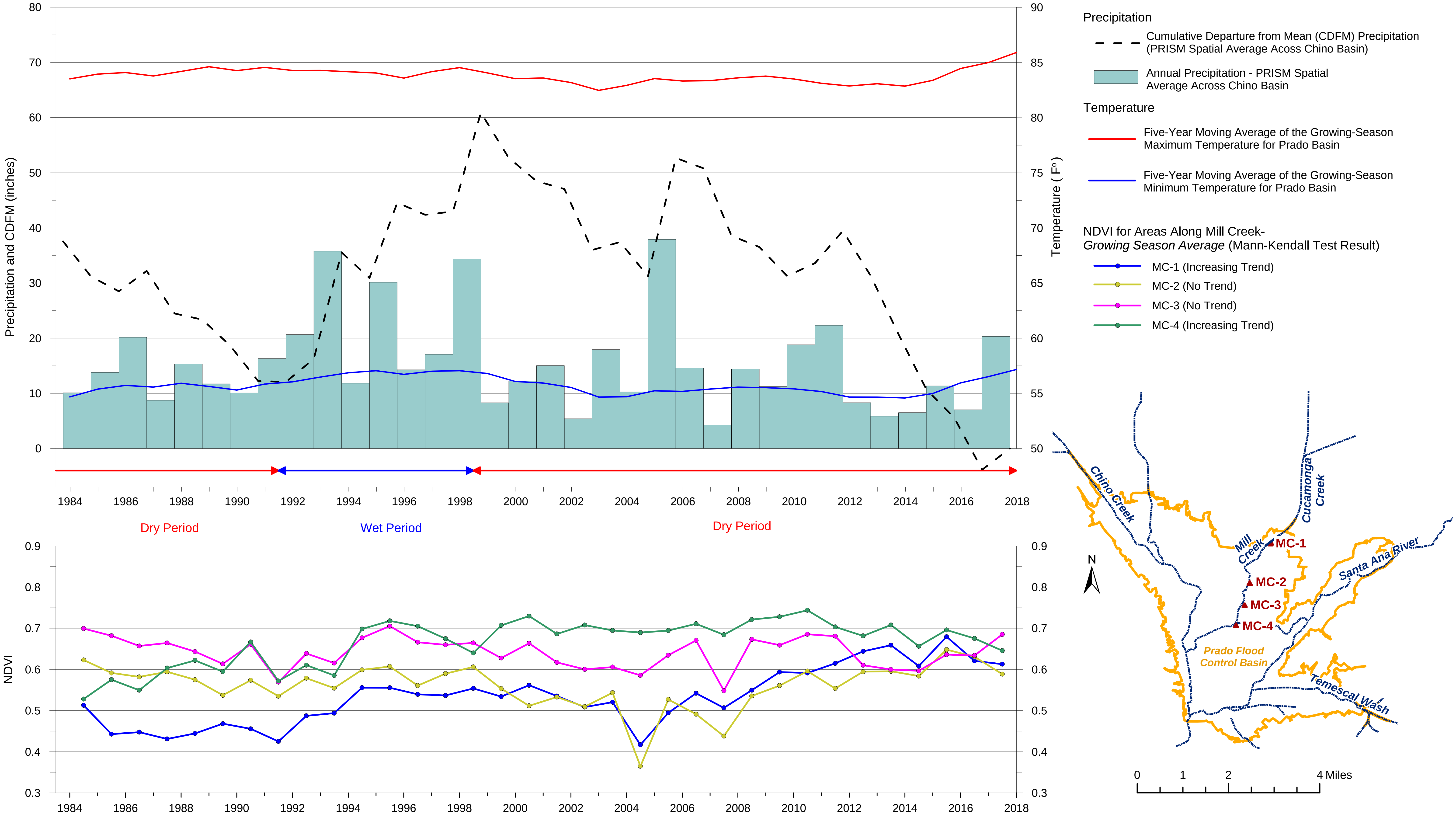

Prepared by:

WEI
Wildermuth Environmental, Inc.

Author: RT
Date: 20180110
Filename: CDFM_Temp_NDVI_ChinoCreek.grf

2017 Annual Report
Prado Basin Habitat Sustainability Committee

Climate versus NDVI
Mill Creek Area for 1984-2017

Figure 3-16b

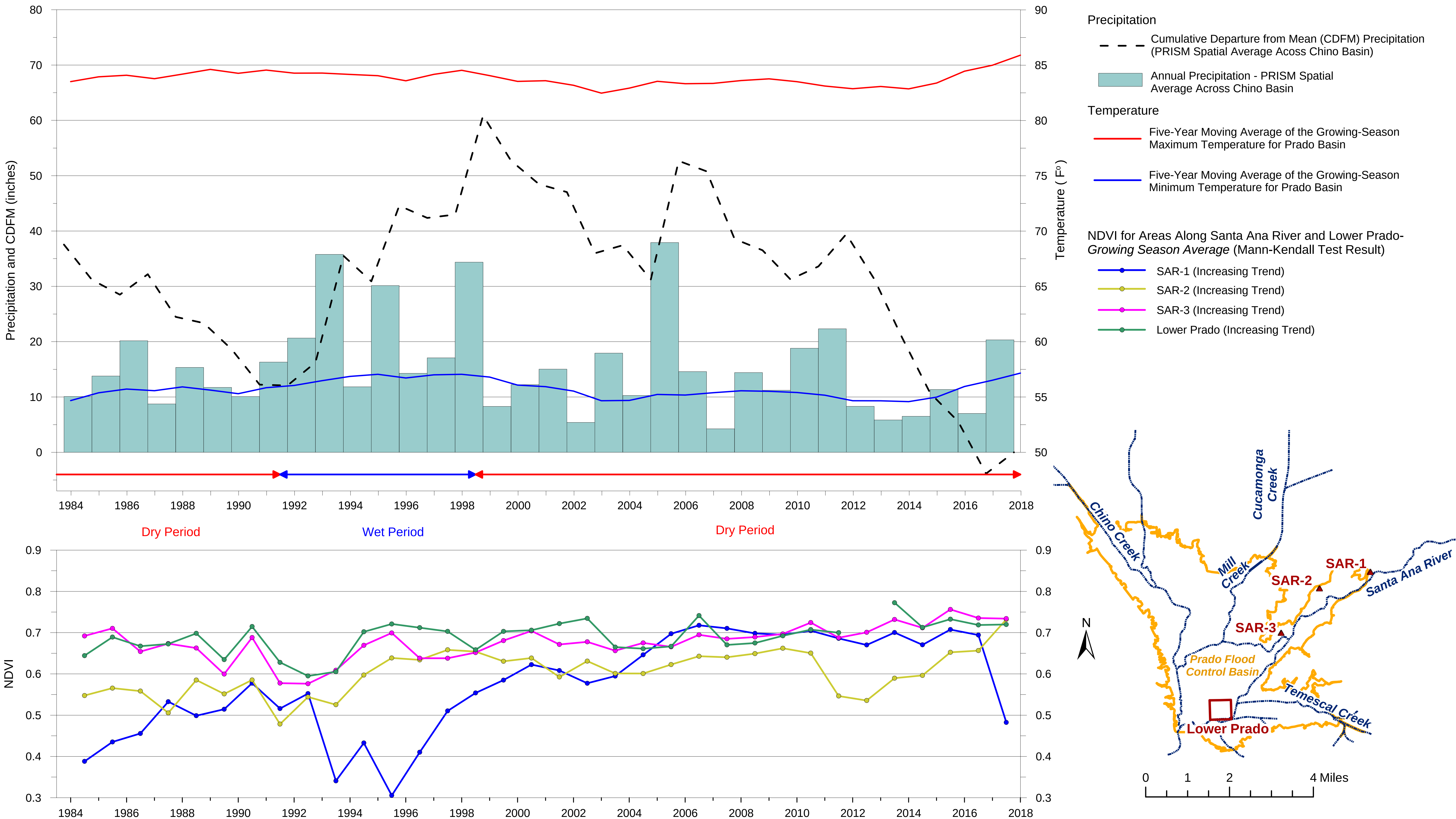

Prepared by:

WEI
Wildermuth Environmental, Inc.

Author: RT
Date: 20180110
Filename: CDFM_Temp_NDVI_ChinoCreek.grf

2017 Annual Report
Prado Basin Habitat Sustainability Committee

Climate versus NDVI
Santa Ana River and Lower Prado Area for 1984-2017

Figure 3-16c

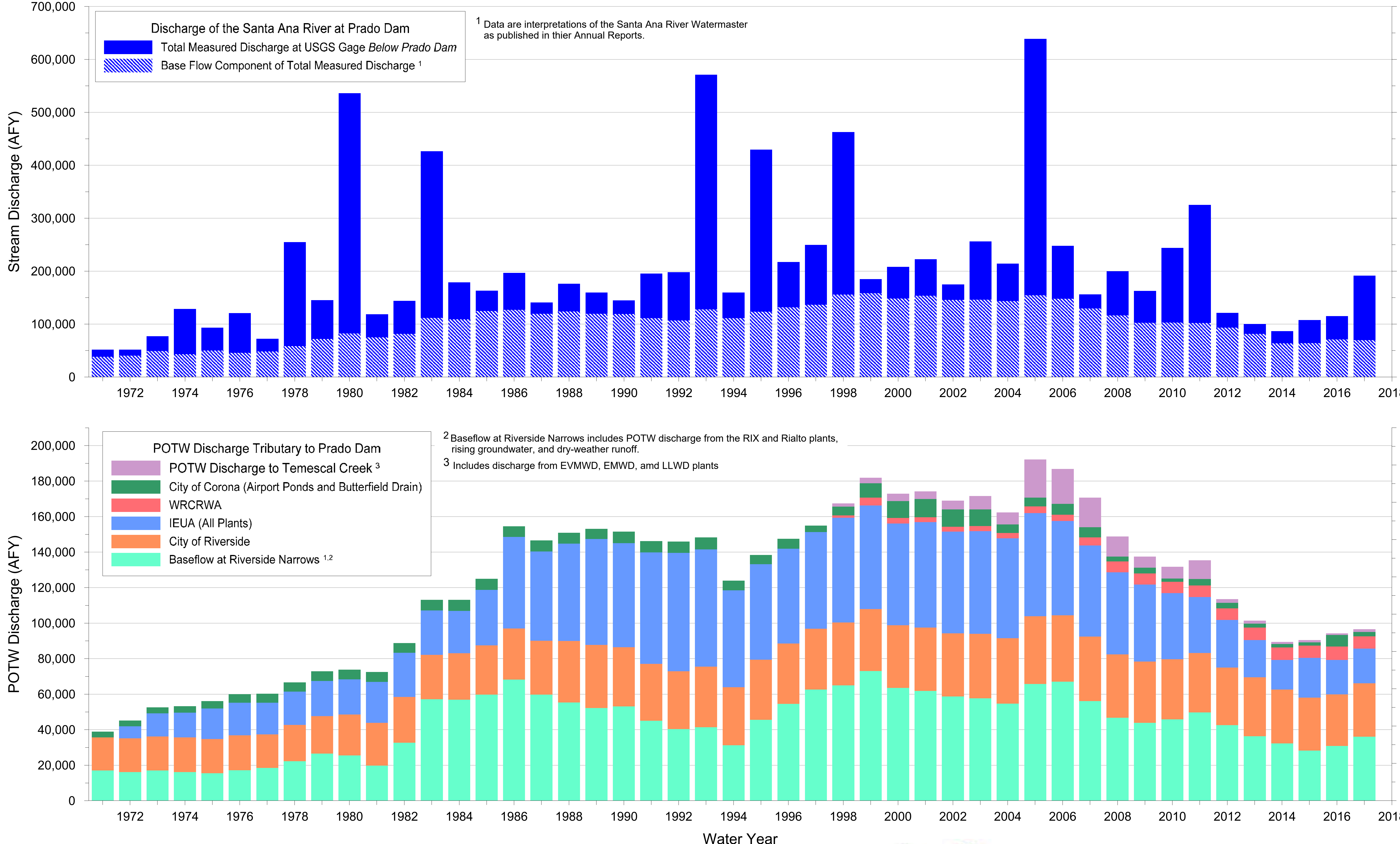

Prepared by:

WEI
WILDERMUTH ENVIRONMENTAL, INC.

Author: RT
Date: 20180215
Filename: 2017_Fig3-13_SW Discharge.grf

2017 Annual report
Prado Basin Habitat Sustainability Committee

Discharge Tributary to Prado Dam
Water Year 1960-2017

Figure 3-17

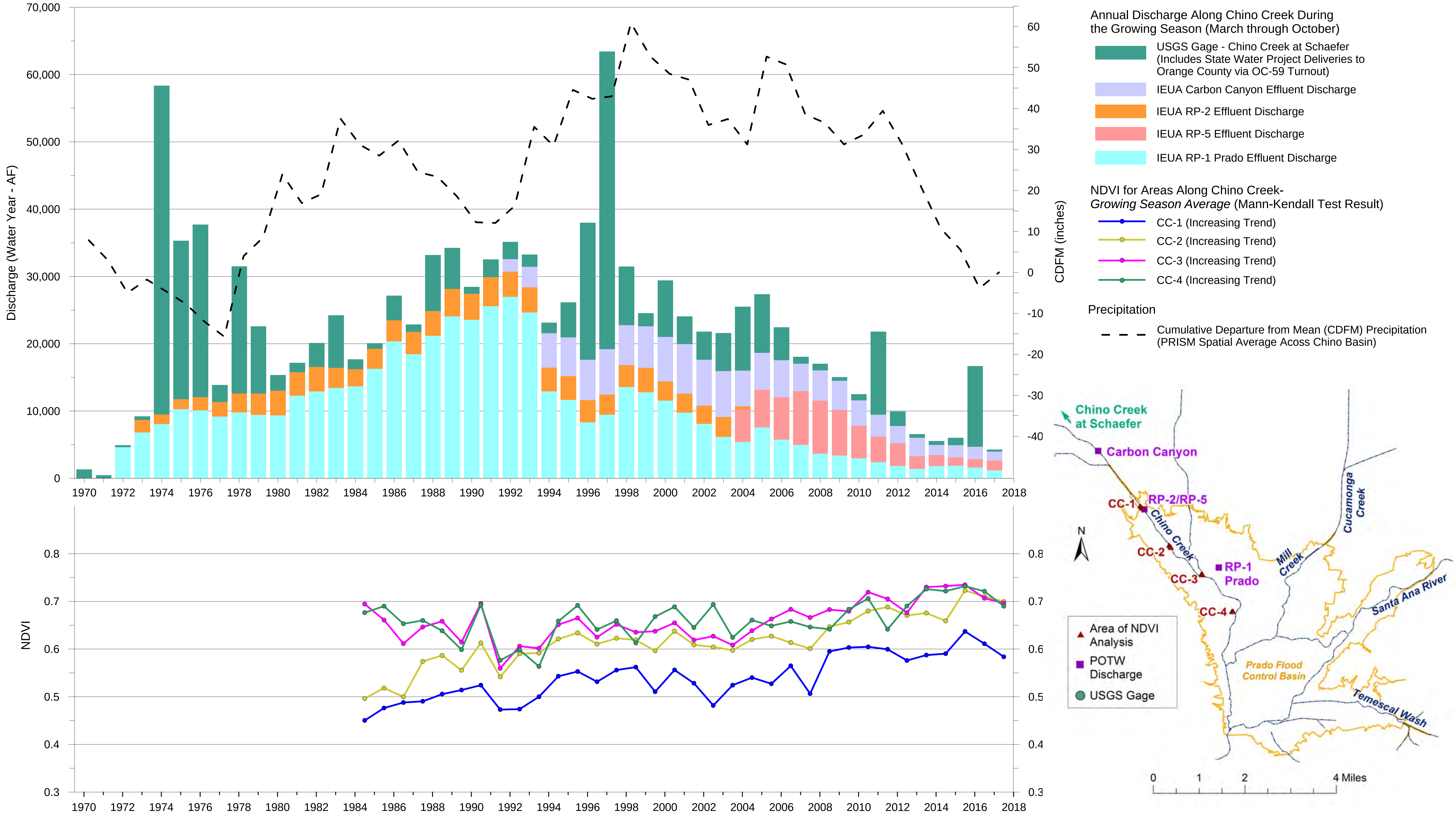

Surface-Water Discharge versus NDVI
Chino Creek Area for 1971-2017

Figure 3-18a

Prepared by:
WEI
Wildermuth Environmental, Inc.

Author: RT
Date: 20170410
Filename: SW Discharge_NDVI_Chino Creek.grf

2017 Annual Report
Prado Basin Habitat Sustainability Committee

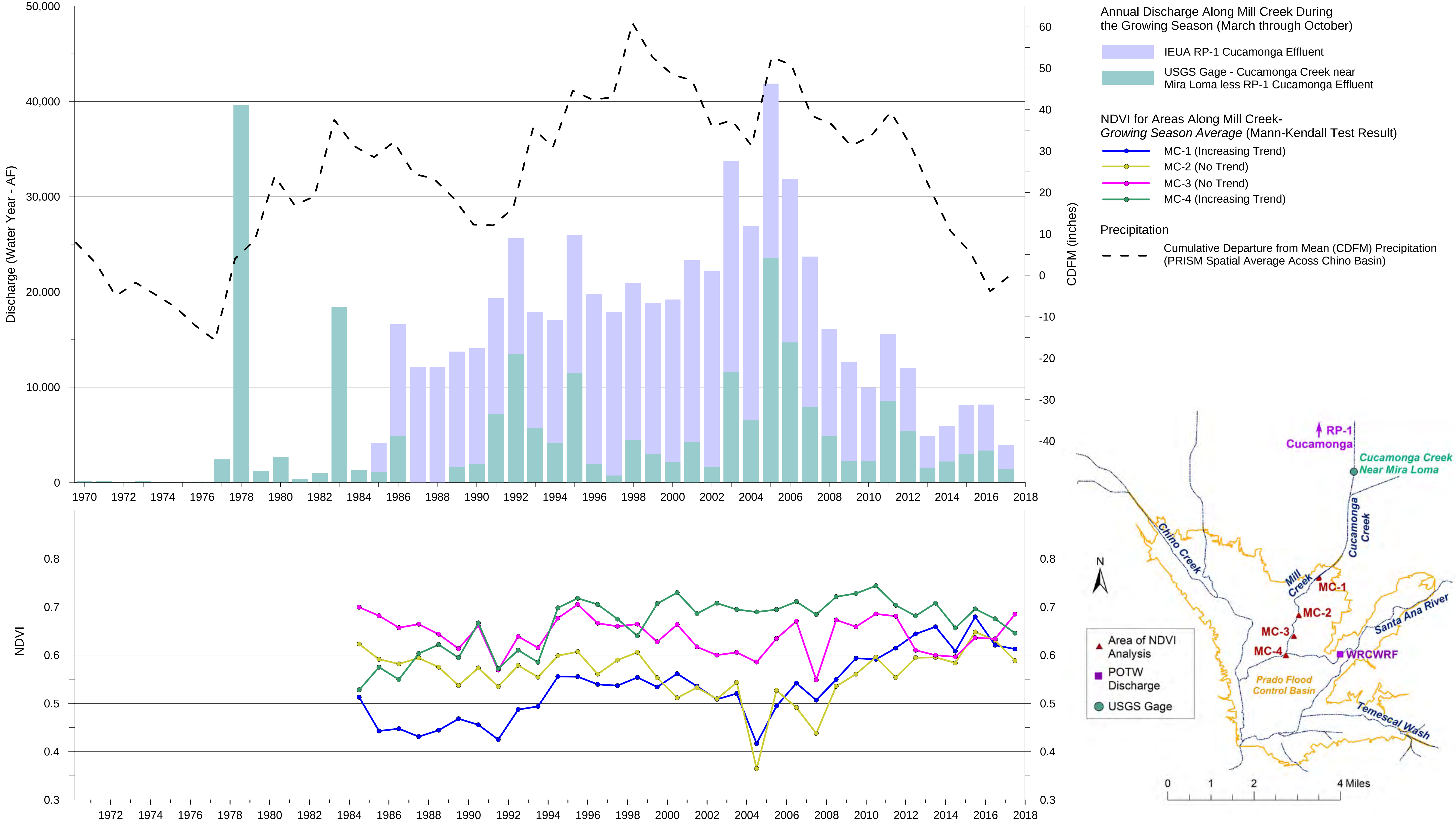

Prepared by:

Author: RT
Date: 20170410
Filename: SW Discharge_NDVI_Mill Creek.grf

2017 Annual Report
Prado Basin Habitat Sustainability Committee

Surface-Water Discharge versus NDVI
Mill Creek Area for 1971-2017

Figure 3-18b

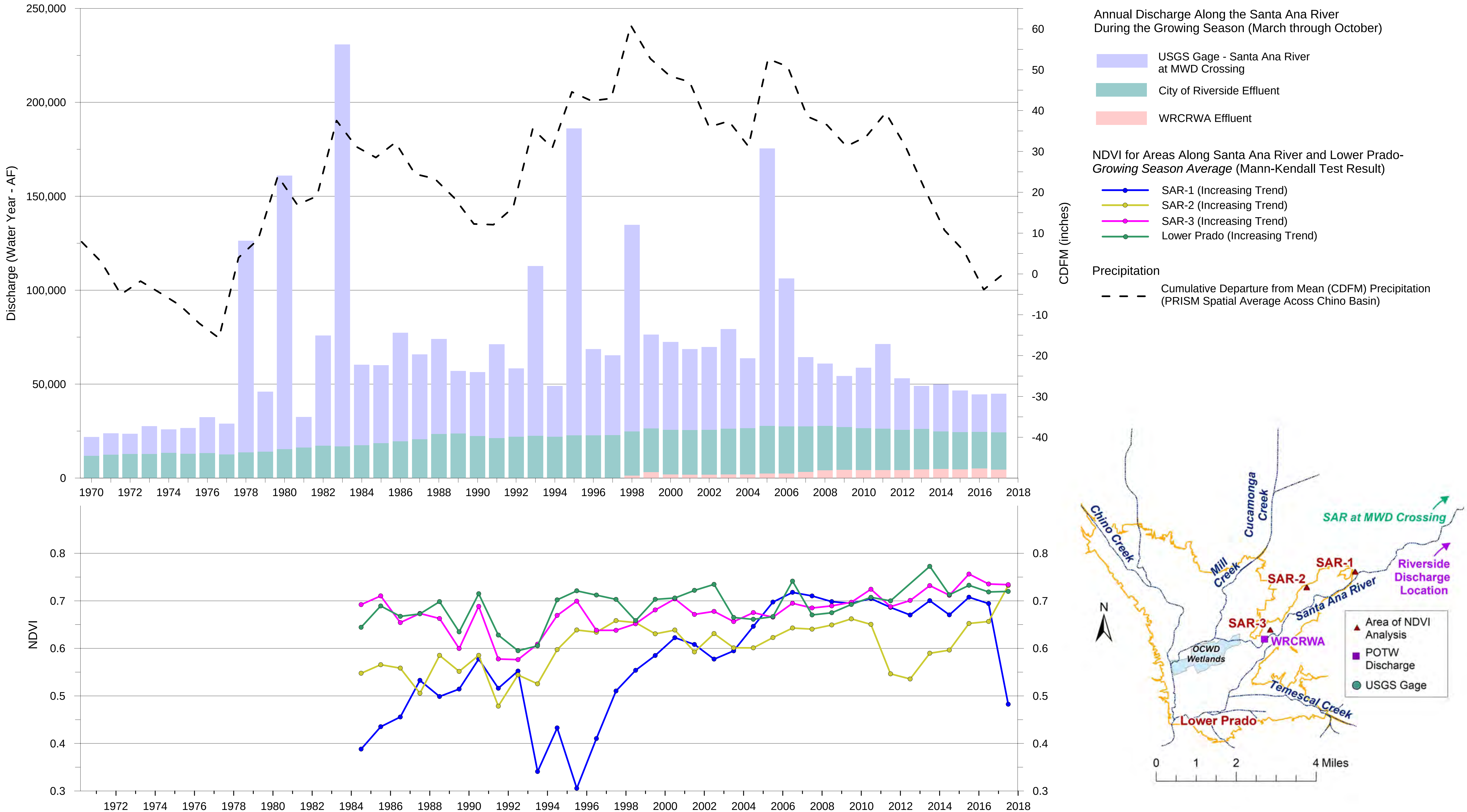

Prepared by:

WEI
WILDERMUTH ENVIRONMENTAL, INC.

Author: RT
Date: 20170410
Filename: SW Discharge_NDVI_SAR and LP.grf

2017 Annual Report
Prado Basin Habitat Sustainability Committee

Surface-Water Discharge versus NDVI
Santa Ana River and Lower Prado Area for 1971-2017

Figure 3-18c

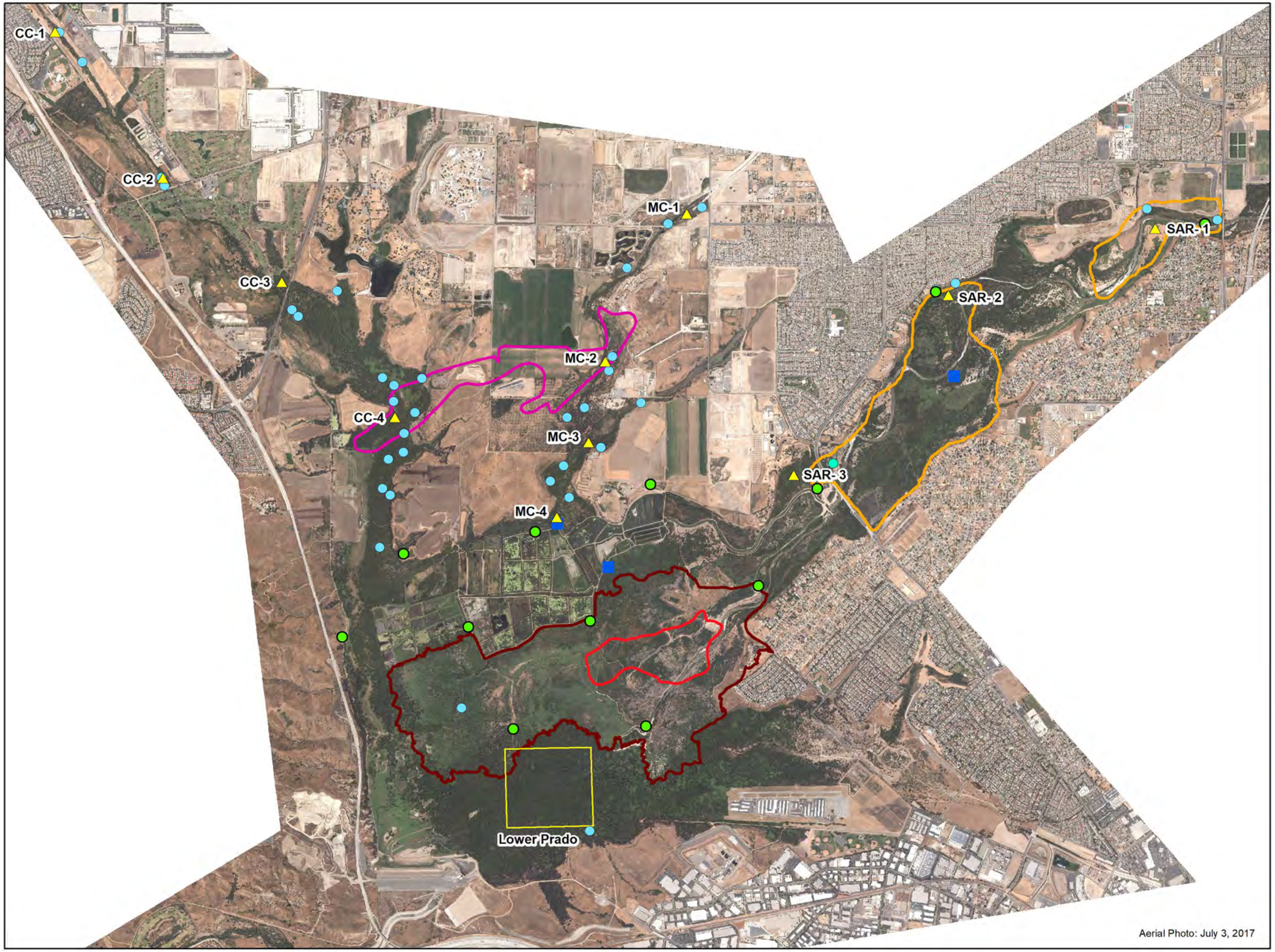

NDVI Area (3,600 square meters)

NDVI Area (19,520 square meters)

Documented Locations of
Polyphagous Shot-Hole Borer (PSHB)

Identified by in USBR during the 2016
Site-Specific Vegetation Surveys

Documented by University of California Division
of Agriculture and Natural Resources According
to PSHB/FD Distribution Map

Location of PHSB Traps Deployed by OCWD
and SAWA from August 2016 to April 2017

Extents of Wildfire Occurrences in Prado Basin

1985

1989

2007

2015

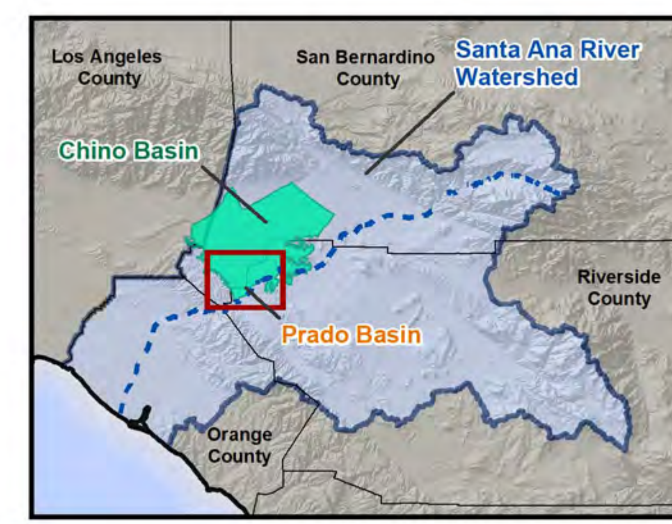

Prepared by:

WEI
WILDERMUTH ENVIRONMENTAL, INC.

Author: RT
Date: 4/5/2018
File: 2017_Figure 3-19_2017_other factors

0 1 2 Miles

0 1 2 3 KM

2017 Annual Report
Prado Basin Habitat Sustainability Committee

Location Map of Other Factors That Can Affect Riparian Habitat

Figure 3-19

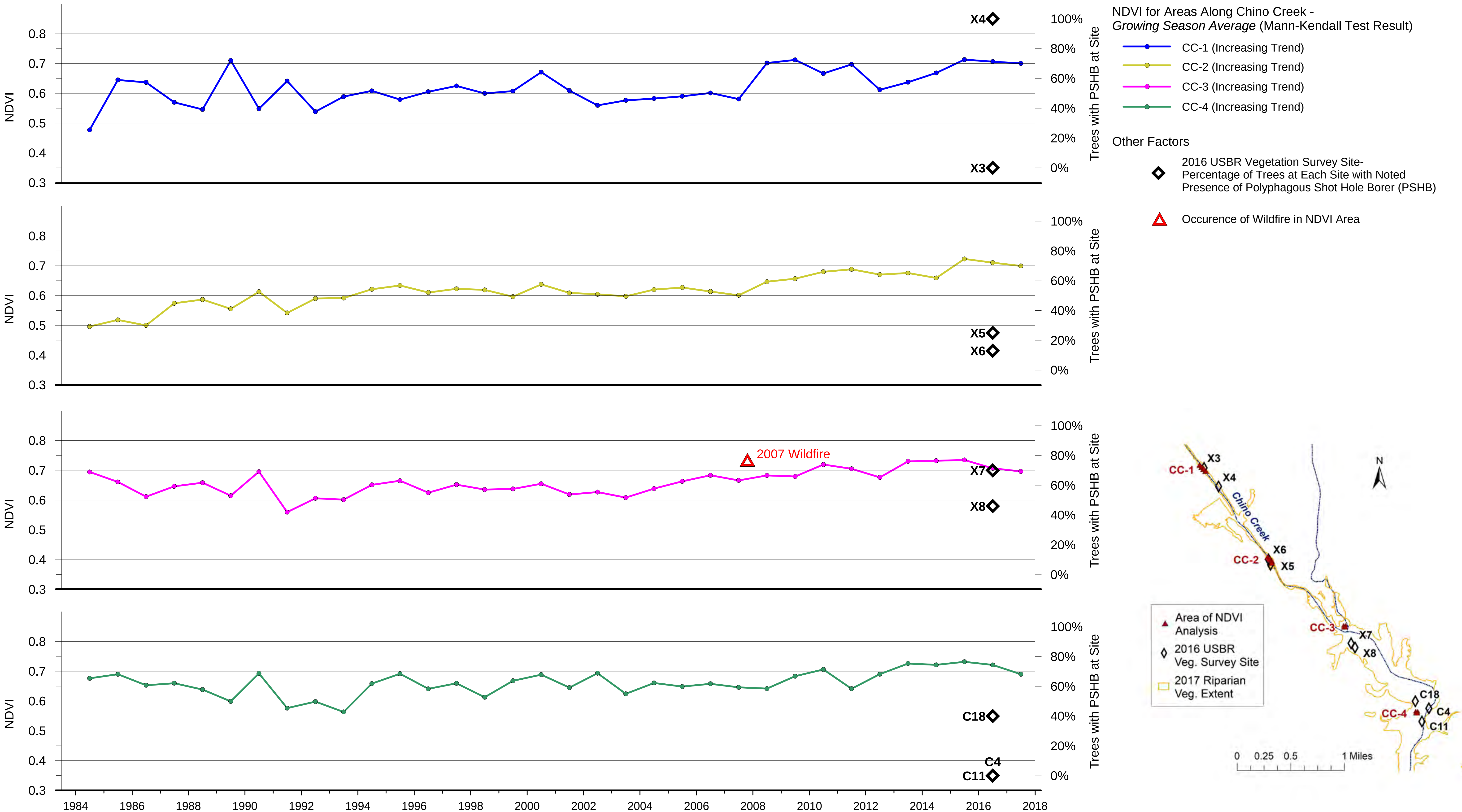

Prepared by:

WEI Wildermuth Environmental, Inc.

Author: RT
Date: 20180111
Filename: Other Factors_NDVI_CC.grf

2017 Annual Report
Prado Basin Habitat Sustainability Committee

Other Factors That Can Affect Riparian Habitat versus NDVI
Chino Creek Area for 1984-2017

Figure 3-20a

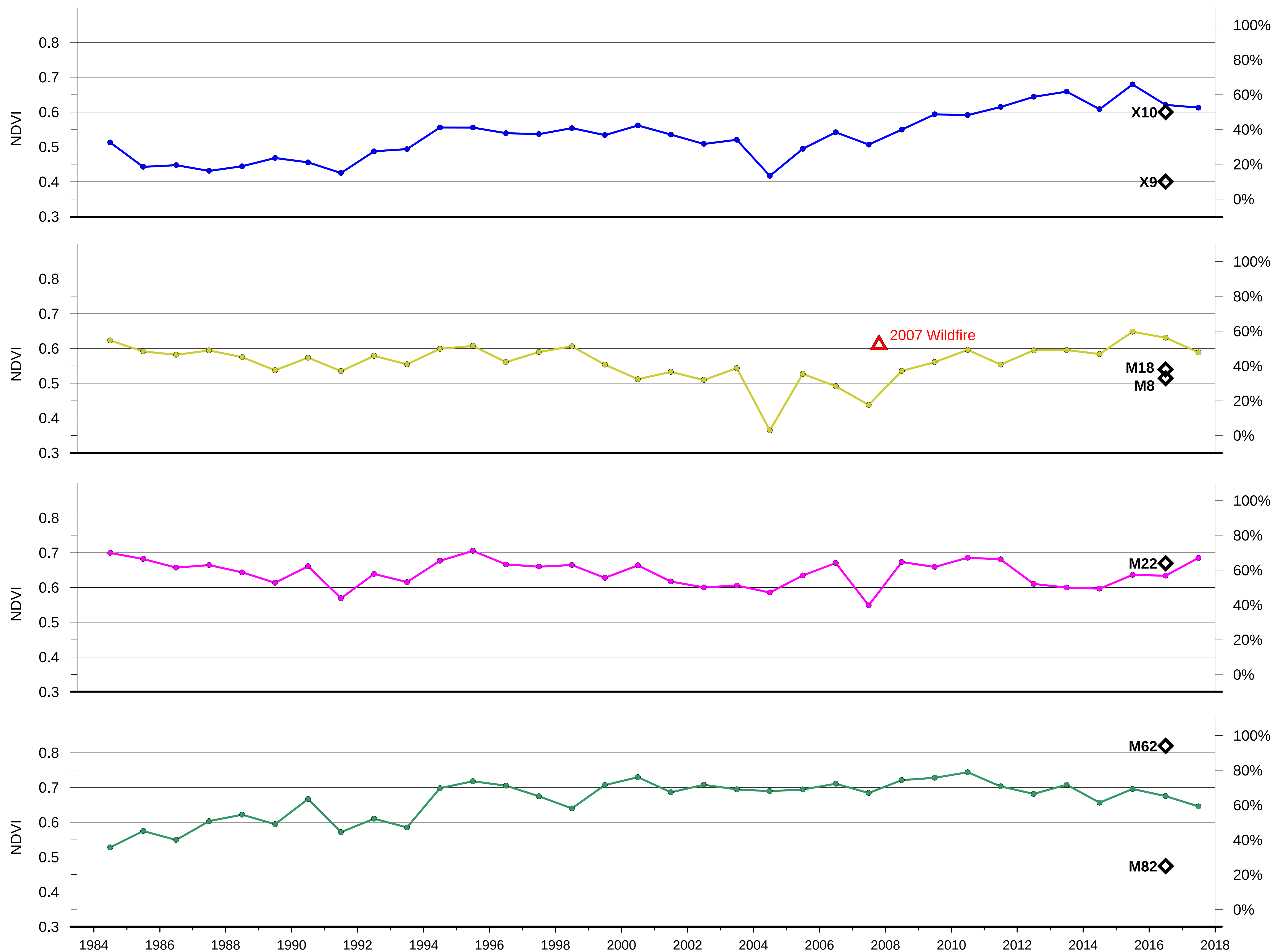

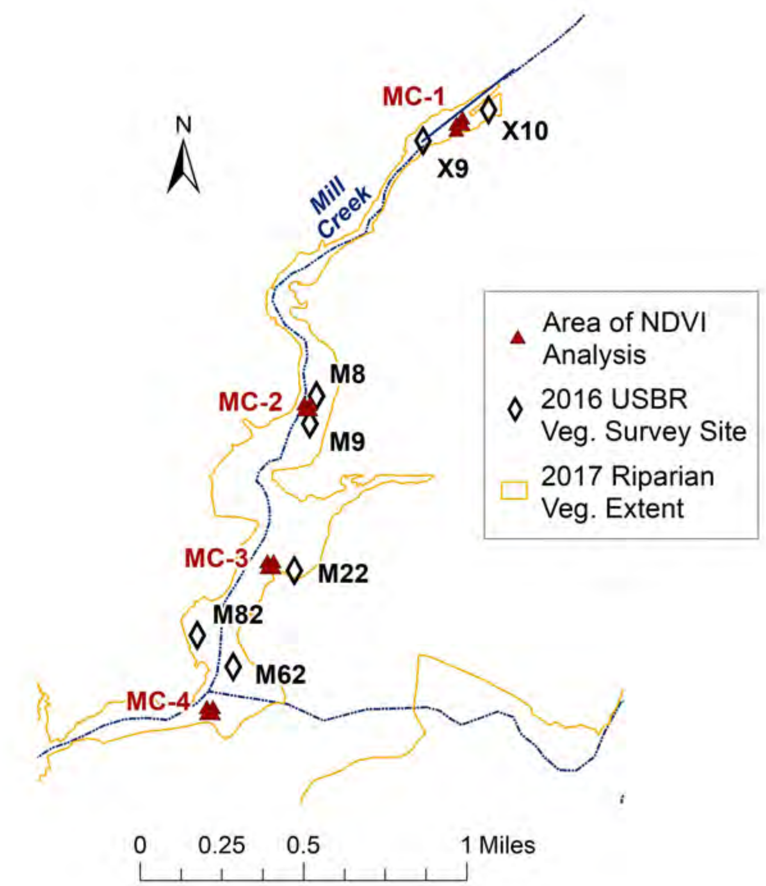

Other Factors That Can Affect Riparian Habitat versus NDVI
Mill Creek Area for 1984-2017

Figure 3-20b

Prepared by:
WEI
Wildermuth Environmental, Inc.

Author: RT
Date: 20180111
Filename: Other Factors_NDVI_CC.grf

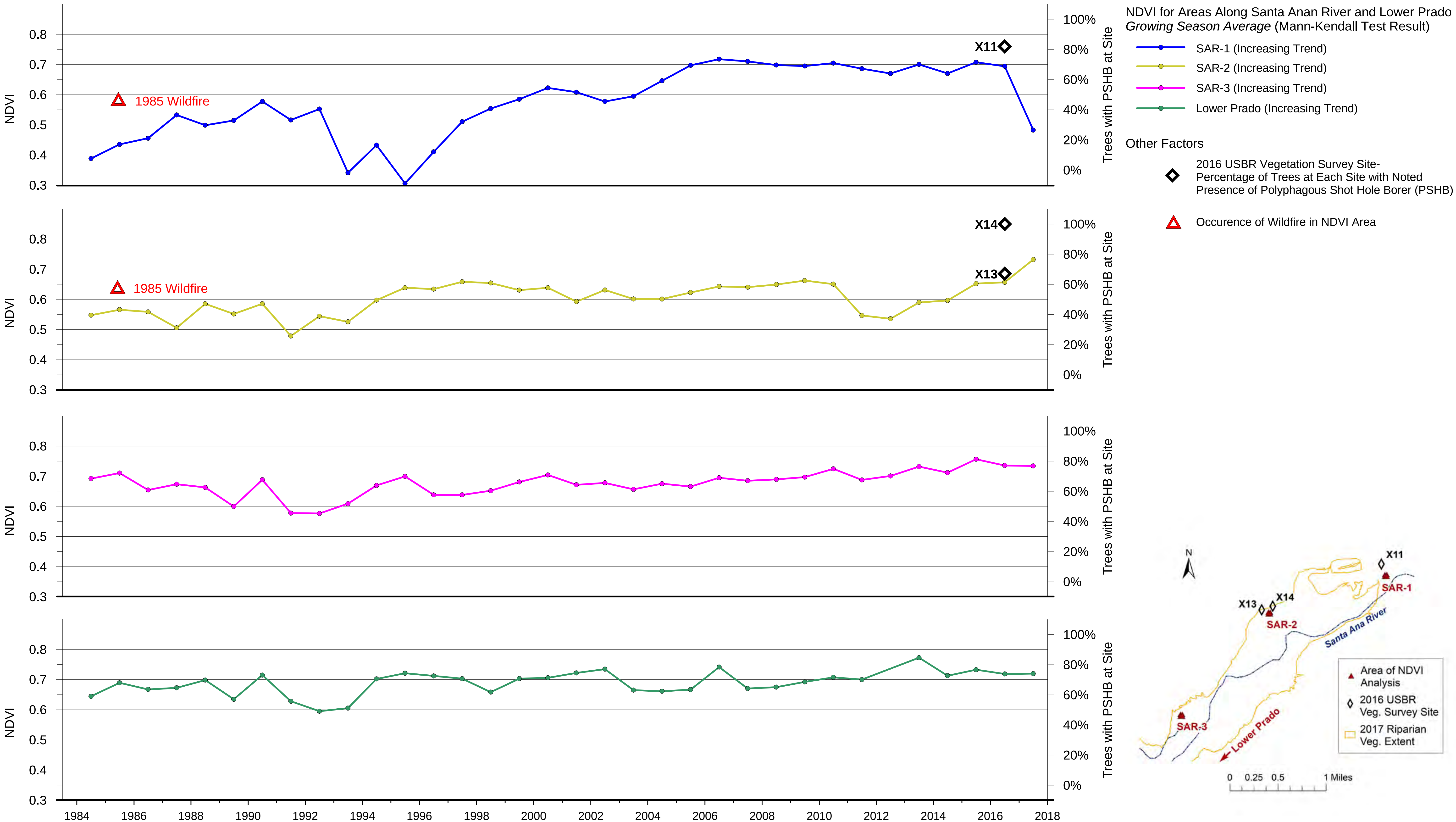

Prepared by:

WEI Wildermuth Environmental, Inc.

Author: RT
Date: 20180111
Filename: Other Factors_NDVI_CC.grf

2017 Annual Report
Prado Basin Habitat Sustainability Committee

Other Factors That Can Affect Riparian Habitat versus NDVI
Santa Ana River and Lower Prado Area for 1984-2017

Figure 3-20c

117°40'0"W

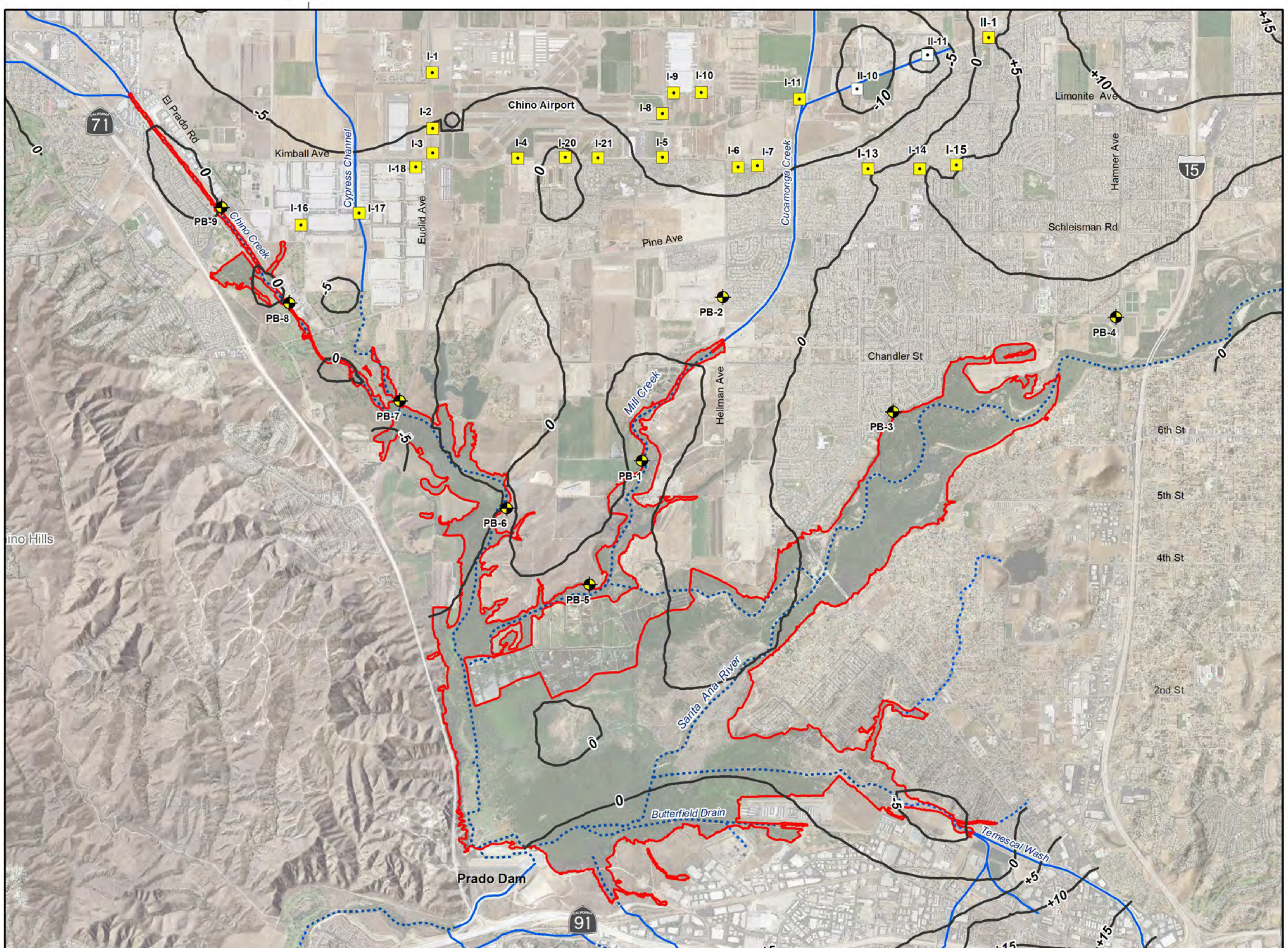

-10 Change in Groundwater Levels *Fall 2017 to Fall 2030, feet*

Chino Basin Desalter Authority Well

Future Chino Basin Desalter Authority Well

PBHSP Monitoring Well

Concrete-Lined Channels

Unlined Rivers and Streams

2017 Extent of Riparian Vegetation in Prado Basin

Aerial Photo: USDA, 2016. Mosaic of photos from June 2, 2016 to June14, 2016

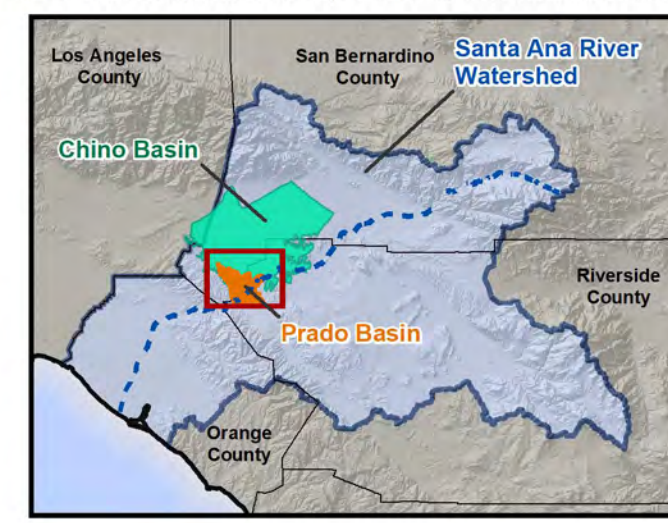

Prepared by:

WEI
WILDERMUTH ENVIRONMENTAL, INC.

Author: VMW
Date: 5/8/2018
File: 2017_Figure 3-21_Model 2017-30

0 1 2 Miles
0 1 2 3 KM

PBHSP 2017 Annual Report
Prado Basin Habitat Sustainability Committee

Projected Change in Groundwater Levels
2017 to 2030 -- Scenario 1A

Figure 3-21

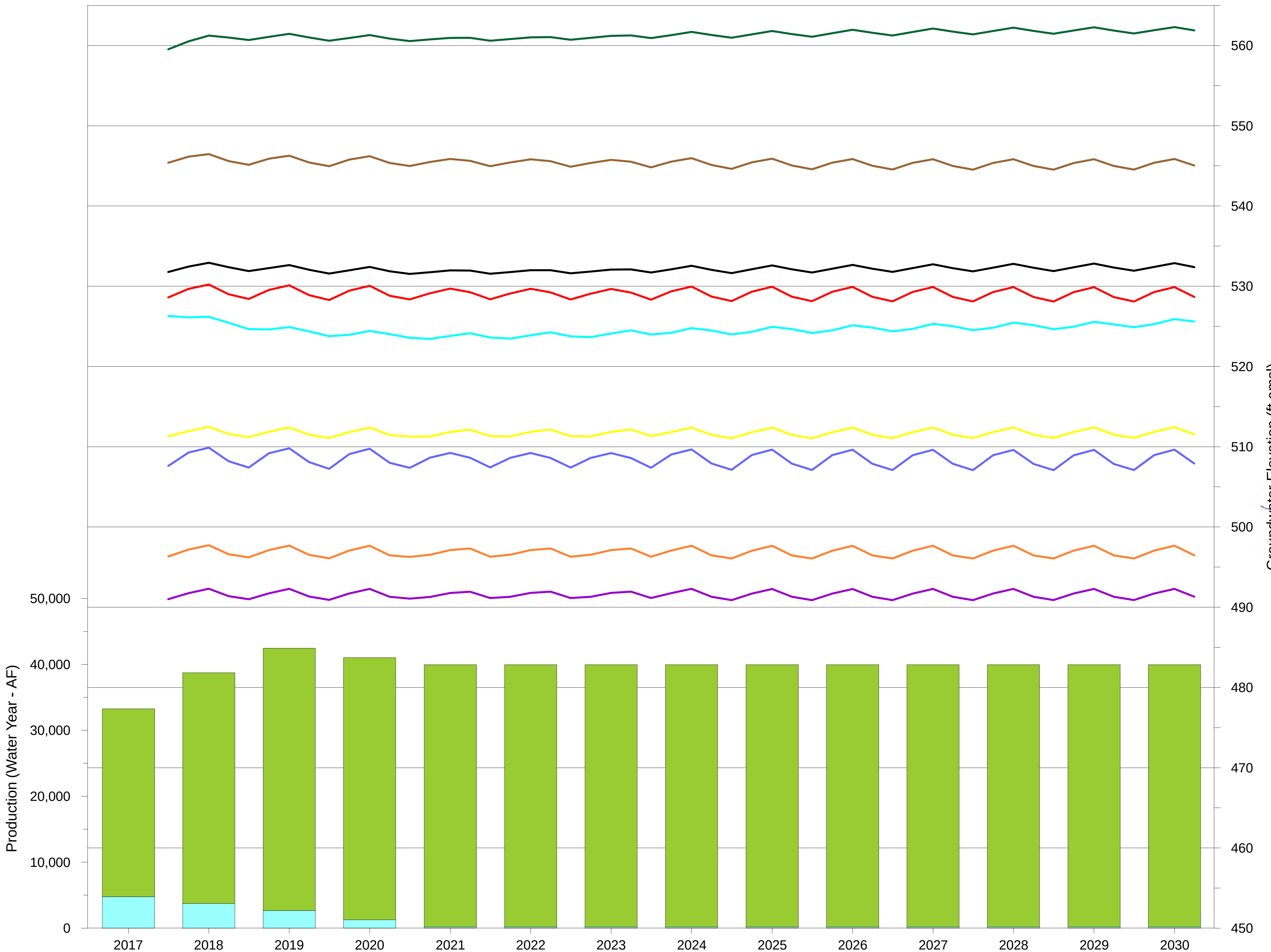

Well Locations

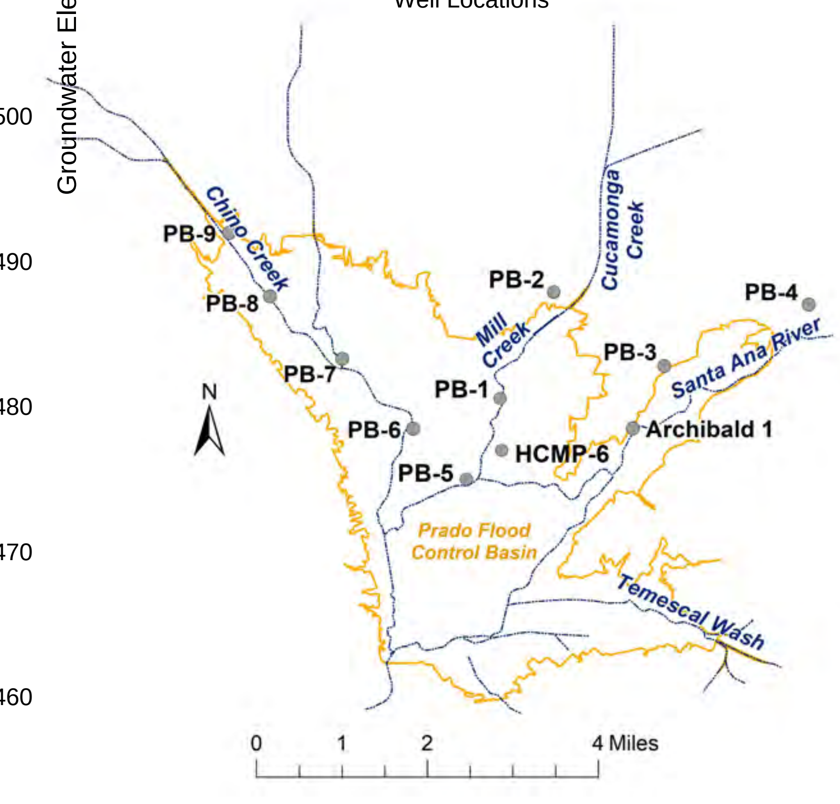

Prepared by:

WEI
WILDERMUTH ENVIRONMENTAL, INC.

Author: RT
Date: 20160601
Filename: Projected_PROD_GWE_2012-2030.grf

2017 Annual Report
Prado Basin Habitat Sustainability Committee

Projected Groundwater Production and Groundwater Levels
2017-2030

Figure 3-22

Section 4 – Conclusions and Recommendations

The monitoring and mitigation requirements in the Peace II SEIR call for annual reporting for the PBHSP:

> *Annual reports will be prepared and will include recommendations for ongoing monitoring and any adaptive management actions required to mitigate any measured loss or prospective loss of riparian habitat that may be attributable to the Peace II Agreement.*

This section describes the main conclusions of this annual report, and provides recommendations for future monitoring, reporting, and mitigation, if any.

4.1 Main Conclusions and Recommendations

This sub-section describes the main conclusions and recommendations for the 2017 Annual Report of the PBHSC. Some conclusions and recommendations are similar to those in the 2016 annual report, and some conclusions and recommendations are new.

The following conclusions and recommendations are similar to those described in the 2016 annual report, and are consistent with the interpretations described in this annual report:

- The assessment of the riparian habitat in the Prado Basin, through the analysis of historical air photos and NDVI estimates show that the riparian habitat has increased in its extent and quality since the 1960s. There is no indication of a long-term trend in degradation of the extent or quality of riparian habitat along Chino Creek, Mill Creek, or the SAR that is contemporaneous with the implementation of the Peace II Agreement. ***Recommendation for 2018:*** Continue the regional monitoring of riparian habitat using NDVI and high-resolution air photos of the Prado Basin

- With two exceptions, groundwater levels underlying the riparian habitat in Prado Basin have remained stable since 1961 and appear to have been unaffected by the implementation of both Peace Agreements starting in 2000. The two exceptions are areas along the northern reaches of Mill Creek and the SAR, where groundwater levels have fluctuated by up to +/-10 feet—apparently in response decreased groundwater production from the southern Chino Basin in the 1990s and increased production after about 2000 with the commencement of CDA pumping. The quality of the riparian habitat in these areas has shown no long-term trend of degradation since the NDVI estimates became available in the early 1980s and may have improved slightly during the Peace II Agreements period. ***Recommendation for 2018:*** Continue the monitoring of groundwater levels with no change in scope.

- The extended dry period from 1999 to 2017 does not correlate with a long-term declining trend in the quality of riparian habitat in Prado Basin during this period, which suggests the availability of source waters for consumptive use by the riparian vegetation other than precipitation and runoff, such as baseflow discharge and shallow groundwater.

- Discharge in the SAR and its tributaries to Prado Dam has declined significantly since 2005. The declining trend in discharge is attributed to dry climatic conditions from 1999-2017 and the decreases in POTW effluent discharge because of increased recycled-water reuse and decreased wastewater discharge due to the economic recession that began in 2008 and the implementation of emergency water-conservation measures during the recent drought. The quality of riparian habitat in the 12 defined areas along Chino Creek, Mill Creek, and the SAR in the Prado Basin show no long-term trend of degradation that coincides with the decline in stream discharge, and may have improved slightly during the implementation of the Peace II Agreement. ***Recommendation for 2018:*** Continue the monitoring of stream discharge with no change in scope. The 2018 annual report should analyze the influence of the elevation of the Prado Dam reservoir on the riparian habitat and groundwater/surface water interactions in the Prado Basin. Additionally, the 2018 annual report should indicate what portion of the USGS gage at *Chino Creek at Schaefer* is composed of discharge from the OC-59 turnout during the growing season.

- There are other factors that have had documented adverse impacts on the riparian habitat, including wildfire and pests, particularly, the PSHB beetle which has been identified as threat to cause adverse impacts to trees in the Prado Basin. The USBR site-specific vegetation surveys performed in 2016 noted presence of the PSHB at about 80 percent of the sites surveyed, and the OCWD and others have indicated that the PSHB is widespread through the Prado Basin and has reduced tree canopy cover throughout the region, and caused tree deaths in local patches. ***Recommendation for future field vegetation surveys:*** The PSHB should be monitored for and documented in future field-based vegetation surveys.

- Depth-to-groundwater is relatively shallow across most of Prado Basin. The riparian vegetation typically overlies areas where the depth-to-groundwater is less than 15 feet-bgs, which suggests that shallow groundwater is an available source water for consumptive use by the vegetation.

The following are new conclusions and/or recommendations derived from this annual report:

- The quality of riparian habitat, characterized by the time series of average-growing season NDVI at 13 defined areas and analyzed using the Mann-Kendall trend test, show 'no trend' or 'increasing trend' in the NDVI during 1984-2017. ***Recommendation for 2018:*** Use the same method to analyze trends in the NDVI for specific intervals within the period of record to characterize changes in the quality of the riparian habitat before and after implementation of both Peace Agreements.

- During WY 2017, groundwater levels fluctuated, in some cases by more than 15 feet, under the seasonal stresses of production and recharge. During the winter months of WY 2017, groundwater levels at the PBHSP monitoring wells increased to their highest recorded levels, likely in response to the recharge of stormwater discharge in unlined creeks and the associated surface-water reservoir that ponds behind Prado Dam. These short-term increases in groundwater levels are temporary, and groundwater levels declined during the growing season under the stresses of groundwater production and evapotranspiration.

Recommendation for 2018: Continue the monitoring of groundwater levels with no change in scope.

- There is a warming trend observed in the Prado Basin as indicated by the increases in the five-year moving average for the growing-season maximum and minimum temperatures. In addition, in 2017 the maximum and minimum temperatures and the five-year moving average were the highest for the entire period of record (1895-2017). ***Recommendation for 2018:*** Continue the monitoring of climate with no change in scope.

- The most recent groundwater modeling of the Chino Basin shows there are two areas within Prado Basin where groundwater levels are projected to decline by 2030 due to the implementation of the Peace II Agreement—the northernmost reaches of Chino Creek and Mill Creek. These projected groundwater-level declines are minor, and based on the current (2017) depth to groundwater in these areas, are not associated with concerns for prospective loss of riparian habitat. ***Recommendation for the PBHSP:*** Continue the monitoring of groundwater levels and utilize updated groundwater model projections of groundwater levels to characterize areas of prospective loss of riparian habitat.

- Several of the defined areas in Prado Basin along Chino Creek, Mill Creek, and SAR show decreases in the average-growing season NDVI from the 2015-2017 period. Except for one area (SAR-1), these two-year decreases in the NVDI are minor and within the historical range of the annual and short-term variability of NDVI at these area, and hence do not necessarily represent degradation of the quality of riparian habitat. In addition, the analysis of air photos does not illustrate signs of degradation of the riparian habitat. Sections 3.2 through 3.6 compare trends in the average-growing season NDVI for the defined areas during 2015 to 2017 with trends in other factors that affect riparian vegetation:

    - Except for the southern portion of Chino Creek, the decreases in the average-growing season NDVI from 2015 to 2017 occurred at locations where groundwater levels remained the same or increased by two feet. In the locations along the southern portion of Chino Creek where the NDVI decreased from 2015 to 2017, groundwater levels declined by up to one foot. The declines in groundwater levels are not a likely cause of the recent declines in NDVI at these locations because the declines in groundwater levels are less than one foot and appear to be within the historical range of short-term variability.

    - The decreasing trends in NDVI observed from 2015 to 2017 occurred during a gradual warming trend in the Prado Basin growing-season maximum and minimum temperature, and the highest recorded maximum and minimum temperatures in 2017. The Chino Basin has been experiencing a dry period since 1999.

    - The decreasing trends in NDVI from 2015 to 2017 occurred as the growing season discharge in Chino Creek and Mill Creek decreased over this period, and were below the five-year averages in 2017; the growing-season discharge remained stable in the SAR.

- o At all areas where NDVI decreased from 2015 to 2017, the presence of the PSHB beetle was noted in stressed trees at nearby locations during the 2016 USBR site-specific vegetation surveys.

These observations suggest that the drawdown of groundwater levels due to the Peace II implementation is not the cause of the recent (2015-2017) decrease in the NDVI estimates observed at some areas in the Prado Basin. It is premature to attribute the recent trends in decreasing NDVI with the increasing temperatures in the Prado Basin over the last five years, a prolonged dry period, the 2015 to 2017 declines in growing-season discharge in Chino Creek and Mill Creek, and the presence of the PSHB noted in 2016. Continued monitoring and analysis is required to identify the relationships between recent trends in these factors with recent trends in the quality of the riparian habitat. ***Recommendation for the PBHSP:*** Continue the monitoring of temperature, precipitation, surface-water discharge, and groundwater levels with no change in scope. Recommended changes to the riparian habitat monitoring program include: (i) in 2018, increase the number of defined areas to analyze NDVI in the Prado Basin to include areas near the defined areas where NDVI decreased from 2015 to 2017—these areas may include locations where the USBR conducted vegetation surveys in 2016; (ii) monitoring for the presence of PSHB in the site-specific vegetation surveys scheduled for 2019; and (iii) modifying the list of sites for the 2019 specific vegetation surveys as deemed necessary to include additional sites where declining trends in NDVI are observed in 2018.

- The average-growing season NDVI at SAR-1 along the upstream reach of the SAR decreased from 2016 to 2017 by 0.21. Analysis of the 2017 air photo indicates that the decrease in NDVI is due to a change in the riparian vegetation at SAR-1. Groundwater levels and baseflow in the SAR remained relatively stable in this area from WY 2015 to 2017. The stress that caused change in the vegetation at SAR-1 is currently unknown. ***Recommendation for 2018:*** Perform a site visit to SAR-1 with OCWD biologists to inspect and document the state of the vegetation. Based on the results of the site visit, revise the monitoring program for this area to characterize changes in the riparian habitat and identify the causes of those changes.

- Shallow groundwater in Prado Basin provides a source water for consumptive use by the riparian vegetation. Analysis of groundwater/surface water interactions in the Prado Basin indicates that the northern reaches of Mill Creek and the SAR are "losing reaches" characterized by streambed recharge. Most other areas along Chino Creek and Mill Creek are "gaining reaches" characterized by groundwater discharge. However, at most locations in Prado Basin, groundwater/surface-water interactions are complex and there appears to be multiple and transient source waters that feed the shallow groundwater. Additional monitoring and testing are needed to better characterize the source waters and the groundwater/surface-water interactions in these locations. ***Recommendation for the PBHSP:*** Discontinue the quarterly groundwater sampling for general minerals at all nine locations (18 wells) performed for the PBHSP thus far, and replace with a monitoring pilot test at two locations along Chino Creek and/or Mill Creek (four wells). The recommended pilot test will use (i) high-frequency water-quality monitoring probes that measure EC and temperature at the wells and the surface water just upstream from the wells and (ii) quarterly sampling and analysis of general minerals at the wells and surface-water site. The high-frequency data may better characterize the groundwater/surface-water interactions and source waters for the shallow groundwater, and enhance the interpretation of the general mineral data. Additionally, the 2018 annual report should analyze the influence of the elevation of the Prado Dam reservoir on the groundwater/surface water interactions.

- NDVI should be integrated with georeferenced field observations for validation. The USBR performed field vegetation surveys in 2007, 2013, and 2016. A field vegetation survey is planned for 2019. It is possible that the field survey methods could be refined to improve the validation of NDVI. Appendix A includes a literature review of field-survey methods that are favorable for validating NDVI results. ***Recommendation for 2018:*** Recruit a biological expert with experience in groundwater-dependent ecosystems to review the field-survey methods used thus far for the PBHSP, perform independent research, and provide recommendations for field surveys and/or other site-specific monitoring methods for the PBHSP.

4.2 Recommended Mitigation Measures and/or Adjustments to the AMP

This annual report documented no trend in degradation of the extent or quality of the riparian habitat along Chino Creek, Mill Creek, or the SAR that is contemporaneous with the implementation of the Peace II Agreement. Hence, no mitigation measures are proposed at this time.

No adjustments to the AMP are recommended at this time.

4.3 Recommended PBHSP for Fiscal Year 2018/19

Based on the conclusions and recommendations described above, a scope-of-work for the PBHSP for FY 2018/19 was developed and recommended by the PBHSC and is shown in Table 4-1 as a line-item cost estimate.

The ongoing costs of the PBHSP are shared between the Watermaster and IEUA per the 2016 Agreement.[31] Watermaster is responsible for the costs associated with Tasks 1 through 3; and IEUA and Watermaster split costs 50/50 for Tasks 4 through 7. The cost for the custom flight to collect a high-resolution air-photo in Task 4 is being shared 50/50 with OCWD.

The following describes the scope-of-work by major task for the PBHSP for FY 2018/19:

[31] Agreement Between Chino Basin Watermaster and Inland Empire Utilities Agency Regarding Reimbursement of the Peace II Subsequent Environmental Impact Report Mitigation Measure 4.4.5 (Prado Basin Habitat Sustainability Program). Signed September 2016.

Task 1—Groundwater-Level Monitoring Program. The monitoring of groundwater levels in the Prado Basin is a key component of the PBHSP, as declining water levels could be a factor related to Peace II implementation that adversely impacts riparian vegetation. Sixteen monitoring wells were installed specifically for the PBHSP during fiscal year 2014/15. These wells, plus monitoring wells HCMP-5/1 and RP3-MW3, are monitored for groundwater levels. These 18 PBHSP monitoring wells are located at nine sites in the Prado Basin along the fringes of the riparian habitat (see Figure 2-2). The 18 monitoring wells are equipped with pressure transducers that record water-level measurements every 15 minutes. This task includes quarterly field visits to all 18 PBHSP monitoring wells to download the transducer data, and processing, checking, and uploading of the data to the database. This task is consistent with the work performed during the previous fiscal year.

Task 2—Groundwater-Quality Monitoring Program. Groundwater-quality data are analyzed along with groundwater-level data, model-generated groundwater-flow directions, and surface-water chemistry data to help characterize groundwater/surface-water interactions in the Prado Basin and determine the source of the shallow groundwater that is available for consumptive use by the riparian vegetation.

Quarterly groundwater-quality grab samples have been collected over the previous three fiscal years at the 18 PBHSP monitoring wells since they were constructed. These data were analyzed for the current annual report. The analysis suggests that the SAR is a losing reach from PB-4 to about River Road, and that the source of the shallow groundwater along this reach is recharge from the SAR. However, the analysis was inconclusive along portions of Chino Creek and Mill Creek. It appears that the groundwater/surface-water interactions along these creeks are more complex, and that the current water-quality monitoring program is not sufficient to definitively characterize the interactions. We recommend discontinuing the current groundwater-quality monitoring procedures used through fiscal year 2017/18, and performing a pilot test of a high-frequency water-quality monitoring program at two groundwater monitoring sites (four wells)—located along Chino Creek or Mill Creek. Each well will be equipped with probes that measure and record EC, temperature, and water levels at a 15-minute frequency. The wells will be visited quarterly to download the data from the probes, measure water levels, and collect grab samples for laboratory analyses of TDS and general mineral analytes listed in Table 4-2. The high-frequency data may better reveal the groundwater/surface-water interactions and enhance the interpretation of the TDS and general mineral data that has been derived from grab sampling. This task also includes quarterly processing, checking, and uploading of the water-quality data into the database.

Conducting this pilot test, instead of continuing the quarterly groundwater-quality monitoring for general mineral chemistry, translates into a $25,015 reduction in cost from the previous fiscal year for Task 2.

Task 3—Surface-Water Monitoring Program. Surface-water discharge data are evaluated in the vicinity of the Prado Basin to characterize trends, and to determine if these trends contribute to impacts on the riparian habitat. The surface-water monitoring program utilizes publicly-available data sets which include: the USGS daily discharge measurements at six sites along the Santa Ana River and its tributaries; daily discharge and water-quality data from Publicly-Owned Treatment Works (POTWs) that are tributary to Prado Basin; US Army Corps of Engineers (ACOE) daily measurements of reservoir elevation and releases from the reservoir at Prado Dam; and Watermaster's quarterly surface-water-quality monitoring at two sites along the Santa Ana River. The locations of these surface-water monitoring sites are shown on Figure 2-3.

Task 3.1 and 3.2 includes the annual collection of the USGS, POTW, and ACOE data for water year 2018 (October 2017 – September 2018), and the processing, checking, and uploading of these data to the PBHSP database. These tasks do not include the processing, checking, and uploading of the Watermaster-collected Santa Ana River data, which is performed for another Watermaster task. Collecting this surface-water data is consistent with the work performed during the previous fiscal year.

The surface-water data were analyzed along with groundwater-quality data for the current annual report to help characterize groundwater/surface water interactions. However, as described in Task 2 above, the analysis was inconclusive along portions of Chino Creek and Mill Creek. Additionally, there are no recent surface-water-quality data along Chino Creek and Mill Creek except for the POTW discharge water-quality data. Starting in fiscal year 2018/19, we recommend collecting quarterly surface-water-quality grab samples at two sites—one site along Chino Creek and one site along Mill Creek (near the two groundwater monitoring sites where the proposed pilot test is to be conducted for Task 2 above). Task 3.3 includes conducting quarterly surface-water-quality sampling at two surface-water sites and laboratory analyses for TDS, nitrate, and general mineral analytes listed in Table 4-2. These data will be used to better characterize groundwater/surface-water interactions along these creeks. Task 3.4 is for the quarterly processing, checking, and uploading of the surface-water-quality data into the database. Collecting Task 3.3 and 3.4 will increase the cost of Task 3 by $11,495 compared to last fiscal year.

Task 4—Riparian Habitat Monitoring Program. Monitoring the extent and quality of the riparian habitat in the Prado Basin is a fundamental component of the PBHSP to characterize how the riparian habitat changes over time. To characterize the impacts of Peace II implementation on the riparian habitat, if any, it is necessary to understand the long-term historical trends of its extent and quality and the factors that have affected it. The riparian habitat monitoring program consists of both regional and site-specific components.

The regional monitoring of riparian habitat is performed via two independent methods that complement each other: mapping and analysis of the riparian habitat using (i) air photos and (ii) the NDVI derived from the Landsat remote-sensing program. Tasks 4.1, 4.2, and 4.3 are for the collection of data for the regional monitoring of the riparian habitat, and include the following:

- Perform a custom flight (outside professional) to acquire a high-resolution air photo (three-inch pixel) of the Prado Basin during summer 2018. The cost for the air photo is shared with the OCWD.
- Catalog and import the 2018 high-resolution air photo to ArcGIS, and digitize the extent of the riparian habitat.
- Collect, review, and upload the Landsat NDVI data for water year 2018.

Task 4.4 is for research and refinement of the regional monitoring methods, as-needed. This includes coordination with OCWD and others to research and identify regional monitoring methods of the riparian habitat that can complement and validate the NDVI data. This includes review of a pilot study that the OCWD is conducting at two transects in Prado Basin during 2018 using infrared imagery collected from drones to analyze vegetation health.

Site-specific monitoring of the riparian habitat consists of periodic field surveys of the riparian vegetation at selected locations. These surveys provide an independent measurement of vegetation quality that can be used to "ground truth" the regional monitoring of the riparian habitat. To date, the field surveys have been conducted by USBR and OCWD staff once every three years. The *Annual Report of the PBSHC for Water Year 2016/17* includes a literature review of field-survey methods that are favorable for ground truthing the NDVI results. No field surveys are planned for FY 2018/19.

Task 4.5 is for research and refinement of the site-specific monitoring methods. This includes effort to identify and contract with a biological expert with experience in groundwater-dependent ecosystems to review the field-survey methods used thus far for the PBHSP, perform independent research, and provide recommendations for field surveys and/or other site-specific monitoring methods for the PBHSP.

Task 4.6 is for planning and coordination for the next field survey that is scheduled for Summer 2019. This may include completing the same scope as past field surveys performed by the USBR and OCWD, or implementing new monitoring methods that are recommended by the biological expert in Task 4.5.

Task 5 – Climate Monitoring Program. Climatic data are evaluated in the vicinity of the Prado Basin to characterize trends, and to determine if these trends contribute to impacts on the riparian habitat. The climate monitoring program utilizes publicly-available data sets. Two types of datasets are compiled: time-series data measured at weather stations and spatially-gridded datasets. Task 5 includes the annual collection of the time-series data and spatially-gridded datasets for water year 2018 (October 2017 – September 2018), and the processing, checking, and uploading of the data to the PBHSP database. The scope of this task is consistent with the work performed for the previous fiscal year.

Task 6—Prepare Annual Report of the PBHSC. This task involves the analysis of the data sets generated by the PBHSP through water year 2018. The results and interpretations generated from the data analysis will be documented in the *Annual Report for Prado Basin Habitat Sustainability Committee for Water Year 2017/18*. This task includes the effort to prepare an administrator draft report for Watermaster and IEUA staff review, a draft report for the review by the PBHSC, and a final report including comments and responses. A PBHSC meeting will be conducted in May 2019 to review the draft report and facilitate comments on the report. The scope of this task is consistent with the work performed for the previous fiscal year.

Task 7—Project Management and Administration. This task includes the effort to prepare the PBHSP scope, schedule, and budget for the subsequent fiscal year. A draft *Technical Memorandum Recommended Scope and Budget of the Prado Basin Habitat Sustainability Program for FY 2019/20* will be submitted to the PBHSC in February/March 2019. A PBHSC meeting will be conducted in March 2019 to review the draft recommended scope and budget and facilitate comments. Also included in this task is project administration, including management of staffing and monthly financial reporting. The scope of this task is consistent with the work performed for the previous fiscal year.

Table 4-1
Work Breakdown Structure and Cost Estimate
Prado Basin Habitat Sustainability Program -- FY 2018/19

Task Description		Labor Total		Other Costs						Notes	Totals						
	No. of sites	Person Days	Total	Travel	Equip. Rental	Lab	Outside Pro	Equip	Total		Recommended Budget 2018/19	Budget 2017/18	Budget 2016/17 (Spent)	Difference 2017/18 to 2018/19	Difference 2016/17 to 2018/19	IEUA Share 2018/19	CBWM Share 2018/19
Task 1: Groundwater Level Monitoring Program		**11.4**	**$12,856**						**$782**		**$13,638**	**$11,931**	**$11,600**	**$1,707**	**$2,038**	**-**	**$13,638**
1.1 Collect Transducer Data from PBHSP Wells (Quarterly)	18	5.0	$4,792	$590	$192				$782		$5,574						
1.2 Collect, Check, and Upload Transducer Data from PBHSP Wells (Quarterly)	18	6.4	$8,064						$0		$8,064						
Task 2: Groundwater Quality Monitoring Program		**6.6**	**$13,612**						**$10,428**		**$24,040**	**$49,055**	**$67,422**	**-$25,015**	**-$43,382**	**-**	**$24,040**
2.1 Initiate a Pilot Test of High-Frequency Water Quality Monitoring using EC and Temperature Probes	4	3.3	$3,879	$236				$6,100	$6,336		$10,215						
2.2 Collect, Check, and Upload High-Frequency Probe Data from Pilot Monitoring Program (Quarterly)	4	2.4	$3,123						$0		$3,123						
2.3 Collect, Check, and Upload Grab Sample General Mineral Chemistry Data (Quarterly)	4	6.6	$6,610	$472	$820	$2,800			$4,092		$10,702						
Task 3: Surface Water Monitoring Program		**2.8**	**$12,940**						**$2,033**		**$14,973**	**$3,744**	**$3,800**	**$11,229**	**$11,173**	**-**	**$14,973**
3.1 Collect, Check, and Upload Surface Water Discharge and Quality Data from POTWs, and Dam Level data from the ACOE (Annual)		2.0	$2,470						$0		$2,470						
3.2 Collect, Check, and Upload Surface Water Discharge and Quality Data from USGS gaging stations (Annual)		0.8	$1,008						$0		$1,008						
3.3 Design and Conduct a Surface Water-Quality Monitoring at Chino and Mill Creeks (Quarterly)	2	7.0	$6,793	$525	$108	$1,400			$2,033		$8,826						
3.4 Check and Upload Grab Surface Water Quality Field and Lab Data (Quarterly)	2	2.0	$2,669						$0		$2,669						
Task 4: Riparian Habitat Monitoring Program		**22.5**	**$36,194**						**$20,000**		**$56,194**	**$50,342**	**$145,927**	**$5,852**	**-$89,733**	**$28,097.2**	**$28,097.2**
4.1 Perform a Custom Flight to Acquire a High-Resolution 2018 Air Photo of the Prado Basin		0.8	$1,224				$10,000		$10,000	1	$11,224						
4.2 Catalog, Check, and Digitize the Extent of the Riparian Vegetation in the 2018 Air Photo of the Prado Basin		3.7	$5,234						$0		$5,234						
4.3 Collect, Check, and Upload 2018 Landsat NDVI Data to the PBHSP Database		5.0	$7,240						$0		$7,240						
4.4 Research and Refine Regional Monitoring Methods		4.0	$7,008						$0		$7,008						
4.5 Research and Refine Site-Specific Monitoring Methods		6.0	$10,432				$10,000		$10,000		$20,432						
4.6 Plan and Coordinate the Site-Specific Monitoring Event for Summer 2019		3.0	$5,056						$0		$5,056						
Task 5: Climate Monitoring Program		**1.0**	**$1,479**						**$300**		**$1,779**	**$1,756**	**$1,700**	**$23**	**$79**	**$889.60**	**$889.60**
5.1 Collect, Check, and Upload Climatic Data (Annual)		1.0	$1,479				$300		$300		$1,779						
Task 6: Prepare Annual Report of the PBHSC		**61.0**	**$95,747**						**$210**		**$95,957**	**$91,082**	**$203,473**	**$4,875**	**-$107,516**	**$47,978.6**	**$47,978.6**
6.1 Analyze Data and Prepare Admin Draft Report for CBWM/IEUA		44.7	$70,007						$0		$70,007						
6.2 Meet with CBWM/IEUA to Review Admin Draft Report		3.0	$5,216	$105					$105		$5,321						
6.3 Incorporate CBWM/IEUA Comments and Prepare Draft Report: Submit Draft Report to PBHSC		5.0	$7,152						$0		$7,152						
6.4 Meet with PBHSC to Review Draft Report		3.0	$5,216	$105					$105		$5,321						
6.5 Incorporate PBHSC Comments and Finalize Report		5.3	$8,156						$0		$8,156						
Task 7: Project Management and Administration		**11.8**	**$20,282**						**$105**		**$20,387**	**$19,033**	**$23,395**	**$1,354**	**-$3,008**	**$10,193.30**	**$10,193.30**
7.1 Prepare Scope and Budget for FY 2019-20		4.0	$6,848						$0		$6,848						
7.2 Meet with PBHSC to Review Scope and Budget for FY 2019/20		3.0	$5,216	$105					$105		$5,321						
7.3 Project Administration and Financial Reporting		4.8	$8,218						$0		$8,218						
Totals		**232**	**$193,110**	**$1,548**	**$928**	**$4,200**	**$20,300**	**$6,100**	**$33,858**		**$226,968**	**$226,943**	**$457,317**	**$25**	**-$230,349**	**$87,159**	**$139,810**

1 - This is half of the cost for the outside professional. OCWD will pay the other half.

Table 4-2
Parameter List for the Groundwater and Surface Water Quality Monitoring Programs for Fiscal Year 2018/19

Chemical Parameter	Method Detection Limit	Analysis Method
Alkalinity in CaCO3 units	2	SM2320B
Ammonia Nitrogen	0.05	EPA 350.1
Bicarbonate as HCO3 *Calculated*	2	SM2320B
Calcium Total ICAP	1	EPA 200.7
Carbonate as CO3 *Calculated*	2	SM2320B
Chloride	1	EPA 300.0
Hydroxide as OH *Calculated*	2	SM2320B
Magnesium Total ICAP	0.1	EPA 200.7
Nitrate as Nitrogen by IC	0.1	EPA 300.0
Nitrate as NO3 *Calculated*	0.44	EPA 300.0
Nitrite as Nitrogen by IC	0.05	EPA 300.0
PH (H3=past HT not compliant)	0.1	SM4500-HB
Potassium Total ICAP	1	EPA 200.7
Sodium Total ICAP	1	EPA 200.7
Specific Conductance, 25 C	2	SM2510B
Sulfate	0.5	EPA 300.0
Silica	0.5	EPA 200.7
Total Dissolved Solids (TDS)	10	E160.1/SM2540C
Total Hardness as CaCO3 by ICP	3	SM 2340B
Total Organic Carbon	0.3	SM5310C/E415.3
Turbidity	0.05	EPA 180.1

Section 5 – References

Achard F., and Estreguil, C. 1995. *Forest classification of Southeast Asia using NOAA AVHRR data.* Remote Sensing of the Environment v. 56, pg. 198-208.

Alfaro, E.J., Gershunov, A., and Cayan, D. 2006. *Prediction of summer maximum and minimum temperatures over the central and western United States: the roles of soil moisture and sea surface temperatures.* J. Clim v. 19, 1407-1421.

Associated Engineers, Inc. 2007. Digital Elevation Model of Southern Chino Basin. Acquired by Airborne 1 Corporation via LIDAR. March, 2007.

California Regional Water Quality Control Board, Santa Ana Region. 2008. Water Quality Control Plan Santa Ana River Basin (Region 8) 1995. Updated February 2008.

Campbell, 2007. *Introduction to remote sensing.* Fourth edition. Published 2007 Guilford Press.

Chino Basin Watermaster. 2000. Peace Agreement, Chino Basin. SB 240104 v 1:08350.0001. 29 June 2000.

Chino Basin Watermaster. 2007. *Peace II Agreement: Party Support for Watermaster's OBMP Implementation Plan, - Settlement and Release of Claims Regarding Future Desalters. SB 447966 v 1:008250.0001.* 25 October 2007.

Chino Basin Municipal Water District v. City of Chino et al., San Bernardino Superior Court, No. 164327. (1978).

Chen, J., Jonsson, P., Tamura, M, Gu, Z., Matsushita, B., and Eklundh, L. 2004. *A Simple method for reconstructing a high-quality NDVI time-series data set based on the Savitzky-Golay filter.* Remote Sensing of Environment v. 91, pg. 332-344.

Flood, N. 2014. *Continuity of Reflectance Data between Landsat-7 ET<+ and Landsay-8 OLI, for Both Top-of Atmosphere and Surface Reflectance: A Study in the Australian Landscape.* Remote Sensing v. 6, pg. 7952-7970. August 26, 2014.

Gandhi, M., Parthiban, S., Thummalu, N., and A., C. 2015. *Ndvi: Vegetation changes detection using remote sensing and gis – A case study of Vellore District.* Procedia Computer Science v. 57, pg. 1199-1210.

Hatfield, J.L., and Prueger, J.H. 2015. *Temperature extremes: Effect on Plant growth and development.* Weather and Climate Extremes v. 10, pg. 4-10.

Hatfiled, J.L, Boote, K.J, Kimball, B.A, Ziska, L.H, Izaurralde, R.C., Ort, D., Thomson, A.M., and Wolfe, D. 2011. Climate impacts on agriculture: implications for plant production. Agron J, v. 103, P.351-370.

Hird, J., and McDermid, G. 2009. *Noise reduction of NDVI time series: An empirical comparison of selected techniques.* Remote Sensing of Environment v. 113, pg. 248-258.

H. T. Harvey & Associates. 2015. *Prado Basin Preliminary Riparian Habitat Health and Vigor Assessment.* Memorandum to the Orange County Water District. October 26, 2015.

James, M., and Kalluri, S. 1994. The Pathfinder *AVHARR land data set; an improved coarse resolution data set for terrestrial monitoring.* International Journal of Remote Sensing v. 15, pg. 3347-3363.

Jenson, J. 2007. *Remote Sensing of the Environment: An Earth Resource Perspective*, second edition. Published 2007 by Prentice-Hall, Upper Sadle River, N.J.

Jones, H., and Vaughan, R. 2010. *Remote Sensing of Vegetation: Principles, Techniques and Applications.* Oxford University Press, Oxford.

Ke, Y., Im, J., Lee, J., Gong, H., and Ryu, Y. 2015. *Characteristics of Landsat 8 OLI-derived NDVI by comparison with multiple sensors and in-situ observations.* Remote Sensing of Environment v. 164, pg. 298-313.

Knowles, N., Dettinger, M.D., and Canyon, D.R. 2006. *Trends in snowfall versus rainfall in the western United States.* J Clim v.19, pg.4545-4599.

Li, P., Jiang,L.,Feng,Z. 2014. *Cross Comparison of Vegetation Indices Derived from Landsat-7 Enhanced Thematic Mapper Plus (ETM+) and Landsat-8 Operational Land Imager (OLI) Sensors.* Remote Sensing v. 6, pg. 310-329.

Lillesand,T., Kiefer, R, and Chipman, J. 2008. *Remote Sensing and Image Interpretation*, sixth edition. Published in 2008 by John Wiley & Sons, New York.

Markon, C., Fleming, M., and Binnian, E. 1995. *Characteristics of vegetation phenology over Alaskan landscape using AVHRR time-series data.* Polar Records v. 31, pg.179-190.

Markon, C., and Peterson, K. 2002. *The utility of estimating net primary productivity over Alaska using baseline AVHRR data.* International Journal of Remote Sensing, v.23, pg. 4571-4596.

McPherson, D., at United States Bureau of Reclamation. 2016. Verbal communication on November 2, 2016

Merkel & Associates, Inc. 2007. Evapotranspiration Analysis of the Prado Basin Santa Anan River, California. Prepared for Wildermuth Environmental, Inc. November 2007.

Orange County Water District. 2015. *Effects of Reduced Outflow from Prado Dam Water Conservation 2013/2014.* Prepared for the U.S. Fish & Wildlife Service. February 2015.

Palenscar, K., at United States Fish and Wildlife. 2016. Verbal communication on November 2, 2016

Peters, A., Walter-Shea, E., Ji, L, Vina, A., Hayes, M., and Svoboda, M.D. 2002. *Drought Monitoring with NDVI-Based Standardized Vegetation Index.* Photogrammetric Engineering & Remote Sensing v. 68, no. 1, pg. 71-75.

Pettorelli, N. 2013. *The Normalized Difference Vegetation Index*. First edition. Published 2013 by Oxford University Press.

Pinzon, J., Brown, M., and Tucker, C. 2004. Monitoring Seasonal and International Variations in Land-surface Vegetation from 1981-2003 Using GIMMS NDVI. https://landval.gsfc.nasa.gov/pdf/GIMMS_NDVI_8km_doc.pdf

Roy, D., Kovalskyy, V., Zhang, H., Vermote, E., Yan, L., Kumar, S, and Egorov, A. 2016. *Characterization of Landsat-7 to Landsat-8 reflective wavelength and normalized difference vegetation index continuity*. Remote Sensing of Environment v. 185, pg. 57-70. January 12, 2016.

Inland Empire Utilities Agency and Chino Basin Watermaster. 2008. *Memorandum of Understanding, Cooperative Efforts for Monitoring Programs Between the Inland Empire Utilities Agency and the Chino Basin Watermaster, Bright Line Approach*. 17 December 2008.

Intera Inc. 2015. *Memorandum Remote-Sensing Based Evaluation of Temporal Changes in Riparian Vegetation Health Along Temescal Creek, Prado Reservoir, Corona, California*. Prepared for Orange County Water District. January 30, 2015.

Santa Ana River Watermaster. 2017. Forty-Sixth Annual Report of the Santa Ana River Watermaster for Water Year October 1, 2015 – September 30, 2016 (draft). March, 9, 2017.

Schimdt, H. and Karnieli, A. 2000. *Remote sensing of seasonal variability of vegetation in a semi-arid environment*. Journal of Arid Environments v.45, pg. 43-59.

She, X., Zhang L., Cen, Y., Wu, T., Changping, H., and Ali Baig, H. 2015. *Comparison of the Continuity of Vegetation Indices Derived from Landsat * OLI and Landsat 7 ETM+ Data Among Different Vegetation Types*. Remote Sensing v.7, pg. 13485-13506. October 16, 2015.

Tanre, D., Holden, B., and Kaufman,Y. 1992. *Atmospheric correction algorithm for NOAA_AVHRR products; theory and application*. IEE Journal of Geosciences and Remote Sensing, v. 30, pg. 231-248.

Tom Dodson & Associates. 2000. *Program Environmental Impact Report for the Optimum Basin Management Program (SCH#2000041047)*. Prepared for the Inland Empire Utilities Agency. July 2000.

Tom Dodson & Associates. 2010. *Final Subsequent Environmental Impact Report for the Inland Empire Utilities Agency Peace II Agreement Project*. Prepared for the Inland Empire Utilities Agency. 25 September 2010.

Tucker C., Justice, C., and Prince, S. 1986. *Monitoring the grasslands of Sahel 1984-1985. International Journal of Remote Sensing*, v. 71, pg. 1571-1581.

Tucker C., Grant, D., and Dykstra, J.D. 2004. *NASA's global orthorectified Landsat data set. Photogrammetric Engineering & Remote Sensing*, v. 70, pg. 313-322.

United States Bureau of Reclamation, Lower Colorado Regional Office. 2008. *Hydraulic Control Monitoring Plan, Task 5.2: Vegetation Survey at the Prado Reservoir, Report No 2 of 5*. Prepared for the Inland Empire Utilities Agency. March 2008.

United States Bureau of Reclamation, Lower Colorado Regional Office. 2015. Riverside and San Bernardino Counties, California Inland Empire Utility Agency *Hydraulic Control Monitoring Plan, Task 5.2: Report No 3 of 5*. Draft Report. April 2015.

United States Bureau of Reclamation. 2017. Southern California Area Office. *Prado Basin Vegetation Survey October 2016*. Draft Report. February 2017.

United States Department of Agriculture. 1996. *Using NDVI to Assess Departure From Average Greenness and its Relation to Fire Business*. Burgan, R.E., Hartford, R.A, and Eidenshink, J.C. General Technical Report INT-GTR-333. April 1996.

United States Department of Agriculture. 1999. *Percent Canopy Cover and Stand Structure Statistics from the Forest Vegetation Simulator*. April 1999.

United States Department of Agriculture, Forest Service Region Pacific Southwest Region – State and Private Forestry. 2013. *Pest Alert. New Pest Complex in California: The Polyphagous Shot Hole Borer, Euwallacea sp., and Fusarium Dieback, Fusarium euwallaceae*. R5-PR-032. November 4, 2013.

United State Geological Survey. 2013. Landsat Ecosystem Disturbance Adaptive Processing System (LEDAPS) Algorithm Description. Open-File Report 2013-1057. 2013.

United State Geological Survey. 2016. Product Guide – Landsat Surface Reflectance-Derived Spectral Indices. Version 3.3. December 2016.

United State Geological Survey. 2017a. Product Guide – Landsat 4-7 Climate Data Record (CDR) Surface Reflectance. Version 7.2. January 2017.

United State Geological Survey. 2017b. User Guide – Earth Resources Observation and Science (EROS) Center Science Processing Architecture (ESPA) On Demand Interface. Version 3.7. January 2017.

Verbesselt, J., Hyndman, R., Newnham, G., and Culvenor, D. 2010. *Detecting trend and seasonal changes in satellite image time-series*. Remote Sensing of Environmental, v. 17, pg. 231-235.

Weiss, J., Gutzler, D., Allred Coonrod, J., and Dahm, C. 2004. *Long-term vegetation monitoring with NDVI in a diverse semi-arid setting central New Mexico, USA*. Journal of Arid Environments v. 58, pg. 249-272.

Wildermuth Environmental, Inc. 1999. *Optimum Basin Management Program. Phase I Report*. Prepared for the Chino Basin Watermaster. August 19, 1999.

Wildermuth Environmental, Inc. 2007. *2007 Chino Basin Watermaster Groundwater Model Documentation and Evaluation of the Peace II Project Description. Final Report.* November 2007.

Wildermuth Environmental, Inc. 2015. *2013 Chino Basin Groundwater Model Update and Recalculation of Safe Yield Pursuant to the Peace Agreement (Final Report)*. Prepared for the Chino Basin Watermaster. October 2015.

Wildermuth Environmental, Inc. 2016. *2016 Adaptive Management Plan for the Prado Basin Habitat Sustainability Program, Final.* Prepared for the Inland Empire Utilities Agency and Chino Basin Watermaster. August, 2016.

Wildermuth Environmental, Inc. 2017 A*nnual Report of the Prado Basin Habitat Sustainability Committee Water Year 2015/2016*. July 2017.

Wang, J., Rich, P., Price, K., and Kettle, W. 2004. *Relations between NDVI and tree productivity in the central Great Plains.* International Journal or Remote Sensing, v. 25, pg. 3127-3138.

Woodside, G., at Orange County Water District. 2017. Verbal communication on March 15, 2017.

Xie, Y., Sha, Z., and Yu, M. 2008. *Remote Sensing imagery in vegetation mapping: a review.* Journal of Plant Ecology. V. 1, no.1, pg 9-23.

Xue, J. and Su, B. 2017. *Significant Remote Sensing Vegetation Indices A Review of Development and Applications*. Journal of Sensors V. 2017, Article ID 1353691 17 pages

Zembal, R., at Orange County Water District. 2017. Verbal communication on March 14, 2017.

Zembal, R., at Orange County Water District. 2018. Email communication on April 5, 2018.

Appendix A– Field Methods to Validate NDVI

1.1 Introduction

The riparian habitat monitoring program for the Prado Basin Habitat Sustainability Program (PBHSP) consists of regional and site-specific monitoring methods. The regional monitoring is performed via two independent methods that complement each other: mapping and interpretation of the extent and quality of riparian vegetation using (i) air photos and (ii) the normalized difference vegetation index (NDVI) derived from Landsat remote-sensing measurements. The site-specific monitoring consists of periodic field surveys of the structural and compositional attributes of the riparian vegetation at select locations. Where and when possible, field measurements should be used to "ground truth" the NDVI determined from remote sensing measurements.

To date, the field surveys performed for the PBHSP have measured structural and compositional vegetation attributes that are not distinguished by the NDVI. The vegetation attributes can complement the interpretations derived from the NDVI, but cannot be used to validate and/or calibrate the NDVI because the field measurements do not directly correlate to NDVI. Field methods that can be used to validate NDVI should collect data that correlates directly to NDVI. This appendix summarizes a literature review of the field methods that can be used to validate NDVI. These field methods will be considered when designing the site-specific monitoring methods during the upcoming fiscal year 2018/19.

1.2 Field Methods to Validate NDVI

NDVI is a measurement of greenness associated with photosynthesis and is used to assess changes in vegetation distribution, productivity, and dynamics (Pettorelli, 2013). Field survey data that can be used to validate NDVI should have attributes related to photosynthesis. A summary of field methods that can be used to validate NDVI follows:

- ***In-Field NDVI Measurements***. NDVI can be measured in the field with NDVI sensors (i.e. GreenSeeker TM handheld sensor, METER Spectral Reflectance Sensor). Passive or active in-field NDVI sensors can be mounted on a pole or tripod, looking straight down upon a given canopy area to measure NDVI. Passive NDVI sensors measure the ratio of the reflected radiation over the incoming radiation to calculate the NDVI of the canopy. Active NDVI sensors emit red and near-infrared radiation onto a canopy to determine the ratio of reflected to emitting radiation and calculates the NDVI. NDVI field measurements can be compared with NDVI determined from remote-sensing measurements for the same area to validate the NDVI estimates determined from remote sensing. (Gamon et al., 1995; Turner et al., 1999; Pietragalla and Madrigal Vega, 2012).

- ***Leaf Area Index (LAI).*** Leaf area affects the absorption of solar radiation by a plant canopy and the amount of reflectance that can be measured by NDVI sensors (Hardwick et al., 2015). Leaf area measurements are generally converted to LAI, which is the ratio of the one-sided green leaf area per unit of ground surface area. Various field researchers that utilized LAI to verify NDVI generally built a regression analysis between the two datasets to determine the strength of the relationship. LAI in the field is typically measured using the following methods: a) clipping phytomass, b) collecting plant litter, or c) canopy gap analyzing devices.

a) *Clipping Phytomass*: Phytomass is the total amount of living organic plant matter accumulating above the ground, and is harvested by clipping all phytomass in a designated plot area (gram per square meter [g/m^2]). This method is commonly used for crops or pastures (Breda, 2003). LAI is the product of the harvested phytomass (g/m^2), percent leaves, and the specific leaf area (square meters per gram [m^2/g]) (Wolf et al., 1972). The percent leaves in the harvested sample is determined by separating the leaf and non-leaf tissues for each sample. Each live and green leaf is flatted and patted dry in order to insert into a leaf area meter (LAI-3000 for broadleaf species and Delta-T Image Analyzer for conifer species) to measure the species-specific, one-sided leaf area (m^2). The leaf is dried and weighed to obtain the dry biomass (g). Specific leaf area (m^2/g) is calculated from the one-sided leaf area over its dry mass. Studies that used LAI determined from the clipping method and NDVI from remote sensing measurements had field plot sizes ranging from 0.1 x 0.5 m to 0.2 x 0.2 m (Gamon et al., 1995; Turner et al, 1999; Raynolds et al., 2012).

b) *Collecting Plant Litters:* For a deciduous forest, plant litter can be collected in traps distributed below the canopy for a determined frequency during the leaf fall period (Gamon et al., 1995). Litter is collected in a number of traps with a known area at least every two weeks to avoid losses and decomposition (Breda, 2003). Collected litter is dried and weighed to compute the dry mass of litter. Plant litters are sorted by species and leaf area meter is used to measure the leaf area for each species (Gamon et al., 1995). The specific leaf area of each species is determined by dividing the leaf area over its dry mass. Then the total dry mass of leaves for a specific species, collected within a designated plot is multiplied by the specific leaf area and divided by the designated plot size to determine the LAI for each species (Fleck et al., 2012). The LAI is the accumulated leaf area over the leaf fall period. This method provides an understanding of the trends in LAI during leaf fall and the contribution of each species to total leaf area.

c) *Canopy Gap Analyzing Devices:* Canopy gap analyzing devices (i.e. LAI-2200C Plant Canopy Analyzer) measure canopy gap fraction, which is the amount of light passing through a canopy without encountering plant matter (Danson et al., 2007). This method is an in-direct and none destructive technique to obtain the LAI. Canopy gap analyzing devices use fish-eye optical sensors to measure reflectance above and below the canopy area to determine canopy gap fraction at various angles (Van Wijk and Williams, 2005; and Persson, 2014). A solar radiative transfer model is applied to the canopy gap fraction measurements to calculate the LAI. The solar radiative transfer model takes into account how solar radiation is transferred through a leaf canopy, the vertical heterogeneities of plant stand, leaf orientations, and solar tracking behavior of plants (Verstraete, 1987).

- ***Canopy Chemical Content (CCC).*** CCC is the content of different chemicals in the live, green portions of the canopy. CCC such as chlorophyll (the green pigment in plants responsible for photosynthesis) and nitrogen (the main nutrient for chlorophyll production) (Loomis, 1997; Muñoz-Huerta et al., 2013) play important roles in canopy photosynthesis rate and can influence reflectance measured by NDVI sensors. Chlorophyll and nitrogen contents can be measured by harvesting the phytomass, similar to the field method described above for clipping phytomass to determine LAI. After phytomass is separated into live and dead portions and green and non-green portions, the live and green leaves are used to determine the chlorophyll content spectrophotometrically in 80:20 (volume : volume) acetone : water extracts (Porra et al., 1989), and total nitrogen can be estimated using the micro-Kjeldahl technique (Isaac and Johnson, 1976). Regression analysis is utilized to determine the strength of the relationship between chlorophyll, nitrogen, and NDVI data.

- ***Leaf and Canopy Fluxes***. Leaf- and canopy-level fluxes are the exchanges of gases like carbon dioxide (CO_2) and water vapor that occur between the leaf/canopy surface and the surrounding atmosphere. During photosynthesis, pores on leaf surface known as stomata open and CO_2 enters the leaf to be used for plant growth and production (Holding and Streich, 2013). In the process of opening stomates, water vapor exits the leaf into the surrounding atmosphere during photosynthesis. In times of limited water resources, the plant will close its stomates to conserve water and photosynthesis will cease (Nogués and Baker, 2000; Holding and Streich, 2013). Due to their close interactions with photosynthesis, CO_2 gas and water vapor flux measurements can help validate/calibrate NDVI measurements. A regression analysis is generally used to determine the correlation between CO_2 gas and water vapor fluxes with NDVI data. CO_2 gas and water vapor fluxes are measured using the following methods: a) eddy covariance, or b) portable gas exchange meters:

    a) *Eddy Covariance:* Eddy covariance technique measures vertical gas exchanges between the canopy and the surrounding atmosphere by measuring the amount of molecules moving up and down over time at various speeds (Burba, 2013). Air flow is composed of horizontal and vertical turbulent flows (eddies) and measurements of different characteristics of these eddies (i.e. wind speed, temperature, etc.) are measured with sensors to determine the gas exchanges between the canopy and the atmosphere (Burba, 2013; Pirvulescu, 2013). Eddy covariance devices are equipped with gas analyzing and air velocity sensors to calculate air speed and CO_2 and water vapor fluxes (Pirvulescu, 2013). Gas analyzing sensors measure CO_2 gas and water vapor exchanges between the canopy and the atmosphere using chemical, electric, or optical sensors.

    b) Portable Gas Exchange Meters: Portable gas exchange meters (i.e. LI-6200 or LI-COR.) measure the rate of changes in CO_2 and water vapor concentrations of a given leaf in a closed or open system to determine the leaf's CO_2 and water vapor fluxes. In a closed system, a leaf is enclosed in a sealed chamber to monitor and calculate the rate of changes of CO_2 and water vapor concentrations. In an open system, air is allowed to pass through the leaf chamber and the CO_2 and water vapor concentrations are calculated from the difference in CO_2 and water vapor concentrations that flow into the leaf chamber to that which flows out of the leaf chamber (Ferrari et al., 2015). Gas exchange measurements can be made on top-canopy leaves that are exposed to full sun between mid-morning to noon (Gamon et al., 1995).

1.3 Field Survey Design

Often the design of traditional site-specific monitoring programs does not enable easy integration with remotely senses data (Lawley et al., 2016) When integrating field survey data with remotely sensed data such as NDVI, design factors, such as the location and size of the field survey area, and timing of field surveys and the remote sensing measurements should be considered.

- *Location of field survey area.* Locations of field measurements should spatially align with locations of the remote-sensing pixels and be representative of the vegetation conditions within the study area (Razzhivin, 1999; Reinke and Jones, 2006; Raynolds et al., 2012). The field survey area should be at least one-pixel width from the boundary of the vegetation of interest to reduce the effects of relative positioning errors between the edge of the field measurements and remote-sensing data pixel (Reinke and Jones, 2006).
- *Size of field survey area.* The size of the field survey area should be sufficient to adequately sample the features of interest at a scale consistent with the spatial resolution of the remote sensing sensor, however it is should also be appropriate for the spatial distribution or size of the features measured in the field (Reinke and Jones, 2006). From a remote sensing perspective, the minimum field survey area should equal the area of at least one remote-sensing pixel (Reinke and Jones, 2006). The minimum field survey area can also be determined using the ground width of a pixel and the geometric accuracy of the pixel (Justice and Townshed, 1981) using the following: *minimum plot size = pixel width (1+(2* geometric accuracy of the pixel))*^{2}. For example, Landsat NDVI data has a pixel size of 30 m x 30 m; if the geometric accuracy is 0.5 pixels, this would result in a plot size of 60 m x 60 m.
- *Timing of field surveys and remote sensing.* When possible, field data should be collected within the same date as the remote-sensing measurements to ensure temporal compatibility for data comparison (Reinke and Jones, 2006). For example, the Landsat 7 and 8 remote sensing data both have temporally frequency of every 16 days, so a field survey can be planned for the desired season/month to be on the same date as the remote-sensing measurement. The time of day should also be considered when planning the field surveys. Landsat 7 and 8 daytime acquisition times occur at a given location around the same time each pass+/- 15 minutes (USGS, https://landsat.usgs.gov/what-acquisition-schedule-landsat). Field data to ground truth NDVI determined from remotes-sensing measurements are more effective during the growing season when

plants are photosynthetically active (Gamon et al., 1995; Reinke and Jones, 2006; Raynolds et al., 2012).

1.4 Next Steps

During the upcoming fiscal year 2018/19, a biological expert will be recruited to review and refine the field-survey methods used thus far for the PBHSP, and provide recommendations for the field surveys and other site-specific monitoring methods for the PBHSP. This literature review of field-survey methods that are favorable to validate NDVI derived from remote sensing measurements will be considered when designing the site-specific monitoring for fiscal year 2019/20.

1.5 References

Baker, J.M., and van Bavel, C.H.M. 1987. *Measurement of mass flow of water in the stems of herbaceous plants.* Plant Cell Environment v.10, pg. 777-782.

Breda, N.J.J, 2003. *Ground-based measurements of leaf area index: a review of methods, instruments, and current controversies.* Journal of Experimental Botany, v. 54, pg. 2403-2417.

Burba, G. 2013. *Eddy covariance method for scientific, industrial, agricultural and regulatory applications: A field book on measuring ecosystem gas exchange and areal emission rates.* LI-Cor Biosciences.

Burgess, S.S.O., Adams, M.A., Turner, N.C., Beverly, C.R., Ong, C.K., Khan, A.A.H., Bleby, T.M. 2001. *An improved heat pulse method to measure low and reverse rates of sap flow in woody plants.* Tree Physiology v.21, pg. 589-598.

Campbell, G.S. 1991. An overview of methods for measuring sap flow in plants. In *Collected summaries of papers at the 83rd annual meeting of the American Society of Agronomy, Division A-3:* Agroclimatology and agronomic modelling. (p.2-3), Denver, Colorado, Oct.27-Nov.2, 1991.

Cohen Y. 1994. Thermoelectric Methods for Measurement of Sap Flow in Plants. In Stanhill G. (eds) *Advances in Bioclimatology.* Advances in Bioclimatology v.3 (pp. 63-89). Berlin, Heidelberg.: Springer.

Danson, F. M., Hetherington, D., Morsdorf, F., Koetz, B., & Allgower, B. 2007. *Forest canopy gap fraction from terrestrial laser scanning.* IEEE Geoscience and remote sensing letters v. 4, pg. 157-160.

Ferrari, F. N., Parera, C. A., & Passera, C. B. 2016. *Whole plant open chamber to measure gas exchange on herbaceous plants.* Chilean journal of agricultural research v.76, pg. 93-99.

Fleck, S. Raspe, S. Cater, M., Schleppi, P., Ukonmaanaho, L., Greve, M., Hertel, C., Weis, W., Rumpf, S. 2012. Leaf Area Measurements. In Fleck, S. Raspe, S. Cater, M., Schleppi, P., Ukonmaanaho, L., Greve, M., Hertel, C., Weis, W., Rumpf, S (eds) *Manual Part XVII. Manual on Methods and Criteria for Harmonized Sampling, Assessment, Monitoring, and Analyzing of the Effects of Air Pollution on Forests.* Hamburg, Germany.: UNECE ICP Forests Programme Co-Ordinating Cente.

Gamon, J. A., Field, C. B., Goulden, M. L., Griffin, K. L., Hartley, A. E., Geeske, J. Penuelas, J., and Valentini, R. 1995. *Relationships Between NDVI, Canopy Structure, and Photosynthesis in Three Californian Vegetation Types.* Ecological Applications v. 5, pg. 28-41.

Goulden, M. L., and Field, C.B. 1994. *Three methods for monitoring the gas-exchange of individual tree canopies: ventilated chamber, sap-flow and Penman-Monteith measurements on evergreen oaks.* Functional Ecology v.8, pg. 125-135.

Hardwick, S. R., Toumi, R., Pfeifer, M., Turner, E. C., Nilus, R., & Ewers, R. M. 2015. *The relationship between leaf area index and microclimate in tropical forest and oil palm plantation: Forest disturbance drives changes in microclimate.* Agricultural and Forest Meteorology v. 201, pg. 187-195.

Holding, D. R., & Streich, A. M. 2013. *Plant Growth Processes: Transpiration, Photosynthesis, and Respiration*. Division of the Institute of Agriculture and Natural Resources, University of Nebraska, Lincoln, Nebraska.

Isaac, R. A., & Johnson, W. C. 1976. *Determination of total nitrogen in plant tissue, using a block digestor.* Journal of the Association of Official Analytical Chemists v.59, pg. 98-100.

James, S. A., Clearwater, M. J., Meinzer, F. C., and Goldstein, G. 2002. *Heat dissipation sensors of variable length for the measurement of sap flow in trees with deep sapwood.* Tree physiology v. *224*, pg. 277-283.

Justice, C.O., and Townshend, J.G. (1981). *Integrating ground data with remote sensing.* In: Terrain Analysis and Remote Sensing. pg. 38-58. George Allen and Unwin, London.

Lawley, V., Lewis, M., Clarke, K., and Ostendorf, B. 2016. Site-based and remote sensing methods for monitoring indicators of vegetation condition: An Australian review. Ecological Indicators v. 60, pg. 1273-1283.

Loomis, R. S. 1997. *On the utility of nitrogen in leaves.* Proceedings of the National Academy of Sciences v.9425, pg. 13378-13379.

Muñoz-Huerta, R. F., Guevara-Gonzalez, R. G., Contreras-Medina, L. M., Torres-Pacheco, I., Prado-Olivarez, J., & Ocampo-Velazquez, R. V. 2013. *A review of methods for sensing the nitrogen status in plants: advantages, disadvantages and recent advances*. Sensors v.13, pg. 10823-10843.

Nogués, S., & Baker, N. R. 2000. *Effects of drought on photosynthesis in Mediterranean plants grown under enhanced UV-B radiation.* Journal of Experimental Botany v. 51, pg.1309-1317.

Persson, S. 2014. *Estimating leaf area index from satellite data in deciduous forests of southern Sweden.* Master degree thesis, Physical Geography and Ecosystem Analysis Department of Physical Geography and Ecosystems Science, Lund University.

Pettorelli, N. 2013. *The Normalized Difference Vegetation Index.* First edition. Published 2013 by Oxford University Press.

Pietragalla, J. and Madrigal Vega, Arturo. 2012. Chapter 8: Normalized Difference Vegetation Index. In Pask, AJD., Pietragalla, J., Mullan, DM. and Reynolds, MP. (Eds.), *Physiological Breeding II: A Field Guide to Wheat Phenotyping* (pp. 37-40). Mexico, D.F.: CIMMYT.

Pirvulescu, V. 2013. *Application of the eddy-covariance method under the canopy at a boreal forest site in central Sweden.* Master degree thesis, Physical Geography and Ecosystem Analysis Department of Physical Geography and Ecosystems Science, Lund University.

Porra, R. J., Thompson, W. A., & Kriedemann, P. E. 1989. *Determination of accurate extinction coefficients and simultaneous equations for assaying chlorophylls a and b extracted with four different solvents: verification of the concentration of chlorophyll standards by atomic absorption spectroscopy*. Biochimica et Biophysica Acta (BBA)-Bioenergetics v.975, pg. 384-394.

Raynolds, M. K., Walker, D. A., Epstein, H. E., Pinzon, J. E., & Tucker, C. J. 2012. *A new estimate of tundra-biome phytomass from trans-Arctic field data and AVHRR NDVI*. Remote Sensing Letters v.3, pg. 403-411.

Razzhivin, V.Y. 1999. Zonation of vegetation in the Russian Arctic. In Nordal, I. and Razzhivin, V.Y. (Eds.), *The Species Concept in the High North – A Panarctic Flora Initiative* (pp. 113–130). Oslo, Norway.: The Norwegian Academy of Science and Letters.

Reinke, K., & Jones, S. 2006. *Integrating vegetation field surveys with remotely sensed data*. Ecological Management & Restoration v. 7, pg. S18-S23

Turner, D. P., Cohen, W. B., Kennedy, R. E., Fassnacht, K. S., and Briggs, J. M. 1999. *Relationships between leaf area index and Landsat TM spectral vegetation indices across three temperate zone sites*. Remote sensing of environment v.70, pg. 52-68.

Van Wijk, M. T., & Williams, M. 2005. *Optical instruments for measuring leaf area index in low vegetation: application in arctic ecosystems*. Ecological Applications v.15, pg. 1462-1470.

Valentini, R., Gamon, J. A., & Field, C. B. 1995. *Ecosystem gas exchange in a California grassland: seasonal patterns and implications for scaling.* Ecology v.766, pg. 1940-1952.

Verstraete, M. M. 1987. *Radiation transfer in plant canopies: Transmission of direct solar radiation and the role of leaf orientation.* Journal of Geophysical Research: Atmospheres v.*92*, pg. 10985-10995.

Wolf, D. D., Carson, E. W., & Brown, R. H. 1972. *Leaf area index and specific leaf area determinations*. Journal Agriculture Education v.1, pg. 24-27.

Appendix B– Mann-Kendall Analysis of NDVI Data

1.1 Introduction

The Mann-Kendall statistical trend test (Mann-Kendall test) was performed on the average growing-season NDVI metrics (NDVI) for the period of 1984 to 2017 for all 13 areas where NDVI are analyzed for the *Annual Report of the Prado Basin Habitat Sustainability Committee Water Year 2016/2017*. The Mann-Kendall test was utilized to evaluate whether the average growing-season NDVI increased, decreased, or remained stable over time.

1.2 Methods

The primary objective of a statistical trend test is to quantitatively characterize the relationship among a series of observations. Trend analysis determines whether the probability distribution of a data-set changes over time (Helsel and Hirsch, 2002). The Mann-Kendall test is a non-parametric hypothesis test and is analogous to parametric trend testing such as regression (linear regression) except the data do not need to have a particular probability distribution (normal) and be accurately described by a particular measure of centrally tendency (mean, standard deviation, etc.). The Mann-Kendall test determines whether Y values (NDVI) increase, decrease, or stay the same with time (X) by independently ranking the chronological change among data as either a positive difference (rank: 1), negative difference (rank: -1), or no difference (rank: 0). This comparison of relative relationships among data can be described as monotonic correlation (Meals et al. 2011). The Mann-Kendall test utilizes the null hypothesis (H_o) that there is no trend. Two values, the $\boldsymbol{S}$ test statistic and the **τ(tau)** coefficient are calculated to measure the strength of monotonic correlation of NDVI. If the $\boldsymbol{S}$ test statistic and $\boldsymbol{\tau}$ coefficient are significantly different than zero (tested at a specified significance), H_o is rejected and a trend exists.

The $\boldsymbol{S}$ test statistic, represents the difference of concordant pairs (number of X,Y pairs where Y increases with increasing X) from discordant pairs (number of X,Y pairs where Y decreases with increasing X). A positive $\boldsymbol{S}$ test statistic is indicative of an increasing trend in Y, and conversely a negative $\boldsymbol{S}$ test statistic is indicative of a decreasing trend in Y. The $\boldsymbol{S}$ test statistic is calculated using the following equation (Meals et al. 2011):

$$\boldsymbol{S} = \sum_{i=1}^{n-1} \sum_{j=i+1}^{n} sign(y_j - y_i)$$

Using the $\boldsymbol{S}$ test statistic, the $\boldsymbol{\tau}$ coefficient (analogous to the **r** correlation coefficient in linear associations) is then calculated using the following equation:

$$\boldsymbol{\tau} = \frac{S}{n(n-1)/2}$$

The **τ** coefficient represents the strength of the monotonic relationship between X and Y with a possible a range of -1 to 1. It is the net relative score of association. A perfect positive trend would yield a **τ** coefficient equal to 1, and a perfect negative trend would yield a **τ** coefficient equal to -1. If the **τ** coefficient equals 0, the null hypothesis of 'no trend' cannot be rejected indicating no trend exists in the data.

To test for the statistical significance of the calculated ***S*** test statistic and **τ** coefficient, two possible methods are utilized. For small sample sizes ($n \leq 10$) results are compared to a table of standardized critical values for **τ** coefficient at a level of significance of 0.05 (95% confidence) (Fisher et al. 1989). For large sample sizes ($n > 10$), a normal-approximation test can be applied at a specified level of significance (Kendall, 1975).

1.3 Example

Consider the following dataset: X(time)= 1991, 1992, 1993, 1994 and Y(NDVI)= 0.4, 0.7, 0.6, 0.9 (n=4). The data is organized chronologically by increasing X. The Y values are ranked based on the relative changes between data whereby a rank of 1 indicates the subsequent value increased, and -1 if the subsequent value decreased; Y pair 1 (0.4, 0.7) receives a rank of 1. Performing this ranking exercise on all Y data combinations yields the following table:

Y Pair	Rank
(0.4, 0.7)	1 (positive difference)
(0.4, 0.6)	1 (positive difference)
(0.4, 0.9)	1 (positive difference)
(0.7, 0.6)	-1 (negative difference)
(0.7, 0.9)	1 (positive difference)
(0.6, 0.9)	1 (positive difference)
Total (increasing)	5
Total (decreasing)	1
S = Total (increasing) - Total (decreasing)	4
τ (tau)	0.67

For this data set, the positive ***S*** test statistic of 4 indicates an increasing trend in Y(NDVI), and the positive **τ** coefficient of 0.67 represents the strength of the relationship between X and Y, on a scale of 0 to 1.

1.4 Data Analysis and Results

The ***S*** test statistic and **τ** coefficient were computed for average-growing season NDVI from 1984 to 2017 for the 13 areas in Prado Basin, using 'Kendall' package in R *studio*[1]. A two-tailed p-value was calculated in R *studio* to test for significance of the ***S*** test statistic. Table B-1 lists the results of Mann-Kendall test. The ***S*** test statistics were evaluated at 0.05 level of significance (95% confidence) using a normal-approximation test typically done for sample sizes where n >

[1] RStudio Team (2015). RStudio: Integrated Development for R. RStudio, Inc., Boston, MA URL http://www.rstudio.com/.

10. A p-value below the specified level of significance of 0.05 indicates a rejection of the null hypothesis of 'no trend', and an increasing trend is the ***S*** test statistic and **τ** coefficient are positive, and a decreasing trend if the ***S*** test statistic and **τ** coefficient are negative. A p-value above the specified level of significance of 0.05 indicates a failure to reject the null hypothesis of 'no trend', and a determination of no trend. For all 13 sites where NDVI data were evaluated with the Mann-Kendall test, 10 resulted in an 'increasing trend', and three resulted in 'no trend'

1.5 References

Helsel, D.R., and Hirsch R.M. 2002. *Statistical Methods in Water Resources*. Techniques of Water Resource Investigations of the United States Geological Survey, Book, 4 Hydrological Analysis and Interpretation. September 2002.

Fisher, Sarah R. and Potter, Kenneth W. *Appendix A; Recommended Statistical Tests*. Methods for determining compliance with groundwater quality regulations at waste disposal facilities (Wisconsin groundwater management practice monitoring project, [DNR-014b]) Madison, Wisconsin: Wisconsin Department of Natural Resources, 1989.

Meals, D.W., Spooner, J., Dressing, S.A, and Harcum. J.B. 2011. *Statistical Analysis for Monotonic Trends; Tech Notes 6*. Developed for U.S. Environmental Protection Agency by Tetra Tech, Inc., Fairfax VA. November 2011.

HydroGeoLogic, Inc. (2005). *Appendix D; Mann-Kendall Analysis*. OU-1 Annual Groundwater Monitoring Report – Former Fort Ord, California. July 2005.

Kendall, M.G., 1975. *Rank Correlation Methods, 4th ed.* Charles Griffin, London.

Table B-1

Site	n (number of (X, Y) pairs)	S test statistic	τ (tau) coefficient	p-value (two-tailed)	Confidence (1-(p-value))	Trend at 0.05 Significance Level
Riparian Vegetation Extent	33	104	0.20	0.1105	0.8895	No Trend
Lower Prado	33	198	0.38	0.0023	0.9977	Increasing
CC-1	34	357	0.64	1.19E-07	1.0000	Increasing
CC-2	34	397	0.71	2.22E-16	1.0000	Increasing
CC-3	34	255	0.46	0.0002	0.9998	Increasing
CC-4	34	171	0.31	0.0117	0.9883	Increasing
MC-1	34	325	0.58	1.55E-06	1.0000	Increasing
MC-2	34	-21	-0.04	0.7669	0.2331	No Trend
MC-3	34	-79	0.14	0.2476	0.7524	No Trend
MC-4	34	217	0.39	0.0014	0.9986	Increasing
SAR-1	34	313	0.56	3.70E-06	1.0000	Increasing
SAR-2	34	229	0.41	0.0007	0.9993	Increasing
SAR-3	34	269	0.48	7.09E-05	0.9999	Increasing

Appendix C - Response to PBHSC Comments

Annual Report of the PBHSC – Water Year 2017

U.S. Fish and Wildlife Service and California Department of Fish and Wildlife – comments provided by Rebecca Gordon

Comment 1 – Baseline Condition

As previously stated, we are concerned with the lack of an established baseline to compare changes over time since the Peace II Agreement was first implemented.

Response:

In determining whether a project's impacts are significant, an EIR compares those impacts with existing environmental conditions that exist in the area affected by the project at the time the EIR process begins, which are referred to as the "baseline" for the impact analysis. (14 Cal Code Regs § 15125(a).) As noted in the Peace II SEIR, the baseline condition is the absence of implementation of the Peace II Agreement (Basin Re-operation and the expansion of the CDA facilities to achieve Hydraulic Control). All prior groundwater extraction, recharge, and management activities (e.g. Peace Agreement activities) have been through certified environmental review pursuant to the California Environmental Quality Act (CEQA), and are part of the current and future baseline conditions. Thus, any new projects must consider the Peace Agreement activities in their baseline analysis.

While the Peace II SEIR concluded, based on modeling data, that implementation of the Peace II Agreement would not cause significant adverse effects on Prado Basin riparian habitat, a monitoring program was adopted as a contingency mitigation measure in response to comments from Orange County Water District (OCWD). The Prado Basin Habitat Sustainability Program (PBHSP) is an adaptive management program to ensure that the Prado Flood Control Basin riparian habitat will not incur any unforeseeable significant adverse effects due to the implementation of the Peace II Agreement. The specific intent of this monitoring program is to characterize the historical, current, and future extent and quality of the riparian habitat in Prado Basin, and if degradation of the riparian habitat is documented, to provide the data necessary to describe the cause(s) of that degradation. This Annual Report includes historical data dating from the 1960s and vegetation surveys that were performed before and after the Peace II Agreement was implemented. In sum, the assessment of the Prado Basin riparian habitat, through the analysis of air photos, NDVI, and vegetation surveys, shows that the riparian habitat has increased in its extent and quality since the 1960s. There is no indication of a trend in degradation in the extent or quality of the riparian habitat that is contemporaneous with the Project at issue.

Comment 2 – Section 3.3

Groundwater elevations and thalweg elevations for 2017 were determined using a 1-meter horizontal resolution digital elevation model (DEM) of the ground surface obtained in 2007. These DEM data are approximately 10 years old and should be updated for future analyses. There is known aggradation occurring within the Prado Basin and the Santa Ana River, and elevations are likely higher in at least some locations than they were in 2007. Please obtain more current DEM data for next year's report.

Response:

Comment noted. While the recommended PBHSP for fiscal year 2018/19 does not include the development of an updated DEM for the Prado Basin area, the PBHSC may determine that it should be explored, and potentially considered for fiscal year 2019/20.

Comment 3 – Site-specific monitoring

Orange County Water District is currently implementing an updated field protocol to measure habitat quality within Prado Basin. Please coordinate with them to determine if their new methods may support ground-truthing efforts in conjunction with future remote-sensing data.

Response:

Concur. The Watermaster and IEUA have coordinated with OCWD on their monitoring efforts in the Prado Basin throughout the development and implementation of the PBHSP. The scope of the PBHSP for the upcoming fiscal year 2018/19 includes a refinement of the site-specific or regional monitoring methods of riparian vegetation and incudes coordination with OCWD and recruiting a biological expert to review the field-survey methods used thus far for the PBHSP, perform independent research, and provide recommendations for field surveys and/or other site-specific monitoring methods for the PBHSP.

Comment 4

We appreciate your continued efforts to monitor groundwater within the Chino Basin and implement the Prado Basin Habitat Sustainability Program

Response:

Comment noted and thank you.

Orange County Water District (OCWD) – Comments provided by Greg Woodside

Comment 1 – Monitoring and Reporting

OCWD appreciates the data collection and analysis efforts by the Chino Basin Watermaster and Inland Empire Utilities Agency. The data and analyses in the draft report are presented in an understandable manner and the graphics are well-designed.

Response:

Comment noted and thank you.

Comment 2 - Section 1.1

The report says 'The US Army Corps of Engineers, in coordination with the Orange County Water District (OCWD), regulates releases of water from Prado Dam for both purposes of flood control and groundwater recharge in Orange County.' The Corps coordinates with OCWD for releases of water temporarily held in storage for groundwater recharge, but does not coordinate with OCWD regarding flood control. Suggest change text to something like 'The US Army Corps of Engineers regulates releases of water from Prado Dam for both purposes of flood control and groundwater recharge in Orange County. Releases of water temporarily held in Prado Basin for groundwater recharge in Orange County are coordinated with OCWD.'

Response:

The report text was updated to read "The US Army Corps of Engineers regulates releases of water from Prado Dam for both purposes of flood control and groundwater recharge in Orange County. Releases of water temporarily held in storage in Prado Basin for groundwater recharge in Orange County is coordinated with the Orange County Water District (OCWD)".

Comment 3 - Section 2.1

The draft report utilizes LANDSAT satellite imagery and the calculated index referred to as 'NDVI' to characterize temporal trends in the extent and quality of Prado Basin's riparian habitat. As discussed in comments submitted on last year's report, NDVI is a useful tool to assess potential changes but it is important to note that as we continue to collect data in the future, we will need to assess the degree to which NDVI measurements correlate with on the ground measurements of vegetation health. As stated in the report, NDVI measurements cannot be interpreted in isolation. The report provides a good discussion of NDVI measurements in light of other data. OCWD appreciates the discussions we have had in the last year with Wildermuth Environmental and agency staff regarding NDVI measurements and available options for collecting data remotely from above the earth's surface. We will need to continue to carefully assess future NDVI measurements in light of other data regarding vegetation health, such as vegetation surveys conducted by biologists in the field. OCWD looks forward to continued collaboration with IEUA, CBWM, and Wildermuth Environmental regarding the most effective data collection efforts

Response:

Concur. As stated in the annual report: "Interpretations of the NDVI (vegetative changes) should be (i) verified with other georeferenced datasets, such as air photos and field vegetation surveys, and (ii) explained by comparison to datasets of causal factors of vegetative changes, such as water availability."

Comment 4 - Air Photo

OCWD appreciates the cost sharing for aerial photo collection in the summer of 2017 by IEUA and CBWM. OCWD is willing to share the cost of the aerial photo collection in July 2018 with IEUA and CBWM

Response:

The Watermaster and IEUA appreciate OCWD cost sharing for the 2017 air photo. The high-resolution air photo collected in July 2017 is a valuable tool to analyze the riparian vegetation extent and quality and to verify the NDVI. Watermaster and IEUA have allocated budget in fiscal year 2018/19 to share the cost with OCWD for acquiring a high-resolution air photo in July.